Columbia

Early Sighting Assessment Team

Final Report

13 June 2003

DA8/Paul S. Hill
DM4/Ron Spencer, Chris Edelen, Ryan W. Proud
DM4/Marc Abadie, John Gowan
DM4/Richard B. Mrozinski, Sarah R. Graybeal, Gavin F. Mendeck
DM4/Scott Hartman, Marissa Herron
OZ4/Craig Schafer

National Aeronautics and Space Administration
Johnson Space Center
Mission Operations Directorate

Table of Contents

1. Executive Summary

2. Early Sightings Assessment Team Overview
   - 2.1. Early Sightings Assessment Team Summary
   - 2.2. Early Sightings Assessment Team Lessons Learned

3. Debris Sighting Report Evaluation
   - 3.1. Types of reports and priorities
   - 3.2. Process for handling videos
   - 3.3. Debris Sighting Report Evaluation Lessons Learned

4. Debris Trajectory Analysis
   - 4.1. Debris Sighting Timeline
     - 4.1.1. Debris Sighting Timeline Summary and Methodology
     - 4.1.2. Detailed Time Sequencing
   - 4.2. Relative Motion and Ballistics
     - 4.2.1. Relative Motion and Ballistics Summary and Methodology
     - 4.2.2. Detailed Relative Motion and Ballistic Analysis
   - 4.3. Trajectory and Footprints
     - 4.3.1. Trajectory and Footprints Summary and Methodology
     - 4.3.2. Primary Debris Footprint
     - 4.3.3. Generic Pre-Breakup Debris Swath
     - 4.3.4. Pre-Breakup Shedding Debris Footprints
     - 4.3.5. Estimated Separation Time for Littlefield Tile
   - 4.4. Debris Trajectory Analysis Lessons Learned

5. Radar Search Areas
   - 5.1. Radar Analysis Team Summary
   - 5.2. Radar Database and Search Method
   - 5.3. California Fence Search
   - 5.4. Radar Based Search Boxes
   - 5.5. Radar Test Implications for Radar Based Search Boxes
   - 5.6. Radar Search Areas Lessons Learned

6. Witness Reports
   - 6.1. Witness Report Summary
   - 6.2. Credible Sightings
   - 6.3. Witness Reports Lessons Learned

7. DOD Data
   7.1 Remote sensors during entry
   7.2. Imagery: AMOS, Kirtland
   7.3. FD2 Radar Data
   7.4. Radar Tests
   7.5. Miscellaneous Other DOD Data
   7.6. DOD Data Lessons Learned

8. Other Sensor Data
   8.1. Infrasonic
   8.2. Seismic
   8.3. Other Sensor Data Lessons Learned

9. References

10. Appendices
   10.1. Team Members and Contributors
   10.2. Entry Debris Events Timeline, Version 6 - 05/27/03
   10.3. DOD - JSC Actions

The following appendices are under separate cover:

   10.4. STS-107 Early Entry Debris Sighting Timeline; May 2003
   10.5. STS-107 ESAT Final Report Relative Motion and Ballistics Analysis; May 20, 2003
   10.6. STS-107 Columbia Accident Debris Footprint Boundary Estimates; May 24, 2003
   10.7. JSC Radar Assessment Team Final Report; May 23, 2003
   10.8. Results of Search for Observed Debris Landing Events, and EOC Hotline and Database Lessons Learned for STS-107 Accident Investigation
   10.9. Infrasonic Data: Report to the Department of Defense on Infrasonic Re-Entry Signals from the Space Shuttle Columbia (STS-107) (Revision 3.0)
   10.10 Seismic Data: Analysis of Sonic Booms from the Reentry of the Space Shuttle Columbia over California and Nevada

1. Executive Summary

The Early Sightings Assessment Team (ESAT) was formed two days after the Space Shuttle Columbia accident on February 1, 2003. The ESAT had two primary goals:

- Sift through and characterize the witness reports during entry.
- Obtain and analyze all available data to better characterize the pre-breakup debris and ground impact areas. This included providing the NASA interface to the DOD through the DOD Columbia Investigation Support Team (DCIST).

Video supplied by the general public showed 20 distinct debris shedding events and three flashes/flares during Columbia's entry over the CONUS. Analysis of these videos and corresponding air traffic control radar produced 20 pre-breakup search areas extending from the California-Nevada border through West Texas. These search areas ranged in size from 1 to 1,700 square miles.

In an effort to characterize various orbiter materials and their ability to be detected by available radar, tests were performed by AFRL, Wright-Patterson AFB, OH. A complement of materials and components from inside the payload bay and on the exterior of the Orbiter were tested. These tests characterized both the material radar cross-sections and the detection ranges for the radars that tracked during ascent, orbit operations and entry.

Final analysis concluded there are no reliable indications of off-nominal events in any DOD, DOE, NOAA, and USGS remote sensor data during ascent or pre-breakup during entry, including debris shedding. The only anomalous event detected by remote sensors during the mission was a series of DOD radar tracks indicating an object originating from the Orbiter on flight day 2. A subset of the radar tests and related analyses were designed to identify this object. Conclusions are deferred to the tiger team specifically formed under the OVE Working Group to study the Flight Day 2 event.

2. Early Sightings Assessment Team Overview

2.1. Early Sightings Assessment Team Summary

The Early Sightings Assessment Team (ESAT) was formed 2 days after the Space Shuttle Columbia accident on February 1, 2003. The ESAT had two primary goals:

- Sift through and characterize the witness reports during entry.
- Obtain and analyze all available data to better characterize the pre-breakup debris and ground impact areas. This included providing the NASA interface to the DOD through the DOD Columbia Investigation Support Team (DCIST).

Of the 17,400 public phone, e-mail, and mail reports received from February 1 through April 4, more than 2,900 were witness reports during entry, prior to the vehicle breakup. Over 700 of the reports included photographs or video of Columbia during entry. It was quickly discovered that public imagery provided a near complete record of Columbia's entry over the United States and that the video showed debris being shed from the Orbiter. Final analysis showed 20 distinct debris shedding events and three flashes/flares during entry over the CONUS. To facilitate the trajectory analysis, these witness reports were prioritized in order to process entry imagery with precise observer location and time calibration first, with an emphasis on video.

The ESAT set up a process to time synchronize all video, determine the exact debris shedding time, measure relative motion, determine ballistic properties of the debris, and perform trajectory analysis to predict the potential ground impact areas or footprints. Key videos were hand carried through the JSC system, expedited through the Photo Assessment Team, and put into ballistic and trajectory analysis as quickly as possible. The Aerospace Corporation independently performed the ballistic and trajectory analysis for Debris 1, 2, 6, and 14 for the purpose of process verification.

Figures 2-1 and 2-2 summarize the debris shedding events and flashes/flares observed in public video. These are shown on the entry ground track and include each photographer's location and approximate field of view recorded in video. Times listed in the figures for each event indicate the earliest each is seen in video. Exact debris shedding times were calculated based on detailed relative motion analysis as explained in detail in Section 4.2. Figure 2-3 shows the predicted ground impact areas for each debris shedding event.

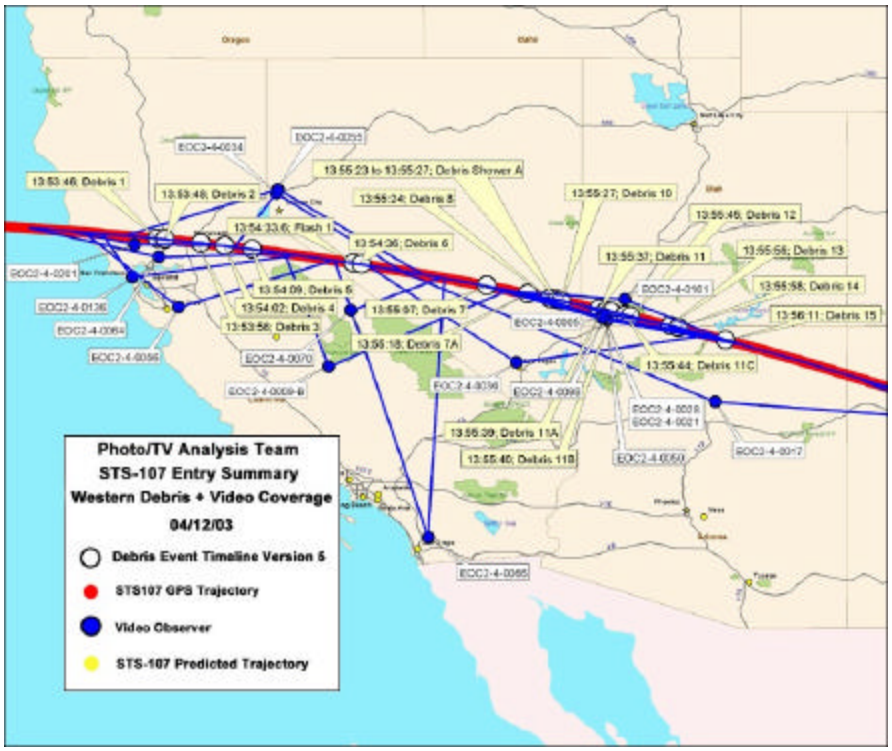

Figure 2-1: Public Video Coverage of the Western United States STS-107 Entry Trajectory [21]

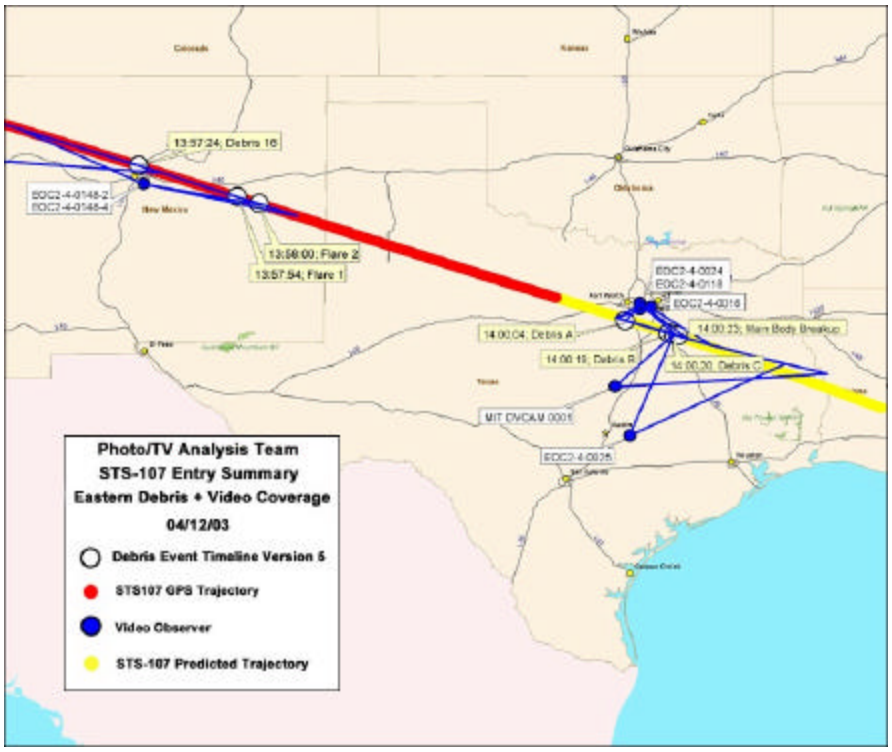

Figure 2-2: Public Video Coverage of the Central United States STS-107 Entry Trajectory [21]

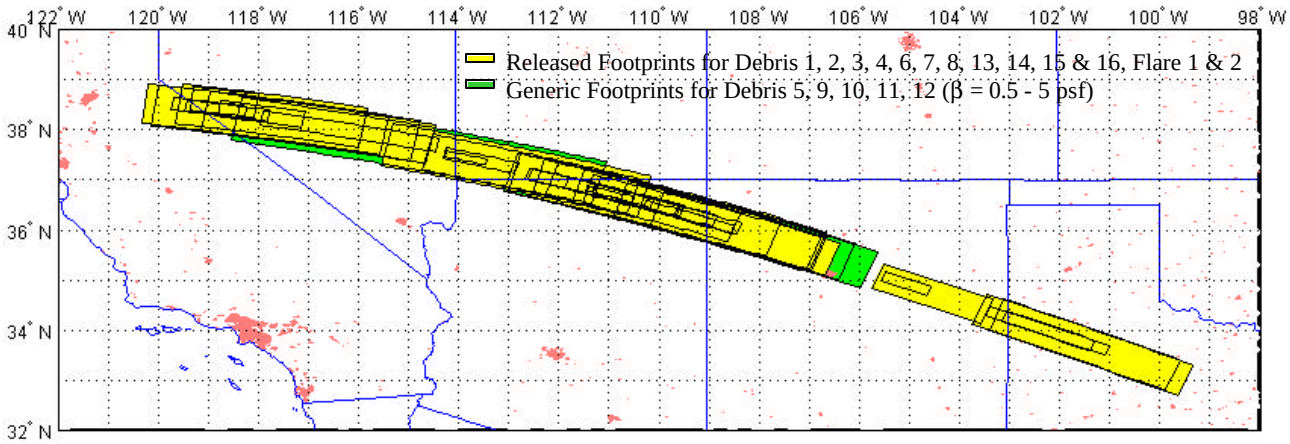

Figure 2-3: Combined Ground Impact Footprints
of Observed Debris 1 Through 16 and Assumed Debris at Flare 1 & 2
Constant Ballistic Coefficients, 0-0.15 L/D, C_d 1.0 [24]

Similar footprints were generated for 35,000 and 80,000 ft altitude for use in searching recorded FAA and DOD air traffic control radar in close partnership with the NTSB and FAA. The Radar Analysis Team searched through more than 2 million individual radar returns generated between 1330 and 1500Z on February 1, 2003. Footprints for all debris observed in video were searched by analysts at JSC and the NTSB for indications of any uncorrelated radar threads falling through the air space. A generic debris swath extending from California through break-up in Texas was also searched for radar threads in long range radar.

The combination of trajectory analysis and radar searches led to 20 pre-breakup search areas extending from the California-Nevada border through West Texas. The search areas were prioritized by overall confidence based on the trajectory analysis, radar data quality, and in one case a supporting witness account. The search areas ranged in size from as low as 1 - 11 square miles for the radar based areas, to 300 - 1700 square miles for trajectory-only based areas. All areas were typically in high desert or mountainous terrain. Although ground searches of several of the smaller areas did not produce any Columbia debris, the "Littlefield Tile" (KSC Database object #14768) was determined to have been shed from the Orbiter in the approximate time of Flare 1 through Flare-2 seen in public video.

Results from a series of radar tests by the Air Force Research Laboratory at Wright-Patterson AFB, OH show that the various Orbiter external materials have low maximum detection ranges for the air traffic control radars. Although the larger, leading edge components have much higher radar detection ranges, ballistic analysis and telemetry analysis suggest the long stream of debris observed in video is comprised of smaller objects, not a series of large, near intact, leading edge components. Thus, confidence was reduced that the radar threads used as the basis for search boxes are Columbia debris. This leaves the much larger trajectory based areas as best predictions for pre-breakup debris.

Emphasis was then given to the areas in which the highest probability regions of multiple early debris shedding footprints overlap as shown in Figure 2-4. The darkest regions in the plot indicate the most overlap.

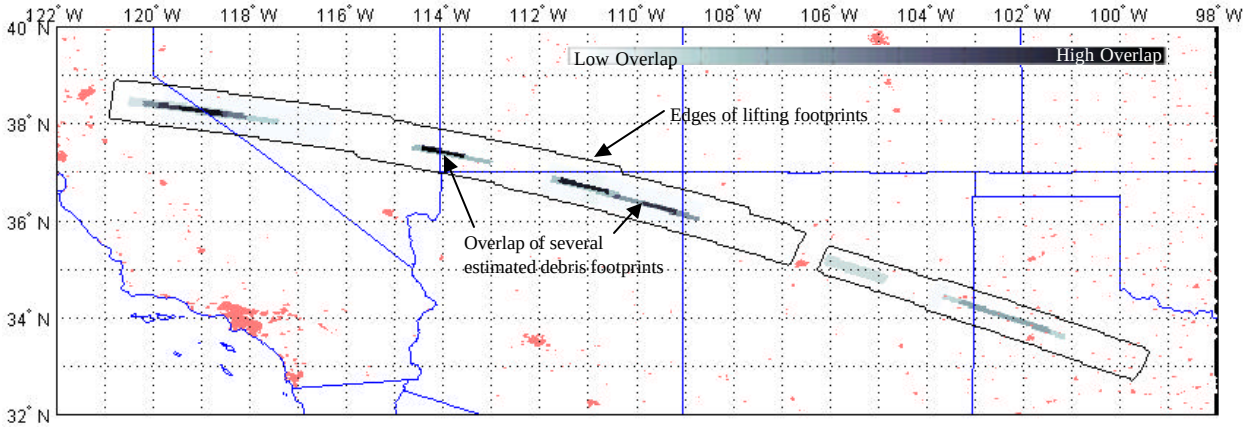

Figure 2-4: Combined Overlapping Ground Impact Footprints of Observed Debris 1 Through 16 [24]

Table 2-1 lists the ten high confidence ballistics and radar based search areas in priority order. The full list is shown in Section 5.

JSC/NTSB Priority	Box	Location Description	# radar hits	# radar antennas	Box Area Sq. NM / Acres (size of Non-lifting areas reflects ONLY the PRIMARY NL areas)	Inside any Lifting or Non Lifting (Ballistic) Footprint? Y/N (see separate Lookup Table)	Thread ID	Comment
1	8	west of Elgin, NV	11	1 (QAS)	1.68 / 1424	Y (Lifting 01 thru 06)	QAS-11-114.77	Delamar Lake, NV witness
2	7-1	Near Pioche, and Caliente, NV	75	1 (CDC)	4.25 / 3602	**Y (Non lifting 02 thru 04, and Lifting 01,05,06)**	CDC-075-114.4689	Well outside non-lifting, but in Debris-6 lifting foot print.
3	3	Near Floydada, TX	10	2 (QXS,LBB - ASR)	169.02 / 143251	Y(Lifting 16, non-lifting for Flare 1 and Flare2)	LBB-ASR-18-101.3186	Tile found 40 NM west of box
4	7-2	Near Pioche, and Caliente, NV	75	1(CDC)	11.03 / 9384	Y (Lifting 01 thru 06)	CDC-075-114.4690	Well outside non-lifting, but in Debris-6 lifting foot print.
5	6-south	Dixie Natl Forest - Zion Natl Park, UT	18	2 (QXP, CDC)	1.42 / 1203	Y (Lifting 02 thru 07)	QXP-18-113.1506	In/near Debris-6 dense overlap
6	6-north	Dixie Natl Forest - Zion Natl Park, UT	18	2 (QXP, CDC)	1.58 / 1339	Y (Lifting 02 thru 07)	QXP-18-113.1505	In/near Debris-6 dense overlap
7	Dense overlap non-lifting debris 04 thru 06	Near St. George Utah	N/A	N/A	Approx 300 Sq. NM	N/A	N/A	Best relmo cues and ballistics. Considered 1 of 2 most significant events in video. Most dense overlap area.
8	Dense Overlap non-lifting 07 thru 14	NE Arizona, Navajo Indian Reservation	N/A	N/A	approx 1162 Sq. NM	N/A	N/A	Measured relmo, but not as good as Debris-6. Considered 2 of 2 most significant events in video. 2nd most dense overlap area.
9	7-3	Near Pioche, and Caliente, NV	75	1 (CDC)	9.19 / 7789	Y (Lifting 01 thru 06)	CDC-075-114.4691	Outside non-lifting, but in Debris-6 lifting foot print.
10	Dense overlap - non-lifting Debris 01 thru 04	CA/NV Border	N/A	N/A	approx 775 Sq. NM	N/A	N/A	Measured relmo, but not as good as Debris-14. 3rd most dense overlap area.

Table 2-1: High Confidence Western Search Box Priorities [25]

AFRL performed additional radar tests on materials and components inside the payload bay and on the exterior of the Orbiter. This was done in order to fully characterize the radar cross-sections for correlation with the C-band radars which track during ascent and two deep space tracking radars. The C-band radar tests were added to investigate the ability to track debris during ascent, with a primary goal of quantifying the likelihood of discriminating Shuttle debris in the ascent plume and the ability to track the most likely Shuttle debris with the C-bands in general. The deep space tracking radar tests were used to evaluate radar data from an object tracked by Air Force Space Command during the mission that was shown to have originated at the Orbiter on Flight Day 2. Detailed discussion of the evaluations of the Flight Day 2 object are deferred to the tiger team formed under the OVE WG to study this data.

In the first 2 weeks of the investigation, there were preliminary indications in various unclassified and classified sensors of some anomalous events during entry. There were similar preliminary indications of anomalous events during ascent. After additional analysis, however, there are no reliable indications in any DOD remote sensor data of anomalous events during ascent or pre-breakup during entry, including debris shedding.

Columbia was imaged during 3 days of STS-107 orbit operations by the Air Force Maui Optical & Supercomputing (AMOS) site and during entry by employees of the Starfire Optical Range at Kirtland AFB, NM. The AMOS and Kirtland images are the only DOD images taken of Columbia during STS-107 from any source, unclassified or classified. The AMOS images are predominantly of the upper surfaces with payload bay doors open, obscuring a significant portion of the wings, and showing no discernible damage. Detailed discussion of the Kirtland images are deferred to the tiger team formed under the OVE WG to study them.

DOD, DOE, and NOAA infrasound researchers collaborated to study infrasonic signals recorded during STS-107 entry. Similarly, the USGS studied seismic data recorded throughout the southwest CONUS during entry. Although signals associated with the Orbiter are found in both sets of data, analysis to date does not provide any data that can be positively identified as off-nominal, such as debris shedding, high energy release, ground impact, etc.

Analysis of luminosity data, embedded in public imagery, was initiated in an effort to extract an estimate of the size and mass of specific debris material. Ames Research Center has developed a series of tests to explore this possibility, but at the time of this writing, these tests had not yet begun, but the confidence that this will yield significant data is considered low. Also investigated early on was the use of spectral data for constituent determination, but this is not expected to be pursued based on the relatively poor quality video data.

The top level interfaces and data paths within the JSC team are shown in Figure 2-5 below. Not depicted are the interfaces to the various non-NASA groups.

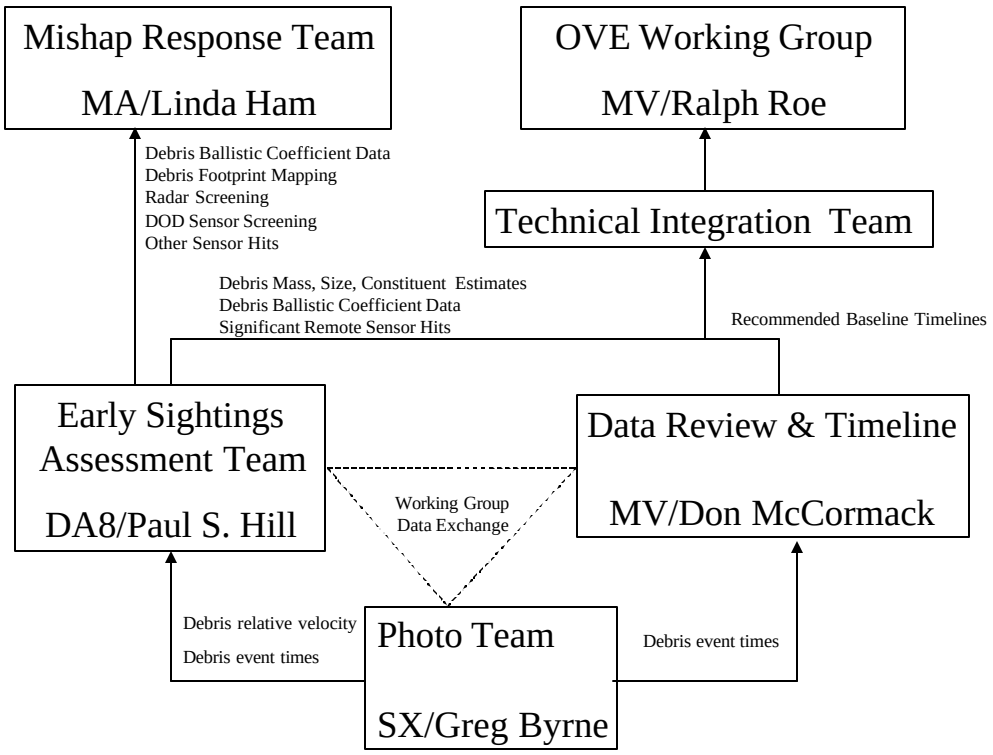

Figure 2-5: ESAT Interfaces

2.2. Early Sightings Assessment Team Lessons Learned

2.2.1 Debris Sighting Report Evaluation Lessons Learned

1) The public report form should be standardized and ready for use in any future incident to maintain uniformity of collected information. This form should include key interview questions, detailed locations, contact information and zip codes.

2) All phone interviews (and any public reports) should be entered directly into an electronic form as the interview takes place to facilitate immediate accessibility by all investigation teams. These should include fields to distinguish reports of human remains, debris, and visual sightings. Additionally, the database should have a search function for the various types of input fields.

3) Eyewitness reports should be treated as a 'case file' rather than as separate reports. This would allow the team to add to an existing report and note when video or other media was received without logging repeated calls from the same witness as separate reports.

4) A single point of contact should be used for responding to EOC reports whenever possible due to sensitivity among some of the public to being contacted repeatedly for the same EOC report.

5) Various products referencing EOC reports should be built using the EOC reference number not the public caller's name.

6) Record exact location, weight, dimensions, and a digital still of all debris as it is recovered and input it into a single database daily. This would allow the use of some back-propagation techniques to better define the debris field, identify debris separation times, and confirm validity of objects as debris. Additionally, it should be noted how the location was determined (GPS coordinates, map location, street address, etc.)

2.2.2 Debris Trajectory Analysis Lessons Learned

1) Observer provided information on location, camera specifications, zoom settings, and time synchronization was invaluable as the debris analysis progressed.

2) The combination of automation and parallel processes for calculating a relative range for each time step in video ensured both a quick and accurate answer and is highly recommended to anyone performing a similar analysis in the future.

3) The Debris Footprint Team generated the method to shape a debris footprint between the heel and toe specifically for this accident to aid the Search and Recovery Team in avoiding unnecessary search areas, and will be used in all future debris footprint predictions.

4) In this incident, the first debris footprint predictions were not available until 4 hours after the accident. To improve the possibility of crew rescue, either:
   - a "running" debris footprint should be designed for future STS missions such that as soon as telemetry is lost, a debris footprint and estimated crew module impact point are available, or
   - a footprint prediction team should be available during entry.

5) An upper bound on ballistic coefficient was not known for an Orbiter on entry; the Debris Footprint Team now has a maximum ballistic coefficient to use in any future Orbiter-only debris field analysis, based on the Columbia observed value of 220 psf.

2.2.3 Radar Search Areas Lessons Learned

1) Focus energy looking for localized "blob" tracks, vice linear radar tracks.

2) Focus the search for tracks closer to the groundtrack within the non-lifting footprint.

3) Integrate eye-witness reports into radar search as early as possible.

4) Station NASA Radar Analysis Team representative at the field operations center for debris searches to help coordinate search box data and act as primary liaison between the RAT and MIT/Search Coordinators.

5) Conduct daily telecons with NTSB/FAA/RADES to discuss radar tracks, search boxes, etc.

2.2.4 Witness Reports Lessons Learned

NASA should consider developing a method of educating the public on how best to record future reentries so that, if such a mishap ever occurs again, the video would more easily facilitate post-flight analysis. This would include all important imagery characteristics and supporting data which are key to the analysis.

2.2.5 DOD Data Lessons Learned

1) A single DOD POC, located at the NASA center conducting the investigation, is essential to effectively exchanging data and requesting additional support.

2) Generic DOD tracking capability and the resulting routine taskings on Shuttle flights should be reviewed and updated as required for all phases of flight.

3) Generic DOD imaging/sensor capability and the resulting routine and contingency taskings on Shuttle flights should be reviewed and updated as required for all phases of flight.

4) NASA and the USAF should study the use of Orbiter-specific material maps to facilitate AMOS' thermal mapping of all Orbiters during orbit operations.

2.2.6 Other Sensor Data Lessons Learned

1) The state of the art for infrasonic and seismic data does not support their use for monitoring Orbiter entry.

2) The state of the art for infrasonic and seismic data does not provide significant engineering value for Columbia's post-incident investigation.

3. Debris Sighting Report Evaluation

3.1. Types of reports and priorities

The Emergency Operations Center (EOC) at JSC received 17,400 public phone, e-mail, and mail reports from February 1 through April 4, with approximately 50 percent of them received in the first week. These reports ranged from people who saw or heard something, to condolences, offers to help, photographs and video of Columbia in flight,or some part of the sky after Columbia had flown past.

Of the total reports received, more than 2,900 were witness reports during entry, over 700 of which included photographs or video. As it became clear that public imagery provided a near complete record of Columbia's entry over the United States, the highest priorities were placed on identifying credible imagery of Columbia in flight and debris on the ground. The ESAT then focused exclusively on imagery and witness reports of debris in the sky, while reports of debris on the ground were forwarded to the MIT. [6]

All witness reports were sorted geographically with an emphasis on the western most reports. These were then judged for credibility by comparing the time of the observation and location of the observer to the known entry ground track and an estimated debris swath from California through Texas. (Refer to section 5 for a description of the trajectory analysis and debris swaths.) Reports that were considerably before or after entry and from areas which could not have observed entry were easily eliminated from consideration. This includes reports of observations hours or days before entry or from hours after entry. Similarly, witness reports from areas like Jacksonville, Florida could obviously be eliminated since Columbia could not have been observed there from entry interface through break up. The less credible reports were not discarded, but they were moved to low confidence files for follow up later, if necessary.

Of the remaining reports, highest priority was given to reports with photographs and video and with witness descriptions of debris falling near the ground. The ESAT made direct contact with the witness for each of these reports in order to further screen the less credible reports. Extreme examples of the less credible reports would be video from parking lot security cameras after sunrise that show views of parked cars or traffic on a city street, or offers to explain premonitions from days or weeks before the flight which foretold the accident.

It quickly became clear that some of the public imagery showed debris being shed from Columbia. With this discovery, the witness descriptions of small objects appearing to separate from the Orbiter became much less important, and the strong emphasis was given to finding all video and key still photographs. Further, many of the photographers had measured their positions with GPS receivers and/or provided the address of their viewing location. The observer position data enabled JSC to establish accurate relative geometry to the Orbiter, since we had GPS and tracking radar-based Orbiter state vectors. Several of the videos also had clear celestial references, which combined with the observer's location, gave JSC a means to establish absolute time for the video. (Refer to section 4 for more detail on time synchronizing video.)

As a minimum, the ESAT concluded early on that exact times could be determined for the debris shedding captured in time-correlated video. In a best case, the goal was to use the time and geometry to measure ballistic properties of each discrete piece of debris in video. If ballistic properties could be accurately determined, this would lead to predicted areas the debris would fall through at altitude and predicted ground impact areas or footprints. This, in turn, would enable JSC to calculate pre-breakup debris footprints with a goal of locating early debris. There was also a low probability objective of using luminosity and spectral data in the imagery to estimate mass and constituents of the specific debris. (Refer to section 5 for more detail on trajectory analysis.)

Ultimately, witness report priorities were processed as follows, with the highest priority first: entry imagery with precise observer location and time calibration, with an emphasis on video; remaining entry imagery with an emphasis on video; witness reports of debris falling near the ground. As the analysis progressed, these priorities updated to emphasize videos which included: knowledge of field of view, length of debris observation at a constant zoom setting, potential significance of debris, accuracy of time sync for video, accuracy of observer location information, and multiple views of the same debris event. Knowledge of the field of view was important for scaling of the motion of the debris relative to the Shuttle. Brighter and longer duration debris observations were suggestive of a relatively higher ballistic coefficient than other debris observations. Westernmost debris or debris with a unique characteristic such as a flash were also higher priority. Multiple views for debris events such as debris 6 and 14 allowed for cross checking of field of view and time sync estimates.

This led to a prioritized video “hot list” of the most promising witness reports. The videos on this list were given highest priority when routing through JSC for analysis. The final Hot List is shown in Table 3-1.

Priority	Event	Tape #	Time Debris First Observed Aft of Vehicle GMT	Tape Time (TCR)	FOV info	Observer Location	Event Description	Observed duration
1	Debris 6	EOC2-4-0026 Sparks, NV	13:54:38	23:05:35.16	Venus in FOV during events	Lat: 39.5409 Lon: -119.7682 Alt: 4444 ft	Flash, plasma brightening, bright debris	6 sec
	Debris 6	EOC2-4-0009B, Springville, CA	13:54:36	19:50:35.17	Plasma trail brightening visible during event	Lat: 36.2264 Lon: -118.8052 Alt: 2230 ft	Flash, plasma brightening, bright debris	12.2 sec
	Debris 6	EOC2-4-0030, Las Vegas	*13:54:38*	01:11:06.28	Plasma trail brightening visible during event	Lat: 36.3099 Lon: -115.2744 Alt: 2513 ft	plasma brightening, bright debris	2.4 sec
2	Debris 14	EOC2-4-0017, N. of Flagstaff	13:55:56.4	01:05:40.23	*Observer reports ~80% zoom*	Lat: 35.5745 Lon: -111.5294 Alt: 5600 ft	very bright debris, subsequent breakoff of secondary debris from primary debris	5.4 sec
	Debris 14	EOC2-4-0005, Ivins, UT	13:55:58.1	20:04:07.11	Observer reports max zoom	Lat: 37.1681 Lon: -113.6575 Alt: 3080 ft	Very bright debris	4 sec
	Debris 14	EOC2-4-0028, St. George, UT	13:55:57.7	04:34:03.26		Lat: 37.1048 Lon: -113.5721 Alt: 2713 ft		3.6 sec
	Debris 14	EOC2-4-0030, Las Vegas	13:55:58.0	01:12:28.20	*zoomed in and out since debris 9 observation*	Lat: 36.3099 Lon: -115.2744 Alt: 2513 ft		1.1 sec
3	Debris 1	EOC2-4-0056, Lick Observatory	13:53:46	07:57:13.03	Observer reports max zoom	Lat: 37.3416 Lon: -121.6430 Alt: 4232 ft	Westernmost debris to date	2.5+ sec
	Debris 1	EOC2-4-0064, Fairfield, CA	13:53:46	00:50:59.17	Vega in view later in video	Lat: 38.2804 Lon: -122.0065 Alt: 69 ft	NOTE: Appears to have occasional missing frames.	0.8+ sec
4	Debris 16	EOC2-4-0148-2, Kirtland AFB	13:57:24	23:11:54.24	5 deg FOV	Lat: 34.9646 Lon: -106.4636 Alt: 6155 ft	Easternmost early debris event, very faint	0.9 sec
5	Debris 2	EOC2-4-0056, Lick Observatory	13:53:48	07:57:14.26	Observer reports max zoom	Lat: 37.3416 Lon: -121.6430 Alt: 4232 ft		2.8 sec
	Debris 2	EOC2-4-0064, Fairfield, CA	13:53:48	00:51:01.12	Vega in view later in video	Lat: 38.2804 Lon: -122.0065 Alt: 69 ft	NOTE: Appears to have occasional missing frames.	0.8+ sec
6	Debris 3	EOC2-4-0026 Sparks, NV	13:53:58	23:04:55.08	celestial object in FOV shortly after event	Lat: 39.5409 Lon: -119.7682 Alt: 4444 ft	Debris possibly reacquired at 13:54:03 after zoom-out	2.7 sec
	Debris 3	EOC2-4-0056, Lick Observatory	13:53:56	07:57:23.04	Observer reports max zoom	Lat: 37.3416 Lon: -121.6430 Alt: 4232 ft		2.9 sec
7	Debris 4	EOC2-4-0056, Lick Observatory	13:54:03	07:57:30.17	Observer reports max zoom	Lat: 37.3416 Lon: -121.6430 Alt: 4232 ft		1.4 sec
8	Debris 13	EOC2-4-0005, Ivins, UT	13:55:56.1	20:04:05.12	same FOV as debris 14	Lat: 37.1681 Lon: -113.6575 Alt: 3080 ft	Debris 13 breaks up at the end	0.8 sec
	Debris 13	EOC2-4-0017, N. of Flagstaff	13:55:55.6	01:05:39.29	same FOV as debris 14	Lat: 35.5745 Lon: -111.5294 Alt: 5600 ft		0.7 sec
	Debris 13	EOC2-4-0021	13:55:56.2	03:06:43.27		Lat: 37.0952 Lon: -113.5561 Alt:		0.6 sec
9	Debris 8 (9?)	EOC2-4-0030, Las Vegas	13:55:22.0	01:11:52.20	zoom in and out since debris 6 & 7, observer reports max optical zoom	Lat: 36.3099 Lon: -115.2744 Alt: 2513 ft		3.7 sec
	Debris 9	EOC2-4-0005	13:55:26.2	20:03:40.00	observer reports max zoom, pre-event plasma trail brightening. Possibly same FOV as debris 14.	Lat: 37.1681 Lon: -113.6575 Alt: 3080 ft	Overtaken by debris 10 later	5.0 sec
	Debris 9	EOC2-4-0098 Santa Clara, UT	13:55:27.6	17:35:48.04		Lat: 37.1327 Lon: -113.6470 Alt: 2846 ft		2.4 sec
10	Debris 10	EOC2-4-0005	13:55:26.8	20:03:40.18	observer reports max zoom, pre-event plasma trail brightening. Possibly same FOV as debris 14.	Lat: 37.1681 Lon: -113.6575 Alt: 3080 ft	Overtakes debris 9	3.2 sec

Table 3-1: Video Hot List [17]

Priority	Event	Tape #	Time Debris First Observed Aft of Vehicle GMT	Tape Time (TCR)	FOV info	Observer Location	Event Description	Observed duration
11	Debris 11C	EOC2-4-0098 Santa Clara, UT	13:55:44.4	17:36:04.27	probably same FOV as debris 9	Lat: 37.1327 Lon: -113.6470 Alt: 2846 ft	Measure head of secondary plasma trail, since debris view is intermittent	4.6 sec
	Debris 11C	EOC2-4-0028, St. George, UT	13:55:45.2	04:33:51.10	same FOV as debris 14	Lat: 37.1048 Lon: -113.5721 Alt: 2713 ft	debris not visible, measure head of secondary plasma trail	
	Debris 11C	EOC2-4-0050, St. George, UT	13:55:45.5	07:33:18.27		Lat: 37.2195 Lon: -113.6218 Alt: 3940 ft	debris not visible, measure head of secondary plasma trail	
12	Debris 7	EOC2-4-0030, Las Vegas	13:55:04.9	01:11:35.19	same FOV as debris 6	Lat: 36.3099 Lon: -115.2744 Alt: 2513 ft	Debris 7 splits midway through pass	2.3 sec
13	Debris 5	EOC2-4-0026 Sparks, NV	13:54:09	23:05:06.24	Antares and Venus in FOV after event, prior to change in zoom setting	Lat: 39.5409 Lon: -119.7682 Alt: 4444 ft		1.3 sec
14	Debris 12	EOC2-4-0028, St. George, UT	13:55:45.3	04:33:51.13	same apparent FOV as in debris 14	Lat: 37.1048 Lon: -113.5721 Alt: 2713 ft		1.5 sec
	Debris 12	EOC2-4-0098 Santa Clara, UT	13:55:45.4	17:36:05.28	probably same FOV as debris 9	Lat: 37.1327 Lon: -113.6470 Alt: 2846 ft		1.4 sec
	Debris 12	EOC2-4-0050, St. George, UT	13:55:46.0	07:33:19.12	same FOV as debris 11C	Lat: 37.2195 Lon: -113.6218 Alt: 3940 ft		0.5+ sec
15	Debris 15	EOC2-4-0017, N. of Flagstaff	13:56:10.1	01:05:54.15	zoom change between debris 14 and debris 15	Lat: 35.5745 Lon: -111.5294 Alt: 5600 ft	Easternmost debris of continuous western U.S. coverage	2.2 sec
16	Debris 11	EOC2-4-0050, St. George, UT	13:55:37.2	07:33:10.20		Lat: 37.2195 Lon: -113.6218 Alt: 3940 ft		
	Debris 11	EOC2-4-0098	13:55:37.2	17:35:57.21	probably same FOV as debris 9	Lat: 37.1327 Lon: -113.6470 Alt: 2846 ft		0.9 sec
17	Debris 7A	EOC2-4-0161	13:55:18.1	23:57:24.08	zooming during 1st 0.2 sec	Lat: 37.4875 Lon: -113.2250 Alt:		0.9+ sec
18	Debris 11B	EOC2-4-0098 Santa Clara, UT	13:55:40.1	17:36:00.17		Lat: 37.1327 Lon: -113.6470 Alt: 2846 ft		0.5 sec
19	Debris 11A	EOC2-4-0098 Santa Clara, UT	13:55:39.3	17:35:59.24		Lat: 37.1327 Lon: -113.6470 Alt: 2846 ft		

Table 3-1: Video Hot List, continued [17]

3.2. Process for handling videos

There were many organizations involved in receiving, distributing, processing, and evaluating imagery, and still more who were users of any usable data from the images. As already described, this imagery followed several routes getting to JSC, some of which were to individual's personal e-mail accounts or through regular mail. As the report priorities and Hot List were developed, the volume of reports flowing in made it apparent we also needed a standard procedure for each piece of the process to efficiently route the video to facilitate immediate analysis, as well as to ensure no images went overlooked. This procedure follows:

Information Handling/Processing

General: Always include EOC tracking number(s) if available in any correspondence.

Telephone Calls

1. EOC takes call, records pertinent information onto Information Sheet, assigns EOC tracking number, enters info into data base
2. For debris on the ground, EOC forwards Information Sheet to the MER and faxes to Barksdale, Lufkin, and FEMA regions.
3. For sightings, EOC forwards two copies of Information Sheet to Early Sighting Assessment Team (ESAT).
4. For human remains, EOC immediately faxes Information Sheet to FBI Lufkin with follow-up phone call. Then EOC faxes to B.L. FEMA regions.

E-mail (Columbiaimages.nasa.gov)

1. Electronic media should be e-mailed to Columbiaimages.nasa.gov
2. If e-mail is received in personal e-mail account that did not come from Columbiaimages.nasa.gov, forward to that address. Include EOC tracking number or cross-references, if available.
3. EOC Information Systems Directorate (ISD) personnel screen e-mail in the Columbiaimages.nasa.gov account, move to appropriate folder, and assign an EOC tracking number.
4. For electronic images, Bldg 8 (e.g., Maura White) scans the e-mail folders and posts images to website, includes information in body of e-mail in caption. (Currently don't have EOC number on the Bldg 8 website - in work by Pat Chimes, Maura White, etc.)
5. ISD EOC rep will be in EOC to follow-up with individuals who have e-mailed that they have video or images but have not yet sent them in. The ISD EOC rep will ask the individual to reference the EOC tracking number on the information they supply.

Hard Copy (tapes, cards, CDs, etc.)

EOC Operations

1. Hard copy material should be mailed (preferably FED EX or similar carrier which tracks items) to Columbia MIT/JA17, 2101 NASA Rd 1, Houston, TX 77058
   - For sightings, include "Attention: Paul Hill" on outside of envelope and EOC tracking number inside envelope.
2. When the EOC receives mail, the EOC screens out sympathy cards, condolences, etc.
3. EOC rep completes an Information Sheet for each hard copy media and assign a 2-4-xxxx EOC tracking number.
4. The EOC rep contacts the ESAT (x34013) for media that contains video or images, and notifies them they have material to be picked up. The material will be labeled with the 2-4-xxxx EOC tracking number and will be accompanied by three copies of the Information Sheet (one copy inside the envelope with the media for Building 8 and two copies for the ESAT).
5. The ESAT rep signs for each piece of media removed from the EOC.

ESAT Transfer Operations

6. The ESAT rep logs the tracking numbers of received media onto a blank Transfer Log, compares the received media to the "Hot List," and annotates any "Hot items" on the Transfer Log with an asterisk. The ESAT rep also writes a brief summary of each item to expedite screening media in building 8 (EOC number, Name of sender, City and State, type of media, and brief description, e.g., video with clock sync).
7. The ESAT rep carries the received media with the blank Transfer Log and summary sheet to the Building 8 Help Desk and informs the Help Desk that they have media to be transferred.
8. The Help Desk calls the Building 8 point of contact (different people for video versus still images - generally, Jason Fennelly for videos, Cara Johnston/Maura White for still images). The POC then meets the ESAT rep at the front desk.
9. For videos:
   a. The Building 8 video POC plays each video for the ESAT rep to confirm "Hot items." "Hot Items" are marked with an asterisk on the Transfer Log.
   b. If required, the ESAT rep will update the Information Sheet describing the video/images and the summary sheet.
   c. For video of human remains, contact CB/Andy Thomas for further directions (i.e., do not follow process below).
   d. The Building 8 Video POC signs for each piece of media on the Transfer Log and photo copies the Transfer Log (so they know which are "Hot Items").
   e. The Building 8 video POC copies the video and retains the original media, following their standard process for logging and archiving the information.
      (1) For sightings, one high quality (D2) copy for the Imagery personnel and two VHS copies for the ESAT rep are made. Note: the ESAT copies will contain multiple "cuts" so they will not be provided immediately - expect to return for pickup at a later time.
      (2) For debris on the ground, one VHS copy is made for the MER.

f. The Building 8 Video POC will distribute their log of EOC received items on a daily basis via e-mail including DL ESAT on the distribution list.

10. For still images:
    a. The Building 8 Still Images POC signs for each piece of media on the Transfer Log.
    b. The Building 8 Still Images POC retains the original media, following their standard process for logging and archiving the information.
    c. For CD's, the Building 8 POC provides one copy to the ESAT rep.
        (1) For sightings, copy is for the ESAT.
        (2) For debris on the ground, the ESAT rep delivers the copy to the MER Manager.
    d. The Building 8 Still Images POC posts the images on the Imagery web site.

ESAT Follow-up Operations

11. The ESAT rep updates the "Hot List" indicating which media are being processed by Building 8.
12. The ESAT rep attempts to cross-reference any applicable EOC tracking numbers from phone calls or e-mails and notes these EOC tracking numbers on the Information Sheet that was provided by the EOC with the hard copy media. A copy of this updated Information Sheet will be returned to the EOC to update the database.
13. The ESAT rep notifies the Imagery, FDO, and MMACS personnel when "Hot Items" are being processed by Building 8.
14. When VHS or CD copies are received, the ESAT rep notifies FDO and MMACS personnel that a quick-look copy is available. Any media removed from the CSR must be logged out on the posted Hard Copy Media Sign-Out Sheet.

3.3. Debris Sighting Report Evaluation Lessons Learned

1) The public report form should be standardized and ready for use in any future incident to maintain uniformity of collected information. This form should include key interview questions, detailed locations, contact information, and zip codes.

2) All phone interviews (and any public reports) should be entered directly into an electronic form as the interview takes place to facilitate immediate accessibility by all investigation teams. These should include fields to distinguish reports of human remains, debris, and visual sightings. Additionally, the database should have a search function for the various types of input fields.

3) Eyewitness reports should be treated as a 'case file,' rather than as separate reports. This would allow the team to add to an existing report and note when video or other media was received without logging repeated calls from the same witness as separate reports.

4) A single point of contact should be used for responding to EOC reports whenever possible due to sensitivity among some of the public to being contacted repeatedly for the same EOC report.

5) Various products referencing EOC reports should be built using the EOC reference number not the public caller's name.

6) Record exact location, weight, dimensions, and a digital still of all debris as it is recovered and input it into a single database daily. This would allow the use of some back-propagation techniques to better define the debris field, identify debris separation times, and confirm validity of objects as debris. Additionally, it should be noted how the location was determined (GPS coordinates, map location, street address, etc.)

4. Debris Trajectory Analysis

4.1. Debris Sighting Timeline

Unless otherwise footnoted, Section 4.1 is referenced to [22], Spencer, J.R.; JSC-DM; STS-107 Early Entry Debris Sighting Timeline; May 2003. This is included in its entirety in Appendix 10.4.

4.1.1. Debris Sighting Timeline Summary and Methodology

The Early Sighting Assessment Team worked in conjunction with the Photo/TV Analysis Team to screen over 140 public videos of the STS-107 entry. Of these, 19 videos show a total of twenty debris shedding events and three flares, or flashes, as the vehicle flew from California to New Mexico. Videos had poor timing information, so synching the videos to true GMT had to be done by timing any celestial observations and comparing times across videos for common debris/flash event observations. One video had set internal GMT, which was verified as correct. Another video was time synched by the observer's reported calibration to true GMT from WWV (a National Institute of Standards and Technology radio station which broadcasts time and frequency information).

The blue dots in Figures 4-1 and 4-2 represent videographer locations and the blue lines represent video coverage of the Shuttle filmed by that videographer. Although there is overlapping video coverage from just off the California coast to Eastern New Mexico, all of the videos contain short periods when the Shuttle is out of the camera field of view (FOV), out of focus, or obscured by clouds. Therefore, additional off-nominal events may have occurred during this timeframe which were not observed.

There was a lack of good quality video coverage from Eastern New Mexico to the Dallas/Fort Worth Area. The only available video in this region was recorded from Lubbock looking east, and briefly shows the orbiter possibly at the start of the breakup sequence just prior to disappearing over the horizon. Videos from the Dallas/Fort Worth area were not reviewed by the Early Sighting Assessment Team, but were screened by the Photo/TV Analysis Team alone.

Times listed in these figures indicate when the debris was first observed aft of the vehicle and is not the time the debris was shed from the vehicle. These are listed in tabular form with more detail in Appendix 10.2: Entry Debris Events Timeline, Version 6 - 05/27/03.

Twenty distinct debris shedding events and three Shuttle plasma envelope flashes or flares were filmed as the Shuttle flew from California to Eastern New Mexico during STS-107. Many of these events were seen in multiple videos, in one case as many as seven videos recorded the same event.

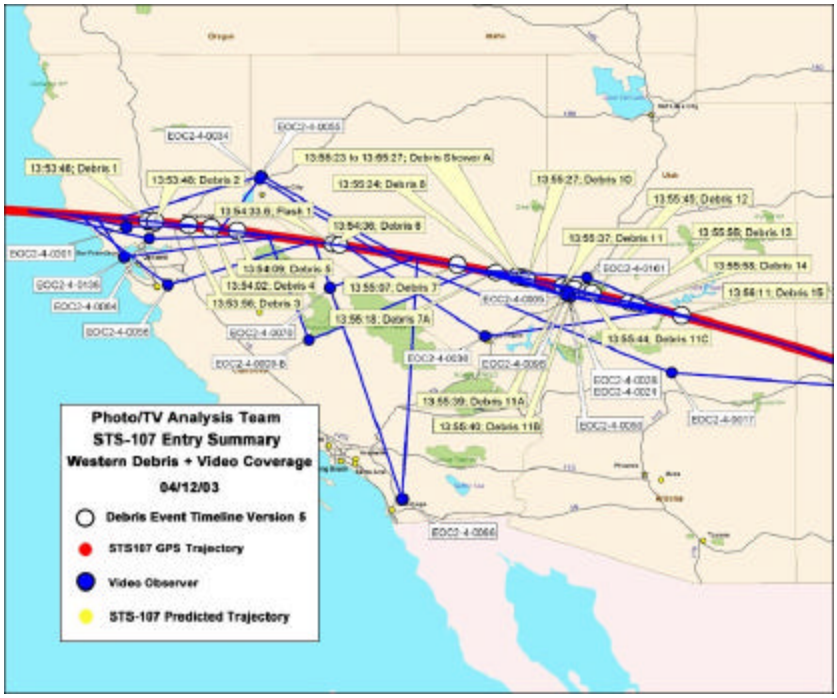

Figure 4-1: Public Video Coverage of the Western United States STS-107 Entry Trajectory [21]

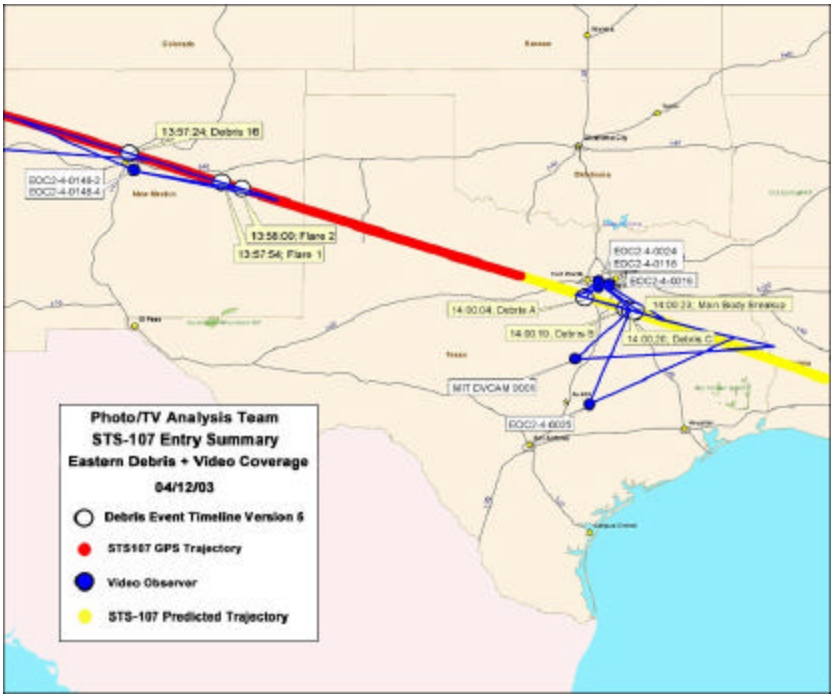

Figure 4-2: Public Video Coverage of the Central United States STS-107 Entry Trajectory [21]

Figure 4-3: STS-107 Early Debris Shedding Events [21]

STS-107 videos were screened for off-nominal events. Observed off-nominal events include debris shedding, bright segments of the plasma trail, flares and flashes in the Shuttle plasma envelope, forks in the plasma trail emanating from the Shuttle plasma envelope, and parallel plasma trails. Entry videos from previous flights were also screened to characterize nominal events such as RCS firings. In none of the previous entry videos were any of the anomalous events described above seen. Examples are shown in Figure 4-4.

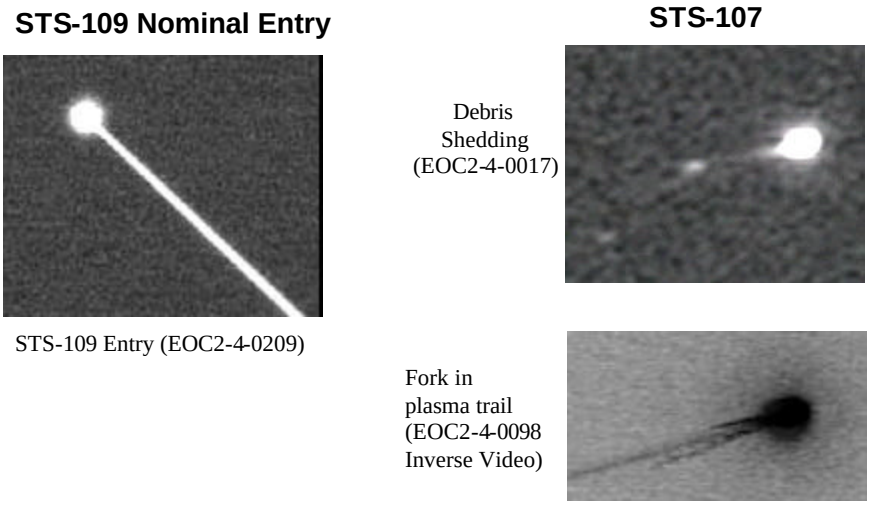

Figure 4-4: Example of Nominal Entry vs. STS-107 Entry

In no video was the Shuttle structure directly discernible. In nearly all the videos, it was displayed as a saturated bright plasma disc. In the Kirtland AFB telescope videos, the plasma

envelop of the orbiter has a shape similar to the orbiter but actual orbiter structure is most likely not seen.

Videos varied greatly in quality, and were initially screened to determine whether they contained footage of the STS-107 entry and if so, for evidence of off-nominal events. Skywatch was used to determine what portion of the STS-107 trajectory, if any, each viewer could have possibly seen. (Skywatch is a JAVA-based celestial acquisitions program developed by the NASA/JSC Flight Design and Dynamics Division.)

In order to use Skywatch, the observer's position and the Shuttle's trajectory had to be known. The as-flown STS-107 GPS trajectory was the source of Shuttle position data. In a few cases, observer-provided GPS coordinates were utilized in Skywatch, but in most cases, this data had to be determined from the viewer's location description, or from video landmarks. Commercially available mapping programs TOPO USA and MapQuest were used to determine/verify latitude, longitude, and altitude locations. Once the observer's location was known, Skywatch was used to determine the viewing arc and maximum elevation angle for the STS-107 flyover.

Nearly all of the videotapes had missing or inaccurate time information. One of the biggest challenges was to accurately time synchronize each videotape. The first step in this process was done by using Skywatch to determine the time of maximum elevation from each viewer's perspective. This time was then applied to the video at the point that depicted the apparent max elevation, assuming that the camera was level. Since the camera was nearly always handheld, this assumption was known to be subject to some error, therefore the accuracy of this initial time sync was only valid to a few seconds.

Refined time synchronization was then done based on celestial references, observer WWV time sync, asset internal GMT, camcorder clock drift measurement, and event correlation across tapes. (WWV is a radio station that broadcasts time, including UT1 corrections, 24 hours a day, 7 days a week.)

Figure 4-5 is a summary of the multiple videos linked to provide times for the entire debris timeline. Some of these debris events were seen in videos not shown above. In those cases, the videos were not useful in providing timing information for the debris event but may be useful for further analysis of the event.

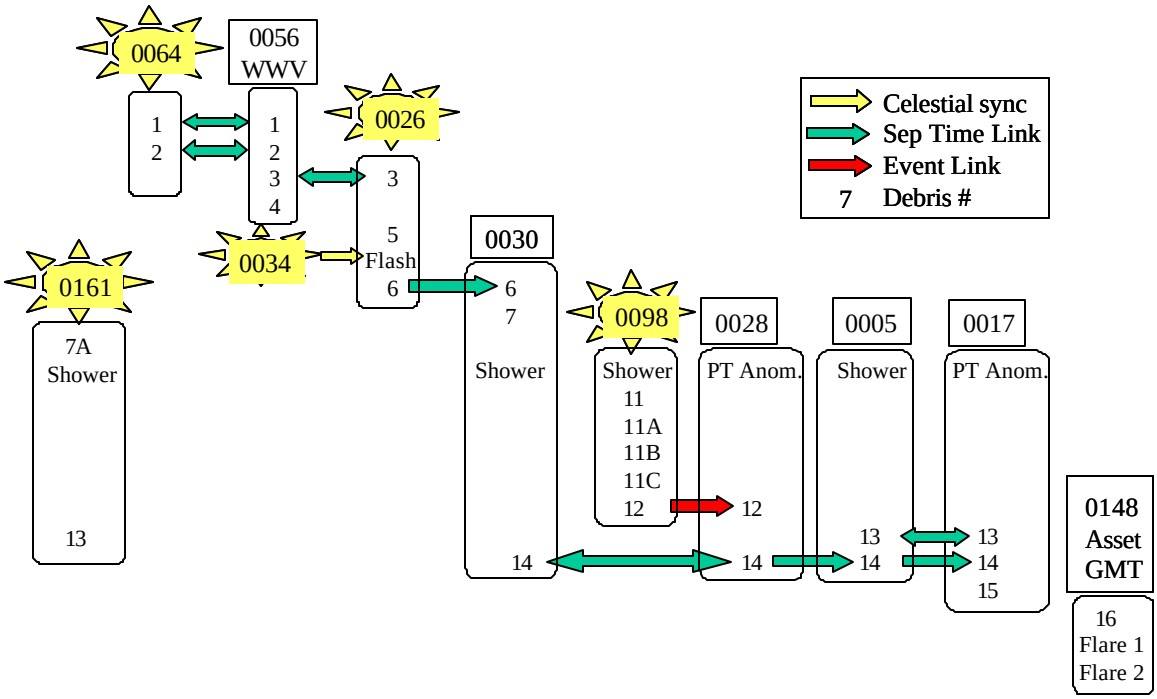

Figure 4-5: STS-107 Early Debris Shedding Events

Synchronizing the videos based on the time of closest approach (TCA) of the Shuttle passage near a celestial body is the most accurate method of time synchronization. Skywatch was used to identify candidate celestial objects seen in the videos based on proximity to the Shuttle's trajectory from the viewer's perspective and a rough TCA (within a few seconds). Positive identification of candidate celestial objects was done by selecting the highest magnitude object in the correct proximity to the Shuttle within the expected time range. Personnel from the NASA/JSC Shuttle Flight Planning and Pointing Group then provided the TCA of the Shuttle with respect to that celestial body from their Supersighter program. (Supersighter is a celestial acquisitions program certified for operational use in the Mission Control Center.)

These TCA's were accurate to 0.1 seconds. One video, EOC2-4-0161, had footage of Venus and the Shuttle but Venus was not in the field of view during TCA, due to zoom in. Several images before and after Venus TCA were used to generate a curve fit of the Shuttle passage near Venus. The image frame that would have depicted the TCA of the Shuttle to Venus on this videotape was then calculated from the curve fit and synced to the actual TCA from this viewer's perspective.

Tape Reference	Observer Location	Celestial Reference
EOC2-4-0026/0055	Sparks, NV	Venus eclipse (Antares, Gienah also seen)
EOC2-4-0034	Reno, NV	Venus TCA
EOC2-4-0064	Fairfield, CA	Vega TCA
EOC2-4-0136	Mill Valley, CA	Vega TCA
EOC2-4-0098	Santa Clara, UT	Tania Australis TCA
EOC2-4-0161	Kolob Arch, UT	Venus TCA curve fit (Venus not in FOV at TCA)

Table 4-1: Public Video Tapes of Columbia with Celestial References

Even though only a small percentage of the videos that saw debris were able to be celestially referenced, these few videos did have observations of over 70% of the off-nominal events. These videos served as the starting point for the time sequencing of all the videos depicting the STS-107 entry between California and Arizona and eventually time synching debris 1 through 15.

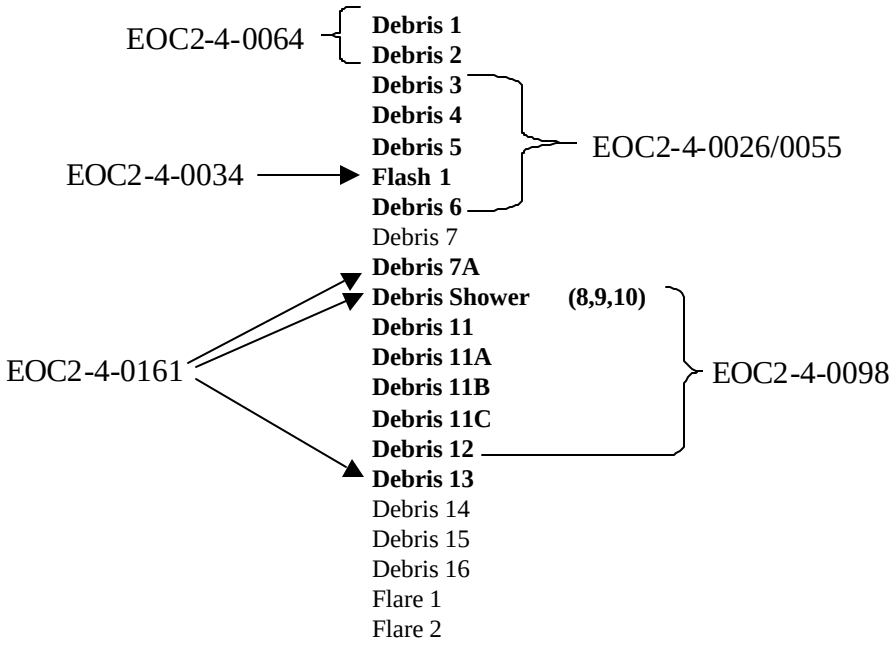

Figure 4-6: Debris Events Observed on Public Video Tapes with Celestial References

EOC2-4-0026/0055 was the most accurate celestial sync of all the videos because it actually captured the Shuttle eclipsing Venus, instead of just a close approach. Also the observer's location was well known since the observer provided his GPS coordinates. Altitude of the observer's location was then determined by referencing his latitude and longitude in TopoUSA. From Supersighter, NASA/JSC personnel determined the time of Venus eclipse to be 13:54:38.3 GMT. The margin of error for this time sync was less than 0.1 seconds. Two additional celestial references were available in this video, the stars Antares and Gienah, but were not needed due to the more accurate Shuttle eclipse of Venus. (This video has two EOC numbers: EOC2-4-0026

is a VHS copy but was the original video reviewed. EOC2-4-0055 is reported to be the original but is not an improvement in quality.)

Figure 4-7: Shuttle Eclipse of Venus as Seen in EOC2-4-0026/0055 from Sparks, Nevada

Some videos without celestial syncs were able to be time synchronized very accurately due to event correlation with videos with celestial syncs. Flash 1 and the Debris 12 brightening well aft of Shuttle are considered such marker events. These had duration of 0.1 sec or less and were seen on multiple videos, including some with celestial syncs.

Other videos without accurate time syncs were synchronized based on matching debris separation times with those of celestially synced videos. Also, in some cases, multiple videos with accurate time syncs contained footage of the same debris object. When possible, separation times for these events were compared between the videos and showed agreement within 0.2 seconds. All separation times were computed by the relative motion team by calculating the ballistic number of the debris and propagating its relative motion back to an origin at the Shuttle.

Debris Event	**Tape of Debris Event with Celestial Reference**	**Tape with Same Debris Event, Time Synchronized/Correlated to Tape with Celestial Reference**
Debris 1	EOC2-4-0064	EOC2-4-0056
Debris 2	EOC2-4-0064	EOC2-4-0056
Debris 3	EOC2-4-0026/0055	EOC2-4-0056
Debris 6	EOC2-4-0026/0055	EOC2-4-0030
Debris 14		EOC2-4-0005, EOC2-4-0017, EOC2-4-0028, EOC2-4-0030

Table 4-2: Public Video Tapes which Were Time Synchronized via Overlapping Coverage

Debris 14 was not depicted on a video that had a celestial time sync, but an accurate time sync was able to be performed for one of the tapes which depicted debris 14 via the debris 12 brightening event.

4.1.2. Detailed Time Sequencing

EOC2-4-0056 provided a link between the celestially synced EOC2-4-0064 which had footage of debris 1 and 2 and the celestially synced EOC2-4-0026/0055 which had footage of debris 3-6 plus the flash. The videographer of EOC2-4-0056 reported a WWV sync of his tape. A coarse verification of this was done by the NASA/JSC Flight Design and Dynamics Division using Skywatch. Even though EOC2-4-0056 did not depict any celestial objects, the observer took a time-elapsed still photo simultaneous with his video which did depict several celestial objects. This is due to the greater light gathering capability of a still camera with the shutter held open versus a camcorder. The Aerospace Corporation was able to time sync the video based on changes in the plasma trail in the time-elapsed still photo to within 0.25 seconds of the observer's reported WWV sync.

The relative motion team calculated the separation times for debris 1 and 2 using EOC2-4-0064 and EOC2-4-0056. The separation times for these debris agreed between the 2 videos to within 0.2 seconds. Similar analysis was done for debris 3 using videos EOC2-4-0056 and EOC2-4-0026. Debris 3 separation times agreed within 0.1 seconds. Therefore EOC2-4-0056 showed good agreement with both EOC2-4-0064 and EOC2-4-0026, providing an overlapping link between those two celestially synced videotapes.

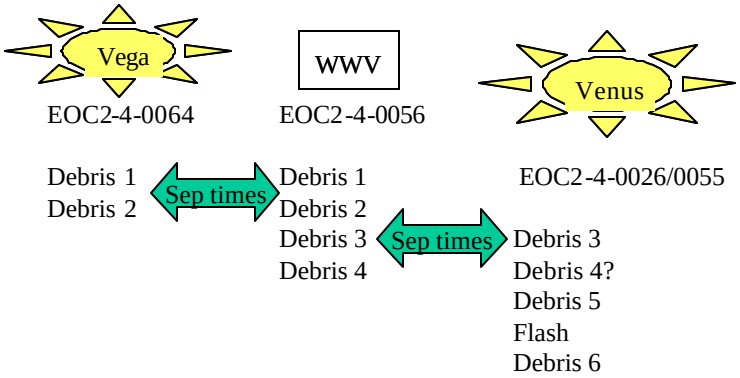

Figure 4-8: Overlapping Debris Observations with EOC2-4-0064 and EOC2-4-0026/0055

The Flash was observed on five videotapes. Four of these observed a brief brightening of the plasma trail, followed by debris 6 emerging from the Shuttle plasma envelope shortly after the flash. EOC2-4-0034 was too noisy to observe any debris (i.e., the brightness of random static, or noise, was the same or greater magnitude as that expected for the debris). Also, it was determined from the STS-107 RCS firing history that aft RCS jets R2R and R3R fired for a total of 0.26 seconds at the same time as the flash was observed. This duration matches the duration of the flash to within 0.04 seconds. However, based on analysis of previous nominal entry overflights, RCS firings do not result in a flash of the Shuttle plasma envelope or a brightening of the plasma trail. It is impossible to determine if the RCS firings contributed to the cause, or are an effect of this event. Therefore, it is concluded that the flash is an off-nominal event which may or may not be related to the RCS jet firing. The previous RCS firing occurred at GMT 13:51:45, which was prior to any video coverage of the STS-107 entry. Later RCS firings, at

13:56:17 and 13:56:53, did occur during video coverage but no unusual signature was seen. However, any flashing may have been difficult to detect since it was daylight by then and all events were more difficult to discern.

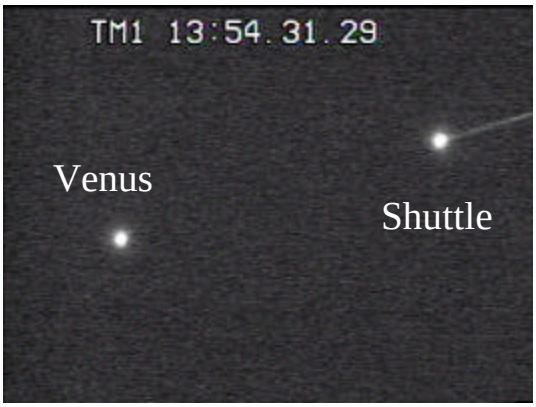

Shuttle at nominal brightness

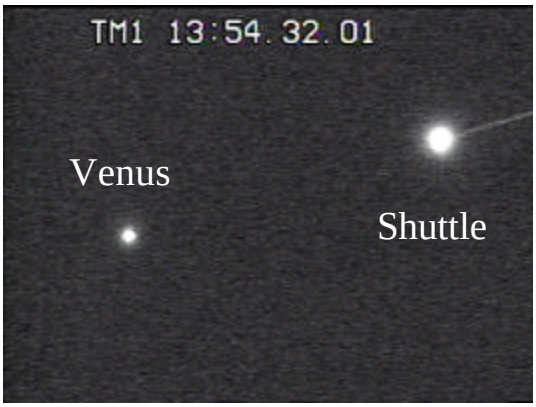

Shuttle at peak brightness

Figure 4-9: Flash 1 as Seen in EOC2-4-0026/0055

Two of the tapes showing the flash had celestial syncs (EOC2-4-0026/0055, EOC2-4-0034). The peak brightening of the flash lasted for only 0.1 seconds and occurred at GMT 13:54:33.6 in both EOC2-4-0026/0055 and EOC2-4-0034, which were celestially synced. EOC2-4-0009B, EOC2-4-0066, and EOC2-4-0070 were then time synced based on the above peak flash time.

Debris 6 was visible for 12 seconds in EOC2-4-0009B, which was the longest duration that any debris was seen in any video.

Note that even though four of the videos observed debris 6, the difference between the time of first observance of debris 6 emerging from the Shuttle plasma envelop varied by as much as 2.2 seconds. This can be explained by differences in field-of-view, viewer look angle to the Shuttle, and camera capability. In each of these cases, the debris may have had to travel a different distance away from the Shuttle before it could be distinguished as a separate object.

The relative motion team determined that debris 6 was shed immediately after the flash.

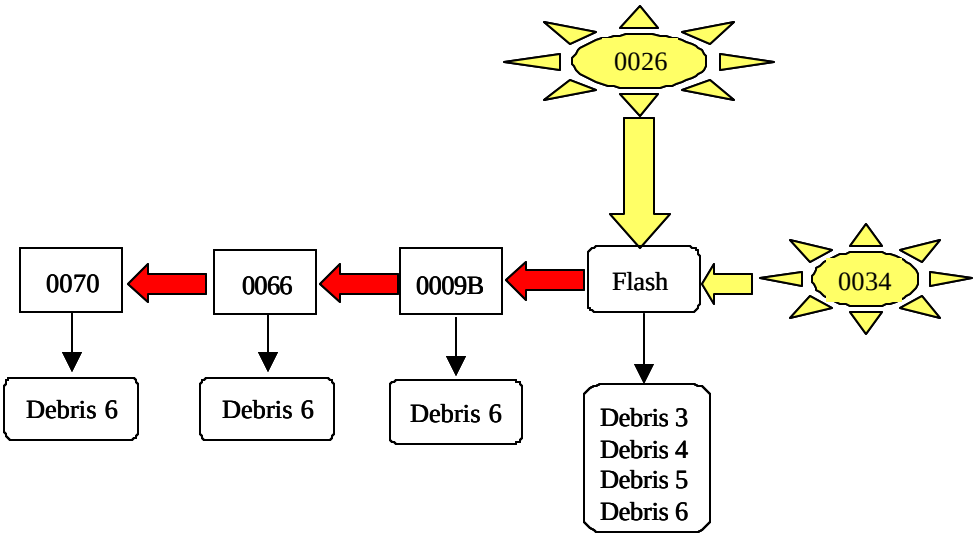

Figure 4-10: Overlapping Observations of Flash 1 and Debris 6

Debris 12 brightened significantly for 1/30th of a second (one frame) in three videotapes (EOC2-4-0028, 0050, 0098), as it was well aft of the Shuttle plasma envelope. EOC2-4-0098 was celestially synced based on a visible TCA with the star Tania Australis; therefore, the time of this brightening event was known to be GMT 13:55:46.5. EOC2-4-0028 and EOC2-4-0050 were then time synchronized to this time for the debris 12 brightening. EOC2-4-0028 contained footage of debris 14, an event that was not on a celestially synced video, thereby providing an accurate time source for this debris event.

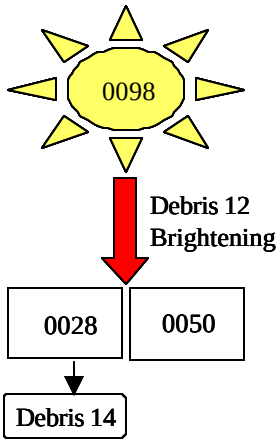

Figure 4-11: Debris 12 Brightening and Time Synchronization of Debris 14

Only one video, EOC2-4-0030, provided overlap between the California/Reno area observations and the Utah/Arizona observations of the STS-107 entry. EOC2-4-0030 starts with observations of debris 6 as the observer reported turning on his video camera shortly after seeing the Shuttle flash and ends with debris 14. No valid time sync information was reported by the observer, so the video was initially time synced to the apparent maximum elevation with the time from Skywatch. This time sync proved that the initial debris depicted on the tape was debris 6 and

the final debris on the tape was debris 14. Since the separation time for debris 6 was known based on relative motion analysis of EOC2-4-0026, the time sync for EOC2-4-0030 was updated to match the debris 6 separation time. The separation time for debris 14 was also known due to relative motion analysis of EOC2-4-0028 (which was linked to celestially synced EOC2-4-0098 through the debris 12 brightening). The separation time for debris 14 in EOC2-4-0030 matched the separation time of debris 14 in EOC2-4-0028 to within 0.1 seconds, therefore linking the Venus eclipse time sync of EOC2-4-0026/0055 to the Tania Australis TCA time sync of EOC2-4-0098.

EOC2-4-0030 was the only videotape that showed footage of debris 7. By linking this tape to EOC2-4-0026 and indirectly to EOC2-4-0098, the time of this debris event was now known.

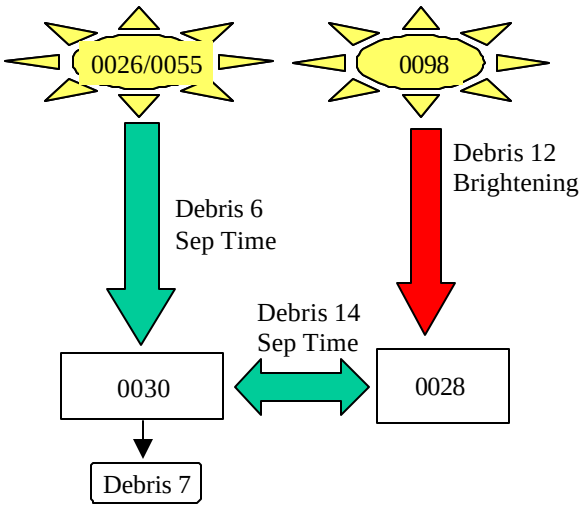

Figure 4-12: EOC2-4-0030 LinksSecond Two Celestially Referenced Segments

Five videos show debris 14: EOC2-4-0005, EOC2-4-0017, EOC2-4-0021, EOC2-4-0028, and EOC2-4-0030. EOC2-4-0028 and EOC2-4-0030 have accurate time syncs based on the debris 12 brightening and debris 6 separation times, respectively. Based on relative motion analysis of EOC2-4-0028 and EOC2-4-0030, the debris 14 separation time is 13:55:56.7. This time was then used to update the time syncs of EOC2-4-0005 (second half) and EOC2-4-0017. EOC2-4-0005 has a break in the continuous footage in the middle of its track of the STS-107 entry, so only the footage after the break in coverage could be updated with this timing information. Relative motion analysis of EOC2-4-0021 debris 14 could not be done due to changes in zoom during the event. The time syncs for EOC2-4-0017 and EOC2-4-0005 (second half) were confirmed with agreement of debris 13 separation times within 0.1 seconds.

EOC2-4-0017 was originally time synced based on measuring camcorder clock drift at 7 days and 14 days after the STS-107 entry to correct the camcorder clock time imbedded in the video. Camcorder clock drift relative to true GMT was assumed to be linear over this time period but based on different battery uses between the two measurements, may not be. Time syncing EOC2-4-0017 based on the more accurate debris 14 separation time resulted in a 1.2 second shift earlier. Based on engineering judgment, this seemed to be a reasonable refinement of the time sync given the known rough assumptions of the camcorder clock drift.

EOC2-4-0017 was the only videotape which contained footage of debris 15, so the time for this event was now known.

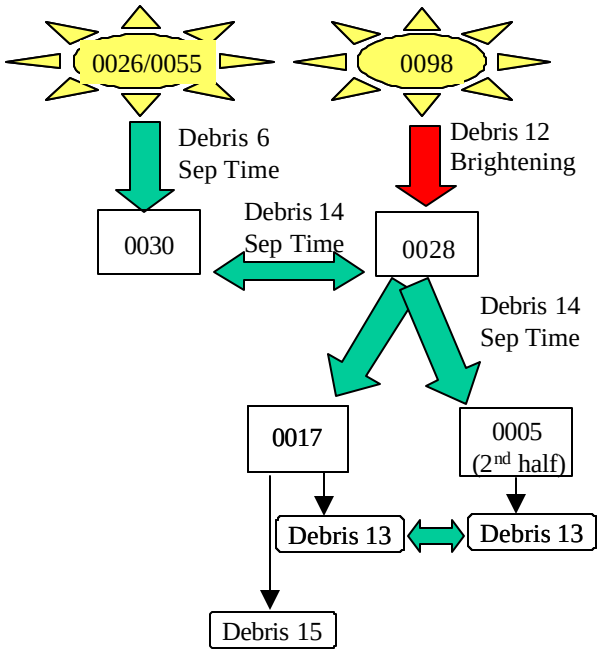

Figure 4-13: Additional Videos Time Synchronized to Establish Debris 15 Separation Time

A debris shower and/or a plasma trail anomaly is visible in seven videos at approximately GMT 13:55:22: EOC2-4-0005, EOC2-4-0017, EOC2-4-0021, EOC2-4-0028, EOC2-4-0030, EOC2-4-0098, and EOC2-4-0161. In the poorer quality videos of this event, only a brief brightening of the plasma trail is seen - approximately 0.5 seconds duration. However, four of the videos - EOC2-4-0005, 0030, 0098 and 0161 - show distinct debris trailing the orbiter from immediately prior to the plasma trail anomaly to 5 seconds after the event. Many pieces are seen briefly flickering aft of the vehicle in and out of the plasma trail on these videos at this time with only two pieces distinctly trackable for more than 0.25 seconds as they trail aft of the vehicle in any one video. EOC2-4-0030 only shows debris 8, at GMT 13:55:22.0, and the plasma trail anomaly. EOC2-4-0098 shows debris 8 at 13:55:24.1, has a zoom-out occur, and acquires another debris object at 13:55:27.2 well aft of the Shuttle plasma envelope with a parallel plasma trail emanating from the Shuttle plasma envelope. Due to the zoom-out, it is unknown whether the debris evident after zoom-out is debris 8 re-acquired, or is a new debris object, debris 9. EOC2-4-0005 clearly shows a shower of debris at GMT 13:55:26.2 with one piece, debris 9, trackable for 5 seconds before it fades from view. Also, the time sync of EOC2-4-0005 (first half) is not nearly as accurate as most of the other videos. This video was synced based on a possible common image of debris 9 as it trailed aft in EOC2-4-0098 and EOC2-4-0005. However, debris 9 did not have any marker events such as the brightening seen in debris 12. Therefore, EOC2-4-0005 could be off in its time sync.

EOC2-4-0161 shows several pieces of debris briefly before they fade from view, but does not show any in continuous track for greater than 0.25 second during this time. Therefore, it is

impossible to correlate any of these debris observations to any single debris shown in any of the other videos.

EOC2-4-0005 did show unique behavior between debris 9 and 10. Debris 10 is observed emerging from the Shuttle plasma envelope 0.6 seconds after debris 9. However, debris 10 quickly decelerates and is overtaken by debris 9. This is the only video evidence of any piece of debris overtaking another piece.

Videos from Kirtland AFB provided the only coverage over most of New Mexico. The observer was viewing the STS-107 entry through daylight by this time, so debris events were more difficult to detect. However, by using inverse video, debris 16 was discernible on EOC2-4-0148-2. This video had imbedded azimuth, elevation, and GMT, which were verified using Skywatch. EOC2-4-0148-4 was a more close-up view from the same telescope mount as EOC2-4-0148-2. This videotape showed two brightening events, or “flares,” of the Shuttle plasma envelope at 13:57:54.5 and 13:58:00.5. The Shuttle plasma envelop was at the edge of the field of view at this time, so it was not known whether debris was ejected during these flare events.

4.2. Relative Motion and Ballistics

Unless otherwise footnoted, Section 4.2 is referenced to [23], Abadie, M.; JSC-DM; STS-107 ESAT Final Report Relative Motion and Ballistics Analysis; May 20, 2003. This is included in its entirety in Appendix 10.5.

4.2.1. Relative Motion and Ballistics Summary and Methodology

Twenty debris objects were viewed in the "early sightings" videos sent to NASA by the general public as the Shuttle passed over the western United States during STS-107 entry. Eleven of the objects viewed in these videos have been fully analyzed for relative motion and ballistics. The objective of the analysis was to determine the ballistic coefficient and separation time of "early sightings" debris pieces from the video footage of each debris shedding event. With ballistic coefficients ranging from 0.1 psf to 4.0 psf, these estimates were then handed off to the JSC-DM Entry Analysis Group for footprint determination as described in Section 4.3.

This analysis was a team effort across JSC, including JSC-DM Flight Design and Dynamics Division, JSC-SX Image Science and Analysis Group, and JSC-EG Aeroscience and Flight Mechanics Division. JSC-SX provided imaging expertise along with scaling and relative motion estimates. JSC-EG provided help in reviewing the analysis methods and simulation tools. JSC-DM focused on the relative motion calculations, separation time estimates, and ballistics estimates. The NASA JSC organizations involved in this effort (DM, EG, and SX) worked cooperatively to obtain a final result, but in certain areas, multiple organizations performed the same tasks using different methods in order to further ensure accuracy.

To verify the results generated by the NASA JSC community, an independent assessment was performed by the Aerospace Corporation, who had previous experience with predicting debris ballistic coefficients from the video footage of the MIR re-entry. The Aerospace Corporation provided an independent assessment for Debris events 1, 2, 6, and 14. They were given access to the videos and any comments provided by the videographers, along with camera specifications or other information derived from tests with the actual cameras. All other information (scaling data, pixel data, etc) was derived independently.

JSC-SX and JSC-DM relative motion calculations agree in most instances. Due to differing assumptions in the calculations, cases where the observer is near the trajectory plane result in larger differences than those where the observer's line-of-sight is nearly perpendicular to the Shuttle trajectory. These differences are well understood and described in more detail later in this section. JSC-EG and JSC-DM show good agreement in simulated relative motion curves. The independent assessment performed by the Aerospace Corporation corroborates the results and conclusions found by NASA-JSC. Overall, the relative motion methodology and results are believed to be accurate due to the agreement in results between all the participating teams and between the different videos that observe the same debris piece.

Table 4-3 below summarizes ballistics for all the "early sighting" debris objects analyzed. Separation time estimates and ranges are listed along with ballistic coefficient estimates and

ranges. These times vary from those displayed in the original timeline. Originally, the separation times were determined by the Debris Timeline Team to be the first GMT the debris object is visible in the video footage. Typically, the debris object becomes visible slightly later than the actual separation time.

Debris 6 reveals the highest ballistic coefficient, estimated at 3.5 psf with an error bar extending as high as 4.0 psf. The lowest ballistic coefficient is estimated at 0.3 psf for Debris 16 with error bar extending as low as 0.1 psf. The density used to simulate the relative motion is listed with each debris object. Finally, all debris objects that were not analyzed are marked as such, and the video footage gathered for these objects is listed.

Debris #	Best Estimate of Separation Time (GMT)	Separation Time Range (GMT)	Best Estimate of Ballistic Coefficient (psf)	Ballistic Coefficient Range (psf)	Density at Altitude (slug/ft^3)
1	13:53:44.80	13:53:44.20 - 13:53:45.40	1.1	0.6 - 1.6	1.18041358E-07
2	13:53:46.50	13:53:45.90 - 13:53:47.10	1.3	0.7 - 1.9	1.19096239E-07
3	13:53:56.10	13:53:55.60 - 13:53:56.60	0.55	0.1 - 1.0	1.21767023E-07
4	13:54:02.90	13:54:02.30 - 13:54:03.50	0.9	0.3 - 1.5	1.25415914E-07
5	Was not analyzed. 1 video : Sparks 0026				
6	13:54:34.20	13:54:33.70 - 13:54:34.70	3.5	3.0 - 4.0	1.40823380E-07
7	13:55:04.10	13:55:03.60 - 13:55:04.60	1.1	0.5 - 1.7	1.54495779E-07
7a	Was not analyzed. 1 video : Kolob Arch 0161				
8	13:55:20.80	13:55:20.20 - 13:55:21.40	3.4	2.6 - 4.0	1.64515972E-07
9	Was not analyzed. 1 video : Ivins 0005				
10	Was not analyzed. 1 video : Ivins 0005				
11	Was not analyzed. 1 video : St. George 0050				
11a	Was not analyzed. 1 video : Santa Clara 0090				
11b	Was not analyzed. 1 video : Santa Clara 0090				
11c	Was not analyzed. 1 video : Santa Clara 0090				
12	Was not analyzed. 1 video : St. George 0028				
13	13:55:53.80	13:55:53.30 - 13:55:54.30	0.65	0.2 - 1.1	1.83054334E-07
14	13:55:56.70	13:55:56.20 - 13:55:57.20	1.7	1.0 - 2.4	1.85877832E-07
15	13:56:09.50	13:56:09.00 - 13:56:10.00	1.4	0.8 - 2.0	1.98522953E-07
16	13:57:23.90	13:57:23.20 - 13:57:24.20	0.3	0.1 - 1.0	2.18514602E-07

Table 4-3: STS-107 Early Debris Ballistics Results

For most debris events, multiple videos observe the event and can therefore be used to verify the accuracy of the relative motion calculations. Some videos that observe debris events are not analyzed for relative motion due to camera zooming or insufficient data. For each video, several inputs are provided by JSC-SX. The JSC-SX team tracks the debris and Orbiter positions in the video, and provides these pixel locations for all frames where both the debris and Orbiter are visible. The video scaling information, which consists of either the focal length or the horizontal field-of-view (HFOV), is also provided by JSC-SX. Once the relative motion / ballistics analysis is complete for a given case, the estimated ballistic coefficient and separation time are passed on to the debris footprint team. In order to perform their calculations, the luminosity team is also given the ballistics results and relative motion raw data.

To automate the detailed process of analytically calculating the relative range between the Orbiter and the debris piece, a relative motion tool was developed to take the video tracking and scaling data and output the relative motion for that video. For each frame of interest, the distance (in pixels) between the Orbiter and debris in the image plane are converted to an actual distance (in feet) in the trajectory plane. One of the assumptions of the analysis is that the debris remains in the trajectory plane during the time region of interest, usually only several seconds in duration. Also during this short time period, the debris is assumed to have zero lift and the ballistic coefficient is assumed to be constant. The error associated with these assumptions is deemed to be relatively small, and the assumption that the debris piece remains in the trajectory plane is considered to be the best assumption that could be made to calculate the relative motion explicitly.

Adjustments to the relative motion calculations include accounting for the off-set of the Orbiter from the principal point (image center) and accounting for camera rotation effects. Once all the relative motion curves for a debris piece are generated, the curves are compared with simulated relative motion data for a constant ballistic coefficient. The ET-SRB simulation, an official range safety external tank (ET) debris footprint tool, models the ballistic trajectory of the debris piece given the initial state vector from the Orbiter best-estimated-trajectory (BET) data. A post processor script then compares the simulated debris trajectory with the actual Orbiter trajectory to calculate a relative motion curve. The video relative motion curve is co-plotted with a set of constant beta, simulated relative motion curves for a given separation time. If none of the constant beta curves match the video relative motion data, then the separation time is adjusted until the closest match is achieved.

Another approach to this analysis would utilize several videos together to triangulate a relative motion solution for a single object. However, this option was not used because several sets of data are erroneous due to zooming or HFOV error. The team felt a more accurate estimation of separation time and ballistic coefficient for each debris object could be made by analyzing each video independently.

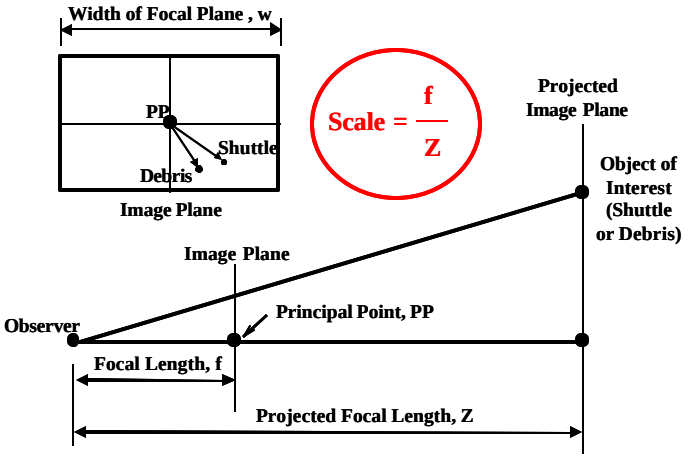

Figure 4-14: Relative Motion Geometry

In the upper left-hand corner of the figure above is an example of the debris and Shuttle positions in the image plane. The actual objects are being projected onto the image plane, which is defined by the focal length (i.e., distance from the observer) and horizontal field-of-view, both of which are a function of the camera specifications and zoom setting. The locations of objects in the image plane correspond directly to their appearance on the screen. The tracking data, which is one of the inputs into the relative motion tool, consists of the location of the debris and Shuttle in the image plane for each frame where the debris is visible. The tracking data is manipulated to calculate the distance (in pixels) from the Shuttle to the debris in the image plane. Another plane, parallel to the image plane, is set at a distance from the observer so that it passes through the location of the Shuttle. Distances (in feet) in this displaced (or projected) image plane are related to distances (in pixels) in the true image plane through a scale factor. Since the two image planes form similar triangles, the scale factor is simply the ratio of the true focal length, f, to the projected focal length, Z. If the trajectory plane was also parallel to the image plane, then the calculated separation distances in the projected image plane would be the actual, true distances between the Orbiter and the debris. In reality, however, the trajectory plane is never parallel to the image plane, so further calculations are necessary.

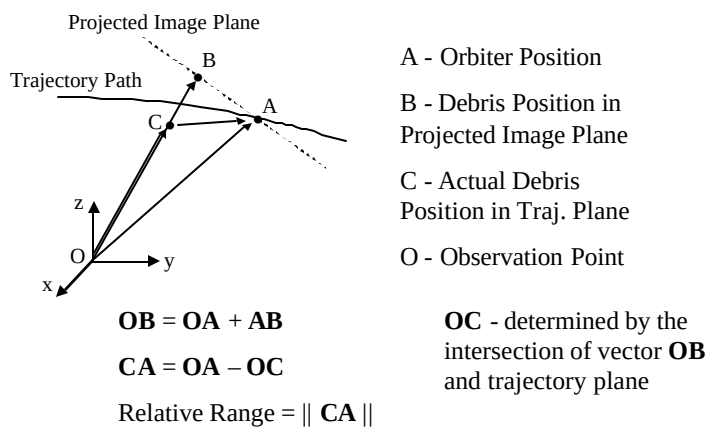

Figure 4-15: Relative Motion Geometry

The dashed line in the figure above represents the projected image plane described earlier. Point A is the actual position of the Orbiter and point C is the actual position of the debris piece, which is assumed to remain in the trajectory plane. Point B represents the point where the projection of the debris piece intersects the image plane. In other words, point B is the debris location as seen on the video, without accounting for the viewing geometry. Point O represents the observer's location. The vector from point O to point A is determined based on the trajectory data, and the vector from point A to point B is calculated using the measured distances on the screen (in pixels) and the scale factor shown on the previous figure. Vector OB is calculated by adding vectors OA and AB. The vector from point O to point C is determined by finding the point of intersection between vector OB and the trajectory plane. The vector from point C to point A is then calculated by subtracting vector OC from vector OA, and the magnitude of vector CA is equal to the relative range from the Orbiter to the debris.

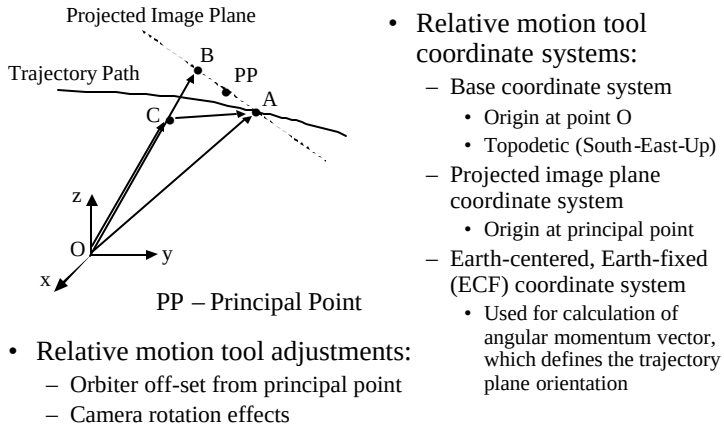

Figure 4-16: Relative Motion Geometry

All vector operations mentioned are calculated in the base coordinate system, located at the observation point. Coordinate systems are also established at the Earth's center and at the projected image plane principal point. Coordinate transformations are then derived to transform vectors in the projected image plane coordinate system and the Earth-centered, Earth-fixed coordinate system to the base coordinate system. The orientation of the trajectory plane is defined by the angular momentum vector of the Orbiter at the time of the given frame. The angular momentum vector is calculated in the Earth-centered, Earth-fixed coordinate system and then transformed to the base coordinate system, which is a topodetic (South-East-Up) coordinate system. The trajectory data is also manipulated to calculate the range, azimuth, and elevation from the observer to the Orbiter.

Since the Orbiter location is not coincident with the principal point (PP), the orientation of vector OA is adjusted to determine the projected image plane orientation, which is needed to perform the necessary coordinate transformation. This adjustment is performed by a series of intermediate coordinate transformations utilizing the scaled tracking data in the projected image plane. The camera rotation effects also needed to be taken into account since the methodology described earlier assumes zero camera rotation. To visualize the effects of the camera rotation on the desired solution, consider what happens to vector OB as the camera rotates from 0 deg to 360 deg. As the camera rotates a full 360 deg, the orientation of vector OB rotates around to form a cone that intersects the trajectory plane at a series of points instead of one exact location. To calculate the camera rotation angle for a given frame, the plasma trail orientation in the video is compared with the trajectory data and then adjusted by iterating on the rotation angle until its orientation matches the trajectory. The solution of the camera rotation angle iteration is then applied to the relative motion calculations to nullify the effects associated with the rotation.

Ranges on separation time and ballistic coefficient have been determined for each debris object. These ranges are derived through an error analysis that takes into consideration all significant error sources. As it turns out, the same error sources applied to separation time also apply to ballistic coefficient. Most of these are independent of which video or debris object is being analyzed and are assigned a constant value for each case. However, a few of the error values are debris/video specific. Conservatism is used throughout the error analysis because small

increases in separation time and ballistic coefficient ranges have little impact on the overall footprint area when these estimates are used as initial conditions for footprint analysis. Once the contribution from each error source is estimated, the errors are stacked in a worst-on-worst fashion. Worst-on-worst analysis was chosen over a RMS calculation for the added conservatism. There are six significant error sources: time synchronization, horizontal field-of-view, beta curve fit method, relative motion calculations, video tracking, and simulation errors.

Time synchronization error is a measure of how well the actual GMT is known for each video. By the end of the analysis, most times were synchronized through celestial references, either directly or indirectly. However, a conservative estimate for error is used. An error of +/- 0.2 seconds is applied to separation time, and an error of +/- 0.05 psf is applied to ballistic coefficient for time synchronization error. While many of the cases truly have less than 0.2 seconds of error because the celestial references are quite accurate, 0.2 is still used for conservatism.

Horizontal field-of-view (HFOV) error is a measure of how well the zoom for a particular camera is known. In most cases, HFOV estimates were done by the Image Science and Analysis Group (JSC-SX). HFOV is known quite well for some video data, while others rely on the observers' estimates of zoom. In some cases, the camera zoom is in the digital zoom region. This region of zoom provides a noise characteristic that can be measured in order to obtain a HFOV estimate. Other cases of footage have camera zoom in the optical zoom region. Without specific zoom information, the actual camera zoom cannot be determined. In cases where zoom was not well defined, a relative motion calculation is performed with multiple HFOV's. For these situations, the error is then included in the beta curve fit error calculation as will be discussed next. Fortunately, changes in HFOV affect separation time estimates very little. For this reason this error source is neglected for separation time estimates. However, HFOV errors certainly impact ballistic coefficient estimates. HFOV error for the ballistic coefficients is assessed on a case-by-case basis, and values range from as little as +/- 0.05 psf to as large as +/- 0.2 psf.

Errors in the beta curve fit method are a measure of how well separation time and ballistic coefficient can be estimated by fitting the ET-SRB generated relative motion curves with the relative motion curves derived from video data. This method is quite accurate because small changes in separation time and ballistic coefficient (on the order of 0.1 sec and 0.1 psf, respectively) are noticeable in the curve fitting. However, errors creep into the beta curve fit method when the relative motion data is dispersed, either because the observer is close to the trajectory plane or because the relative motion data from several videos has less than perfect agreement. This error source applies to both separation time and ballistic coefficient estimates, and the magnitude is determined on a case-by-case basis. The magnitude of this error source can range from 0.1 seconds to 0.2 seconds for separation time and from 0.1 psf to 0.3 psf for ballistic coefficient.

Errors in the relative motion calculations measure the combined accuracy in the components of this calculation. Early in the development of the relative motion tool, assumptions were used to simplify the calculations. Eventually, the calculations were refined, and the simplifications were extracted. For instance, original calculations were made assuming the Earth is a perfect sphere

until the proper coordinate transformations were developed to incorporate the 1960 Fischer Ellipsoid model. To account for this error source, a value of 0.05 seconds and 0.05 psf is included in the error ranges for separation time and ballistic coefficient, respectively.

Additionally, there are small errors associated with tracking the debris and Shuttle from the video footage. The Image Science and Analysis Group uses a tool called ISEE to obtain pixel location as a function of time for objects in a video. This tool approximates the location of the "light source" on the screen. Due to distortion, the pixel data will have errors on the order of a few pixels. The errors in separation time and ballistic coefficient estimates associated with these tracking errors are estimated at less than 0.05 seconds and 0.05 psf, respectively.

Finally, the ET-SRB simulation contains slight errors in the calculations of the relative motion curves. Since these curves are used to estimate the separation time and ballistic coefficient, this error must be accounted for in the estimates. Aerospace Corporation and the Aeroscience and Flight Mechanics Division at JSC (JSC-EG) used independent simulations to derive these curves. The good agreement between the simulations justifies a rather low error range for this error source. Separation time error due to this source is less than 0.05 seconds. Ballistic coefficient error due to this source is less than 0.1 psf. Table 4-4 summarize the error components for debris 6 as an example.

Error in Separation Time (sec) : 0.45	
Error Source	**Error (plus/minus seconds)**
Beta Curve Fit Method *	0.1
Time Synchronization	0.2
FOV	0
Relative Motion Calculations	0.05
Tracking	0.05
Simulation Errors	0.05

Error in Ballistic Coefficient (psf) : 0.55	
Error Source	**Error (plus/minus psf)**
Beta Curve Fit Method *	0.1
Time Synchronization	0.05
FOV *	0.2
Relative Motion Calculations	0.05
Tracking	0.05
Simulation Errors	0.1

Table 4-4: Example Error Calculation for Debris 6

As mentioned above, relative motion between the debris and Columbia has been calculated independently by JSC-DM, JSC-SX, and Aerospace Corporation. The calculation methods differ in the assumptions that were made. There is simply not enough information available to solve this relative motion problem in three dimensional space with video information from one camera, so some simplifying assumption is required. JSC-SX and the Aerospace Corporation assume the debris object remains in the Shuttle trajectory path. JSC-DM assumes the debris object remains in the Shuttle trajectory plane, allowing vertical motion in the plane. Both methods neglect motion out of the trajectory plane. The only force with a component acting outside of the trajectory plane is lift. Neglecting debris motion out of the trajectory plane is a good assumption because debris objects tend to tumble, canceling out lift in any one direction, and because the video observations are only on the order of a few seconds typically.

The difference in assumptions do significantly impact the data; however, these impacts are well understood. JSC-SX and the Aerospace Corporation both project the debris object into the trajectory path. This method works well unless the observer happens to be very close to the

trajectory plane. When this is the case, projecting the debris object introduces some error in the calculation of relative range between the debris and the Shuttle if it is true that the debris has fallen out of the trajectory path. Assuming the debris is falling vertically out of the trajectory path, two possible cases can result. First, if the Shuttle is moving towards the observer, projecting the debris into the trajectory path results in a larger relative range. Unfortunately, none of these cases were analyzed. Alternatively, if the Shuttle is moving away from the observer, projecting the debris into the trajectory path results in a smaller relative range. Ivins 0005 Debris 14 and St. George 0028 Debris 14 illustrate this scenario. This will be discussed in detail subsequently.

The table below lists relative azimuth between the Orbiter trajectory and the line-of-sight of the observer for several Debris 14 videos. A range of azimuths are listed for each video. This range corresponds to the beginning and end of video footage. In other words, Ivins 0005 has a relative azimuth of 7 deg when video footage is acquired, and this decreases to 6 deg when video footage is lost. Note that Flagstaff 0017 is the only case listed where the azimuth increases over the time span. This is because Flagstaff is the only case where the Shuttle is moving toward the observer.

Debris	Video	Relative Azimuth between Orbiter Trajectory and Line-of-sight (degrees)
14	Ivins 0005	7 - 6
	Flagstaff 0017	52 - 61
	St. George 0028	10 - 8
	Las Vegas 0030	32 - 30

Table 4-5: Relative Azimuth Example for Debris 14 Videos

The point here is to illustrate that the cases with a large relative azimuth, Flagstaff 0017 and Las Vegas 0030, are the same cases that demonstrate good agreement using both relative motion assumptions of JSC-DM and JSC-SX/Aerospace Corporation. This result is further illustrated in figure 4-18. The cases with small relative azimuth are scenarios where the observer is close to the Shuttle ground track. Ivins 0005 and St. George 0028 both have small relative azimuths, and thus, do not agree as well between the different teams (figure 4-18).

All teams show very good agreement in the relative motion for Debris 6 as shown in Figure 4-17 below. (These plots are described in detail in Section 4.2.2.) JSC-SX analyzed all three videos: Sparks 0026, Springville 0009B, and Vegas 0030. The differences in the assumptions for the relative motion calculations should not affect the data for Debris 6 because all three observers are not close to the trajectory plane; therefore, the relative azimuths between the Shuttle trajectory and line-of-sight should be large. Aerospace Corporation did not analyze Vegas 0030.

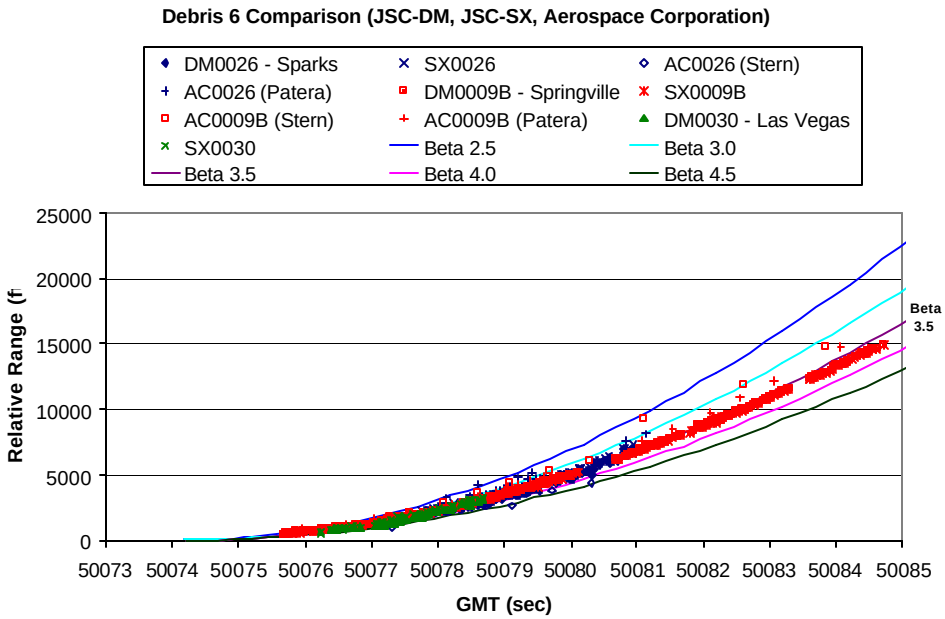

Figure 4-17: Debris 6 Relative Motion Comparison

Variations in Debris 14 data are present due to the different assumptions in the relative motion calculation methods and differences in HFOV estimation for the videos. JSC-DM and JSC-SX Vegas 0030 data matches well. This is expected since the relative azimuth between the Shuttle trajectory and the line-of-sight is 32 deg - 30 deg (table 4-5). JSC-DM and JSC-SX Flagstaff 0017 matches well. Once again the relative azimuth is large (52 deg - 61 deg), so this good comparison is expected.

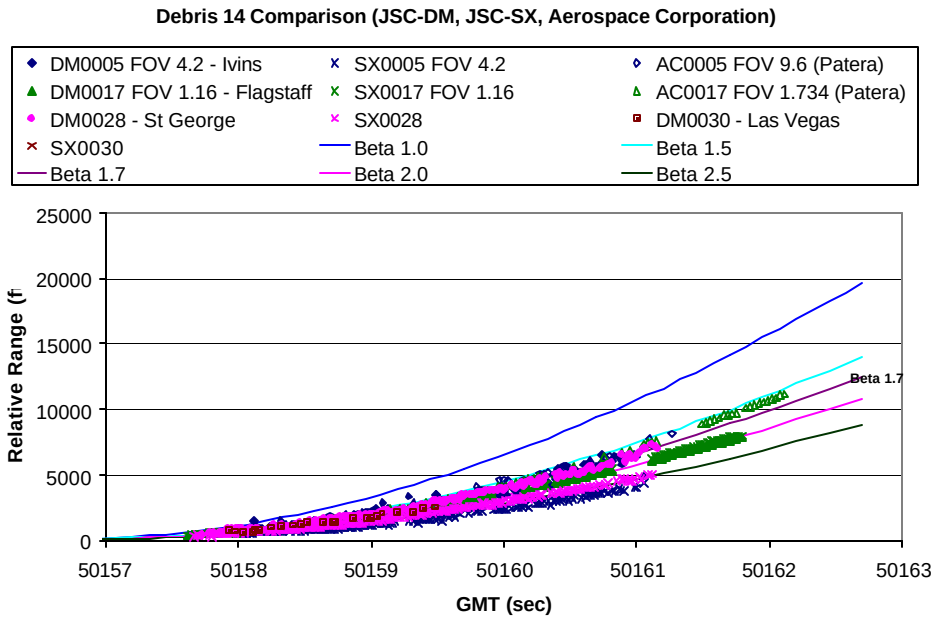

Figure 4-18: Debris 14 Relative Motion Comparison

The comparison between JSC-DM and JSC-SX for Ivins 0005 and St. George 0028 tells a different story. The JSC-SX data indicates a smaller relative range between the debris and the Shuttle for both cases as compared to the JSC-DM data. As discussed above, the difference in assumptions explains this discrepancy. JSC-SX is projecting the debris into the trajectory path; whereas, JSC-DM is accounting for vertical motion of the debris in the trajectory plane. Also, as expected, JSC-DM data for Ivins 0005 and St. George 0028 is more dispersed than the other data sets. This is due to the Line-Plane intersection error present when the observer is close to the trajectory plane as discussed earlier.

The Aerospace Corporation analyzed two of these videos for Debris 14, Ivins 0005 and Flagstaff 0017. Since Aerospace Corporation uses the same assumption as JSC-SX, one would expect the data for both videos to indicate smaller relative range values than the JSC-DM, but this is not the case. The cause is the difference in horizontal field-of-view (HFOV) estimation. JSC-DM uses a HFOV for Ivins 0005 of 4.2 deg; whereas, Aerospace Corporation uses a HFOV of 9.6 deg. JSC-DM uses a HFOV for Flagstaff 0017 of 1.16 deg; whereas, Aerospace Corporation uses 1.734 deg. The larger HFOV estimates Aerospace Corporation uses represent a higher zoom, which results in a larger relative range, as the figure illustrates.

Overall, the agreement between all the teams is quite good, considering the independent efforts and possible error sources. As illustrated, this amount of dispersion in the data still has little effect in the ballistic coefficient estimate - approximately 1 psf.

All teams show good agreement for Debris 1 relative motion. JSC-DM and JSC-SX data matches well for the Lick Observatory 0056 and Fairfield 0064 data sets. Good agreement for both Lick Observatory 0056 and Fairfield 0064 is expected because the observer is well outside of the Shuttle trajectory plane and the relative azimuth is large. Aerospace Corporation estimated one HFOV for Lick Observatory, 3.037 deg, and the data agrees well with the JSC data sets.

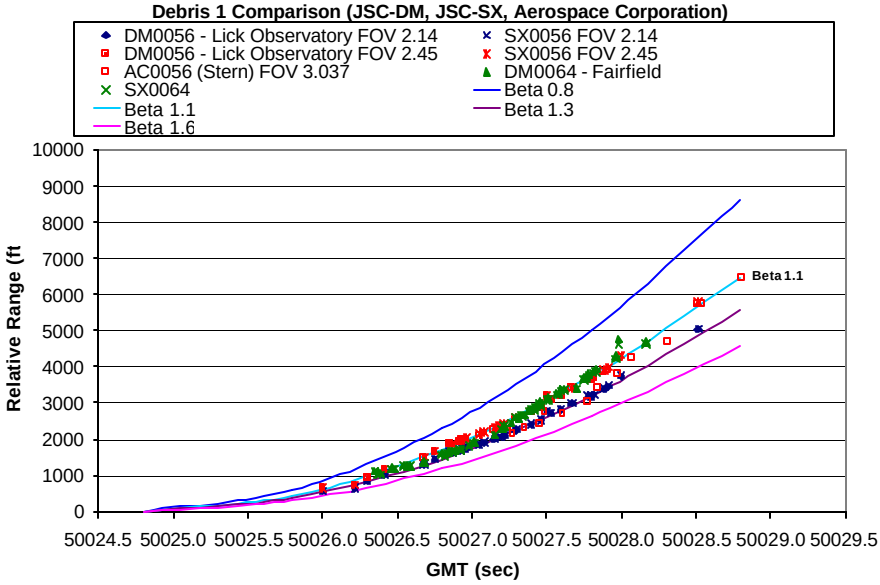

Figure 4-19: Debris 1 Relative Motion Comparison

4.2.2. Detailed Relative Motion and Ballistic Analysis

Relative motion and ballistics data have been organized into several plots, one for each debris object. In each figure, relative range between the Shuttle and the debris object is plotted as a function of GMT in seconds, where 0 seconds corresponds to 12:00 AM February 1, 2003 GMT. Two types of curves are plotted: video data points and simulated beta curves. First, the data points are determined by the relative motion calculations based on pixel data gathered from the videos. The method used in these calculations has been discussed in the methodology section of this report. For each debris, data points are plotted for all videos containing footage usable for relative motion. Second, relative motion curves generated by the ET-SRB simulation and illustrated on the plots as solid lines, are plotted for a range of constant ballistic coefficients. The simulation requires density inputs for each debris, so a constant density corresponding to the estimated separation time for the debris is taken from the flight-derived atmospheric data, which was supplied by the Integrated Entry Environment (IEE) Team.

The simulated curves are compared to the relative motion data points to determine ballistic coefficient and separation time estimates. Typically, simulations are run every 0.1 seconds for separation time and every 0.1 psf for ballistic coefficient. This curve fit method reveals the separation time and ballistic coefficient with a good amount of certainty, as discussed in the Error Analysis portion of this report. The separation time, ballistic coefficient, and error ranges for each are listed on each figure.

Debris 1

The plot below shows the generated relative motion curves for two videos that observe Debris 1. An exact horizontal field-of-view (HFOV) could not be determined for the first video, which filmed from the Lick Observatory in California. As a result, a HFOV range from 2.14 deg to 2.45 deg is applied to the relative motion analysis for this particular video. The HFOV range is based on comments and zoom setting estimations provided by the camera owner. The second video, filmed from Fairfield, CA, provides additional confirmation of the relative motion derived from the Lick Observatory video. The Fairfield relative motion curve is derived based on a HFOV of 5.25 deg and matches well with the relative motion curve for Lick Observatory with a 2.45 deg HFOV. Since the Fairfield relative motion agrees with the Lick Observatory data for the higher HFOV, the estimated ballistic coefficient of 1.1 psf is based on the Lick Observatory 2.45 deg HFOV curve. The estimated separation time is 13:53:44.80 GMT. The error bars for this debris piece are +/- 0.5 psf for ballistic coefficient and +/- 0.60 sec for separation time.

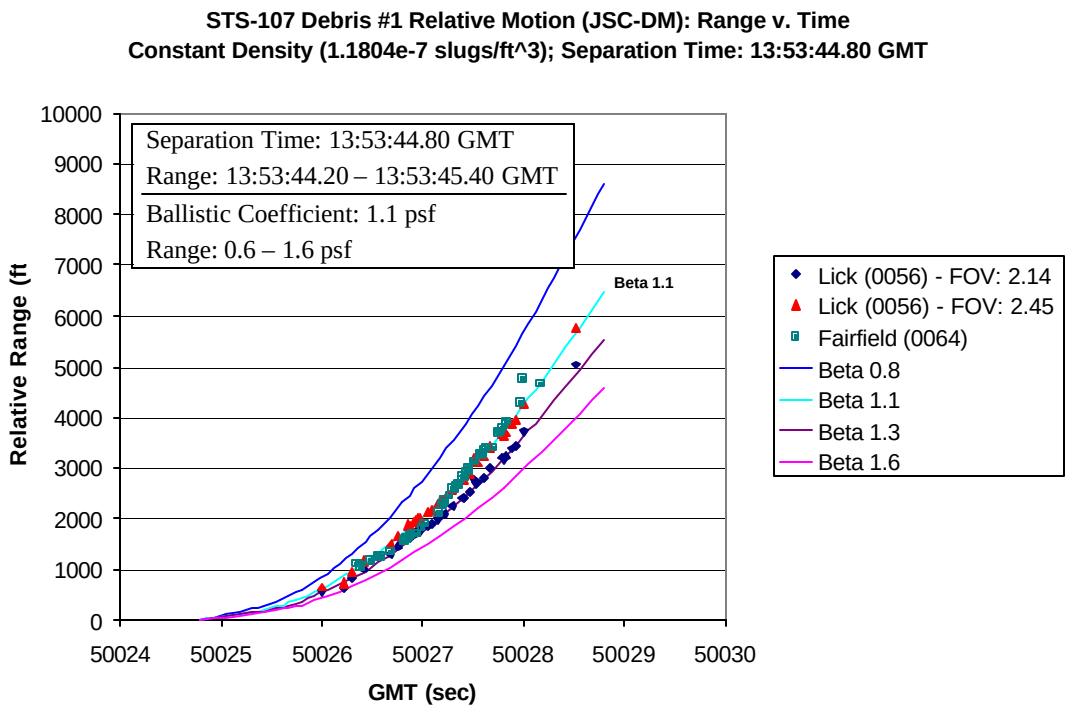

Figure 4-20: Debris 1 vs. Columbia Relative Motion

Debris 2

The same videos and HFOV ranges for Debris 1 are also present for Debris 2. The Fairfield data again suggests that a HFOV of 2.45 deg for the Lick Observatory video is more accurate due to the similarity of the relative motion curves between the two videos at the higher HFOV. Using the Lick Observatory relative motion data with a HFOV of 2.45 deg as the best estimate for ballistic computations, a separation time of 13:53:46.50 GMT and a ballistic coefficient of 1.3 psf are estimated for this debris piece. The estimated error bars for Debris 2 are +/- 0.6 psf for the ballistic coefficient and +/- 0.6 sec for the separation time.

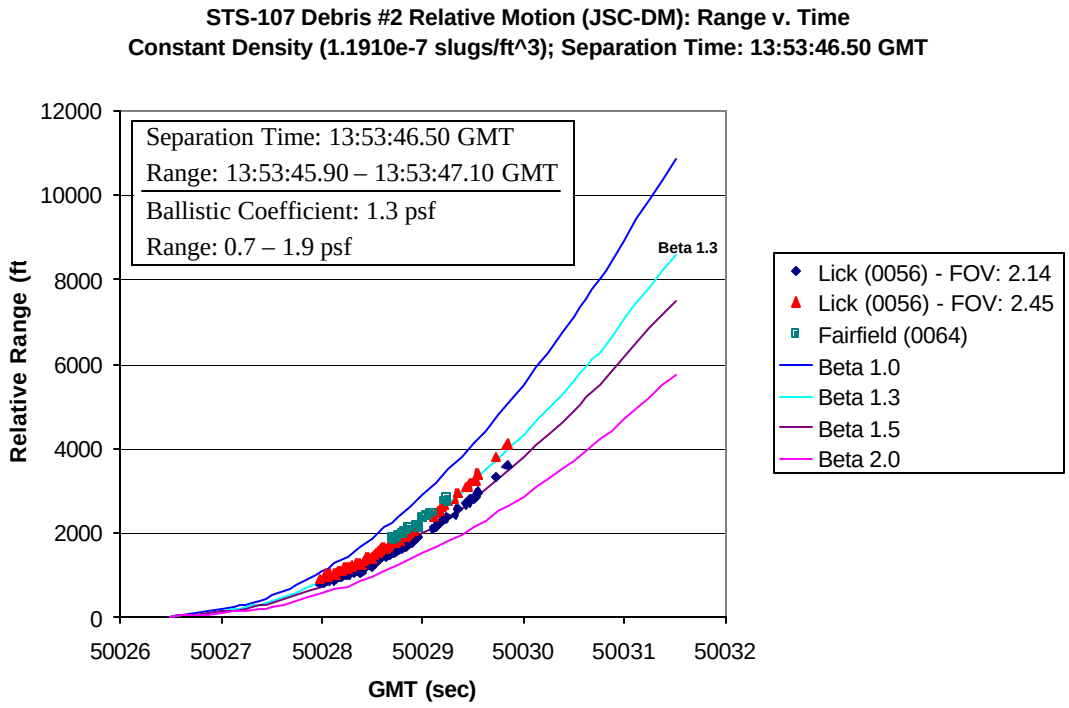

Figure 4-21: Debris 2 vs. Columbia Relative Motion

Debris 3

Two observers capture Debris 3 video footage usable for relative motion calculations: one at Lick Observatory and one in Sparks, NV. Yet again, as in Debris 1 and Debris 2, the Lick Observatory 0056 data cannot be narrowed down to one HFOV, so a range has been used, 2.14 deg - 2.45 deg. As in the plots for Debris 1 and Debris 2, the data seems to indicate a better match with a HFOV of 2.45 deg. A low ballistic coefficient of 0.55 psf with the range 0.1 - 1.0 psf is determined for Debris 3. The estimated separation time is 13:53.56.10 GMT with the range 13:53:55.60 - 13:53:56.60 GMT.

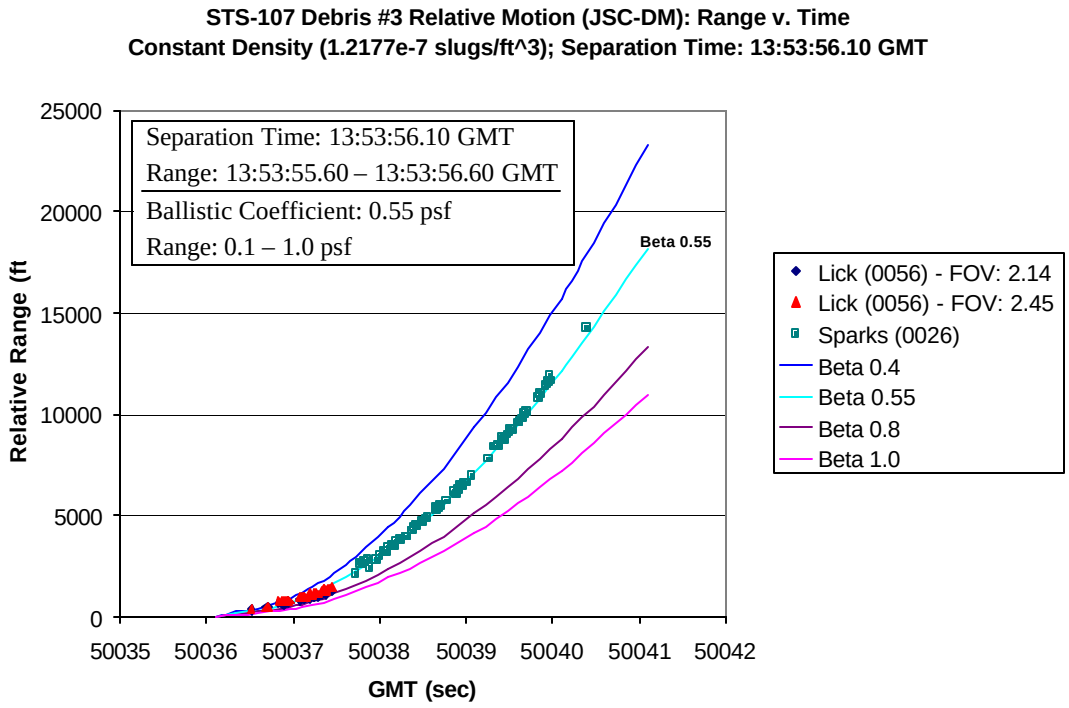

Figure 4-22: Debris 3 vs. Columbia Relative Motion

Debris 4

Only one observer (Lick Observatory 0056) views Debris 4. Once again, relative motion is calculated for both HFOV 2.14 deg and 2.45 deg. However, this time there is no other video data that can help select one HFOV over the other. Here other debris information is used to determine the best ballistic coefficient estimate. Since the relative motion data for Debris 1, 2, and 3 all point to Lick Observatory 0056 with HFOV 2.45 deg as the better HFOV, an assumption is made that the HFOV does not change for Debris 4. Thus, the ballistic coefficient estimate is 0.9 psf with the range 0.3 - 1.5 psf. The separation time is estimated to be 13:54:02.90 GMT with the range 13:54:02.30 - 13:54:03.50 GMT.

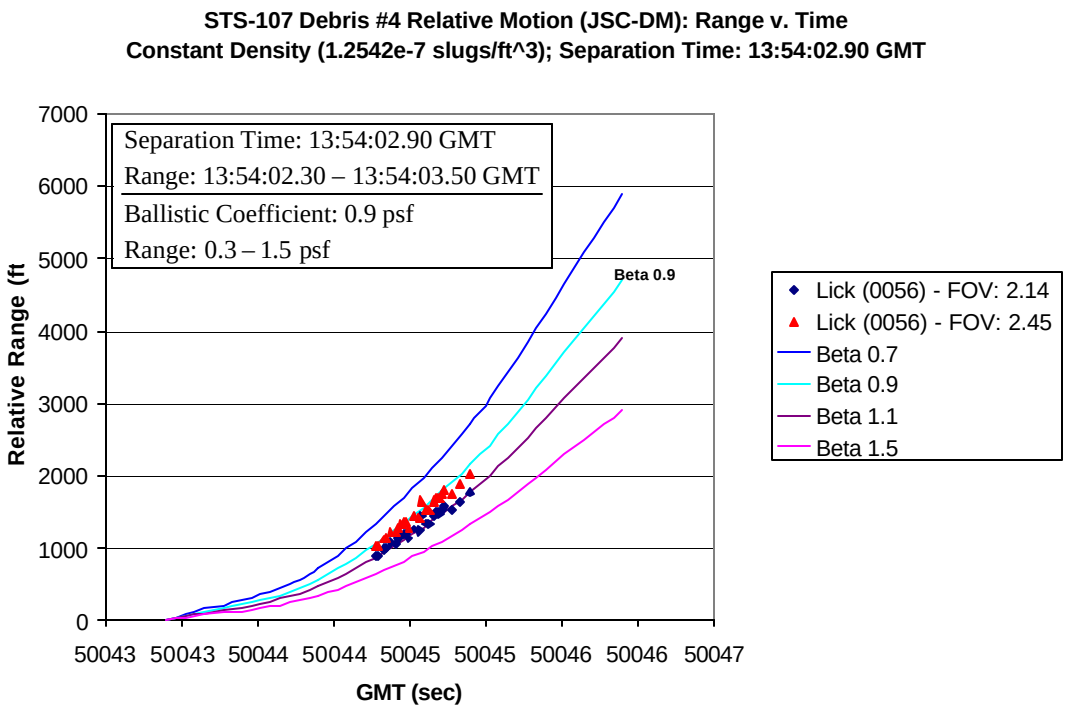

Figure 4-23: Debris 4 vs. Columbia Relative Motion

Debris 6

Debris 6 was the first "early sighting" debris object to be analyzed because several characteristics of this debris event reduced the complexity of the analysis. Foremost, the Sparks, NV 0026 video for this debris event contains a excellent celestial reference. As the debris separates from the Shuttle, not only does Venus enter the field-of-view, but the Orbiter passes directly through Venus from the observing perspective. This convenient event helps provide a very accurate time synchronization and aids in the determination of scaling information for the video. Debris 6 looked promising because it was also viewed for the longest period of time. An observer in Springville, CA 0009B captures close to ten seconds of footage usable for relative motion calculations. Typically, only 2-3 seconds of usable footage was collected by the

observers. And finally, Debris 6 appears bright in the video footage, which increases the accuracy of tracking (pixel) data for the debris.

Three videos contain adequate data for relative motion calculations: Sparks, NV 0026; Springville, CA 0009B; and Las Vegas, NV 0030. Horizontal field-of-view (HFOV) for Sparks is well known due to the celestial reference. The Springville timing is well known, but the HFOV is uncertain because the camera is zoomed somewhere in the optical region. The Image Science and Analysis group (JSC-SX) estimated HFOV for Springville at 3.6 deg because this HFOV forces Springville relative motion to match the Sparks relative motion. Unfortunately, this approach makes the Springville data mostly obsolete, for no new estimates will result from Springville that could not be derived from Sparks. Consequently, while this HFOV for Springville was used, a rather large error bar has been applied to HFOV error source in ballistic coefficient estimates to account for the HFOV uncertainty. Las Vegas separation time and HFOV are uncertain for Debris 6. Thus, the relative motion has been shifted to match Sparks. This also renders Las Vegas obsolete for estimates; however, Las Vegas views several other debris objects. Using the information gained from this shift for Debris 6 provides additional information for other debris.

As listed for Debris 6, a separation time of 13:54:34.20 GMT and ballistic coefficient of 3.5 psf fit the data the best. The error ranges on these estimates are as follows: 13:54:33.70 - 13:54:34.70 GMT and 3.0 - 4.0 psf. Debris 6 has the highest ballistic coefficient of all debris objects analyzed.

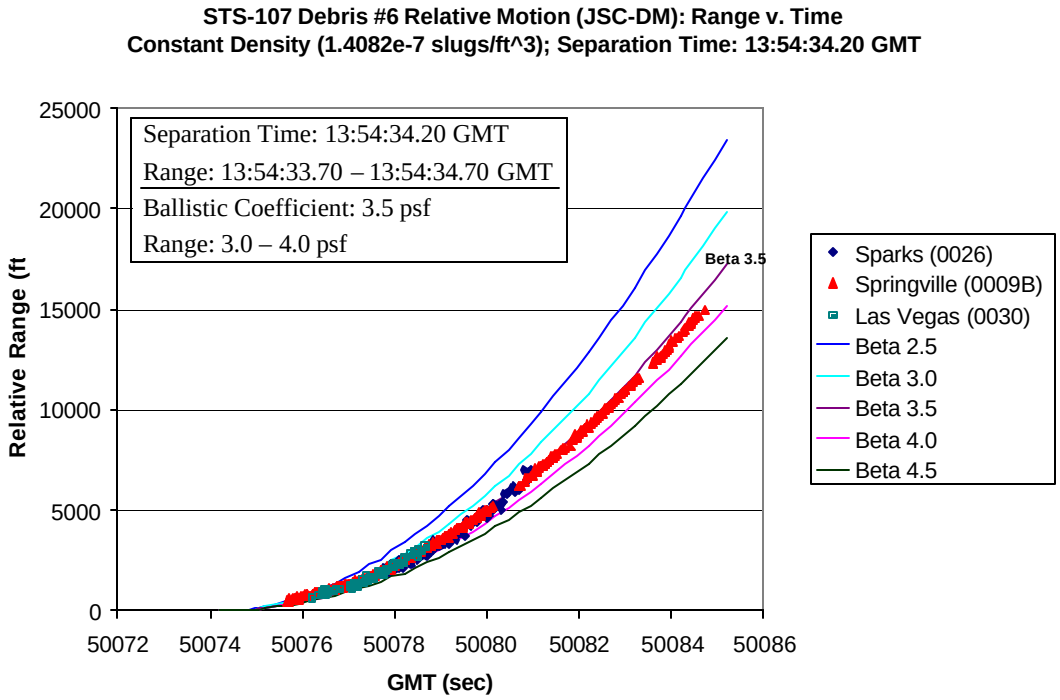

Figure 4-24: Debris 6 vs. Columbia Relative Motion

Debris 7

One observer in Las Vegas, NV views Debris 7. A HFOV range is used: 2.1 deg - 2.3 deg. Since no available information indicates which HFOV is more likely, the ballistic coefficient is estimated using the middle of the HFOV range. However, the error bar on the ballistic coefficient accounts for all possible HFOV's. The estimated ballistic coefficient is 1.1 psf with the range 0.5 - 1.7 psf. The estimated separation time is 13:55:04.10 GMT with the range 13:55:03.60 - 13:55:04.60 GMT.

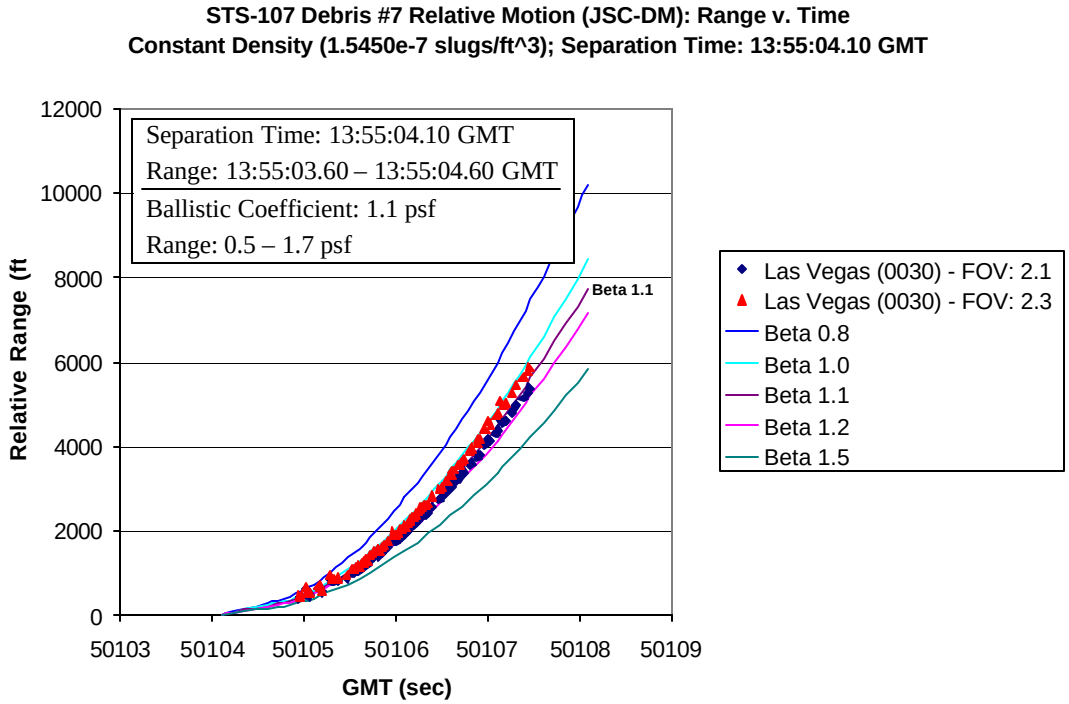

Figure 4-25: Debris 7 vs. Columbia Relative Motion

Debris 8

One observer located in Las Vegas captures video footage suitable for relative motion calculations for Debris 8. This video appears to zoom in from the time Debris 7 is viewed to the time Debris 8 appears. This information indicates that the observer is probably at the maximum optical zoom during Debris 8 footage, corresponding to a HFOV of 2.1 deg. The ballistic coefficient for Debris 8 is surprising because it rivals Debris 6 for the largest beta estimate. The ballistic coefficient for Debris 8 is estimated at 3.4 psf with the range 2.6 - 4.0 psf. The separation time is estimated at 13:55:20.80 GMT with the range 13:55:20.20 - 13:55:21.40 GMT.

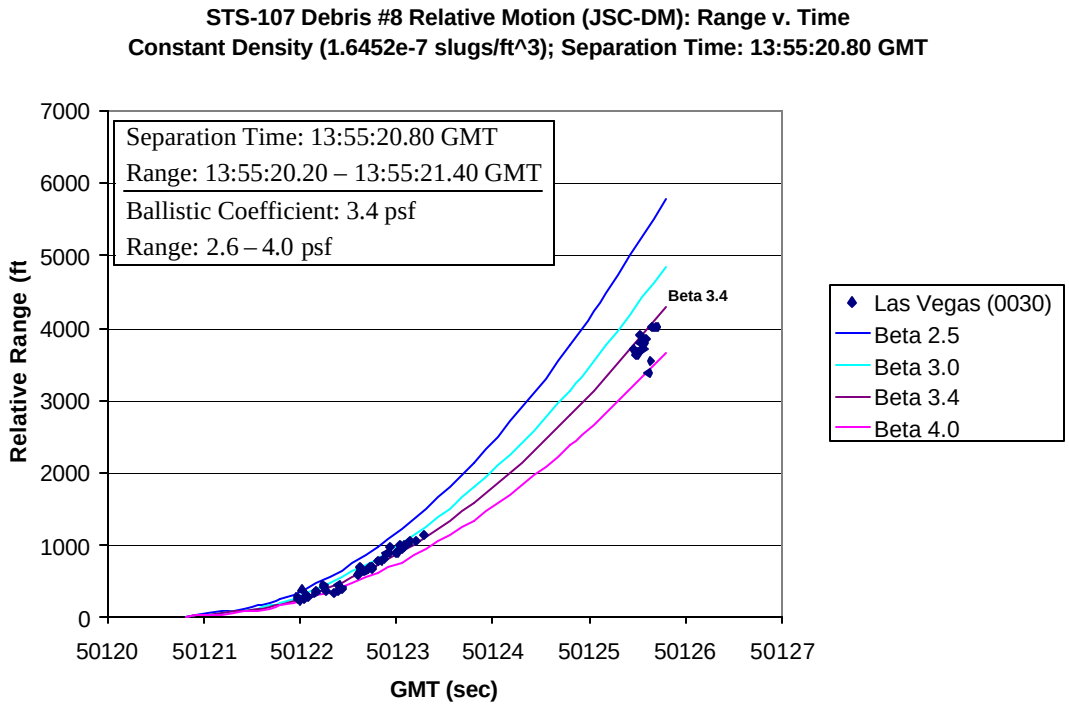

Figure 4-26: Debris 8 vs. Columbia Relative Motion

Debris 13

One of the significant aspects of analyzing Debris 13 is the confirmation of the time sync applied to the Debris 14 videos. The two videos that observe Debris 13 are Ivins and Flagstaff, both of which also observe Debris 14. The time biases that were applied to these two videos for Debris 14 could not be confirmed without the Debris 13 relative motion. As shown in the plot below, the two relative motion curves match very well, thereby significantly increasing the level of confidence in the time syncs. Similarly to Debris 14, the Ivins data for Debris 13 is more noisy than the other relative motion curves analyzed. Again, this is due to the viewing geometry, and one of the beta curves plotted above fits the data quite well. The estimated ballistic coefficient for Debris 13 is 0.65 psf with an error bar of +/- 0.45 psf, and the separation time is estimated at 13:55:53.80 GMT with an error bar of +/- 0.5 sec.

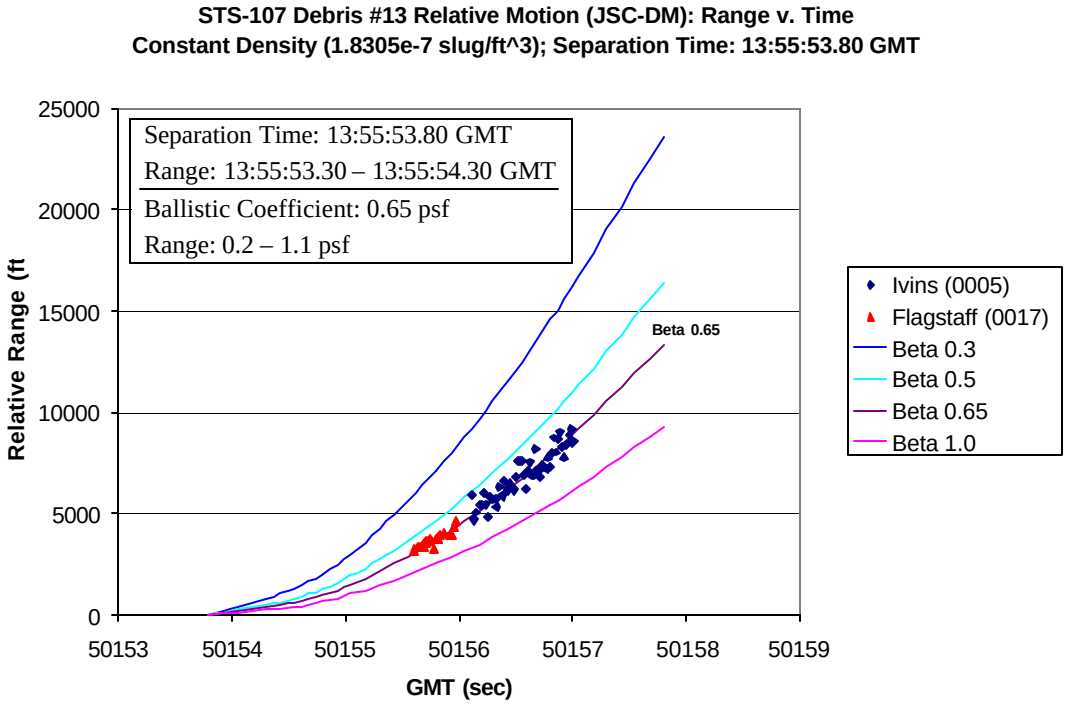

Figure 4-27: Debris 13 vs. Columbia Relative Motion

Debris 14

Debris 14 has the largest amount of relative motion data of all the debris pieces, and along with Debris 6, it was initially considered to be one of the most promising debris pieces. The relative motion curves plotted below are derived from the following videos: St. George, UT (0028), Flagstaff, AZ, Las Vegas, NV, and Ivins, UT. Relative motion was also completed for another video, St. George, UT (0021), but this relative motion curve was thrown out since there is significant zooming taking place during the region of interest. Since the time synchronization of the St. George, UT (0028) video is considered to be the most reliable time synch, the other video time syncs are biased in order to match all the separation times. The only exception is the Las Vegas video time sync, which is set based on Debris 6 relative motion. The Debris 14 relative

motion for Las Vegas confirms the time synch applied for Debris 6. Once the appropriate time biases are applied, the relative motion curves for all four videos match fairly well with each other. With the exception of Las Vegas, the duration of the tracking data is rather large for each of the videos. The relative motion data for Ivins, UT is slightly more noisy than the other relative motion curves, but a curve fit of the Ivins data matches very well with the other Debris 14 videos. The noisiness of the Ivins data is due to the close proximity of the observer location to the Shuttle trajectory plane. As described earlier, the relative motion tool calculates the intersection between a line (vector OB) and a plane (trajectory plane). When the observation point is close to the trajectory plane, a small shift to the line (vector OB) results in a larger shift to the line-plane intersection point, thereby amplifying any errors in the tracking data.

The estimated ballistic coefficient for Debris 14 is mostly based on the St. George, UT (0028) relative motion curve since it is has the most reliable time sync and scaling information. The other videos all agree to within +/- 0.2 psf on the ballistic coefficient, and this range is incorporated in the error bar applied to this debris piece. The estimated ballistic coefficient is 1.7 psf with a beta range of 1.0 to 2.4 psf. The separation time is estimated to be 13:55:56.70 GMT with a +/- 0.5 sec error bar.

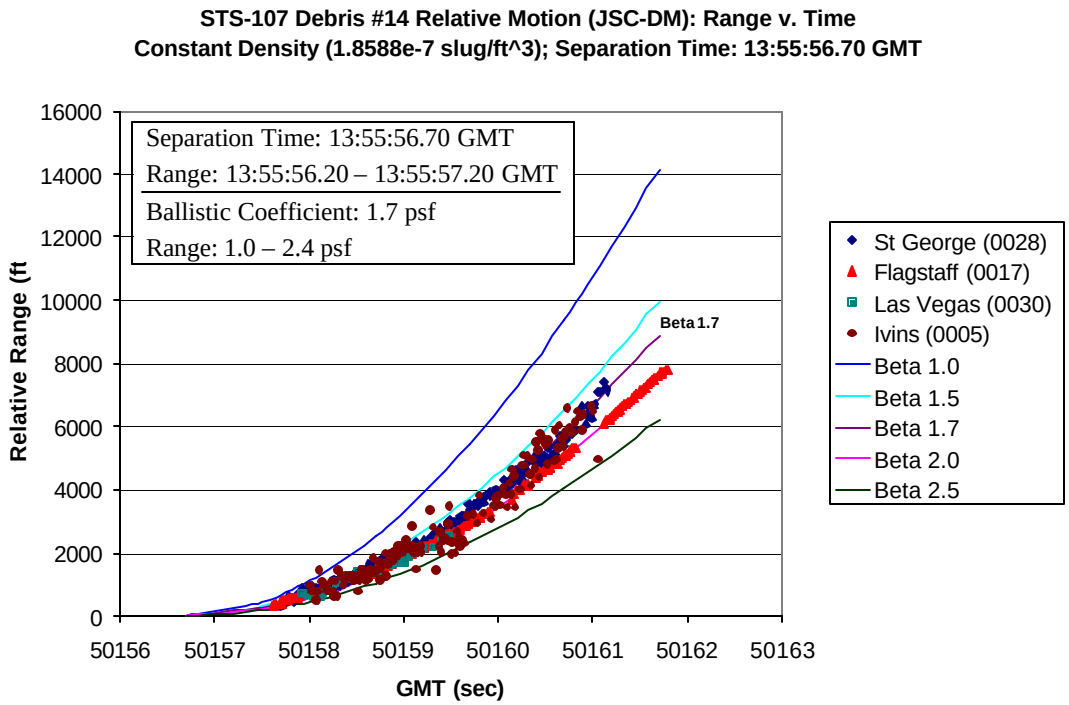

Figure 4-28: Debris 14 vs. Columbia Relative Motion

Debris 16

A video from Kirtland AFB in New Mexico is the only video to observe Debris 16. The amount of relative motion data for this video is quite limited. The debris piece is extremely faint in the video and is therefore very difficult to extract from the video noise. As a result, the chance for inaccurate tracking data is significantly higher, and the error bars are adjusted accordingly. Since this particular video was filmed using a telescope mount, the camera rotation effects are neglected and a high level of confidence is placed on the HFOV estimations. A ballistic coefficient of 0.3 psf is estimated for Debris 16, which is the smallest ballistic coefficient of all of the debris pieces analyzed. The separation time is estimated to be 13:57:23.90 GMT with an error bar of +0.3, -0.7 sec. The error bar on the positive side is limited to +0.3 sec because the beginning of the relative motion data is soon after the estimated separation time. The range for ballistic coefficient is 0.1 to 1.0 psf. The +0.7 psf error bar on beta reflects the low level of confidence in the tracking data.

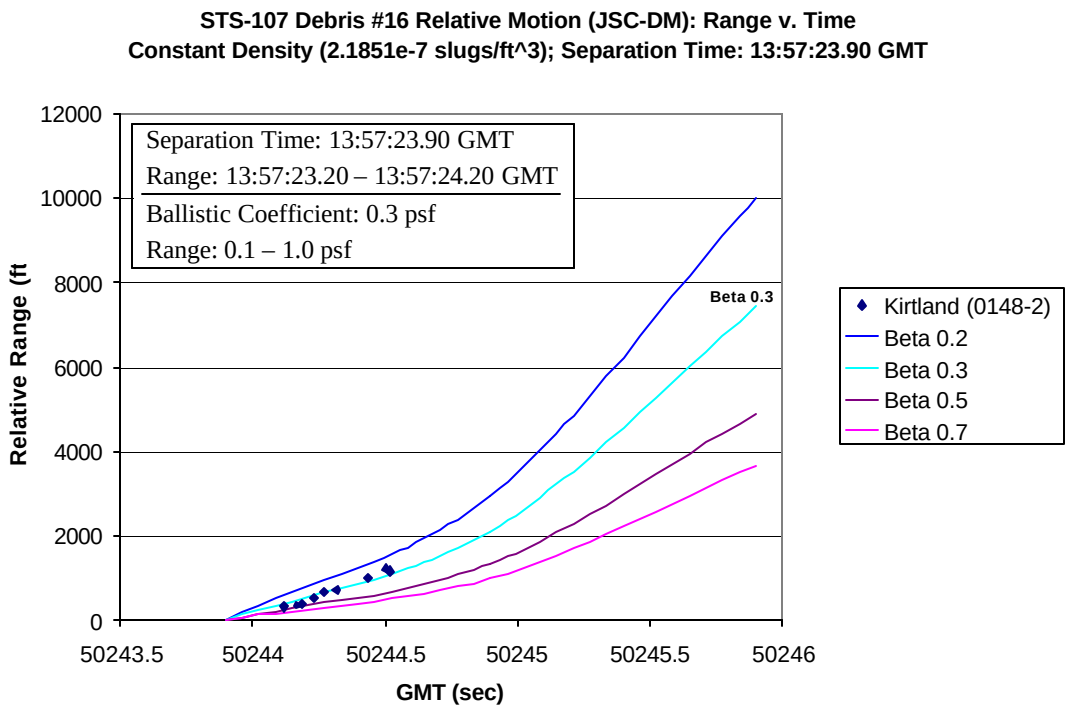

Figure 4-29: Debris 16 vs. Columbia Relative Motion

4.3. Trajectory and Footprints

Unless otherwise footnoted, Section 4.3 is referenced to [24], Mrozinksi, R. B.; JSC-DM; STS-107 Columbia Accident Debris Footprint Boundary Estimates; June 3, 2003. This is included in its entirety in Appendix 10.6.

4.3.1. Trajectory and Footprints Summary and Methodology

The Flight Design and Dynamics Division (JSC-DM) within JSC's Mission Operations Directorate (MOD) estimated debris footprint boundaries for:

1) The primary debris field resulting from Columbia's catastrophic breakup, for which found debris strongly validates the results,
2) The debris impact areas for debris observed in video to have separated from Columbia prior to the catastrophic breakup, and
3) A general swath that would contain all debris that could have separated from Columbia, whether or not it was seen on video.

Additionally, JSC-DM estimated the separation time of the tile found in Littlefield, Texas (KSC Database object number 14768). This work started on February 01, 2003 and continued through June 03, 2003.

The bulk of the content of this section is devoted to footprint boundary estimates for three categories:

1) The Texas/Louisiana debris field resulting from the primary, catastrophic breakup
2) A generic debris swath along the entire STS-107 entry trajectory predicting all possible impact locations for pre-breakup debris in the United States for any possible debris characteristics, and
3) Specific debris footprint boundaries for debris observed to have separated from the orbiter prior to catastrophic breakup.

JSC MOD-DM has been updating debris footprint boundary estimation methodology since 1998, primarily in support of the X-38/CRV program, and in preparation for the eventual disposal of the International Space Station. Several papers document this evolving methodology and its application to various projects [26], [27], [28].

The X-38/CRV vehicle would dispose of its Deorbit Propulsion Stage (DPS) just prior to entry interface. The DPS would trail the crewed Entry Vehicle on entry, and it would breakup and scatter debris into the ocean, while the Entry Vehicle would use its lifting capabilities to move further downrange to a runway landing. Since the placement of the DPS debris footprint must be entirely over water, and since this requirement severely reduces the available landing locations around the globe, JSC's footprint boundary estimation methodology had to adjust to produce a conservative, but not overly conservative, result. This was very important, because as the DPS footprint grows larger, the number of acceptable landing site locations decreases quickly.

JSC MOD-DM has presented the methods and assumptions used in this investigation to several NASA peer-reviews and in international and U. S. forums for feedback, and continuously refined the methodology presented here.

Air Traffic Control (ATC) radar data, and debris found thus far, both strongly support the STS-107 primary footprint boundary results.

A 3 degree-of-freedom simulation predicts the boundaries of the debris footprints. The simulation in this case is called the Simulation and Optimization of Rocket Trajectories [29].

The simulation uses a fourth-order Runge-Kutta method to integrate the equations of motion. MOD-DM assumed that integration method effects on the footprints were minimal, and did not investigate integration methods further.

This work modeled Earth as an oblate spheroid, as set by the equatorial and polar radii (20,925,741.47 ft and 20,855,591.47 ft, respectively). The model assumes that the polar axis is an axial axis of symmetry, and is the planet's rotational axis with an Earth rotation rate of $7.292115146 \times 10^{-5}$ deg/sec. The gravitational model consisted of the central gravitational force (planet gravitational constant of 1.40764685328 x 1016 ft^3/sec^2), adjusted via the first three oblate zonal harmonic coefficients (J2, J3, and J4 with unitless values of 1.0826271×10^{-3}, $-2.5358868 \times 10^{-6}$, and $-1.6246180 \times 10^{-6}$ respectively). JSC-DM assumed that planet and gravity model effects on the footprints were minimal, and did not investigate these further.

The simulation assumes an instantaneous breakup, not a multi-stage breakup as occurs in reality, because the breakup is simply too chaotic to predict any breakup sequence. Due to the chaotic nature of a breakup, and due to non-linearities in the large number of variables involved, especially in atmospheric effects, a parametric approach is ruled out in favor of a Monte Carlo approach. This study uses a sample size of 500, and by using the maximum and minimum ranges and crossranges flown in the simulation, arrives at footprint boundaries that bound 99% of the debris pieces with 95% confidence, given our assumptions [31].

Experience with the methods used here demonstrates that winds have significant impact on the width of the footprint (more pronounced near the heel, or least-range-flown part of the footprint), but negligible impact on the footprint's toe, or most-range-flown point [26]. Thus, the Monte Carlo method used here uses the GRAM-99 atmospheric density and wind database models for dispersions. GRAM models localized winds, density, density variations and shears, and solar activity effects, all in a Monte Carlo environment. (GRAM localizes density perturbations and winds, such that they are specific to the latitudinal and longitudinal position, as well as altitude, month, etc.) This study used GRAM with an entry date of February 01, 2003, and the actual solar activity values for mean solar 10.7 cm radio noise flux and geomagnetic index on February 01 (values of 164.0 Janskys x 10^{-4} and 2.58, respectively) [33]. This methodology utilized the 1999 GRAM model for uncertainties (rpscale = 1.0, or 3σ), applied about a "mean" day-of-entry atmosphere as provided by the DAO (rev D) [32], [34].

JSC-DM did not model explosions for two reasons: 1) there is no evidence thus far of any imparted velocities to debris (debris found thus far does not support an explosion, nor is there

any video evidence of an explosion), and 2) any explosion would have been nearly impossible to model with any certainty without performing a detailed blast analysis.

Initial conditions for the primary breakup are from one of these sources: they are the last BET vector, or the last GPS vector, or they are taken along a 220 psf ballistic trajectory initiated at one of these two vectors. The Debris Footprint Team selected a 220 psf trajectory as it will bound in altitude the entire debris field. The simulation sheds debris off this 220 psf trajectory to define the "feather" shape of the debris footprint as shown later. The team selected 220 psf as it was the maximum ballistic coefficient object observed in the debris field.

The initial condition vector for a piece of pre-breakup shed debris is the orbiter BET vector at the time that the Relative Motion Team computed for that piece of debris to have separated from the orbiter.

Note that the simulation terminates when the altitude relative to the oblate spheroid model is zero. This is not when the local topographical altitude is zero. Thus, the footprint boundaries are conservative when the local topography is above zero feet in elevation.

The assumption of constant mass and aerodynamics is erroneous in reality due to the possible ablation and separation of debris pieces through their entry. However, in modeling the heel of the primary debris footprint, and in modeling the post-breakup shedding debris, the ballistic coefficients used (0.5 psf and 20 psf) are intended to represent an equivalent average value, rather than the actual indeterminable values. In the cases where a ballistic coefficient is observed (the toe of the primary debris footprint, and the footprints for all pre-breakup shed debris), it is impossible to model the ballistic coefficient variation with time without knowing the actual mass, area, and drag characteristics of the object, and without knowing of ablation and interaction with other debris; thus one is forced to a constant β assumption even with an observed β. Furthermore, it has been shown for satellite reentries, that variations in drag coefficient do not affect the overall footprint estimates [35].

Note that for a ballistic (non-lifting) trajectory, designating values of m, S, and C_d is arbitrary, since when the lift is zero it is only the ballistic coefficient that dictates the trajectory of the object. However, when modeling a lifting coefficient, the values are no longer arbitrary. The hypersonic through to subsonic drag coefficient for any debris object is estimated to be approximately 0.5 - 1.5; thus a value of 1.0 is chosen.

The maximum L/D ratio found in the Debris Footprint Team's research of past studies found a maximum L/D of 0.15 in Soyuz launch vehicle studies [27], [36]. Although debris pieces generally can exhibit higher L/D values, they were unlikely to hold the lift vector in a constant orientation as modeled here. The 0.15 value is a reduced L/D that applies when constant bank angles are used [37]. Since the team assumed that the pieces of debris will neither trim at a stable orientation, nor tumble at a high enough rate to generate substantial lift, and since the methodology is conservative in uniformly dispersing L/D, the methodology is able to assume a L/D in the range of 0.0 - 0.15, for all debris.

For the primary debris footprint, the team bounded the lower end of β at 0.5 psf, rather arbitrarily, assuming that the bulk of the debris will be higher than 0.5 psf. In selecting the low end for the primary debris field, the team felt 0.5 psf to be adequately conservative since any identifiable pieces of less than this value would have the lowest capability of all the pieces to cause damage. The team bounded the upper end at 220 psf, as that was the maximum ballistic coefficient observed. The simulations model post-breakup shedding debris at 0.5 psf and 20 psf. 20 psf is the maximum ballistic coefficient modeled in post-breakup shedding, because it maximizes the width of the footprint (increasing β increases width until around 20 - 30 psf), without overextending the toe of the footprint, e.g., increasing this quantity to 30 psf would not significantly widen the footprint, but would significantly extend the length, which is not supported in the debris located thus far.

For pre-breakup shedding debris whose relative motion and ballistic coefficient was analyzed from video, the methodology uses the resulting ballistic coefficient. Otherwise, the methodology uses a range of 0.5 - 5.0 psf to conservatively bound the results of the debris analyzed by the relative motion and ballistics experts, i.e., the methodology assumed that the non-analyzed debris would be similar to the analyzed debris.

The following data were calculated for each debris item based on public video as described in Section 4.2: the best estimated separation time, the separation time range (accounting for the error range), the best estimate of ballistic coefficient, the ballistic coefficient range (accounting for errors), and the constant atmospheric density value used in the ballistic coefficient calculation (which comes from the DAO day-of-entry atmosphere model). These are listed in Table 4-3 in Section 4.2.

4.3.2. Primary Debris Footprint

The Debris Footprint Team received a call to come in at 1030 (central time) on the day of the accident, and presented at 1200 central the first prediction of a debris line and an intact crew module impact location. The initial condition was the closest pre-entry predicted trajectory point (at 13:59:23.96 GMT) to the GMT that remained frozen on the screens in Mission Control (13:59:22 GMT). The team assumed that breakup occurred at that time, and that the intact crew module became a free-flying object at this time (because no better data was available). The United Space Alliance provided quick estimates of crew module size and mass: 30000 lb crew and contents; 17.75 ft diameter area (β = 121.2 psf) [39]. A ballistic trajectory predicted an intact crew module impact location of 31.02 N, 93.58 W.

The team estimated the debris line by assuming a ballistic coefficient range of 0.5 - 116 psf, as in previous analyses [26], [27], [28], based on historical studies. Because the first debris line was due at the Mishap Investigation Team at 1200, no time was available to perform a Monte Carlo analysis, so the Debris Footprint Team simulated two ballistic trajectories (0.5 and 116 psf) through a 1976 Standard Atmosphere, without winds, to arrive at a zero-width debris line. Monte Carlo methods would be needed to arrive at a predicted width, but would take several hours to prepare and run, thus the team was released for this day.

The next primary debris footprint release was on February 04. This release added the 1999 Global Reference Atmosphere Model (density, wind speed, and wind direction) for February 01 along the orbiter trajectory. JSC-DM selected a sample size of 500, as done in previous studies [26], [27], [28]. The Debris Footprint Team had also now identified an actual piece of hardware that could have a ballistic coefficient higher than 116 psf, thus the upper limit of ballistic coefficient increased to this value (Reaction Control System jet nozzle β = 180 psf).

The next primary debris footprint release was on February 07. The primary difference was an update the initial condition, now at 13:59:30.4 GMT [40]. Since this time was 6.5 seconds later than the original last-known-position time, the results showed a significant shift in the debris footprint boundaries due to the banking and lifting toward the north for those 6.5 seconds. Also, the Debris Footprint Team had now received information that a 220 psf object was observed in the debris field, thus the methodology updated to a maximum ballistic coefficient of 220 psf (SSME powerhead).

The next primary debris footprint release was on February 14. The Debris Footprint Team corrected a minor simulation error, incorporated a somewhat later (0.04 sec) GPS vector [41], and completely abandoned the 180 psf upper limit on ballistic coefficient in favor of the 220 psf observed value.

The next primary debris footprint release was on April 10, and included several major modeling improvements. The biggest improvement was transitioning from the GRAM-99 atmosphere model for density, wind speed, and wind direction, to rev C of a day-of-entry model provided by the DAO, and including recommended 10% uncertainties about the DAO mean for density, wind speed, and wind direction [42].

The next major change was moving to two initial condition vectors, which the Debris Footprint Team believes bounds the time at which the orbiter became ballistic (lost lift). The first time (13:59:37.00 GMT) is the last vector in the BET version 4 [43]. The final time (14:00:02.12 GMT) is the final GPS downlisted vector during the 32 seconds of additional data following the original loss of signal [44]. The reason for looking at two vectors was to capture the complete sweep in the debris centerline as in the final stages before catastrophic breakup the vehicle was banking toward the north. If the vehicle began losing debris, but still continued to bank and pull lift toward the north, some debris could lie on a centerline south of the centerline generated at the catastrophic breakup point. Thus, the team transitioned to two breakup times and added centerlines to the resulting footprints. There is no GPS data in between these two selected times, and the team strongly believes the vehicle was lifting at the first time and not lifting at the second time; thus the methodology has the shortest possible range of times during which the vehicle became ballistic.

The final major change was simulating shedding debris post-breakup. The simulations did this by shedding debris off of two 220 psf ballistic trajectories starting from each of the two state vectors (BET and GPS) selected above, in 30 second intervals. The 220 psf trajectory will bound all debris in the debris field and will produce upper limits in width of the footprint. As the post-breakup shedding times become closer and closer to the ground, the footprint width begins to shrink, thus forming the “feather” shape.

The current primary debris footprint release incorporates the latest and final DAO day-of-entry atmosphere model. DAO did not provide uncertainties information, other than to use the GRAM model’s uncertainties. Reference 34 states to use the GRAM model with rpscale = 1.0 (3 sigma dispersions).

Figure 4-30 shows the overlaid historical progression of the primary debris footprint boundary predictions. Each box of text highlights the primary differences from the previous footprint prediction.

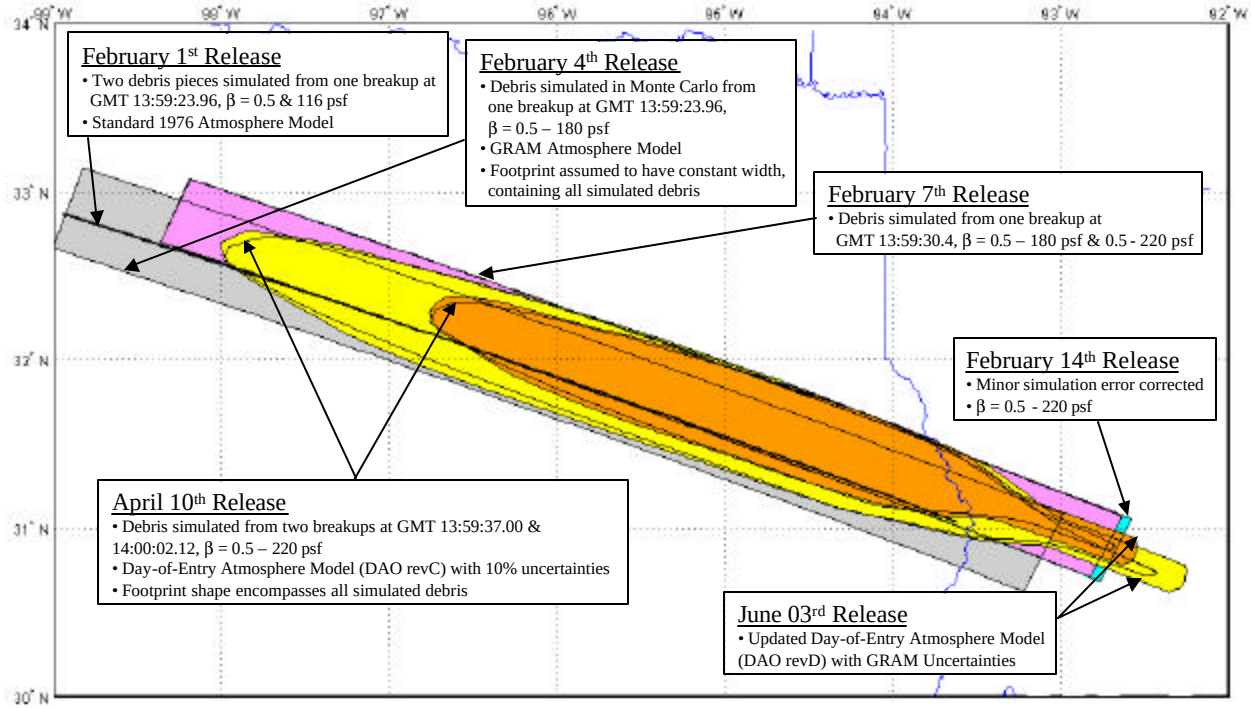

* Bounds 99% of debris trajectories with 95% confidence

Figure 4-30: Overlaid History of Estimated Columbia Primary Debris Fields

The methodology forms the primary debris footprint by combining four "sub" classes of debris footprints. The Debris Footprint Team begins with shaping the heel of the footprint. The entire ability to shape the footprint revolves around the premise that the maximum ballistic coefficient that can sustain lift is 20 psf. Simulations demonstrate that lifting trajectories produce an increasing footprint width as ballistic coefficient is increased from 20 psf to 30 psf, where the width peaks, then begins to decrease with further increases in ballistic coefficient. The simulations use 20 psf to achieve the maximum width (most conservative) rather than 30 psf because the 30 psf results would artificially extend the footprint boundary too far into Louisiana, which is not supported by found debris or radar data. Thus, the team converged on 20 psf as the appropriate value above which the simulations do not model L/D.

The methodology uniformly distributes a full range of L/D of 0.0 - 0.15 for the ballistic coefficients shown, up to the maximum 20 psf.

Figure 4-31 shows the results of the heel-shaping Monte Carlo runs. The impact points are simulated impact points, and are not representative of actual debris or the actual debris distribution within the debris footprint. Note that to arrive at an actual debris distribution, one would have to know three things:

1) A histogram of ballistic coefficients vs. quantity. At some point, if ballistic coefficients are tabulated for ALL Columbia debris, this histogram could be generated. Until then, one could only assume a histogram. The Debris Footprint Team believes that the majority of debris is in the 0.5 - 20 psf range, followed by 20 - 40 psf, 40 - 60 psf, with a minimal amount of debris above 60 psf.

2) A histogram of separation altitude vs. ballistic coefficient. In general, the Debris Footprint Team believes that lower ballistic coefficient objects will tend to separate from their parent objects earlier than higher ballistic coefficient objects. Again, one can only make assumptions about this behavior.
3) A histogram of L/D vs. ballistic coefficient. In general, the Debris Footprint Team believes that only low ballistic coefficient objects are capable of sustained L/D (in magnitude and direction), and that the L/D capability drops off very sharply as ballistic coefficient increases. However, one can only make assumptions about the exact nature of this curve.

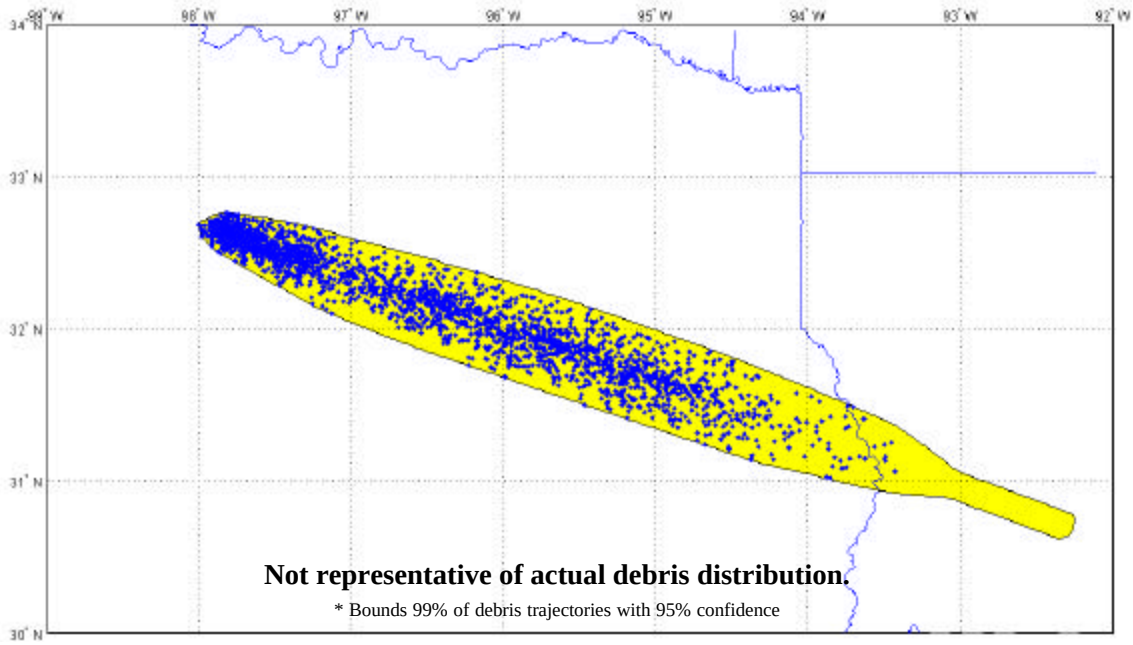

Figure 4-31: Heel Shaping Results of Estimated Columbia Primary Debris Field
Ballistic Coefficients Between 0.5 psf & 20 psf, L/D 0-0.15, C_d 1.0
Propagated from Orbiter State at GMT 13:59:37.00

The methodology continues with finding the toe of the footprint. In Figure 4-32, the Debris Footprint Team simulates no L/D for ballistic coefficients from 10 psf up to 220 psf.

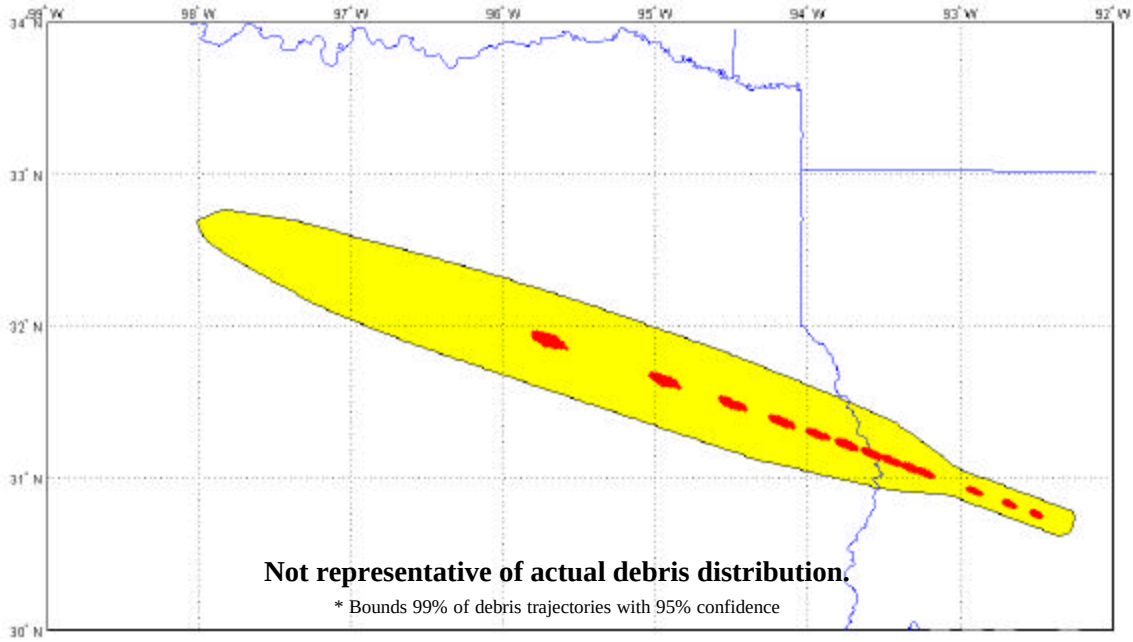

Figure 4-32: Toe Shaping Results of Estimated Columbia Primary Debris Field
Ballistic Coefficients Between 10 & 220 psf, L/D = 0, C_d 1.0
Propagated from Orbiter State at GMT 13:59:37.00

The methodology continues with defining the shape of the footprint between the heel and the toe. Here the Debris Footprint Team uniformly distributes a full range of L/D of 0.0 - 0.15 for 1.5 and 20 psf ballistic coefficients, for IC's every 15 seconds along the 220 psf ballistic trajectories. The footprint is shaped by shedding lifting objects every 15 seconds from the highest-altitude trajectory possible, as defined by a ballistic 220 psf (observed) trajectory from the last BET or GPS vector. These are shown below in Figure 4-33, with the 1.5 psf simulation on the left, 20 psf simulation on the right. The impact points are simulated impact points, and are not representative of actual debris or the actual debris distribution within the debris footprint.

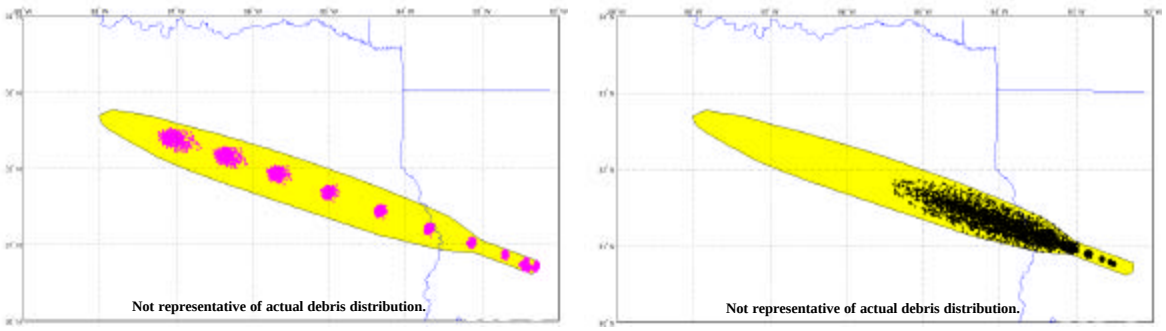

Figure 4-33:
Post-Breakup Shed Debris Shaping Results of Estimated Columbia Primary Debris Field,
Ballistic Coefficient of 1.5 and 20 psf, L/D 0-0.15, C_d 1.0
Propagated from Various States Along a Simulated 220 psf Trajectory

The primary debris footprint is shaped by combining the “sub” footprints from Figures 4-31 through 4-33. This is shown below in Figure 4-34.

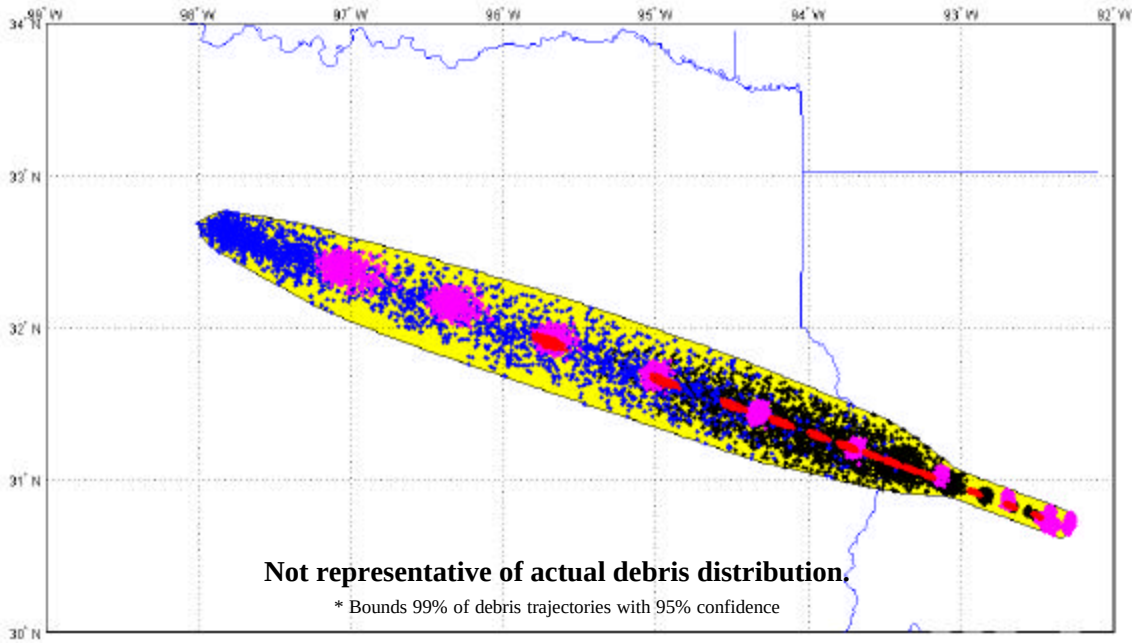

Figure 4-34: Shaping Results of Estimated Columbia Primary Debris Field Propagated from Orbiter State at GMT 13:59:37.00

The final primary debris footprint was derived based on this shaping technique and initial conditions that the Debris Footprint Team believes to bound the time during which the orbiter became a ballistic object. Figure 4-35 shows this footprint.

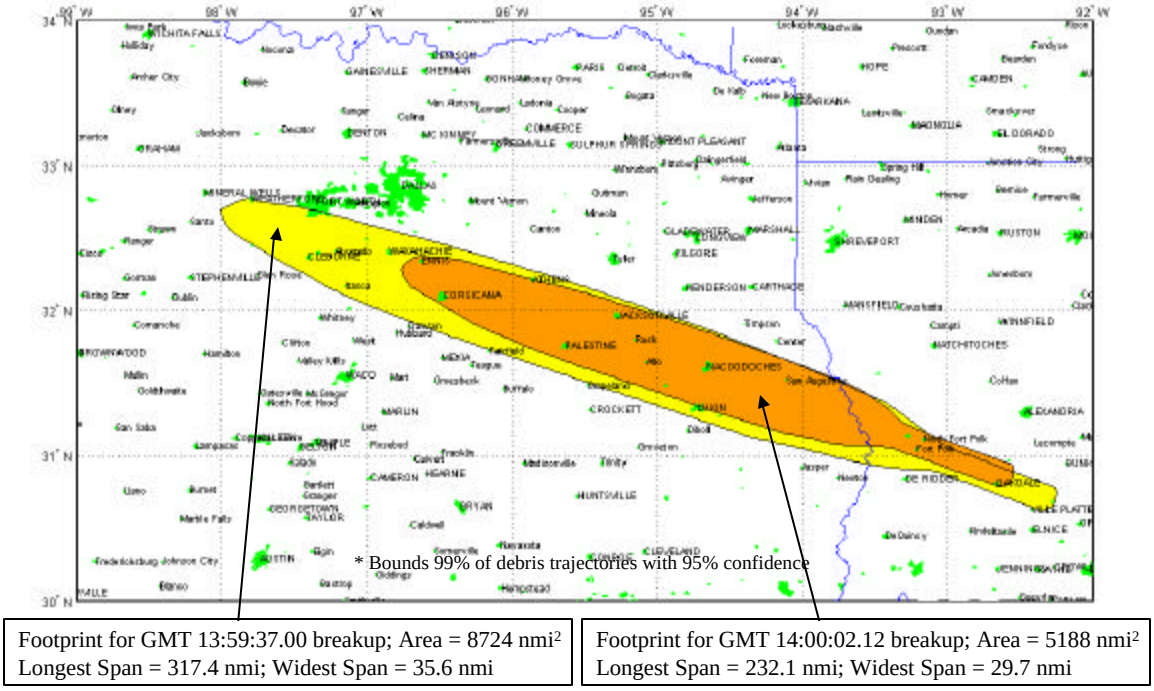

Figure 4-35: Estimated Columbia Primary Debris Fields

Figure 4-36 shows the centerlines of the two predicted primary debris footprints, their relationship to each other and to the "NASA 2/20" (Feb 20) line, as fit to significant debris items found [45]. Figure 4-37 shows the centerlines of the two predicted primary debris footprints and their relationship to the found locations of the three SSME powerheads.

The 13:59:37.00 and 14:00:02.12 centerlines vary in distance from 2.5 - 3.0 nm from each other. The 14:00:02.12 footprint is smaller and shifted north of the 13:59:37.00 footprint. The smaller footprint is due to lower and steeper conditions at 14:00:02.12 as compared to 13:59:37.00 GMT. The northern shift of the 14:00:02.12 footprint relative to the 13:59:37.00 footprint is due to banking lift between these two times.

Excellent agreement is seen between the 14:00:02.12 simulated centerline and the NASA 2/20 curve fit through found debris.

Excellent agreement is seen between the two centerlines and the debris listed in the May 29, 2003 SRIL [46]. The Debris Footprint Team uses the SRIL rather than any of the other debris databases available, based on the belief that investigators have scrutinized the SRIL debris more than the other general debris, and that this scrutiny led to fewer errors in the latitude and longitude coordinates that are common in the other debris databases thus far. (Although the team has spotted some SRIL data that is questionable.) All three Space Shuttle Main Engine (SSME) powerheads landed between the two centerlines, within 3 nm of each other (2 nm in crossrange), and each within 1.0 nm from a centerline (extremely high-β objects should land on the centerline) [47], [48], [49].

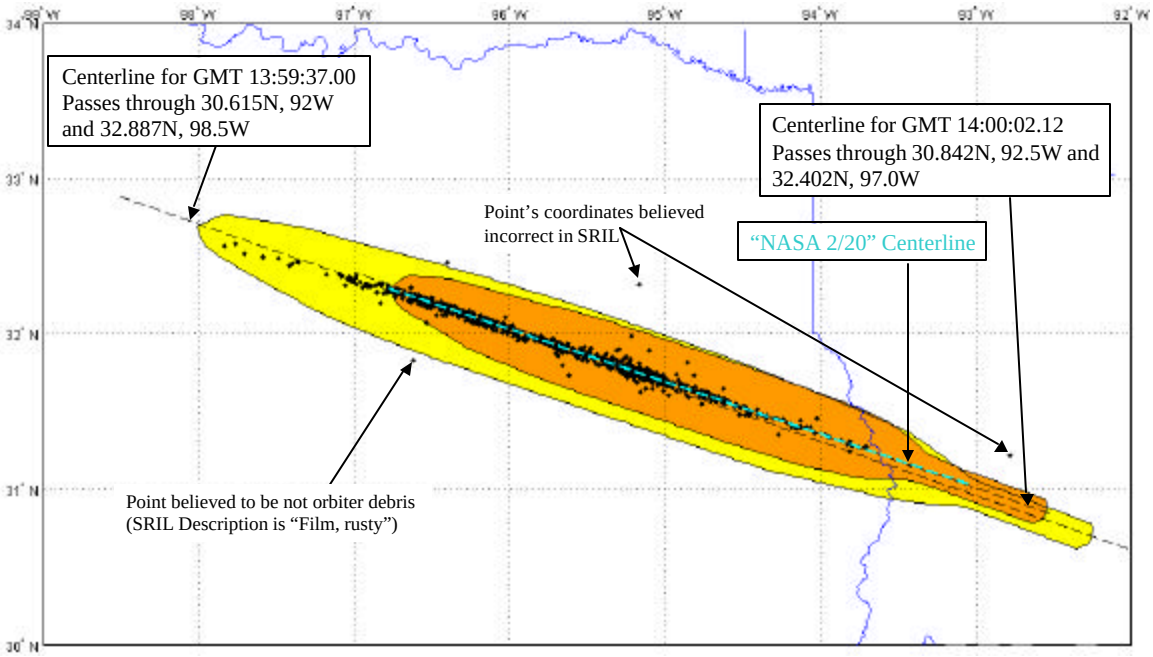

Figure 4-36: Estimated Columbia Primary Debris Fields and Centerlines
Points from Significant Recovered Items List (SRIL 5/29/03 [46])

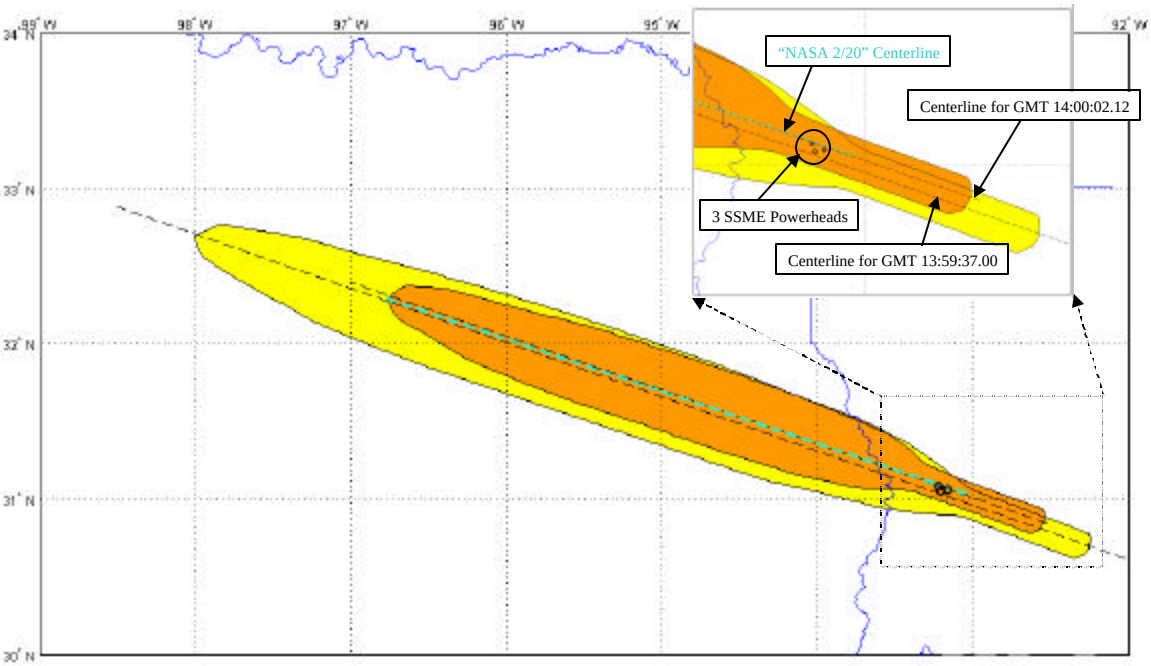

Figure 4-37: Estimated Columbia Primary Debris Fields and Centerlines

Another excellent way to validate the predicted primary debris footprint boundaries is to compare them to Air Traffic Control (ATC) radar hits during the timeframe of the accident. The next five figures coplot ATC radar data with the predicted primary debris footprint boundaries.

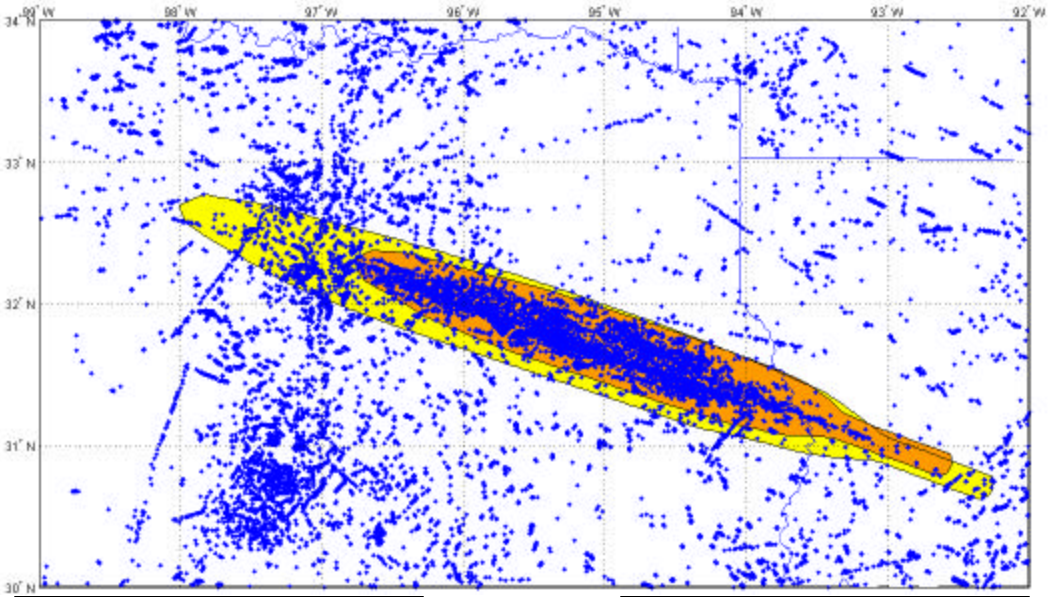

Start of Radar Hits = GMT 13:59:37
End of Radar Hits = GMT 14:10:24

A "Primary Target" is recorded when a radar signal is reflected off an object's surface and returns to the radar site for processing and display.

Figure 4-38: Estimated Columbia Primary Debris Fields and "Primary Targets" from Available ATC Radars, 13:59:37 - 14:10:24Z

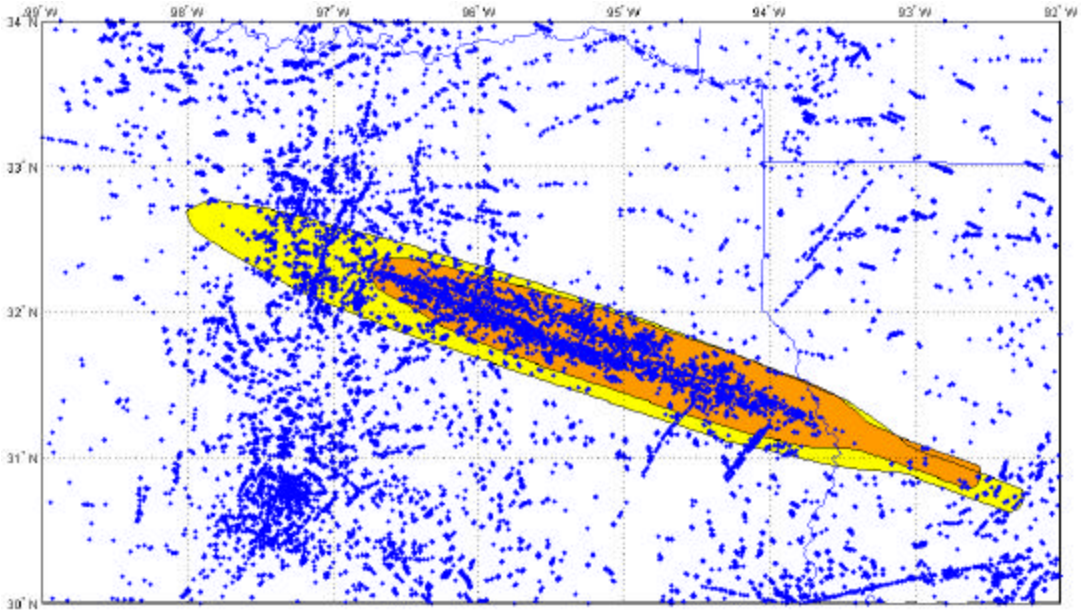

Start of Radar Hits = GMT 14:10:24
End of Radar Hits = GMT 14:20:13

A "Primary Target" is recorded when a radar signal is reflected off an object's surface and returns to the radar site for processing and display.

Figure 4-39: Estimated Columbia Primary Debris Fields and "Primary Targets" from Available ATC Radars, 14:10:24 - 14:20:13Z

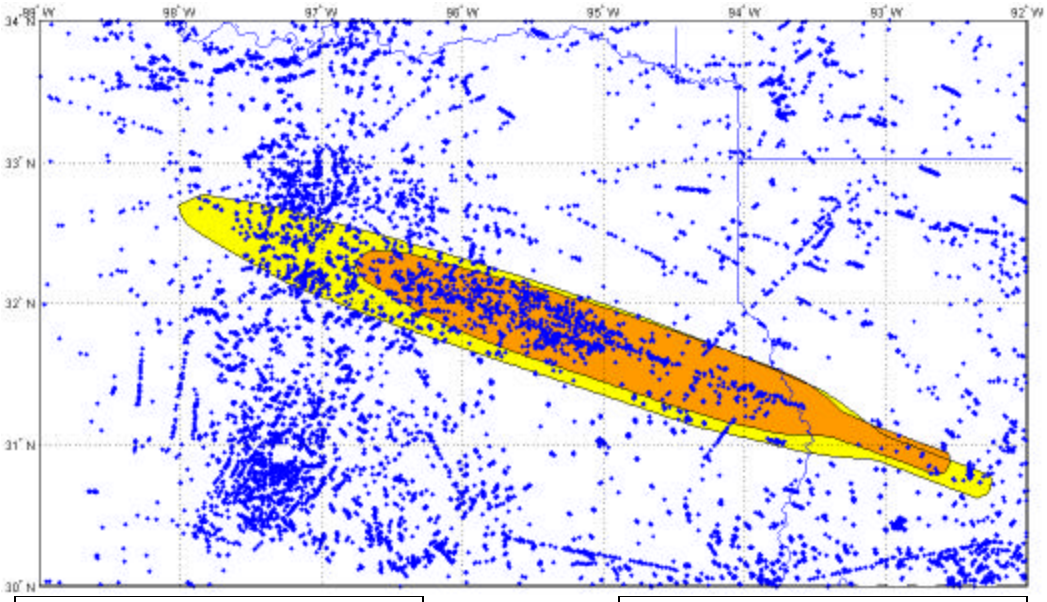

Start of Radar Hits = GMT 14:20:13
End of Radar Hits = GMT 14:30:05

A "Primary Target" is recorded when a radar signal is reflected off an object's surface and returns to the radar site for processing and display.

Figure 4-40: Estimated Columbia Primary Debris Fields and "Primary Targets" from Available ATC Radars, 14:20:13 - 14:30:05Z

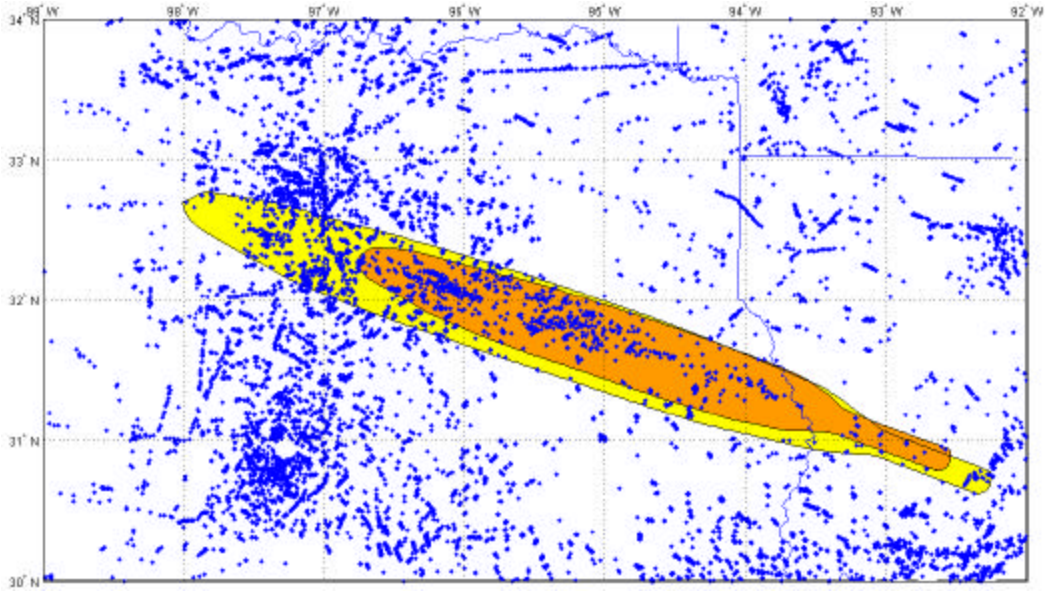

Start of Radar Hits = GMT 14:30:05
End of Radar Hits = GMT 14:40:11

A "Primary Target" is recorded when a radar signal is reflected off an object's surface and returns to the radar site for processing and display.

Figure 4-41: Estimated Columbia Primary Debris Fields and "Primary Targets" from Available ATC Radars, 14:30:05 - 14:40:11Z

Figure 4-42 superimposes all ATC radar hits for the period of time approximately starting at the time of the accident and extending for 40 minutes. This is a composite plot of the previous four figures. A clear clustering of radar hits is seen to fit extremely well in the 14:00:02.12 GMT debris footprint boundary.

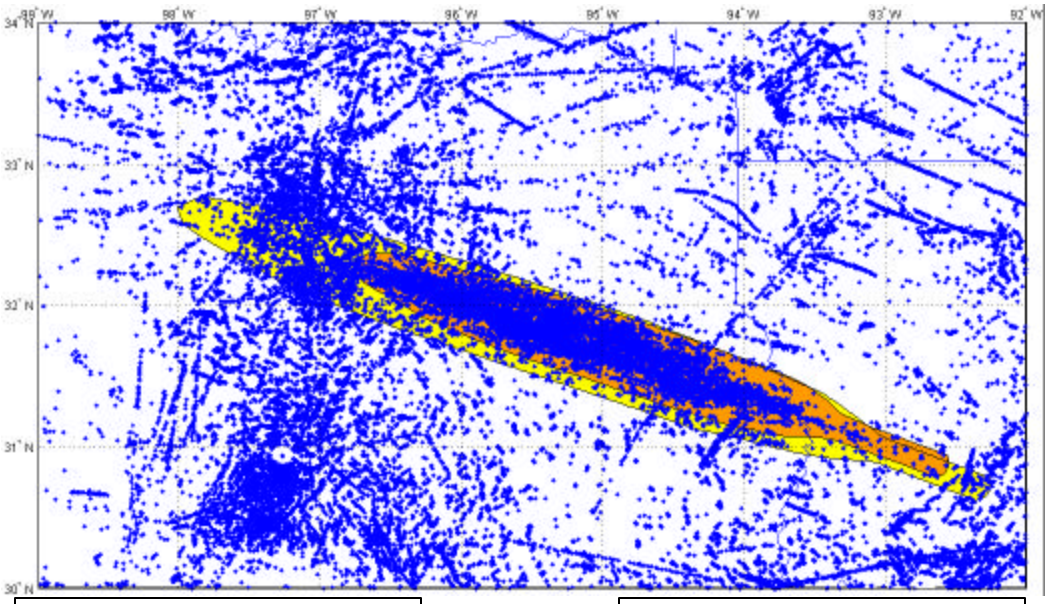

Start of Radar Hits = GMT 13:59:37
End of Radar Hits = GMT 14:40:11

A "Primary Target" is recorded when a radar signal is reflected off an object's surface and returns to the radar site for processing and display.

Figure 4-42: Estimated Columbia Primary Debris Fields and "Primary Targets" from Available ATC Radars, 13:59:37 - 14:40:11

4.3.3. Generic Pre-Breakup Debris Swath

In the days immediately after the accident, the Emergency Operations Center (EOC) fielded hundreds of calls each day from people believing they found Columbia debris, from all over the United States, and some from outside the continental United States. It was necessary to very quickly determine all possible locations in the United States where it was physically possible for debris to have fallen, in order to assist the EOC in focusing on realistic areas and ignoring impossible areas. For example, on the day of delivery of the debris swath, some reports from Phoenix that had previously held a high priority immediately moved to low priority. The EOC needed this information a week before the relative motion and ballistics personnel started analyzing pre-breakup shed debris in video, thus JSC-DM generated a generic debris swath.

Initially, the Debris Footprint Team only considered very low ballistic coefficient objects, as the team believed that only low-β objects could have fallen off of the orbiter without significant flight control activity onboard the vehicle, and without the crew noticing. The first pre-breakup debris analyzed in video (Debris 6) misled the team into assuming this was a very high ballistic coefficient object, perhaps only slightly lower than the approximately 100 psf ballistic coefficient of the orbiter at the Debris 6 time. Thus, the team also looked at very high ballistic coefficient debris to bound the region where debris could have fallen. Later, the video-based relative motion work showed that nothing higher than about 5 psf fell off of the orbiter, indicating that the team could ignore the higher ballistic coefficient swath. However, the team decided to continue analyzing high ballistic coefficient debris for several reasons. First, several videotaped debris awaited analysis. Second, not all of the trajectory has videotape coverage. Finally, it is still important to consider higher ballistic coefficients because if such objects exist, then they would tend to stray farther from the orbiter's groundtrack due to their momentum carrying them "straight" relative to the banking trajectory of the orbiter. This would expand the range of possible impact locations, as the upcoming figures will show.

The simulations assumed a 0.5 psf and a 220 psf piece shed once every minute, starting at Entry Interface, 400 kft altitude. Again, the team chose 220 psf as that was the maximum observed ballistic coefficient in the debris field. Low-ß object assumptions: minimum ß of 0.5 psf; lifting, L/D varied uniformly from 0 - 0.15; bank from 0 deg - 360 deg. High-ß object assumptions: maximum ß of 220 psf; no lift. The resulting "swath" results from merging all resulting debris footprints.

Figure 4-43 shows the "low- ß" debris swath. Figures 4-44 and 45 show this swath laying over the "high- ß" debris swath. Lifting and non-lifting footprints appear. The "without lift" footprints indicate where debris is more likely to land. The "with lift" footprints indicate the total area of expected impact (99% probability with 95% confidence). The footprints shown are the ground impact areas. The Debris Footprint Team also generated footprints for 80,000 ft altitude for use by the Radar Analysis Team as described in Section 5.

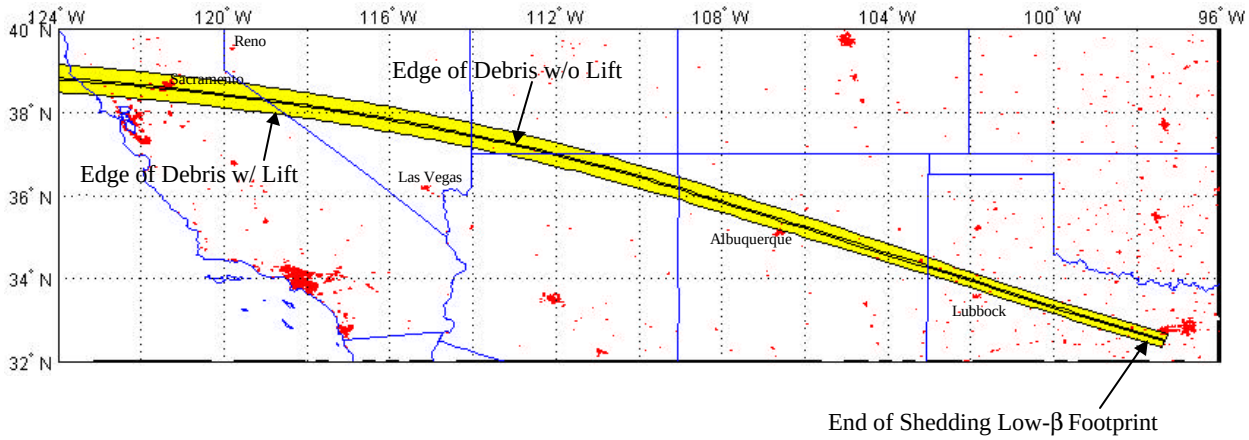

Figure 4-43: Probable Ground Impact Area for Shedding Low-β Debris
Ballistic Coefficient of 0.5 psf, 0-0.15 zL/D, C_d 1.0

Figure 4-44 shows the western half of the resulting ground impact debris swath that would capture any 0.5 psf debris shed pre-breakup, overlaid on the resulting ground impact debris swath that would capture any higher ballistic coefficient (up to 220 psf) debris shed pre-breakup. It is interesting to note that the 220 psf simulated debris footprint is not centered about the groundtrack, but tends to extend quite a bit to the north in this figure. This is due to the momentum of the higher-ß objects carrying them "straight" while the orbiter is banking toward the south.

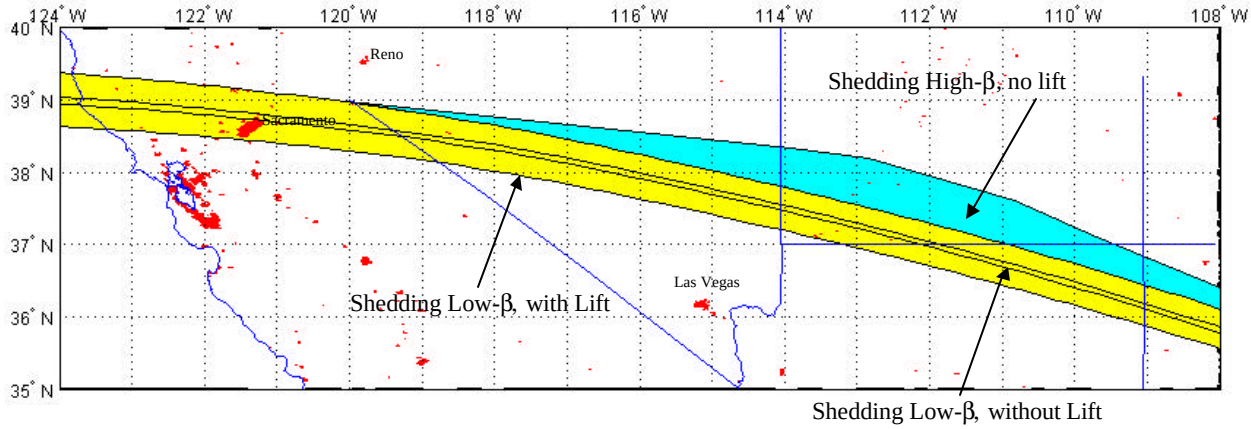

Figure 4-44: Probable Ground Impact Area for Shedding Debris
Ballistic Coefficient of 0.5 psf, 0-0.15 L/D & 220 psf, 0 L/D, C_d 1.0

Figure 4-45 shows the eastern half of the resulting ground impact debris swath that would capture any 0.5 psf debris shed pre-breakup, overlaid on the resulting ground impact debris swath that would capture any higher ballistic coefficient (up to 220 psf) debris shed pre-breakup. Here, note that the 220 psf simulated debris footprint is again not centered about the groundtrack, and begins to shift its extension from north of the groundtrack towards the south on this figure. This is due to the momentum of the higher-ß objects carrying them "straight". While the Orbiter is banking toward the south initially, and thus high-ß objects tend to land north of the

groundtrack, that effect shifts as the Orbiter does a roll-reversal and begins banking toward the north, thus the high-ß objects then tend to land south of the groundtrack. Because of this, if any high-ß objects found south of the primary debris footprint's southern boundary would be a suspect for falling off the orbiter prior to the catastrophic breakup.

Although not shown here, it is possible that debris that fell off the Orbiter prior to catastrophic breakup could have landed within the primary debris footprint boundary. If such debris is found, the more west it is found, the more likely it is debris that came off pre-breakup.

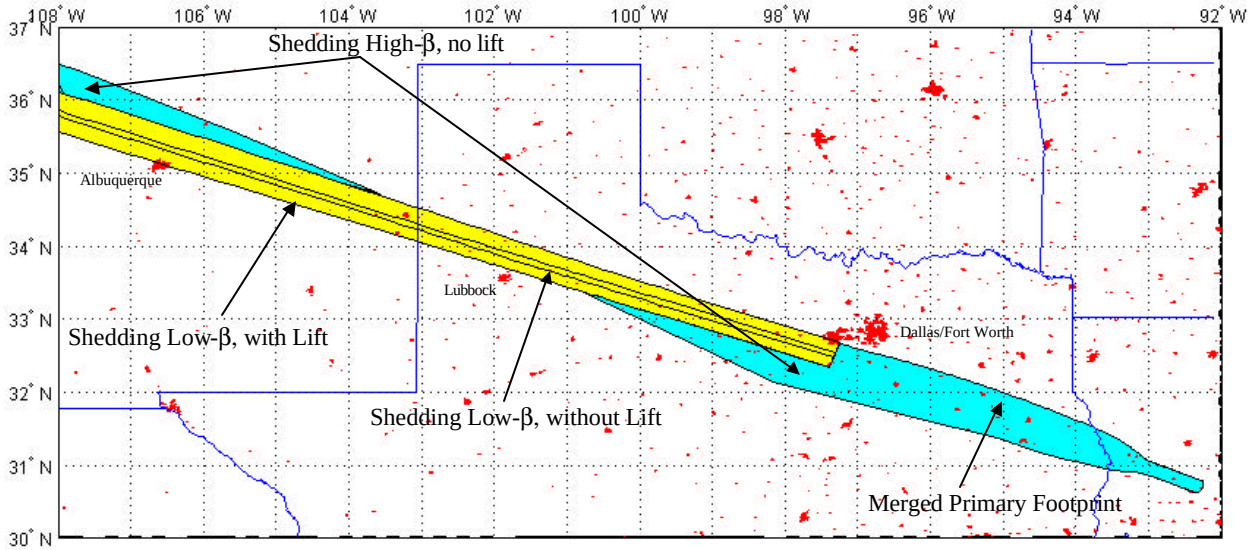

Figure 4-45: Probable Ground Impact Area for Shedding Debris
Ballistic Coefficient of 0.5 psf, 0-0.15 L/D & 220 psf, 0 L/D, C_d 1.0

The next three figures are the low-ß debris swaths with ground impact areas and times of impact for various assumed separation times for debris with an assumed ballistic coefficient of 0.5 psf. These were used to estimate the footprints for low-ß debris shed from any time in the trajectory and were a starting point for trajectory analysis of the debris shedding observed in public video. These results were delivered to the Kennedy Space Center Weather Office, who forwarded them to the Coast Guard and Navy for use with ocean current models to predict beaching locations of any debris that may have landed in the ocean and floated to a beach. The JSC Radar Analysis Team made use of the resulting times over land.

Here is an example of how to read these plots. If one was interested in when a 0.5 psf piece of debris falling off of the orbiter at 13:44:09 GMT would hit the ocean, locate the box with that initial condition (IC) time, and one would see a minimum time and maximum time in the impact time range (in this case 14:27:58.6 - 14:33:17.6 GMT). If one then traces the line from the box down to the "T," then follows left to the dot, and down to the swath, one finds the heel, or western-most line that the debris could have landed. If, instead of left, one traces from the "T" to the right and to the dot, and down again to the swath, one finds the toe, or eastern-most line that the debris could have landed.

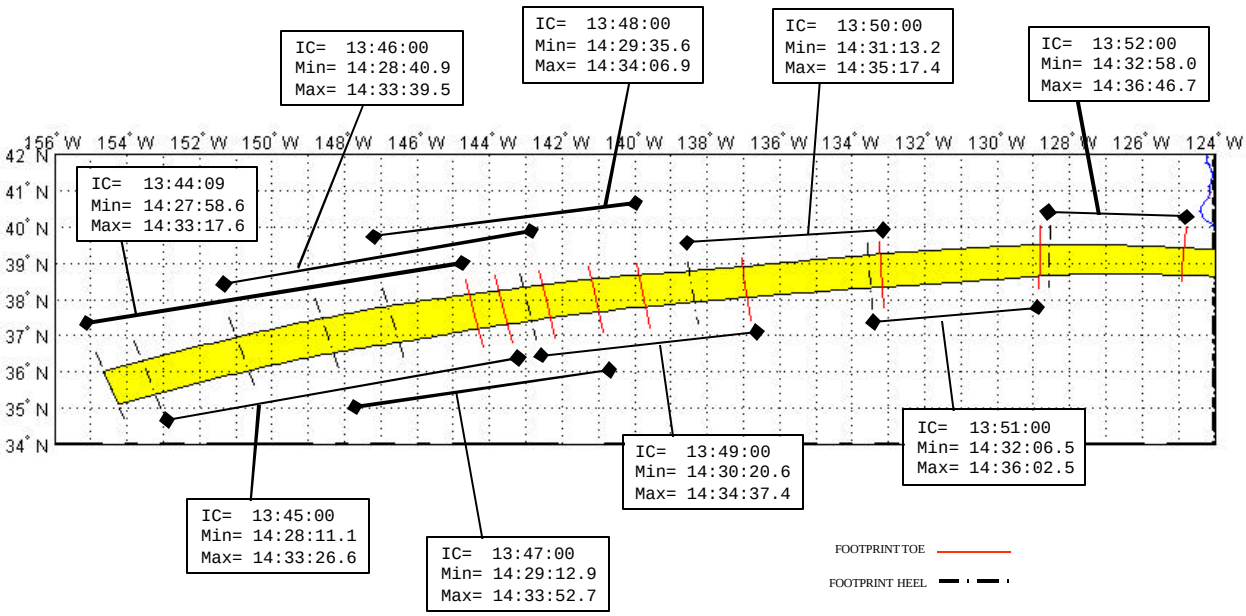

Figure 4-46: Probable Ground Impact Area* for Shedding Low-ß Debris
Off Shore Approaching California
Ballistic Coefficient of 0.5 psf, 0-0.15 L/D, C_d 1.0

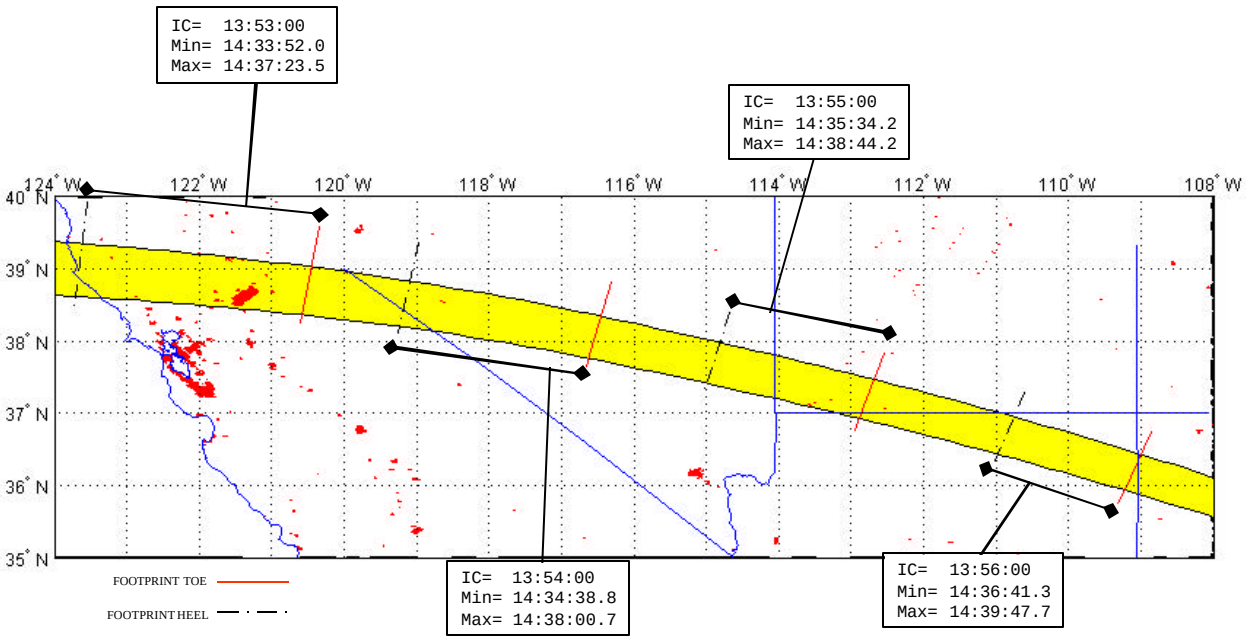

Figure 4-47: Probable Ground Impact Area* for Shedding Low-ß Debris
California through New Mexico
Ballistic Coefficient of 0.5 psf, 0-0.15 L/D, C_d 1.0

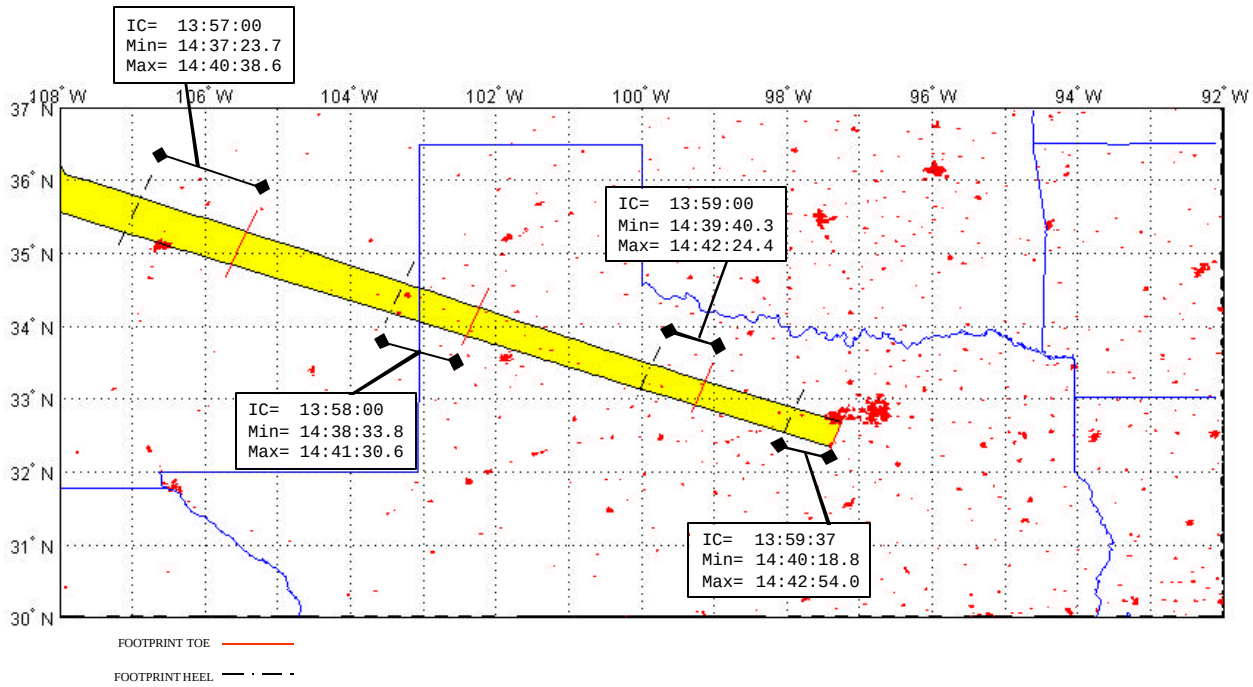

Figure 4-48: Probable Ground Impact Area* for Shedding Low-ß Debris
New Mexico through Texas
Ballistic Coefficient of 0.5 psf, 0-0.15 L/D, C_d 1.0

Based on both the primary debris footprint and the generic swath work, Table 4-6 shows a list of counties across the United States that pre-breakup debris may have landed in as a result of the Columbia entry on February 01, 2003. Some counties are more likely candidates than others, and in some cases only a portion of that county is within any of the debris footprint boundaries.

California Counties	Nevada Counties	Utah Counties	Arizona Counties	New Mexico Counties	Texas Counties			Louisiana Counties
Alpine (a) Amador (b) Calaveras (c) Colusa (b) El Dorado (a) Lake (b) Mendocino (b) Mono (c) Napa (b) Nevada (c) Placer (c) Sacramento (b) Solano (c) Sonoma (b) Sutter (b) Tuolumne (c) Yolo (a) Yuba (c)	Churchill (c) Douglas (b) Esmeralda (c) Lincoln (b) Lyon (b) Mineral (b) Nye (b)	Beaver (c) Garfield (b) Iron (a) Kane (a) Piute (c) San Juan (c) Washington (c)	Apache (b) Coconino (c) Mohave (c) Navajo (c)	Bernalillo (c) Curry (b) De Baca (c) Guadalupe (b) Los Alamos (a) McKinley (b) Quay (c) Rio Arriba (c) Roosevelt (c) San Juan (b) San Miguel (c) Sandoval (a) Santa Fe (b) Torrance (c)	Anderson (b*) Angelina (b*) Bailey (b) Bosque (c) Castro (c) Cherokee (b*) Crosby (b) Dallas (c*) Dickens (b) Eastland (c) Ellis (b*) Erath (b) Floyd (c) Freestone (b*) Hale (b) Haskell (b) Henderson (b*)	Hill (b*) Hockley (c) Hood (a) Houston (c*) Jasper (c*) Johnson (b*) Kaufman (c) Kent (c) King (b) Knox (c) Lamb (b) Leon (c) Limestone (c) Lubbock (c) McLennan (c) Motley (c) Nacogdoches (a*)	Navarro (a*) Newton (c*) Palo Pinto (b) Parker (b*) Parmer (c) Rusk (c*) Sabine (b*) San Augustine (a*) Shackelford (c) Shelby (c*) Somervell (a) Stephens (b) Stonewall (b) Tarrant (c*) Throckmorton (b) Trinity (c*) Young (b)	Allen (c*) Beauregard (c*) Evangeline (c*) Rapides (c*) Sabine (c*) Vernon (b*)

Changes from last list: California: added none; removed Contra Costa, Madera, Marin, Mariposa, San Joaquin, and Stanislaus. Nevada: added none; removed Carson, Eureka, Lander, and White Pine. Utah: added none; removed Wayne. Arizona: added none; removed none. New Mexico: added Los Alamos; removed Cibola, Mora, and Valencia. Texas: added many as list now includes primary debris footprints including Anderson, Angelina, Bosque, Cherokee, Dallas, Ellis, Freestone, Henderson, Hill, Hood, Houston, Jasper, Johnson, Kaufman, Leon, Limestone, McLennan, Nacogdoches, Navarro, Newton, Parker, Rusk, Sabine, San Augustine, Shelby, Somervell, Tarrant, and Trinity; removed Archer, Baylor, Briscoe, Callahan, Cochran, Cottle, Fisher, Foard, Garza, Jack, Jones, Smith, and Swisher. Louisiana: added all counties listed as list now includes primary debris footprints; removed none.

KEY:

(a) The entire area of this county is under the general debris swath (no *), or is within the primary debris footprint boundaries (*).

(b) Most of this county (< 100% but greater >50% of this county's area) is under the general debris swath (no*), or is within the primary debris footprint boundaries (*).

(c) This county is partially under the general debris swath (less than 50% of the county's area) (no *), or is within the primary debris footprint boundaries (*).

Table 4-6: List of Counties Which May Have Columbia Debris

4.3.4. Pre-Breakup Shedding Debris Footprints

NASA has identified nineteen videos that recorded debris falling off of Columbia prior to its catastrophic breakup. Members of the public videotaped twenty distinct debris shedding events and three plasma envelope flashes or flares. In some cases, many of these events appear in multiple videos, and in one case as many as seven videos recorded the same event. NASA carefully screened the videos against previous shuttle entry videos to ensure that debris events were indeed not something that has been seen in previous shuttle entries. [22]

An assessment by the JSC Orbital Debris Program Office predicted that a tile with a ballistic coefficient on the order found in the relative motion results (3.1 psf) would survive to ground impact [51]. Thus, predicting impact points was given a high priority with a goal of locating and recovering pre-breakup debris.

The relative motion and ballistics experts established the initial time of shedding and ballistic coefficient based on videotape analysis. The simulation initializes at the orbiter's state vector at the beginning and end of the computed separation time range. The Debris Footprint Team scaled each derived ballistic coefficient to account for the difference in density used by the relative motion team (the measured value at the orbiter's position at the separation time), and the DAO (rev D) density at this same initial condition in the simulation. The density used by the relative motion and ballistics experts affects the resulting estimate of ballistic coefficient. In all cases, these experts used density values derived from onboard measurements. However, to simulate debris falling below the orbiter trajectory, atmosphere data was needed from the orbiter altitude to the ground along the entire groundtrack. DAO provided this data. When the Debris Footprint Team simulates these debris items with the DAO data, the density at the simulation initial condition never exactly matches these derived density values, because the DAO density is based on meteorological estimates. Thus, a scale factor is used to adjust the ballistic coefficients. This is done via: simulated β = derived β * (simulated density / derived density).

Five hundred Monte Carlo simulations bound the footprint with the simulation initialized at the orbiter's state vector and the computed separation time. The simulation included day-of-entry density, and wind speed, and wind direction (DAO rev D), with GRAM-99 uncertainties (rpscale = 1.0, 3σ). JSC-DM generated lifting and non-lifting debris footprint boundaries. The non-lifting results show the highest likelihood area to find the object. The lifting simulations vary L/D uniformly from 0 - 0.15, and bank angle uniformly from 0 - 360 deg.

As described earlier, the methodology assumes a constant ballistic coefficient for the pre-breakup shedding debris. The mass, area, and material properties of the debris are unknown, so the methodology cannot model ablation, or drag changes with Mach number, even if no ablation were taking place. Also, the methodology assumes the object remains as a single, intact piece with ballistic properties as measured from video.

There is no evidence in video that any imparted velocity was involved in the debris motion. However, during the time the object was within the orbiter brightness envelope, until the time that the distance was sufficient for the object to be discernable as a separate object, it is possible

that something could have happened to impart some delta-V. Then again, once the object is no longer visible because it has dimmed out or it has left the camera's field of view, it is possible that an energy release event could have occurred. Regardless, the methodology cannot model this type of event with no information about it, or even that it existed.

JSC-DM did not "shape" these footprints as was done for the primary debris footprint, but retained a rectangular shape. This is reasonable because any errors in the estimates of ballistic coefficient and/or separation time would manifest themselves as range errors. In accounting for these errors, a shaped footprint would stretch in range, and would approach a rectangular shape around the locations of the footprints presented here.

Unfortunately, the rectangular shaping can give artificially wide footprints, primarily for the ballistic (non-lifting) footprints. Due to varying crosswinds in some cases, the scatter of simulated impact points may bend relative to the groundtrack (it is not entirely parallel to the groundtrack). However, the plotting routine always bounds the impact points with a rectangle, and assumes that the sides of the rectangle are parallel to the groundtrack (the sides of the rectangle cannot bend with the impact points); thus the rectangle ends up showing an area that is too wide in these cases, although two of the opposing points of the rectangle will always correspond to the extreme simulated impact points.

Figure 4-49 shows how rectangular footprint shapes are applied to simulated debris, rather than "form-fitting" shapes, and how the rectangular shapes can be artificially wide whenever the simulated debris centerline is not parallel to the groundtrack, as just described. In this figure, the red points are the simulated ballistic (non-lifting) ground impact points for Debris 3.

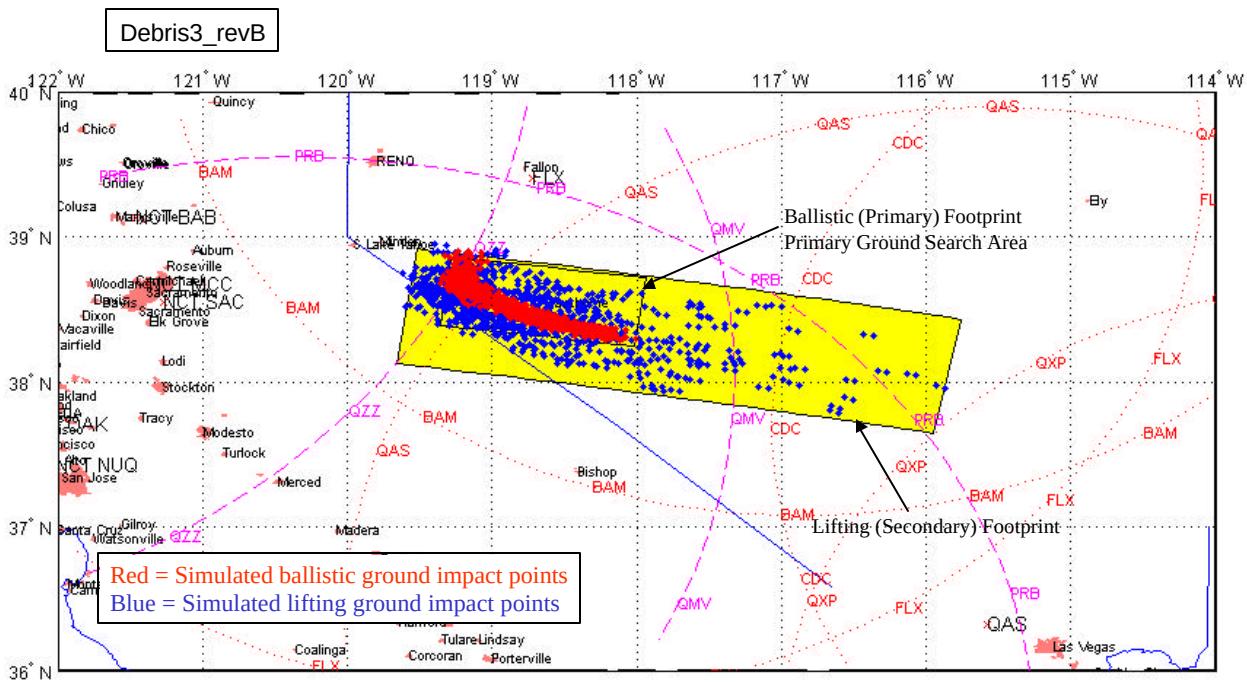

Figure 4-49: Probable Ground Impact Area for Debris 3
and Simulated Impact Points for Observed Debris
Separation Time 13:53:55.6 - 13:53:56.6Z
Constant Ballistic Coefficients between 0.1 to 1.0 psf, 0-0.15 L/D, C_d 1.0

JSC-DM defined Search and Recovery Zones by extending the resulting non-lifting (ballistic) footprint boundaries to the boundaries of the lifting footprint, thus subdividing each entire area into nine different zones, and gave these nine zones likelihood-of-impact values ranging from 1 to 4.

- Zone 1 is the most likely area in which this debris would be found, and is the non-lifting debris footprint.
- Zones 2 are the next most likely areas (errors in separation time and/or ballistic coefficient manifest themselves in range error).
- Zones 3 are the next most likely areas and include lift.
- Zones 4 are the least likely areas, and combine the errors from Zone 2 and lifting.

As with the generic analysis, footprints for each debris shedding event observed in video were generated for 80,000 ft, 35,000 ft and ground impact. Only ground impact footprints are shown in this report. A summary of the observed separation times and ballistic properties are shown in Section 4-2, Table 4-3. The following data are provided in Appendix 10.6 for each of the pre-breakup shedding debris to assist the Radar Analysis Team in locating possible debris tracks:

- latitude/longitude of corner points for all footprints,
- area of all footprints,
- minimum/maximum GMT to altitude,
- airspeed (relative speed) at altitude,

- flight path angle (FPA) (relative topocentric) at altitude,
- groundspeed at altitude,
- Air Traffic Control radar sites which are in range of all lifting debris footprints.

Figure 4-50 shows overlapping debris footprint boundaries for all released debris footprints based on relative motion and ballistics analysis, as well as footprints based on assumed ballistics for Flare 1 and Flare 2, in yellow. This figure shows these results overlaid on results if one assumes a 0.5 - 5.0 psf ballistic coefficient range on videotaped debris whose relative motion and ballistic coefficients are still unknown, in green. Thus, the portion of green that is visible shows potential impact locations for debris 11 and 12 that are outside the released footprints. Note that based on videotaped debris alone, nearly all land under the entire groundtrack is a candidate for potentially finding Columbia debris.

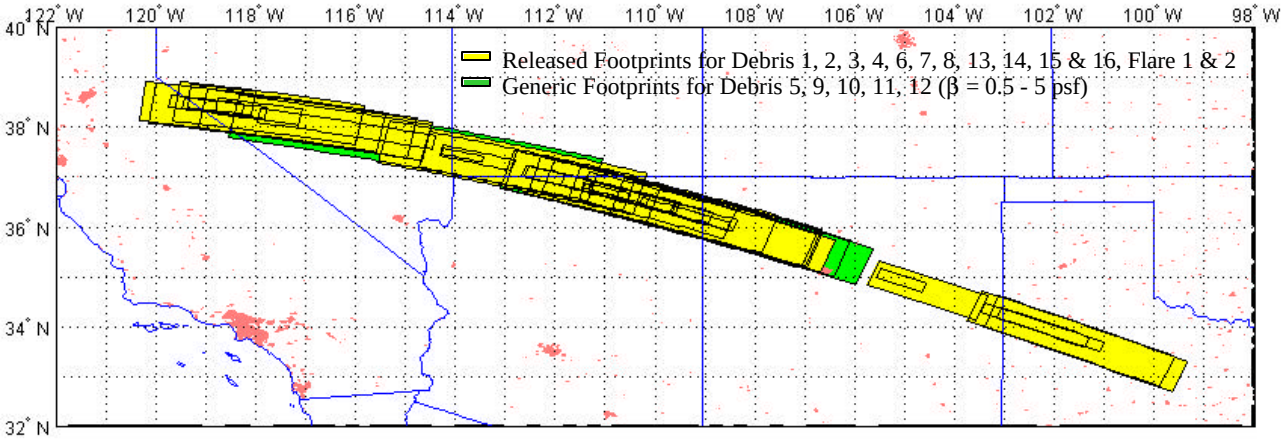

Figure 4-50: Combined Probable Ground Impact Areas
Observed Debris Events 1, 2, 3, 4, 6, 7, 8, 13, 14, 15 & 16 and Assumed Debris at Flare 1 & 2
Constant Ballistic Coefficients, 0-0.15 L/D, C_d 1.0

Figure 4-51 below depicts the amount of overlap among the released (yellow) debris footprints with an emphasis on the non-lifting areas. As more non-lifting areas overlap, the shading becomes darker. The darkest regions in the plot were given higher priority when all areas were prioritized as shown in Table 2-1. Prioritizing these areas and the radar search boxes is described in more detail in Section 5.

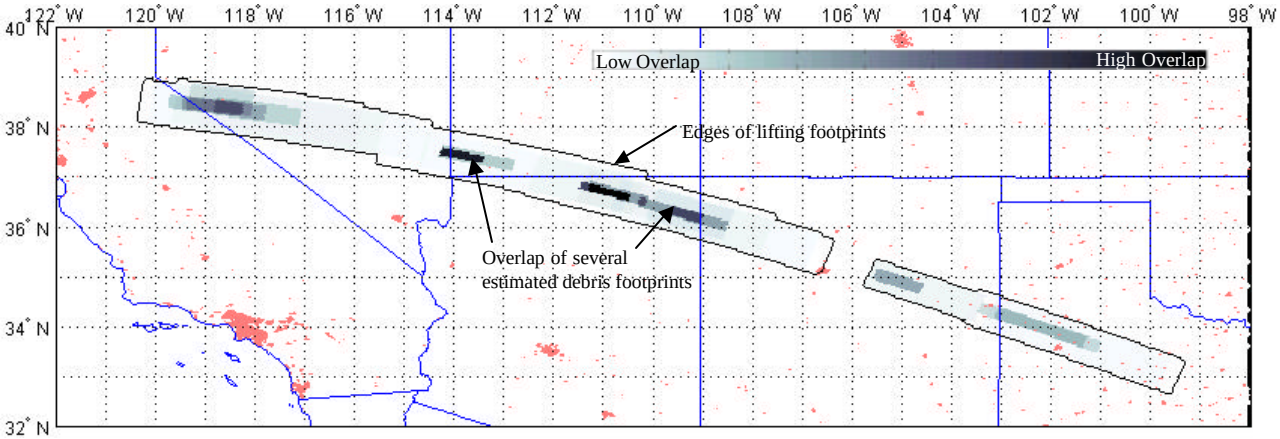

Figure 4-51: Overlapping Non-Lifting Probable Ground Impact Areas
Observed Debris Events 1, 2, 3, 4, 6, 7, 8, 13, 14, 15 & 16 and Assumed Debris at Flare 1 & 2
Constant Ballistic Coefficients, 0-0.15 L/D, C_d 1.0

The following footprints were calculated using the DAO rev D mean atmosphere with GRAM-99 uncertainties (rpscale = 1.0, or 3-sigma) and day-of-entry density at event altitude.

Debris 1

The Aerospace Corporation independently validated the JSC ballistic coefficient, separation time, and both the ballistic (non-lifting) and lifting footprint boundaries, with similar, but slightly different methods for relative motion, ballistic coefficient estimation, and debris footprint estimation [30]. Aerospace calculated an Orbiter/Debris separation time of 13:53:45.4Z compared to a JSC estimate of 13:53:44.2 - 13:53:45.4Z. [23] [30] Likewise, the Aerospace ballistic coefficient was 0.5 - 1.5 psf [30] compared to a JSC estimate of 0.6 - 1.6 psf [23], both derived using day-of-entry density at event altitude.

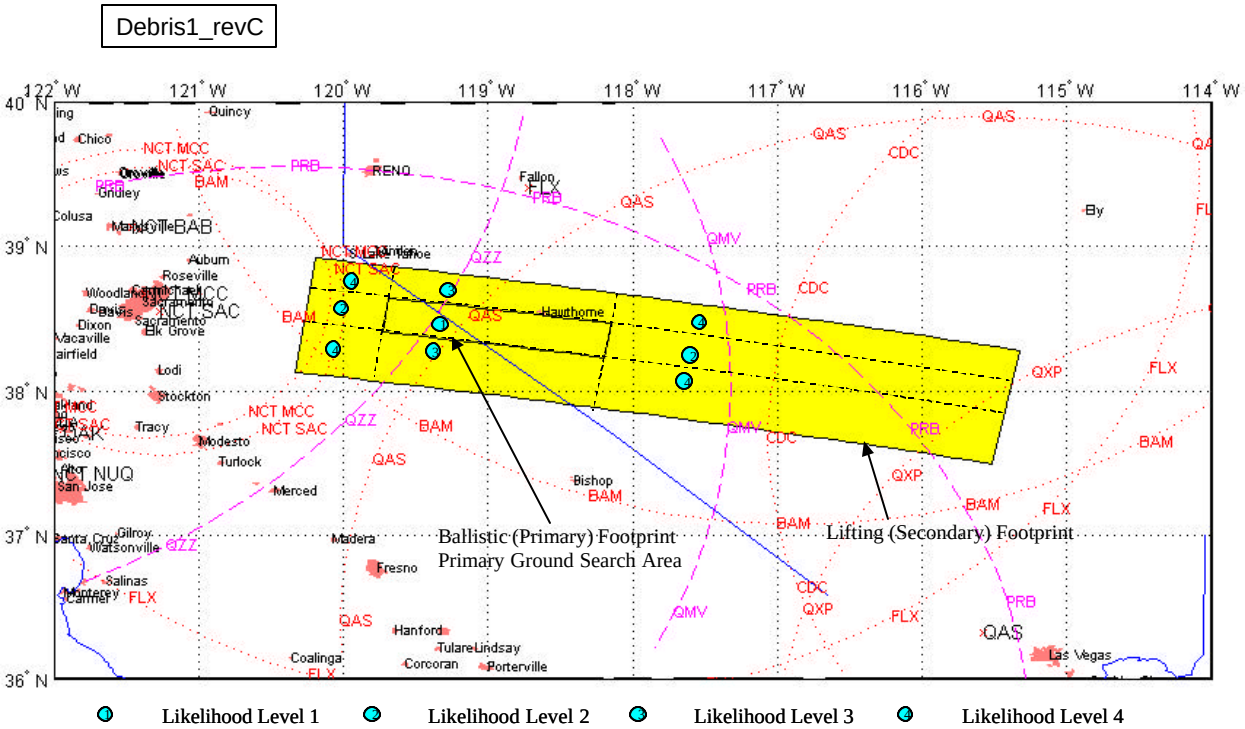

Figure 4-52: Probable Ground Impact Area for Debris 1
Separation Time 13:53:44.2-13:53:45.4Z
Constant Ballistic Coefficients between 0.6 to 1.6 psf, 0-0.15 L/D, C_d 1.0

Debris 2

The Aerospace Corporation independently validated the JSC ballistic coefficient, separation time, and both the ballistic (non-lifting) and lifting footprint boundaries, with similar, but slightly different methods for relative motion, ballistic coefficient estimation, and debris footprint estimation [30]. Aerospace calculated an Orbiter/Debris separation time of 13:53:46.8 compared to a JSC estimate of 13:53:45.9 - 13:53:47.1. [23] [30] Likewise, the Aerospace ballistic coefficient was 1.0 - 2.0 psf [30] compared to a JSC estimate of 0.7 to 1.9 psf [23], both derived using day-of-entry density at event altitude.

Debris2_revB

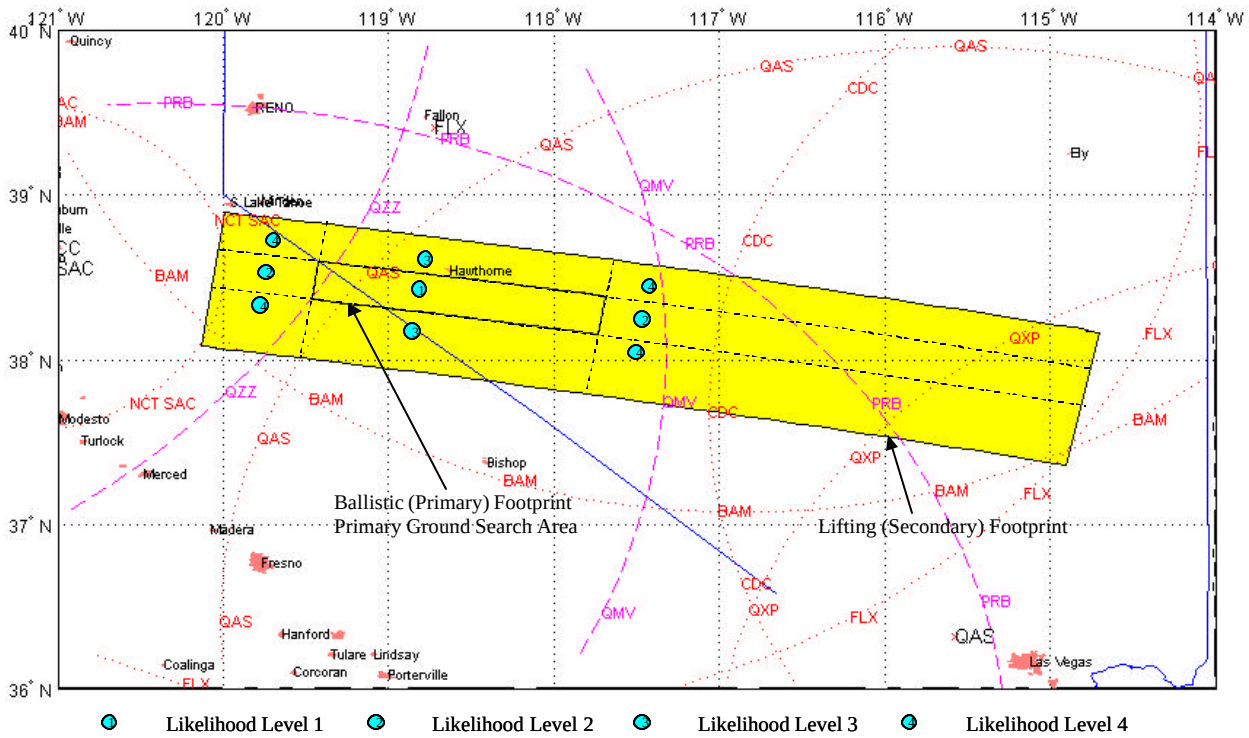

Figure 4-53: Probable Ground Impact Area for Debris 2
Separation Time 13:53:45.9 - 13:53:47.1Z
Constant Ballistic Coefficients between 0.7 to 1.9 psf, 0-0.15 L/D, C_d 1.0

Debris 3

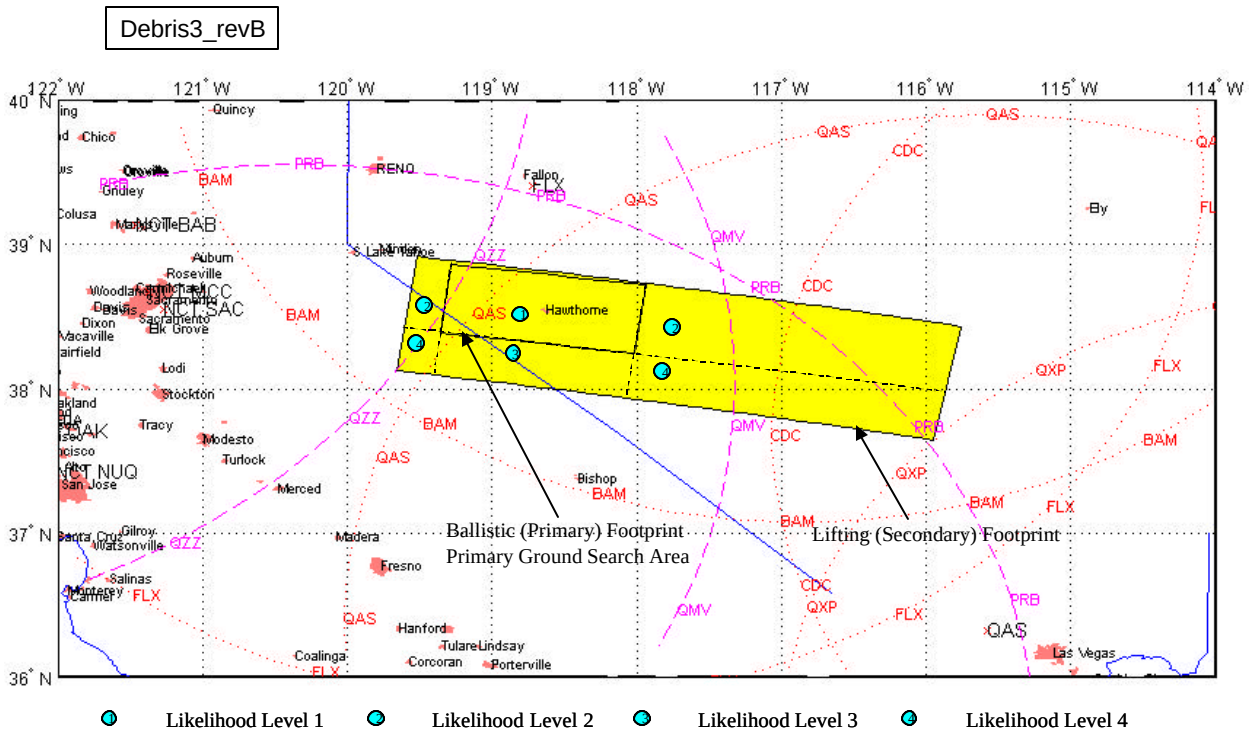

Figure 4-54: Probable Ground Impact Area for Debris 3
Separation Time 13:53:55.6-13:53:56.6Z
Constant Ballistic Coefficients between 0.1 to 1.0 psf, 0-0.15 L/D, C_d 1.0

Debris 4

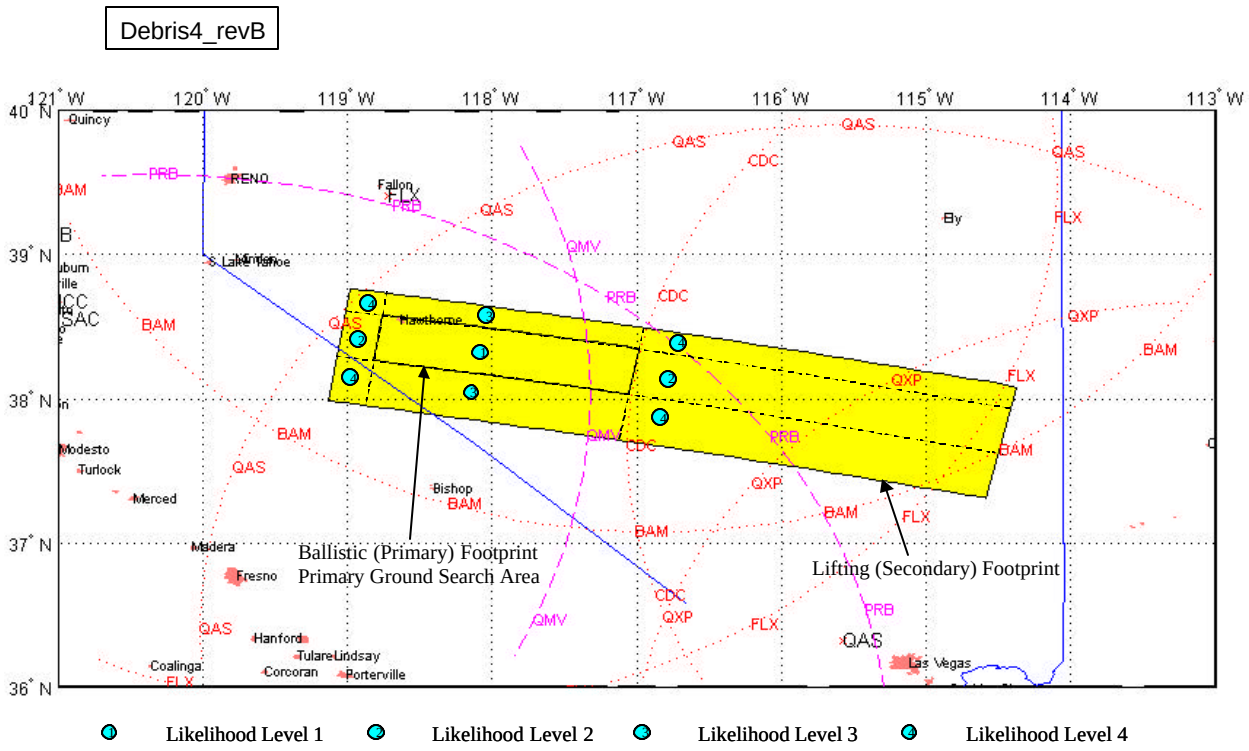

Figure 4-55: Probable Ground Impact Area for Debris 4
Separation Time 13:54:02.3-13:54:03.5Z
Constant Ballistic Coefficients between 0.3 to 1.5 psf, 0-0.15 L/D, C_d 1.0

Debris 6

Video for this object was analyzed first due to the Orbiter and debris crossing of Venus, allowing accurate time estimation

The Aerospace Corporation independently validated the JSC ballistic coefficient, separation time, and both the ballistic (non-lifting) and lifting footprint boundaries, with similar, but slightly different methods for relative motion, ballistic coefficient estimation, and debris footprint estimation [30]. Aerospace calculated an Orbiter/Debris separation time of 13:54:33.72 compared to a JSC estimate of 13:54:33.7-13:54:34.7. [23] [30] The Aerospace ballistic coefficient matched the JSC range of 3.0 - 4.0 psf [30] [23], both derived using day-of-entry density at event altitude.

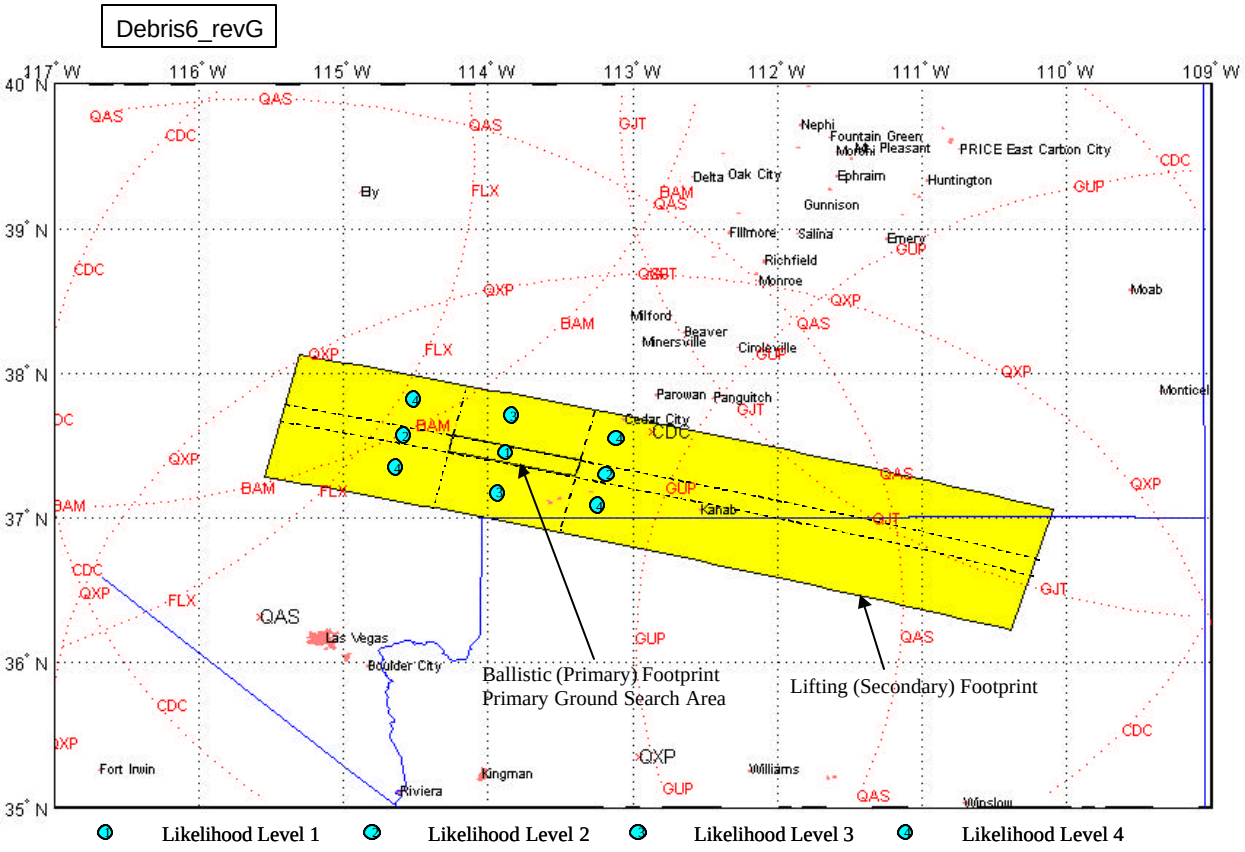

Figure 4-56: Probable Ground Impact Area for Debris 6
Separation Time 13:54:33.7-13:54:34.7Z
Constant Ballistic Coefficients between 3.0 to 4.0 psf, 0-0.15 L/D, C_d 1.0

Debris 7

Debris7_revA

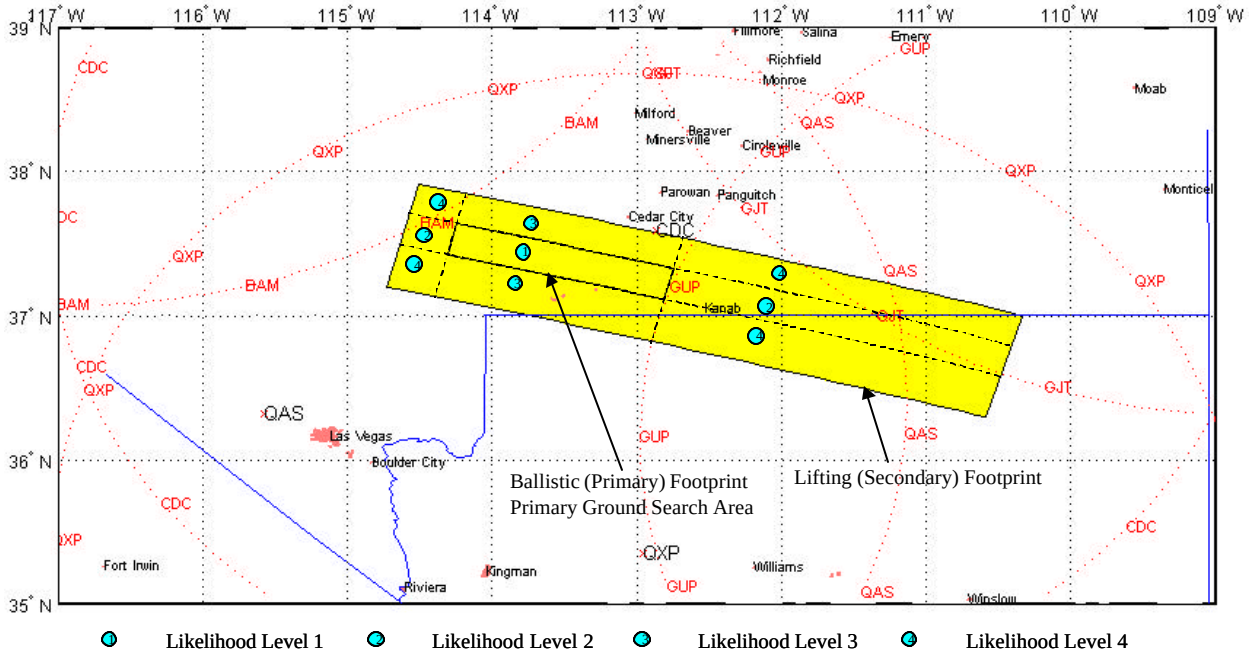

Figure 4-57: Probable Ground Impact Area for Debris 7
Separation Time 13:55:03.6-13:55:04.6Z
Constant Ballistic Coefficients between 0.5 to 1.7 psf, 0-0.15 L/D, C_d 1.0

Debris 8

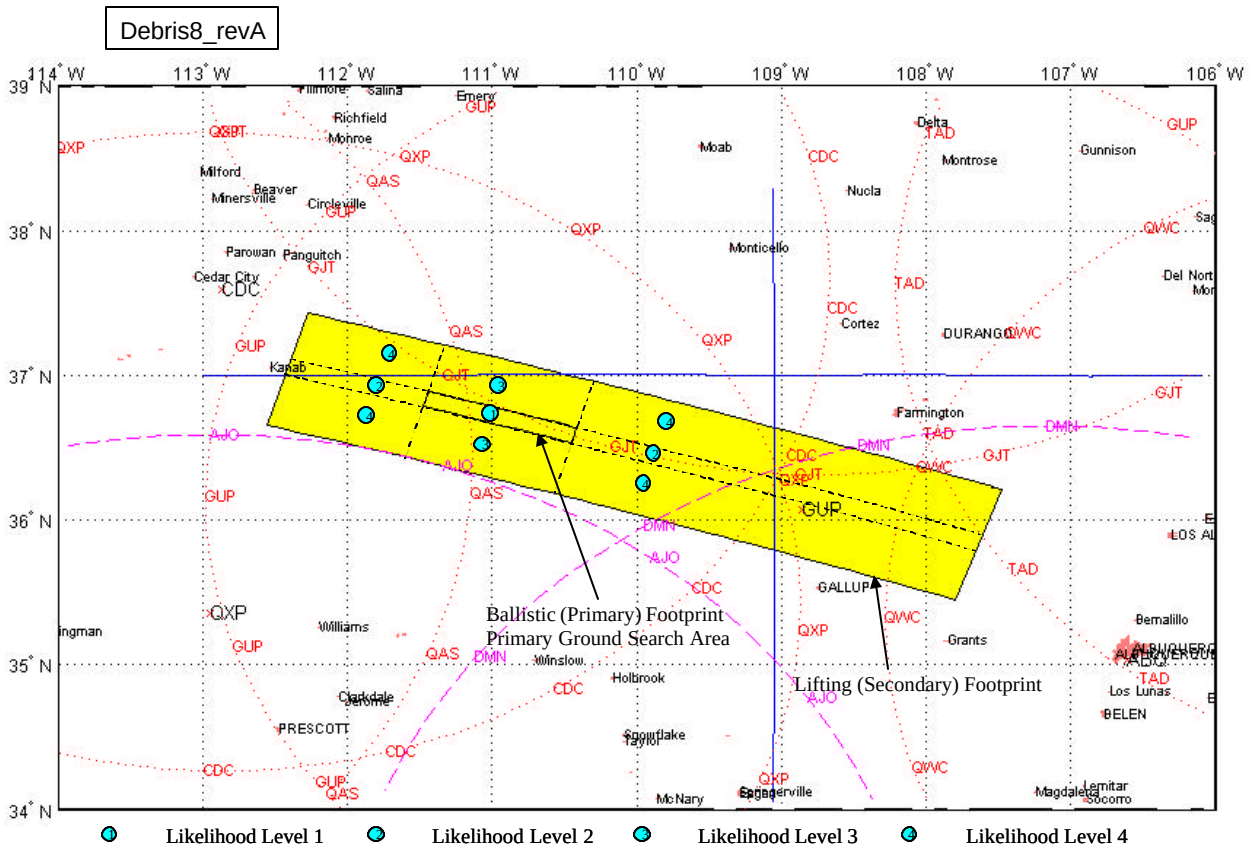

Figure 4-58: Probable Ground Impact Area for Debris 8
Separation Time 13:55:20.2-13:55:21.4Z
Constant Ballistic Coefficients between 2.6 to 4.0 psf, 0-0.15 L/D, C_d 1.0

Debris 13

Debris13_revA

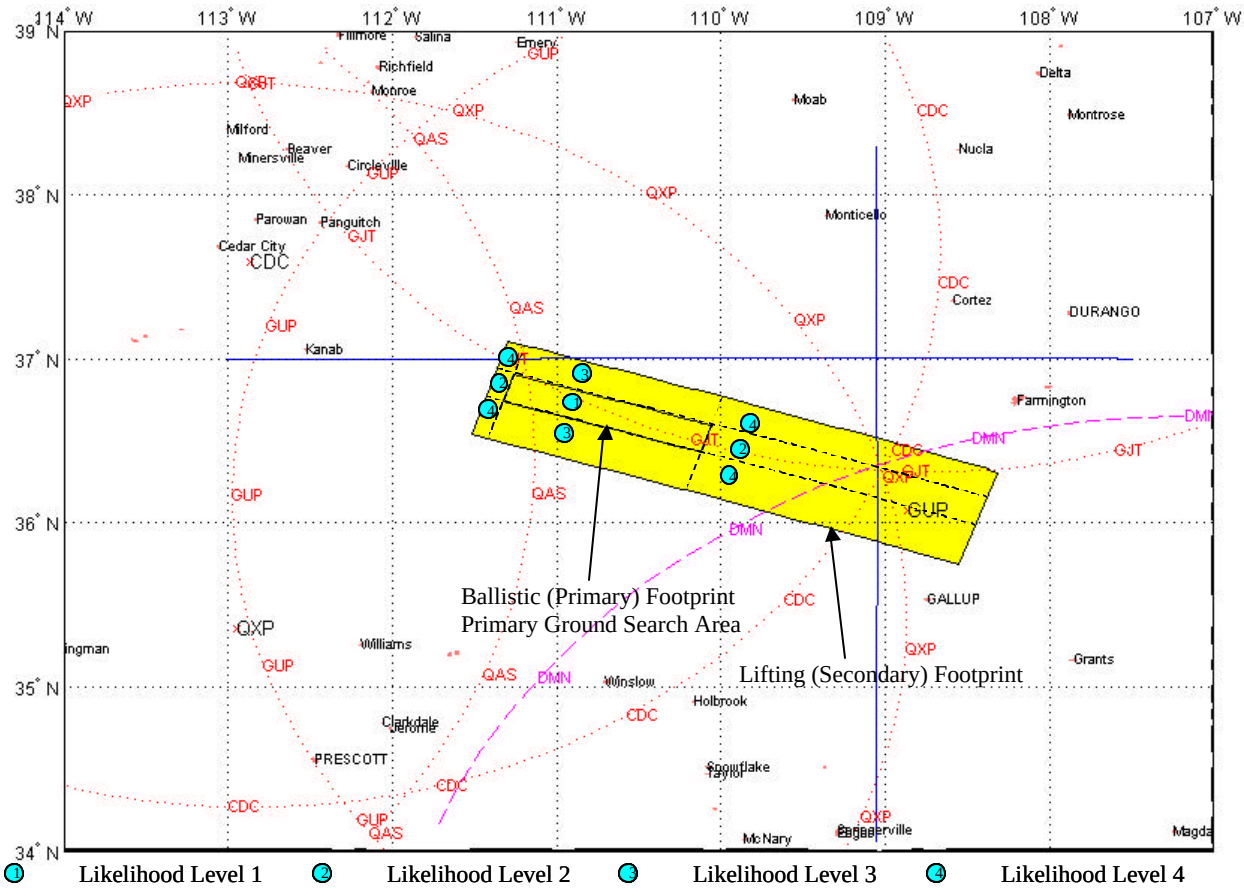

Figure 4-59: Probable Ground Impact Area for Debris 13
Separation Time 13:55:53.3-13:55:54.3Z
Constant Ballistic Coefficients between 0.2 to 1.1 psf, 0-0.15 L/D, C_d 1.0

Debris 14

The Aerospace Corporation independently validated the JSC ballistic coefficient and both the ballistic (non-lifting) and lifting footprint boundaries, with similar, but slightly different methods for relative motion, ballistic coefficient estimation, and debris footprint estimation [30]. Aerospace calculated a ballistic coefficient of 1.0 - 2.0 psf [30] compared to a JSC estimate of 1.0 - 2.4 psf [23], both derived using day-of-entry density at event altitude.

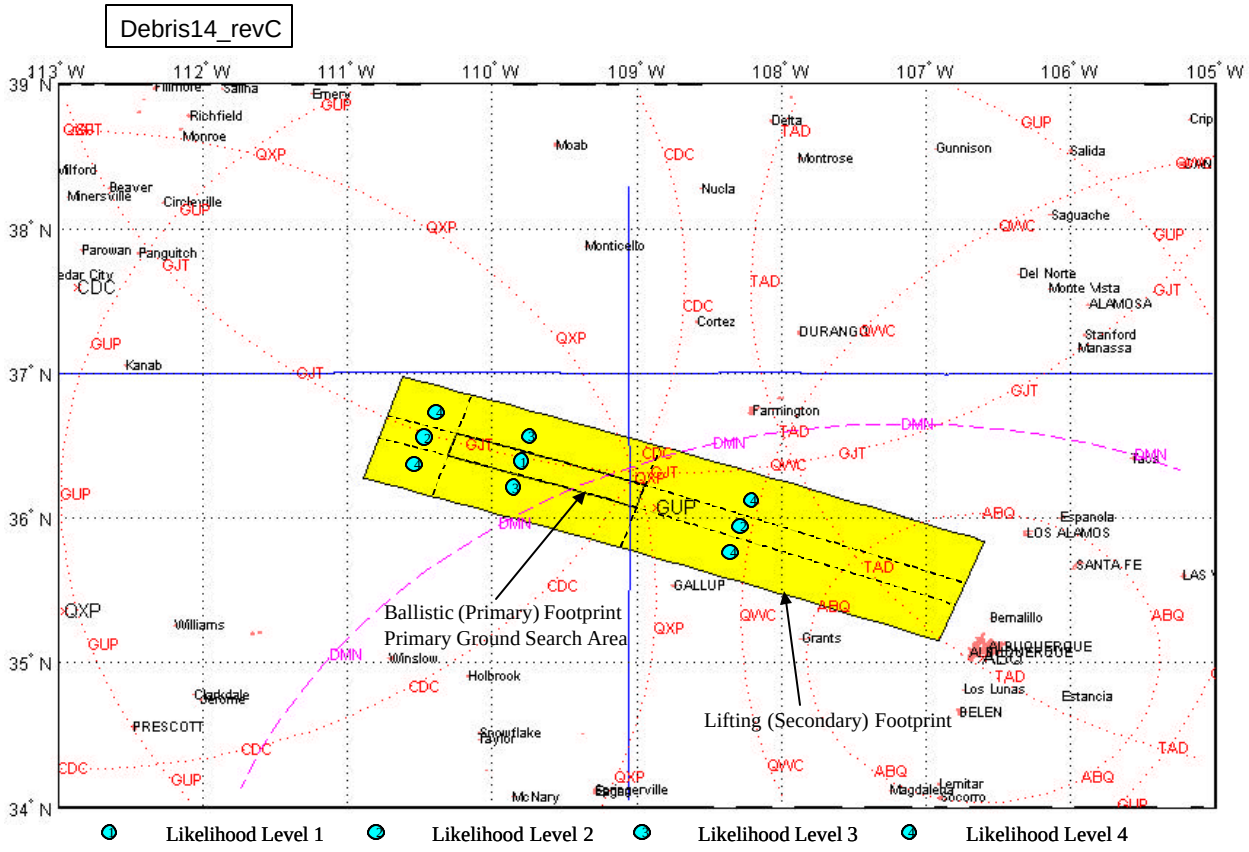

Figure 4-60: Probable Ground Impact Area for Debris 14
Separation Time 13:55:56.2-13:55:57.2Z
Constant Ballistic Coefficients between 1.0 & 2.4 psf, 0-0.15 L/D, C_d 1.0

Debris 15

Debris15_revA

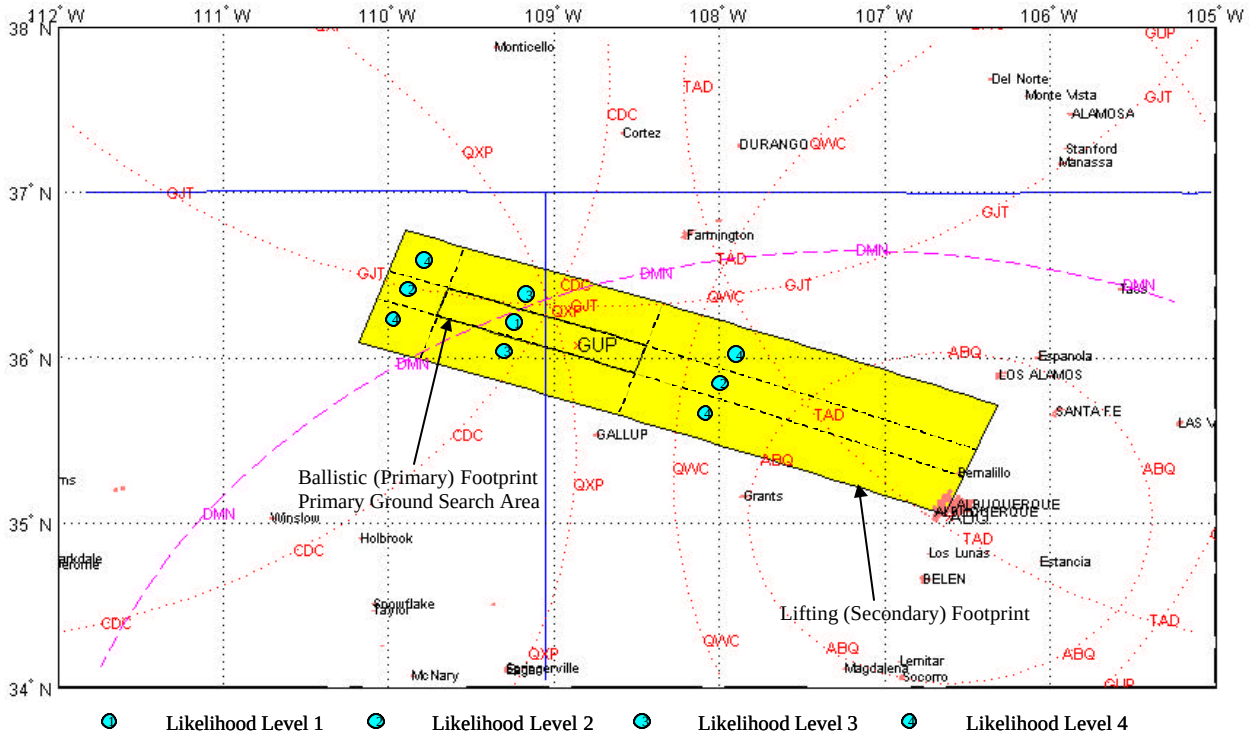

Figure 4-61: Probable Ground Impact Area for Debris 15
Separation Time 13:56:09.0-13:56:10.0Z
Constant Ballistic Coefficients between 0.8 to 2.0 psf, 0-0.15 L/D, C_d 1.0

Debris 16

Debris16_revB

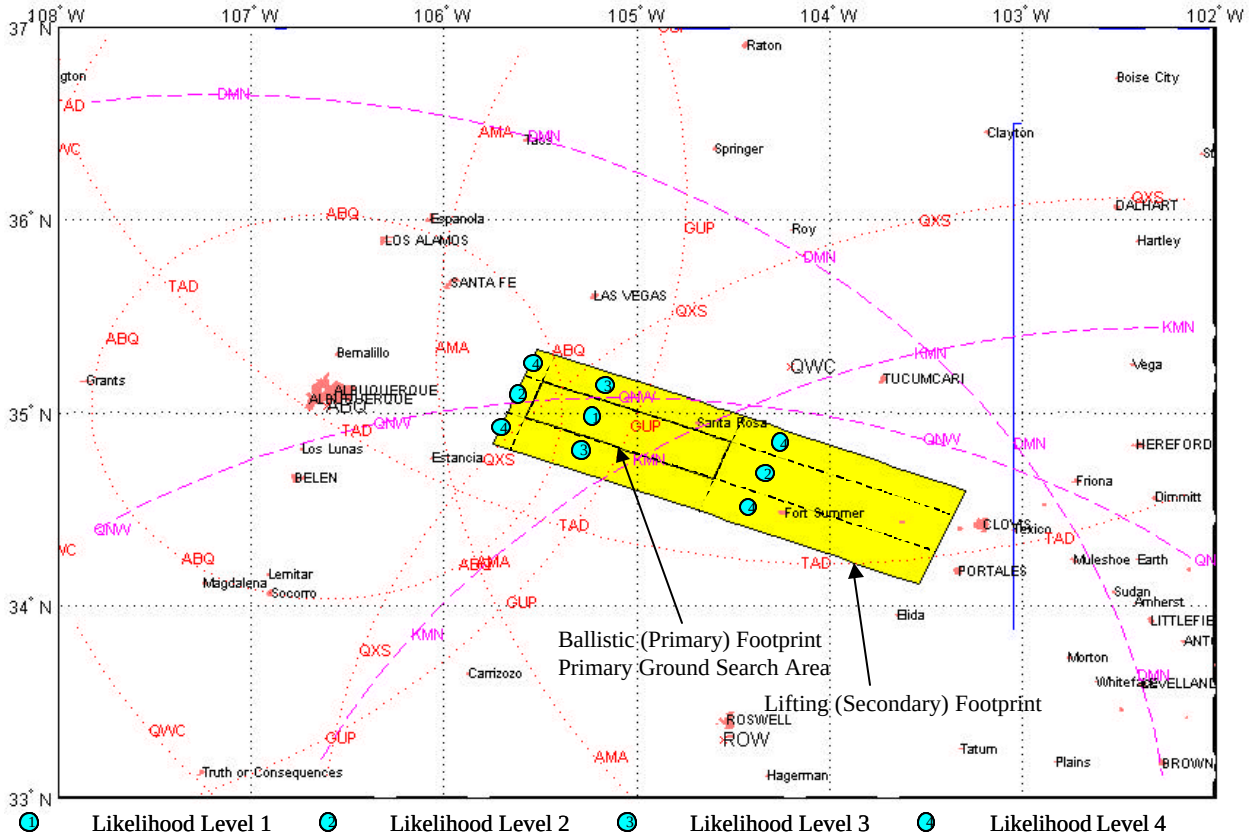

Figure 4-62: Probable Ground Impact Area for Debris16
Separation Time 13:57:23.2-13:57:24.2Z
Constant Ballistic Coefficients between 0.1 to 1.0 psf, 0-0.15 L/D, C_d 1.0

Flare 1 and 2

Two flares are visible in video coverage [22]. No debris is visible in the video at or near the flare times; debris may be there but may not be visible due to: small size; lighting (in daylight now); and/or short time of observation (Orbiter leaves camera field-of-view immediately). It is possible that debris fell off the Orbiter at these two flare times. The simulation uses the assumed ballistic coefficient range of 0.5 - 5.0 psf since this range approximately bounds ballistic coefficients derived from video of other debris thus far.

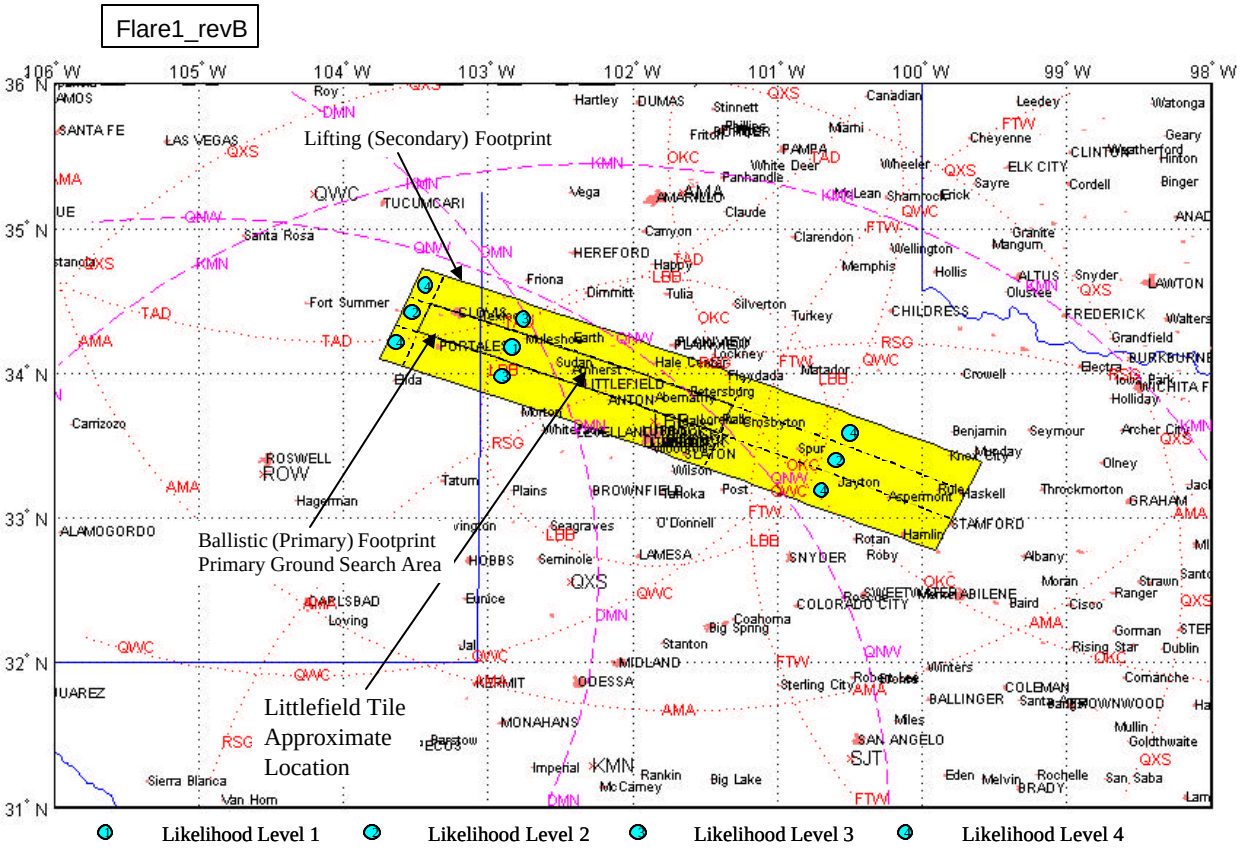

Figure 4-63: Probable Ground Impact Area for Assumed Debris Associated with Flare 1
Observed Flare at 13:57:54.7Z
Constant Ballistic Coefficients between 0.5 to 5.0 psf, 0-0.15 L/D, C_d 1.0

Flare2_revB

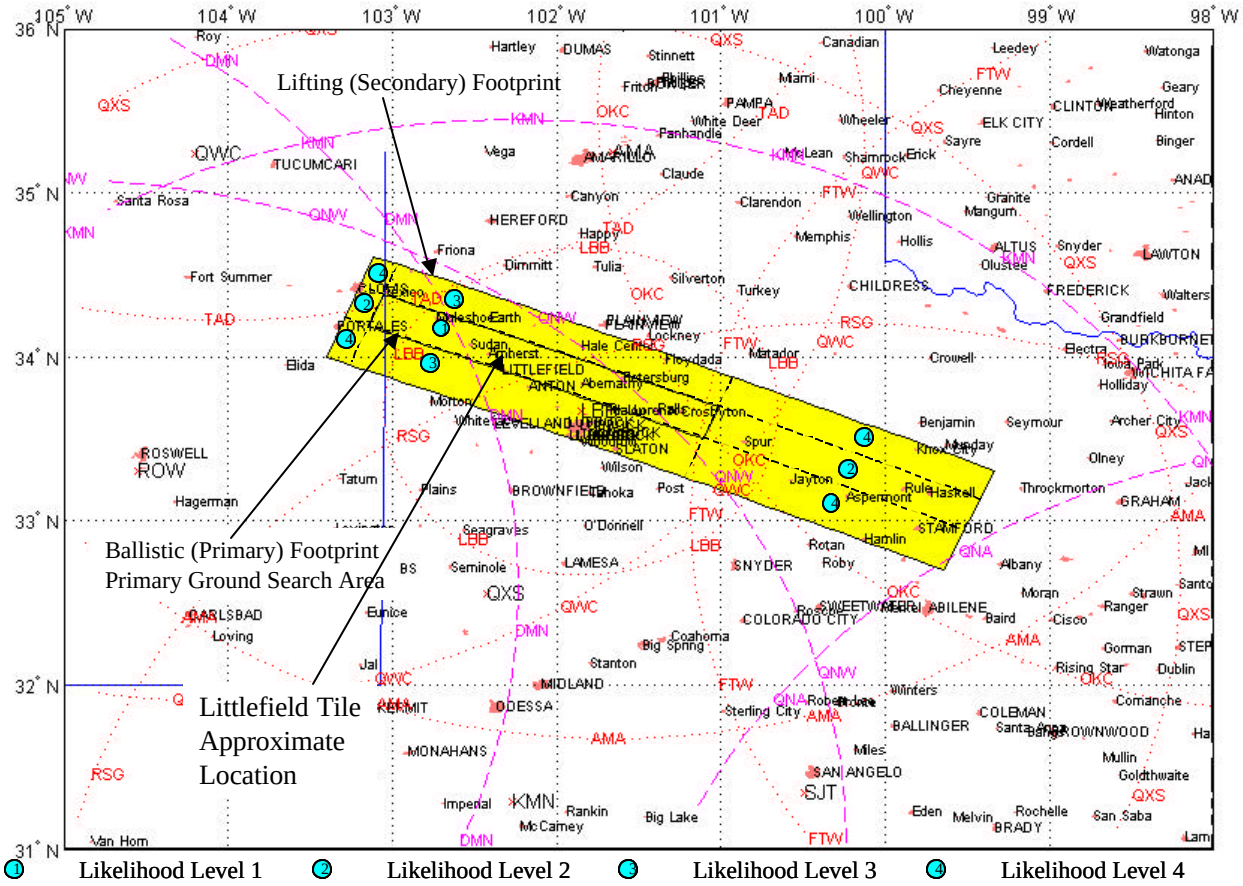

Figure 4-64: Probable Ground Impact Area for Assumed Debris Associated with Flare 2
Observed Flare at 13:58:00.5Z
Constant Ballistic Coefficients between 0.5 to 5.0 psf, 0-0.15 L/D, C_d 1.0

4.3.5. Estimated Separation Time for Littlefield Tile

A tile fragment, KSC Database object number 14768, was found in Littlefield, Texas at 33.97083N, 102.3158W. It weighs 16 grams and is 3.2” x 2.8” x 0.561”. Shown below in Figure 4-65, the Littlefield Tile is the only confirmed pre-breakup debris found -- i.e., it was found outside of the primary debris footprint boundary and shown analytically to have fallen off prior to loss-of-signal.

Figure 4-65: Littlefield Tile

Assuming this tile fragment separated and fell to the ground intact in the shape and size it was discovered, it is possible to estimate the separation time. The Debris Footprint Team first computed the debris’ ballistic coefficient. A series of footprints was then generated based on assumed debris shedding times. These times were iterated on to find the earliest time that results in a footprint boundary with the actual impact location on the edge of the toe, and also to find the latest time that results in a footprint boundary with the actual impact location on the edge of the heel.

Using this method, based on the impact location and ballistic coefficient range of 0.5 - 0.9 psf, the Littlefield Tile is estimated to have been shed between 13:57:49 - 13:58:20Z. This time range encompasses the observed times for Flare 1 and Flare 2. It is possible that if debris fell off the orbiter at Flare 1 or Flare 2, that the Littlefield Tile may be this debris or a portion of this debris. This is shown above in Figures 4-63 and 4-64.

4.4. Debris Trajectory Analysis Lessons Learned

1) Observer provided information on location, camera specifications, zoom settings, and time synchronization are invaluable as the debris analysis progressed.

2) The combination of automation and parallel processes for calculating a relative range for each time step in video ensured both a quick and accurate answer and is highly recommended to anyone performing a similar analysis in the future.

3) The Debris Footprint Team generated the method to shape a debris footprint between the heel and toe specifically for this accident to aid the Search and Recovery Team in avoiding unnecessary search areas, and will be used in all future debris footprint predictions.

4) In this incident, the first debris footprint predictions were not available until 4 hours after the accident. To improve the possibility of crew rescue, either:
   - a "running" debris footprint should be designed for future STS missions such that as soon as telemetry is lost, a debris footprint and estimated crew module impact point are available, or
   - a footprint prediction team should be available during entry.

5) An upper bound on ballistic coefficient was not known for an Orbiter on entry; the Debris Footprint Team now has a maximum ballistic coefficient to use in any future Orbiter-only debris field analysis, based on the Columbia observed value of 220 psf.

5. Radar Search Areas

Unless otherwise footnoted, Section 5 is referenced to [25], Hartman, S.; JSC-DM; JSC Radar Assessment Team Final Report; May 23, 2003. This is included in its entirety in Appendix 10.7.

5.1. Radar Analysis Team Summary

The Radar Analysis Team was chartered to look for debris west of Fort Worth, TX (pre-breakup). The team was composed of personnel from NASA JSC, National Transportation Safety Board (NTSB), Federal Aviation Administration (FAA), and USAF 84th Radar Evaluation Squadron (RADES). The NTSB and FAA teams brought recorded FAA air traffic control radar data and analytical software to JSC and trained the JSC personnel to search for radar threads.

For over 3 months, the Radar Analysis Team searched through more than 2 million individual radar returns generated between 1330 and 1500Z on February 1, 2003. From these, the team developed nine search reports based on radar tracks. Of these, a tile fragment was found approximately 1000 feet north of Search Box 1, a tile was found 3.5 miles east of Search Box 1, and another was found inside Search Box 1. The western-most debris found was a tile in Littlefield, TX.

The team was also the primary liaison for the radar cross-section testing conducted by the Air Force Research Laboratory (AFRL) at Wright-Patterson Air Force Base. These tests were performed on materials and components inside the payload bay and on the exterior of the Orbiter in order to fully characterize the radar cross-sections. These were tested for comparison with data from the C-band radars which tracked during ascent, UHF radars which tracked during orbit operations, and the L-band and S-band air traffic control radars which tracked during entry. The tests quantified material-specific radar return properties, resulting in estimated detection ranges. Results show that the various Orbiter external materials have low maximum detection ranges for the air traffic control radars, reducing confidence in the ability to detect the most probable Columbia pre-breakup debris in radar.

AFRL radar testing results are summarized in Section 6. C, L, and S-band data annexes were fully reported to the Columbia Accident Investigation Board (CAIB) and NASA by Air Force Research Laboratory Sensors Directorate on April 24, 2003.

5.2. Radar Database and Search Method

The term radar *thread* or *track* refers to a sequential series of radar returns, over a span of time, which displays geographical movement of a potential object of interest. A radar *blob* refers to a sequential series of radar returns, over a span of time, which does not display much geographical movement (i.e., multiple radar returns in the same geographic location, one possible explanation of which would be a vertically falling object). Radar *anomaly* is a general term referring to false radar echoes. These can be the result of many different things, including atmospheric phenomena, radar interference, or unknown reflective objects in the path of the radar.

The specific radars of interest to the Radar Analysis Team were:

- L Band - ARSR and FPS air traffic control radars used for long range aircraft tracking, with a maximum range of approximately 250 nm and a radar sweep every 10-12 seconds. The radars operate approximately between 1220 and 1380 MHz. The ARSR-4 is the only type of these radars that produces data in 3 dimensions (i.e., includes altitude information).
- S Band - ASR-9 air traffic control radars used for terminal area control around airports, with a maximum range of approximately 55 nm and a radar sweep every 4-5 seconds. The radars operate approximately between 2400 to 2600 MHz.
- C Band - NASA ascent/entry tracking radars, used for long range shuttle tracking, generally track the shuttle out to approximately 500 nm during ascent. The radars operate at approximately 5.7 GHz.

Archived radar data was collected by NTSB and FAA and brought to JSC on February 10. Data was collected from 72 two-dimensional radars (no altitude data) and 38 three-dimensional radars (altitude data included). Of these, approximately 10 three-dimensional radars and 25 two-dimensional radars were located within proximity of the shuttle groundtrack and generic debris swath.

FAA and USAF radars record and archive radar data for 15 days and 120 days respectively. Consequently, FAA radar data for ascent was lost since it had exceeded the expiration date by the time of Columbia's entry. NTSB collected data from radar sites in any region of the country that had the potential to observe debris.

The NTSB/FAA team brought a number of software tools to aid in the analysis of the radar data. NTSB analysts develop their own tools and are free to use whatever they are most comfortable with individually. The tools they brought were considered by them to be easiest to train on and use. The existing tools were not designed to detect radar threads for objects at Columbia's altitudes and speed, but NTSB personnel were confident the tools would work.

NTSB/FAA tools include: RS3 (developed by 84th RADES) to display raw radar data, RAPTOR to display raw Terminal Control Radar data, TRACKS, FINDTRACK, BALLISTICS, and WINLATS to manipulate the radar data in order to more easily discover radar tracks.

Some of these tools, while useful, needed to be altered in order to be used to search for pre-breakup Columbia debris. The JSC Team developed a number of software tools to aid in the display/analysis of the radar data.

Enhanced Display Tool:

JSC Radar Analysis Tool (JRAT) - Derived by JSC's Flight Design and Dynamics Division from the NTSB "TRACKS" tool. JRAT graphically displays radar returns in both 2-D and 3-D formats to allow the user to better view the data, in order to facilitate the search for any potential tracks.

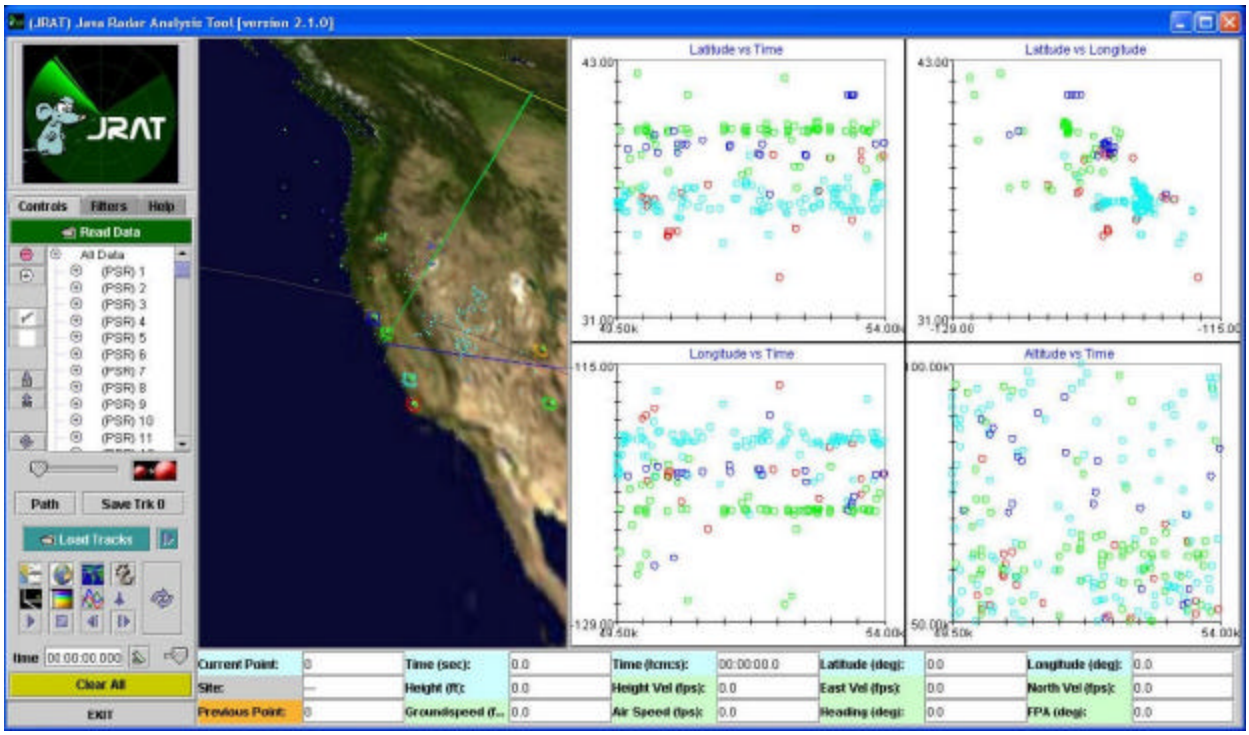

Figure 5-1: JRAT Screenshot

Data Integration Tools:

JSC's Flight Design and Dynamics Division attempted to build a triangulation tool to estimate the altitude of any tracks that were observed by two radars (neither of which was an altitude-finding radar). However, this was not achievable due to the uncertainties inherent in the radar tracks. It was determined that altitude errors would have been on the order of 5000 to 10,000 ft, or greater. Therefore, this tool development was abandoned.

The Concept Exploration Lab (CEL), led by Joe Hamilton, developed: Convert.exe, Vfilter.tcl, Scrub.tcl, Grid.tcl. These tools were used in conjunction with previously available software to attempt to filter the radar database and "automate" the search for potential tracks.

Tools to aid in automating the search for radar tracks:

Convert.exe - Converts 2D radar text files with azimuth and range information from a given sensor location into a comma delimited file for use in multiple plotting and visualization tools. Latitude and longitude of each radar point is calculated based upon a specified assumed altitude. Output files can be filtered by time, range, and azimuth.

Vfilter.tcl - Accepts output from Convert.exe and RS3 to search the data for correlated tracks and calculates an estimated course and speed for each track. Search parameters are selectable to focus on tracks of interest. This has been extremely successful at finding airline tracks. However, attempts to correlate tracks at shuttle entry velocities resulted in numerous false tracks unless the search parameters were kept very tight. Tracks in the RS3 data, of potentially falling objects, were identified but most of them did not match likely ballistic profiles. A version of vfilter.tcl was created to remove airline tracks from the source data. This was mostly successful, but left some points associated with the airlines in the data.

Scrub.tcl - Accepts output from a specially designed session of the 3D visualization tool PRISMS. The PRISMS session was used to visually scrub points out of the data, such as all remaining points associated with airline tracks. Scrub.tcl deletes points that were visually identified in PRISMS from the original source file.

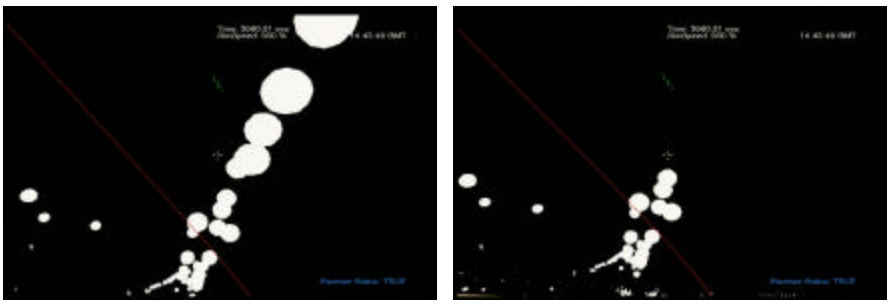

Figure 5-2: PRISMS Screenshots, Before and After Running Scrub.tcl

Grid.tcl - Counts the number of radar returns within specified grids over a time period to create density plots of the radar data. The result is similar to weather radar visualization techniques.

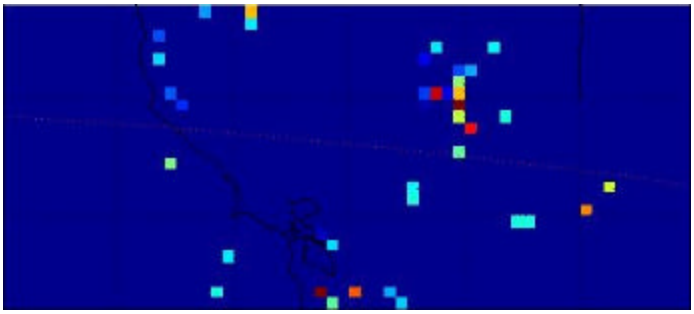

Figure 5-3: Grid.tcl Screenshot

Radar object class information was added to the Global Visualization Process (GVP) trajectory software. This provided the capability to view tens of thousands of radar points simultaneously with color gradients according to time stamp. (Lake Charles radar data and 07Feb03 footprint shown below.)

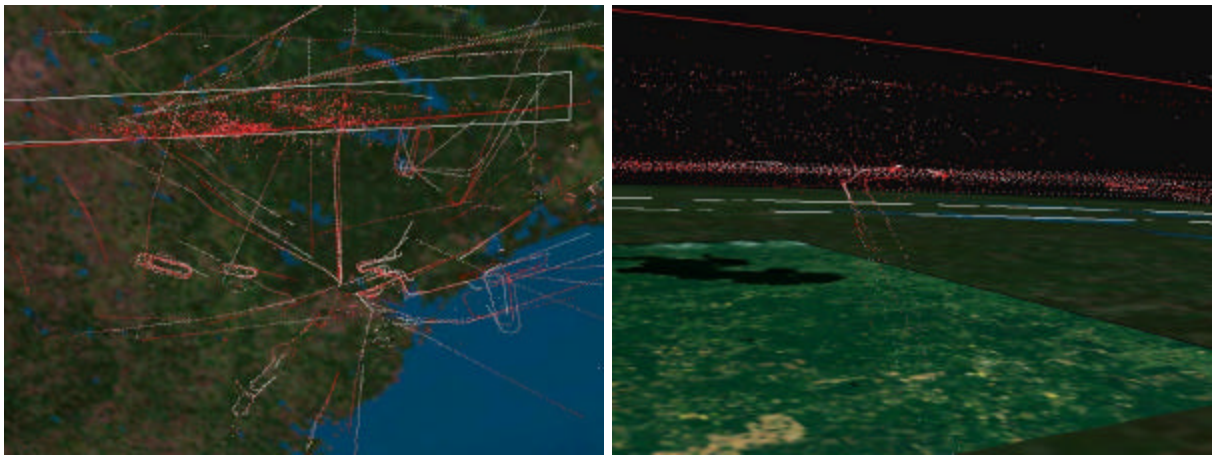

Figure 5-4: Global Visualization Process Screenshots

The NTSB/FAA/JSC team worked together to search for radar tracks. All tracks were reviewed by the full team.

The NTSB set up a password-protected web site that was used as both a repository for data (winds, master radar data file, search reports, etc.) as well as a place to file potential radar track data (accepted, rejected, under review).

The team was split into two sub-teams: groundtrack search and California Fence search.

The Groundtrack Team started by looking for radar tracks near the generic debris swath described in Section 4.3.3. They then focused on areas that reported potential Columbia debris in Albuquerque, New Mexico; Lubbock, Texas; and Littlefield, Texas, as well as the individual ballistic footprints described in Section 4.3.4. Eventually the Groundtrack Team divided the shuttle entry groundtrack into 13 generic search boxes, and completed a systematic search of all radars along the entire groundtrack (three people per box). In addition, the team searched areas near credible eye (and ear)-witness reports. The initial search focused on long radar threads, but migrated more to a "blob" search, looking for objects falling more vertically as the analysis went on. The team tried briefly (mostly unsuccessfully) to automate the search, by trying to look for semi-linear tracks with radar returns having similar velocity, flight path angle, and heading. Analysts attempted to confirm tracks found with RS3, by finding the same (and potentially additional points) using RAPTOR (Terminal Control Radar Data) without much success.

The California Fence Team searched the composite radar picture of four California ARSR-4 radars (Mill Valley, Rainbow Ridge, Paso Robles, Vandenberg). All of these radars have height finding capability, and were combined together in order to best be able to see early debris (potential to be tracked by multiple radars). The California Fence Team also began by searching

the composite radar picture for semi-linear tracks, with similar velocity, flight path angle, and heading. Several software tools were developed to aid in this search; however, the majority of the tracks that they identified were commercial aircraft. This team then transitioned to more of a "Blob" analysis. Specifically, the team attempted to define the density function of the radar returns, and use tools to filter out the background "noise" and identify possible shuttle debris. Thirteen tracks were found that were not identified as commercial aircraft; however, all were dismissed as not being shuttle debris.

Search areas were established which were 2.5 degrees long in longitude, 40 nm wide centered on the ground track as shown below in Figure 5-5. These were intentionally overlapped by 0.5 degrees from the toe of one into the heel of the next. An area search was considered complete when three team members had independently searched each box. Short range radars were not used for these initial searches but were used to confirm a potential radar thread found on a long range radar.

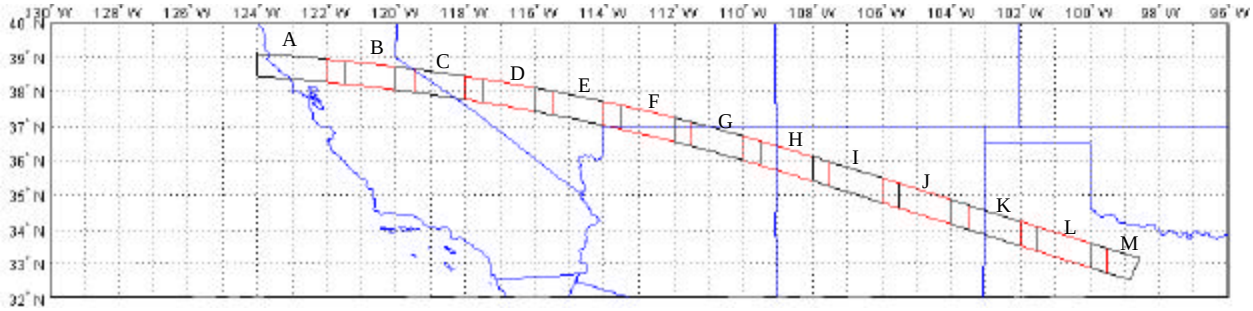

Figure 5-5: Radar Team Search Areas

Area searches of all long range radar were completed from 0 to 20 nm of the CONUS ground track. All areas were searched at least once within 60 nm of the CONUS ground track, but redundant coverage was as low as 79 percent beyond 20 nm from the ground track.

Members of the team searched the radars in one of two different ways: 1) Searching by boxes (defined by the latitude and longitude of their corners), where a teammember searches all radars with coverage in that box. 2) Searching by radars, where one radar's returns were looked at for specific azimuths and within 60 nm of the ground track.

Typically, the NASA team kept track of searching by boxes (such as the generic search boxes or specific footprints.) When a NASA teammember reported an area complete, it meant they had searched all the radars with coverage in the box. Because defining an area as "complete" was not a precise measurement, NASA teammembers were also given the option of calling an area "partially" searched or "fully" searched. If an area was partially searched, the formula only counted that area as 50% searched by one person, or if the area was fully searched, it was counted as 100% searched by one person.

The NTSB/FAA radar teammembers searched by radar, looking at only one radar's returns at specific azimuths and only to a range within 60 nm of the ground track. However, for most areas of the sky near the ground track, anywhere from two to six radars had coverage. The percentage

of the area searched per person was the percentage of radars looked at divided by the total number radars with coverage. For example, if one NTSB member looked at radar ABC, but there were two other radars with coverage in the same area that he didn't search, it was reported as 33% searched by one person.

The long range radar search progress is depicted in Figure 5-6. Arrows point to locations along the ground track where certain "boxes" received even greater scrutiny than the rest of the area. Early revisions of the Debris 1, 6 & 14 footprints received a good amount of scrutiny because they were particularly noteworthy video debris events, and the footprints were generated earlier in the process than when the generic boxes were assigned. This kind of system was not used for distances further out, so those search areas were dependent on different kind of searches (such as NTSB-type single radar searches and looking at specific footprints), resulting in not quite 100% completion.

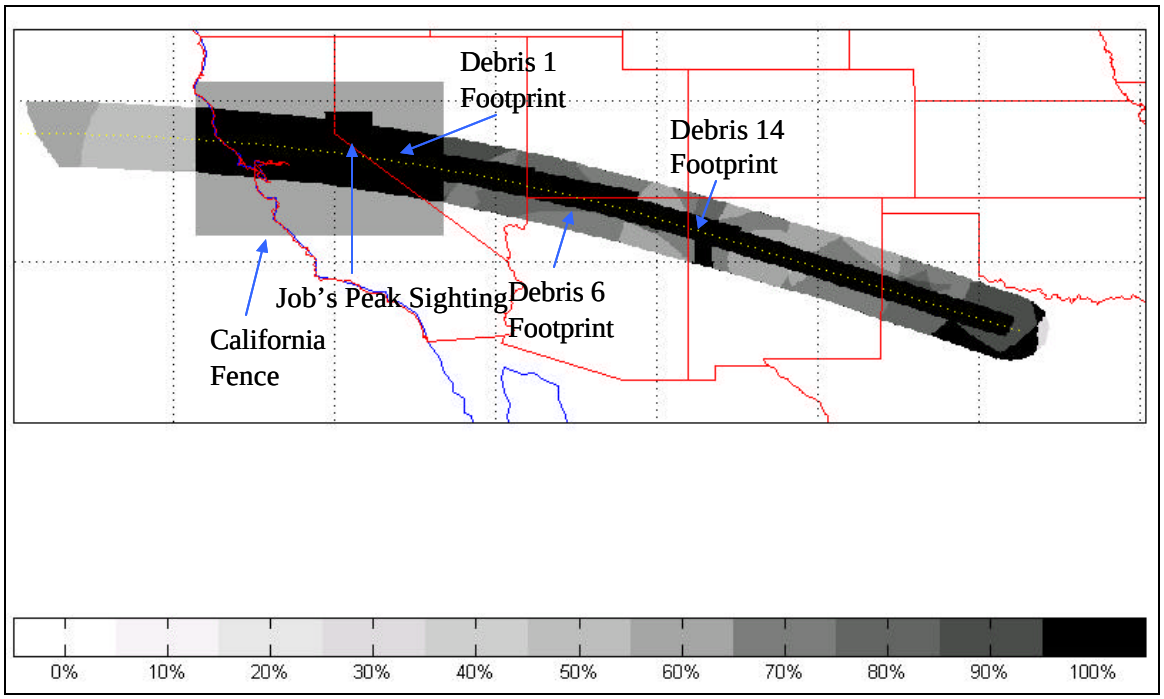

Figure 5-6: NASA/NTSB Team Total Progress (as of May 13, 2003)

Each radar thread was evaluated by the team for the following conditions/characteristics:

- The thread appears at the appropriate time in relation to the shuttle telemetry data - and no radar returns appear before or long after.
- Location of track in relation to the lifting footprint, considered to be the approximate northerly and southerly extent of possible debris.
- Typical behavior of sensor (e.g., noisy data with many spurious returns).
- The behavior of the track is not consistent with an aircraft.
- The location of the track is not consistent with aircraft operations, such as near an airport or an airway.

To be considered, the behavior of the track must be consistent with a valid trajectory of debris in terms of heading, speed, time aloft, known wind conditions, distance from the shuttle groundtrack, and expected range of ballistic coefficient considering the time and location of the track and a range of possible separation times/locations. The track must not be consistent with terrain (peaks or ridges), ground vehicles (located near roadways), or stationary objects such as towers. If a radar thread was determined to be valid, then a search box was generated.

Tracks identified by the Radar Assessment Team were examined for their likelihood of being associated with debris from the space shuttle. Two initial steps were performed to check the validity of the track being associated with a piece of shuttle debris. First, a computer program written by NTSB/Safety Board staff compared the track's location and timing with respect to the Orbiter's known re-entry trajectory. This program iteratively calculates the ballistic coefficient required for the track to be a piece that has departed from the Orbiter and match the radar track's location and timing. For tracks with no associated altitudes, altitude ranges were estimated based on local terrain for the lower bound. The upper bound was based on the upper limit of the range of detection of the respective radar system. This produced a range of calculated required ballistic coefficients for tracks without associated altitudes. The calculated ballistic coefficient was then compared to expected debris in that region, such as tiles or RCC panels, and those ranges of coefficients predicted by the debris footprint team. If the calculated ballistic coefficient for that track was either too large or too small, the track was rejected.

The next validity step performed two functions, as a second validity check and a first step in search box generation. A non-lifting trajectory was calculated using the required ballistic coefficient calculated in the first validity check, the associated (or estimated) altitude of the first return in the track, and the local winds. Tracks that moved in directions close to or in the general direction of the calculated trajectory were considered viable. Factors in this decision included proximity of the track to the local wind measuring point and the local terrain that could change the wind profile.

The calculated trajectory, using the required ballistic coefficient and local winds, was used to calculate the projected ground impact point when the trajectory from the initial point matched subsequent points in the track. If the track differed substantially from the calculated trajectory, then the ground impact trajectory was calculated from the last point in the track. The entire search box area was then defined by running trajectories from the last radar return to the ground and making estimations for: (1) ranges of possible ballistic coefficient, (2) changes in local winds due to terrain, (3) errors in radar return location due to ranging and height estimation errors. All these factors were included in several non-lifting trajectory calculations to define the limits of the search box areas.

5.3. California Fence Search

The California Fence search used California ARSR-4 radar sites (all with altitude data -PSR, RBR, VAN, MIL) in an effort to build a composite radar picture. Data shows 110,751 total radar hits from 1330Z to 1500Z. The data was separated based on time into three groups as shown in Figures 5-7 through 5-9 (Note: STS-107 crossed California coast at approximately 13:53:20.):

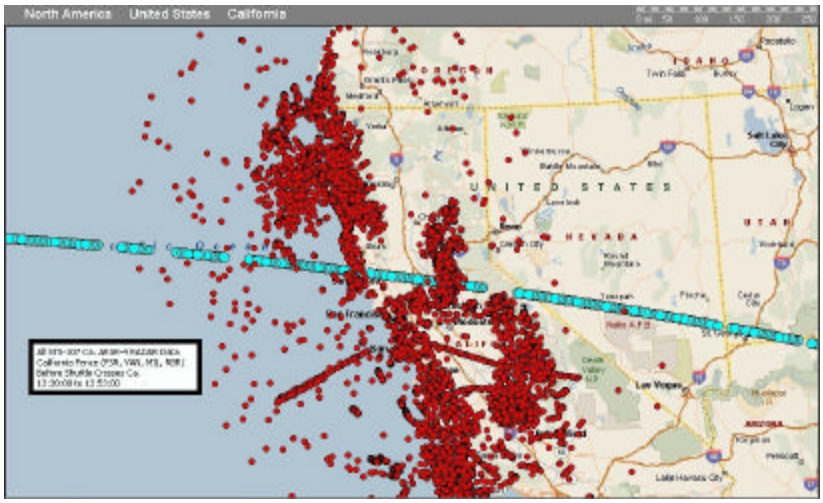

Figure 5-7: California Fence Data, Baseline, 13:30:00 to 13:53:00

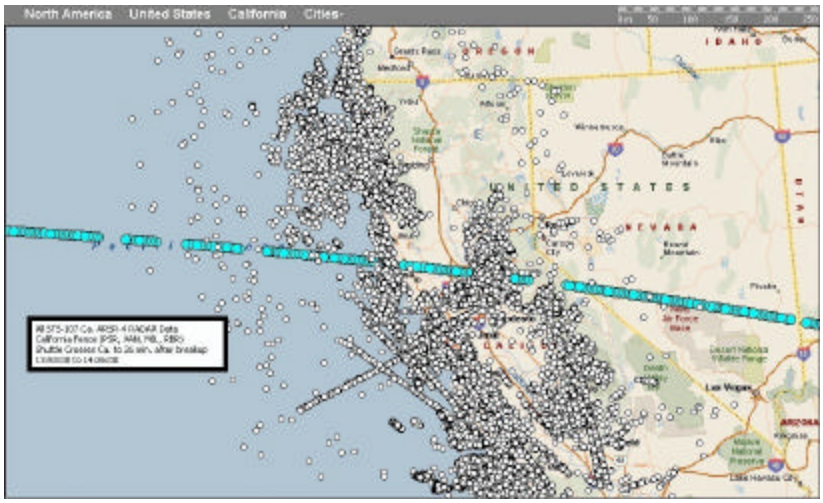

Figure 5-8: California Fence Data, Early, 13:53:00 to 14:26:00

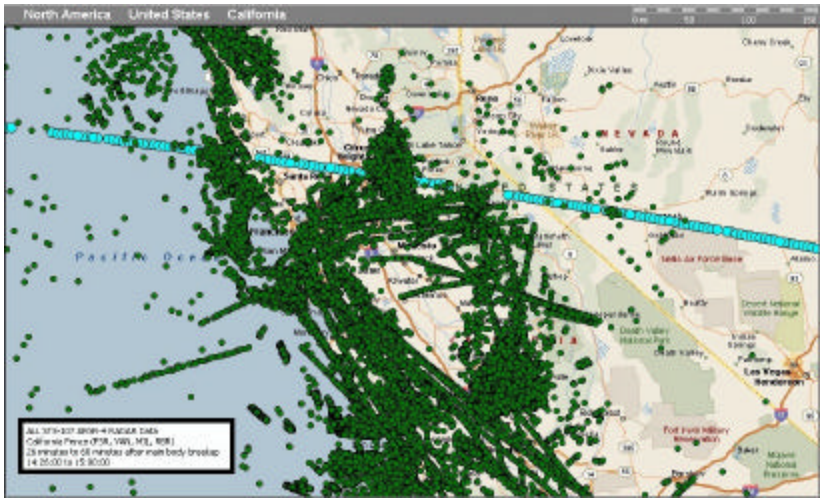

Figure 5-9: California Fence Data, Late, 14:26:00 to 15:00:00

This data was initially searched by analyzing individual tracks. It was postulated that ARSR-4 radar data would generate hits that could be correlated into semi-linear "tracks" with similar velocity, flight path angle, and heading. The team developed several new software packages to correlate data hits and try to automate the search for radar tracks. This resulted in the 13 potential tracks shown in Figure 5-10, but all candidates were rejected as potential shuttle debris.

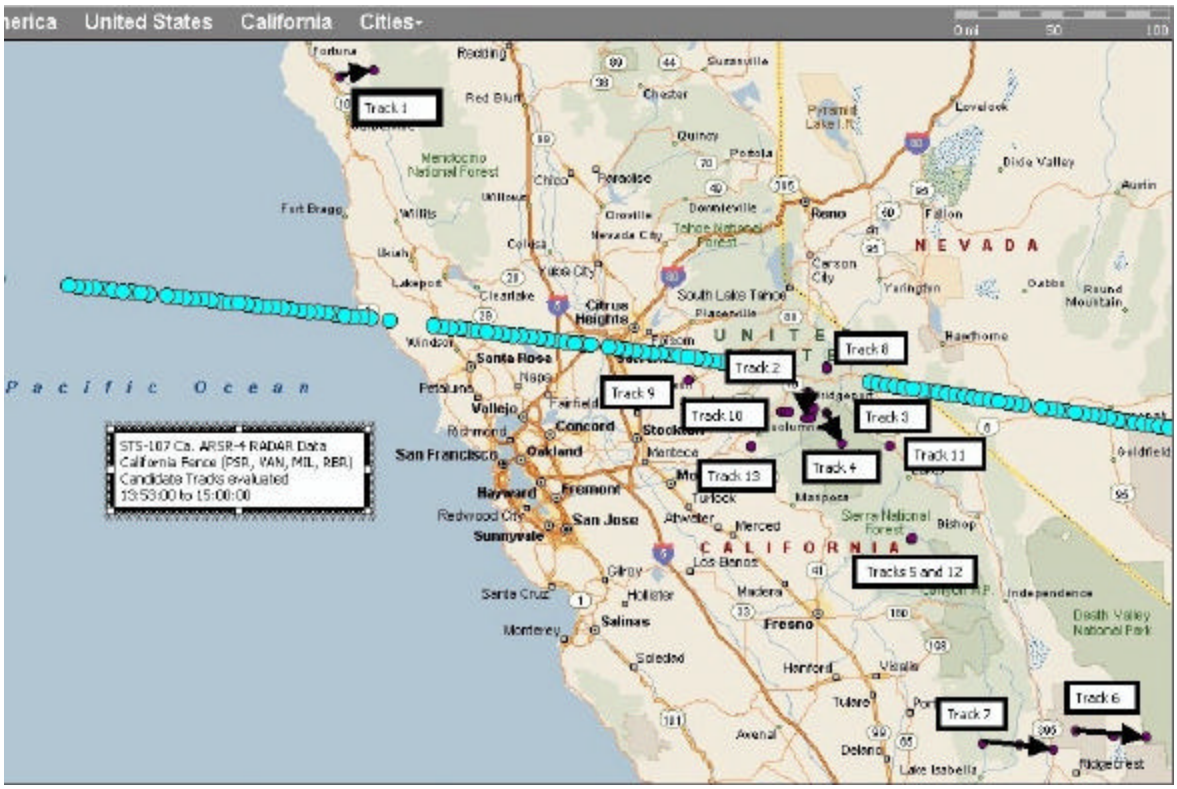

Figure 5-10: Initial "Track" Results: 13 candidates

The second approach used for the California Fence was blob analysis. It was postulated that ARSR-4 radar data would generate hits that could be correlated into groups with corresponding times in a limited latitude and longitude region. This density-approach was intended to identify single particles or "families" of debris falling in non-linear trajectories. The team first scrubbed the database of easily identified "airline" tracks for an approximately 20% reduction in data. They developed new software to count density of data hits within a grid near the groundtrack. This software calculated the number of hits/unit time/unit area before crossing, after crossing, and the change. It then mapped the change in density for easier analysis as illustrated below in Figure 5-11. No footprints have been generated yet from "Blob" analysis.

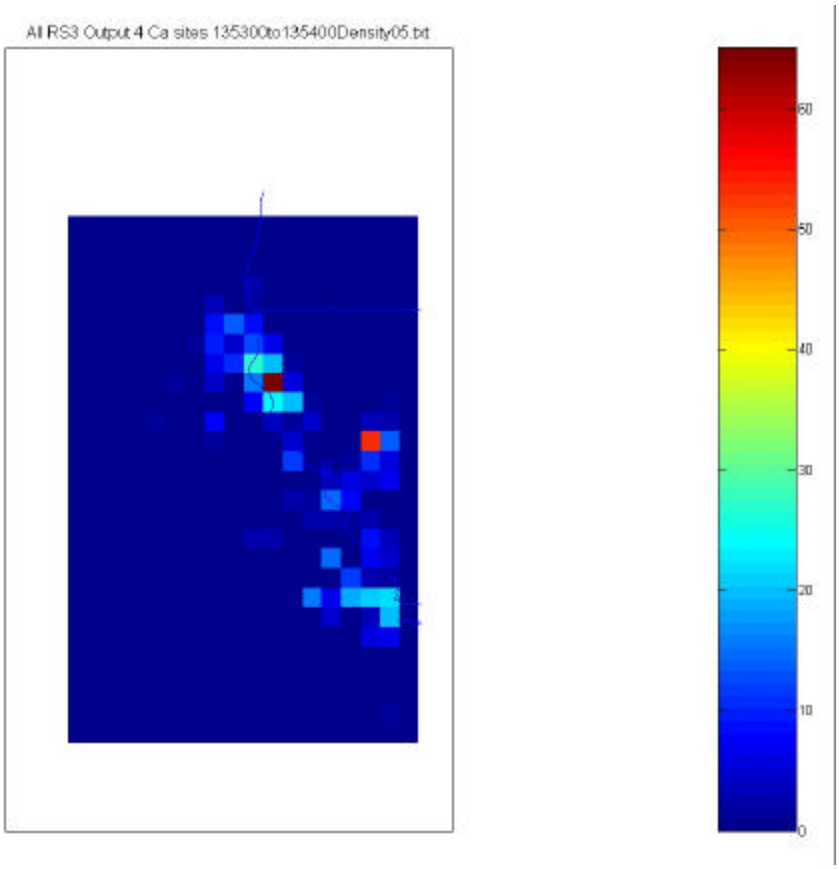

Figure 5-11: Example of Density Map "Blob" Analysis

5.4. Radar Based Search Boxes

The Radar Analysis Team searched through more that 2 million individual radar returns generated between 1330 and 1500Z on February 1, 2003. From these, the team developed nine search reports based on radar tracks. These are summarized in priority order in Tables 5-1 and 5-2. The details for each search box are given after the tables, from west to east. The rationale for the relative priorities is described in Section 5.5.

JSC/NTSB Priority	Box	Location Description	# radar hits	# radar antennas	Box Area Sq. NM / Acres (size of Non-lifting areas reflects ONLY the PRIMARY NL areas)	Inside any Lifting or Non Lifting (Ballistic) Footprint? Y/N (see separate Lookup Table)	Thread ID	Comment
1	8	west of Elgin, NV	11	1 (QAS)	1.68 / 1424	Y (Lifting 01 thru 06)	QAS-11-114.77	Delamar Lake, NV witness
2	7-1	Near Pioche, and Caliente, NV	75	1 (CDC)	4.25 / 3602	**Y (Non lifting 02 thru 04, and Lifting 01.05.06)**	CDC-075-114.4689	Well outside non-lifting, but in Debris-6 lifting foot print.
3	3	Near Floydada, TX	10	2 (QXS,LBB - ASR)	169.02 / 143251	Y(Lifting 16, non-lifting for Flare 1 and Flare2)	LBB-ASR-18-101.3186	Tile found 40 NM west of box
4	7-2	Near Pioche, and Caliente, NV	75	1(CDC)	11.03 / 9384	Y (Lifting 01 thru 06)	CDC-075-114.4690	Well outside non-lifting, but in Debris-6 lifting foot print.
5	6-south	Dixie Natl Forest - Zion Natl Park, UT	18	2 (QXP, CDC)	1.42 / 1203	Y (Lifting 02 thru 07)	QXP-18-113.1506	In/near Debris-6 dense overlap
6	6-north	Dixie Natl Forest - Zion Natl Park, UT	18	2 (QXP, CDC)	1.58 / 1339	Y (Lifting 02 thru 07)	QXP-18-113.1505	In/near Debris-6 dense overlap
7	Dense overlap non-lifting debris 04 thru 06	Near St. George Utah	N/A	N/A	Approx 300 Sq. NM	N/A	N/A	Best relmo cues and ballistics. Considered 1 of 2 most significant events in video. Most dense overlap area.
8	Dense Overlap non-lifting 07 thru 14	NE Arizona, Navajo Indian Reservation	N/A	N/A	approx 1162 Sq. NM	N/A	N/A	Measured relmo, but not as good as Debris-6. Considered 2 of 2 most significant events in video. 2nd most dense overlap area.
9	7-3	Near Pioche, and Caliente, NV	75	1 (CDC)	9.19 / 7789	Y (Lifting 01 thru 06)	CDC-075-114.4691	Outside non-lifting, but in Debris-6 lifting foot print.
10	Dense overlap - non-lifting Debris 01 thru 04	CA/NV Border	N/A	N/A	approx 775 Sq. NM	N/A	N/A	Measured relmo, but not as good as Debris-14. 3rd most dense overlap area.

Table 5-1: High Confidence Western Search Box Priorities

JSC/NTSB Priority	Box	Location Description	# radar hits	# radar antennas	Box Area Sq. NM / Acres (size of Non-lifting areas reflects ONLY the PRIMARY NL areas)	Inside any Lifting or Non Lifting (Ballistic) Footprint? Y/N (see separate Lookup Table)	Thread ID	Comment
11	7	Near Pioche, and Caliente, NV	75	1 (CDC)	8.91 / 7551	Y (Lifting 01 thru 06)	CDC-075-114.4688	Well outside non-lifting, but in Debris-6 lifting foot print.
12	9-1	Modena, UT	7	1 (CDC)	1.36 / 1153	Y (Lifting 01 thru 04)	CDC-007-114.0324	
13	2	Near Weinert, TX	4	1 (KNM)	33.2 / 28138	Y (Lifting for Flare 1 and Flare 2)	KMN-4-99.8039	
14	5	Albuquerque, NM	54	2 - (QAS and ABQ-ASR)	7.14 / 6051	Y (lifting 8 thru 13 and 15)	QSA-ABQ-054-106.36	**about 17 miles from Probabilty "2" area of Debris 14 footprint**
15	Remaining Non-lifting Debris Footprint 06	Southern Utah/Nevada border	N/A	N/A	NL 06 is 296 Sq. NM but net is **0** - covered by Dense overlap 04 - 06	N/A	N/A	Best relmo cues and ballistics. Considered 1 of 2 most significant events in video.
16	Remaining Non-lifting Debris Footprint 14	Northern Arizona /New Mexico border	N/A	N/A	(1255 Total NL 14 - 1162 Dense overlap 07-14) = **93** Sq. NM	N/A	N/A	Measured relmo, but not as good as Debris-6. Considered 2 of 2 most significant events in video.
17	Remaining Non-lifting Debris Footprint 01	Sacramento, CA to Tonopah, NV	N/A	N/A	(1670 total NL 01 - 775 Dense overlap 01-04) = **895** Sq NM	N/A	N/A	Measured relmo, but not as good as Debris-14.
18	4	Brad, TX Possum Kingdom Lake	16 (2 tracks)	2 - FTW, DFWs (ASR)	73.2 / 62039	Y (Lifting -Flare 2)	FTW-7-098.5959	
19	Remaining Lifting Debris Footprint 01	Sacramento, CA to Tonopah, NV	N/A	N/A	16096 Total - 1670 NL = **14426** Sq. NM	N/A	N/A	Measured relmo, but not as good as Debris-14. Lifting considered very improbable by JSC.
20	Remaining Lifting Debris Footprint 06	Southern Utah/Nevada border	N/A	N/A	(12,026 Total- 296 NL) = **11730** Sq. NM	N/A	N/A	Best relmo cues and ballistics. Considered 1 of 2 most significant events in video. Lifting considered very improbable by JSC.
21	Remaining Lifting Debris Footprint 14	Northern Arizona /New Mexico border	N/A	N/A	(10121 Total - 1255 NL) = **8866** Sq. NM	N/A	N/A	Measured relmo, but not as good as Debris-6. Considered 2 of 2 most significant events in video. Lifting considered very improbable by JSC.

Table 5-2: Lower Confidence Western Search Box Priorities

Search Box 8 Near Elgin, NV

Number of sensors tracking: 1
Number of tracks: 1
Total number of returns: 11
Time span: 1 minute, 48 seconds
Ballistic footprints in proximity: Lifting 01 thru 06

A witness (EOC #2-1-1297) reported sighting objects falling ~1.5 statute miles north of the last radar hit in this search box. This report is described in more detail in Section 6. An expanded search area was created using the witness's recommendations.

The topographical map includes:
Thin, red line = search box
Yellow dots = radar hits

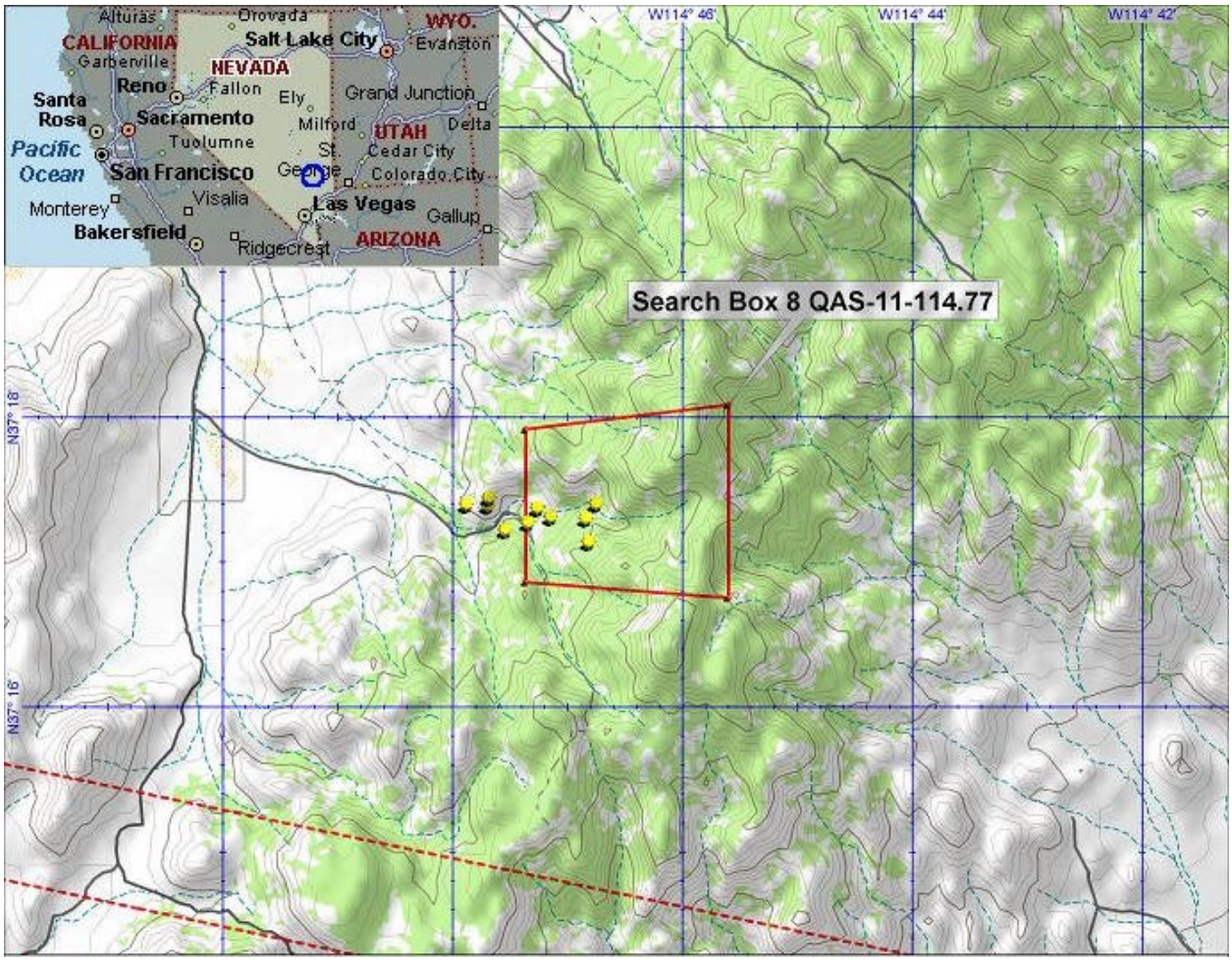

Figure 5-12: Search Box 8 Near Elgin, NV

Search Boxes 7, 7-1, 7-2, 7-3 Near Pioche, NV

Number of sensors tracking: 1
Number of tracks: 1, but may have split into 4 separate pieces
Total number of returns: 75
Time span: 39 minutes, 6 seconds
Ballistic footprints in proximity: 7-1: Non lifting 02 thru 04, and Lifting 01,05,06
7, 7-2 and 7-3: Lifting 01 thru 06

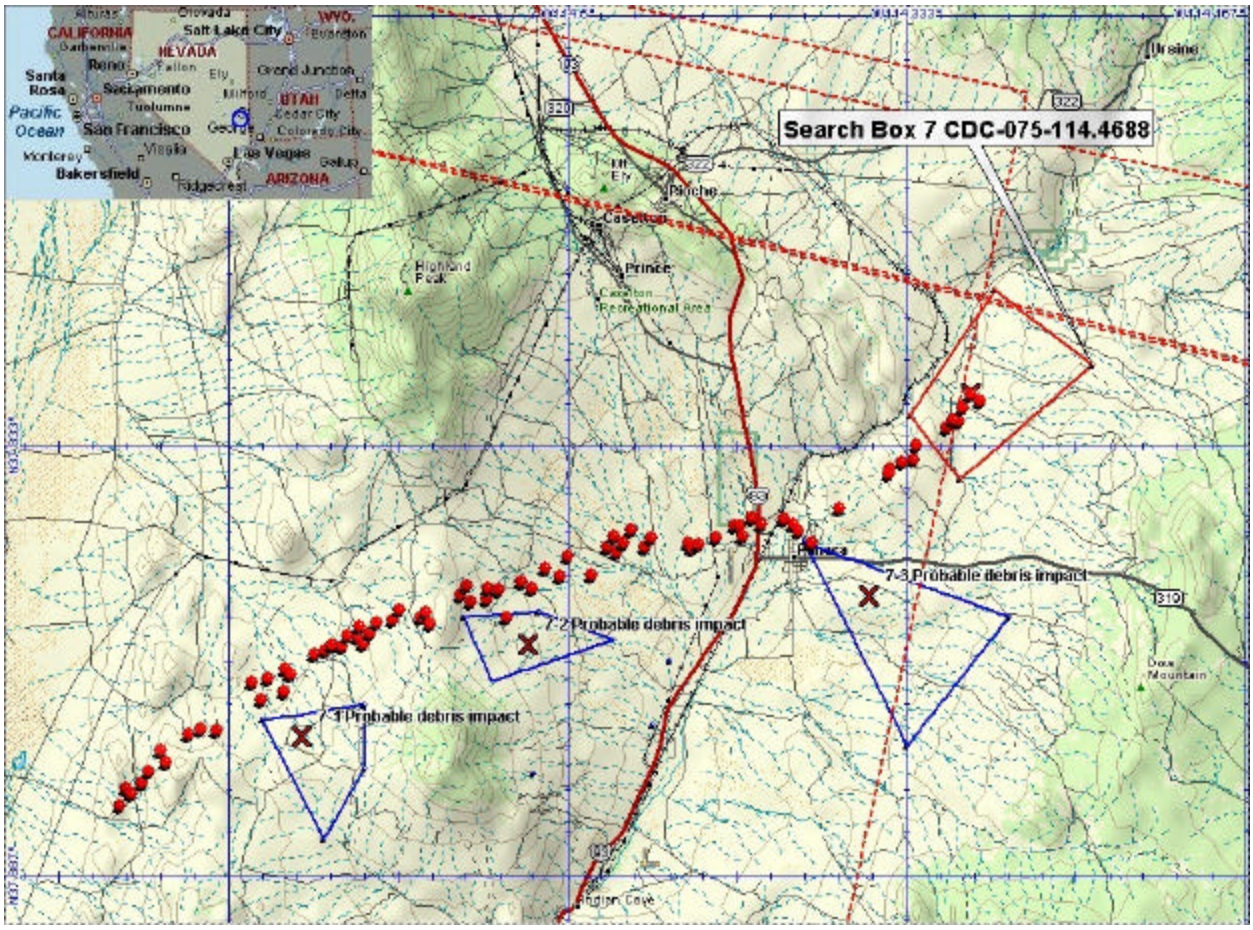

Figure 5-13: Search Boxes 7, 7-1, 7-2, 7-3 Near Pioche, NV

Search Box 9-1 Near Modena, UT

Number of sensors tracking: 1
Number of tracks: 1
Total number of returns: 7
Time span: 3 minutes, 12 seconds
Ballistic footprints in proximity: Lifting 01 thru 04

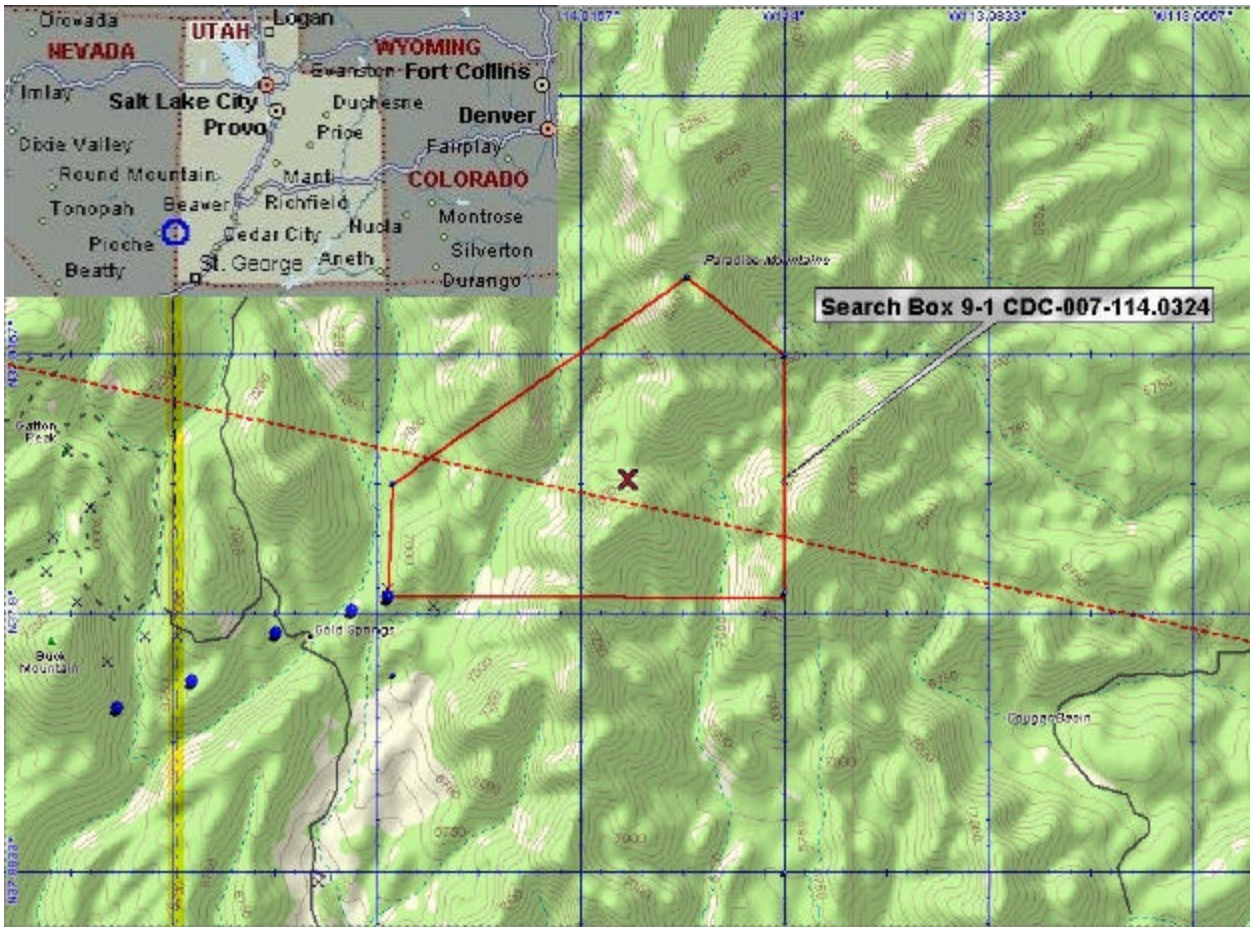

Figure 5-14: Search Box 9-1 Near Modena, UT

Search Box 6 Near Zion National Park, UT

Number of sensors tracking: 2
Number of tracks: 1, but may have split into 2 separate pieces – 2 adjoining search areas were defined
Total number of returns: 18
Time span: 7 minutes, 52 seconds
Ballistic footprints in proximity: Lifting 02 thru 07

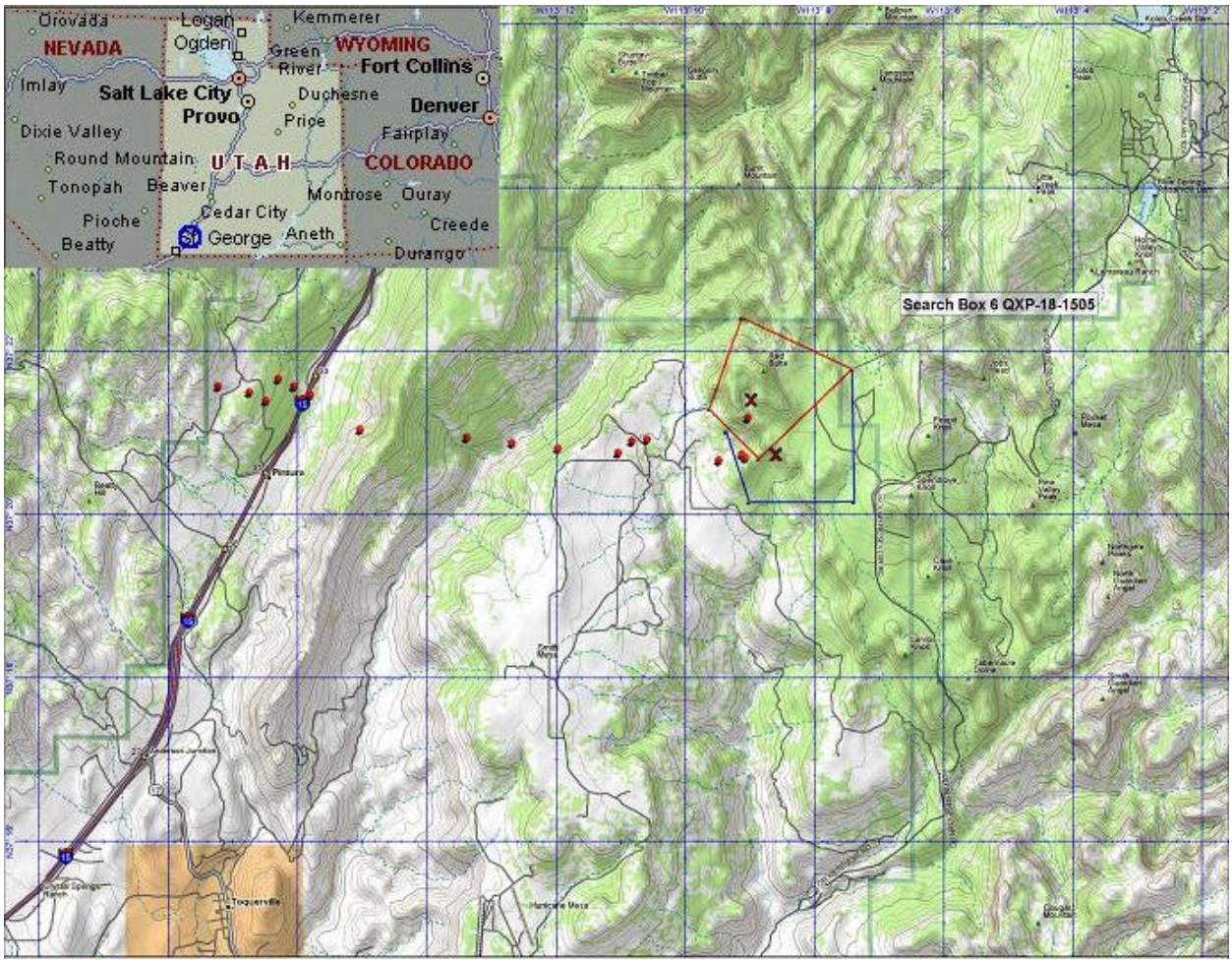

Figure 5-15: Search Box 6 Near Zion National Park, UT

Search Box 5 Near Albuquerque, NM

Number of sensors tracking: 2, 1 of these is a high rate (4.5 second sweeps) sensor
Number of tracks: 1, but may have split into 2 separate pieces – 2 adjoining search areas were defined
Total number of returns: 69
Time span: 11 minutes, 37 seconds
Ballistic footprints in proximity: Lifting 8 thru 13 and 15

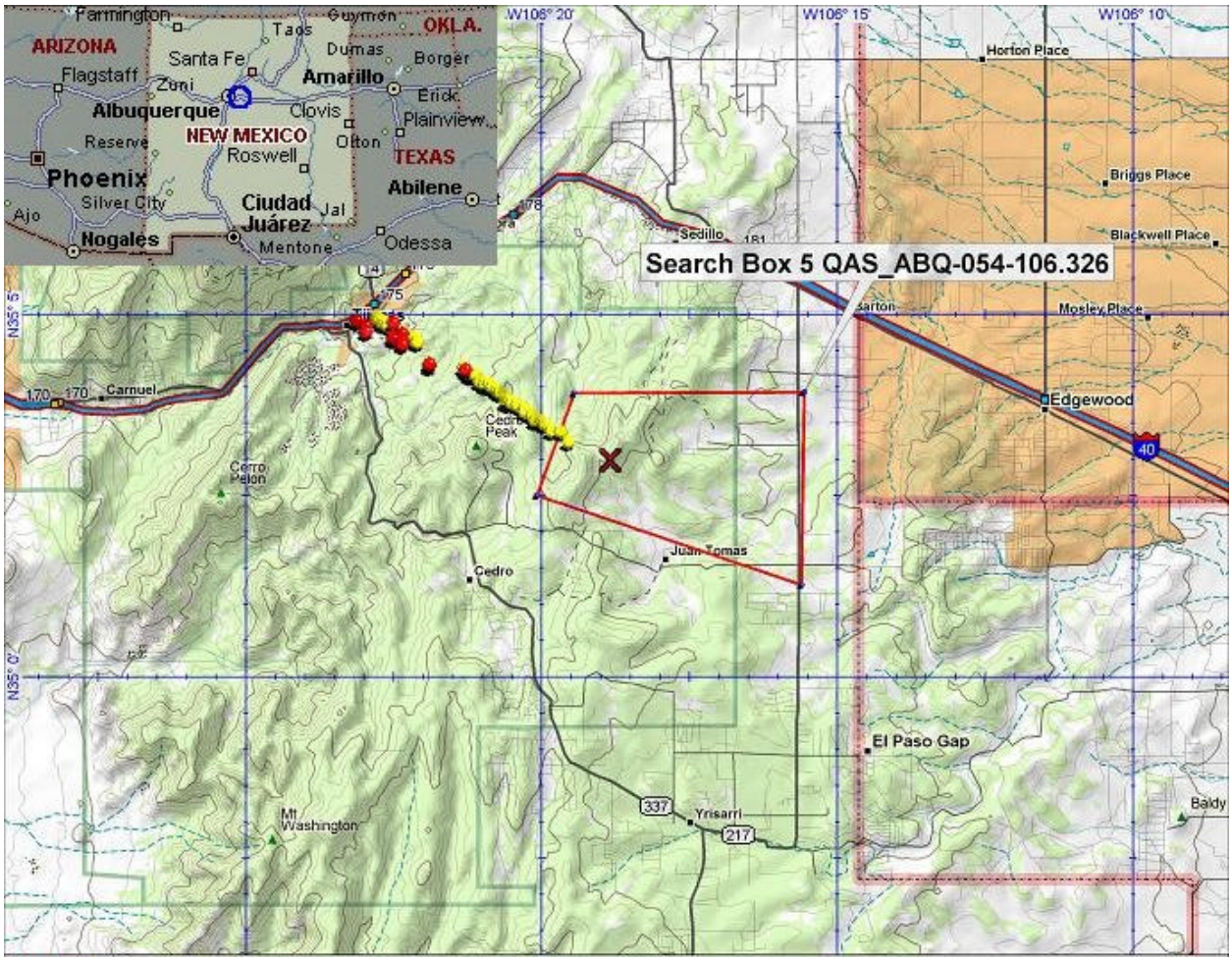

Figure 5-16: Search Box 5 Near Albuquerque, NM

Search Box 2 Near Weinert, TX

Number of sensors tracking: 1
Number of tracks: 1
Total number of returns: 4
Time span: 12 minutes, 16 seconds
Ballistic footprints in proximity: Lifting Flare 1 and Flare 2

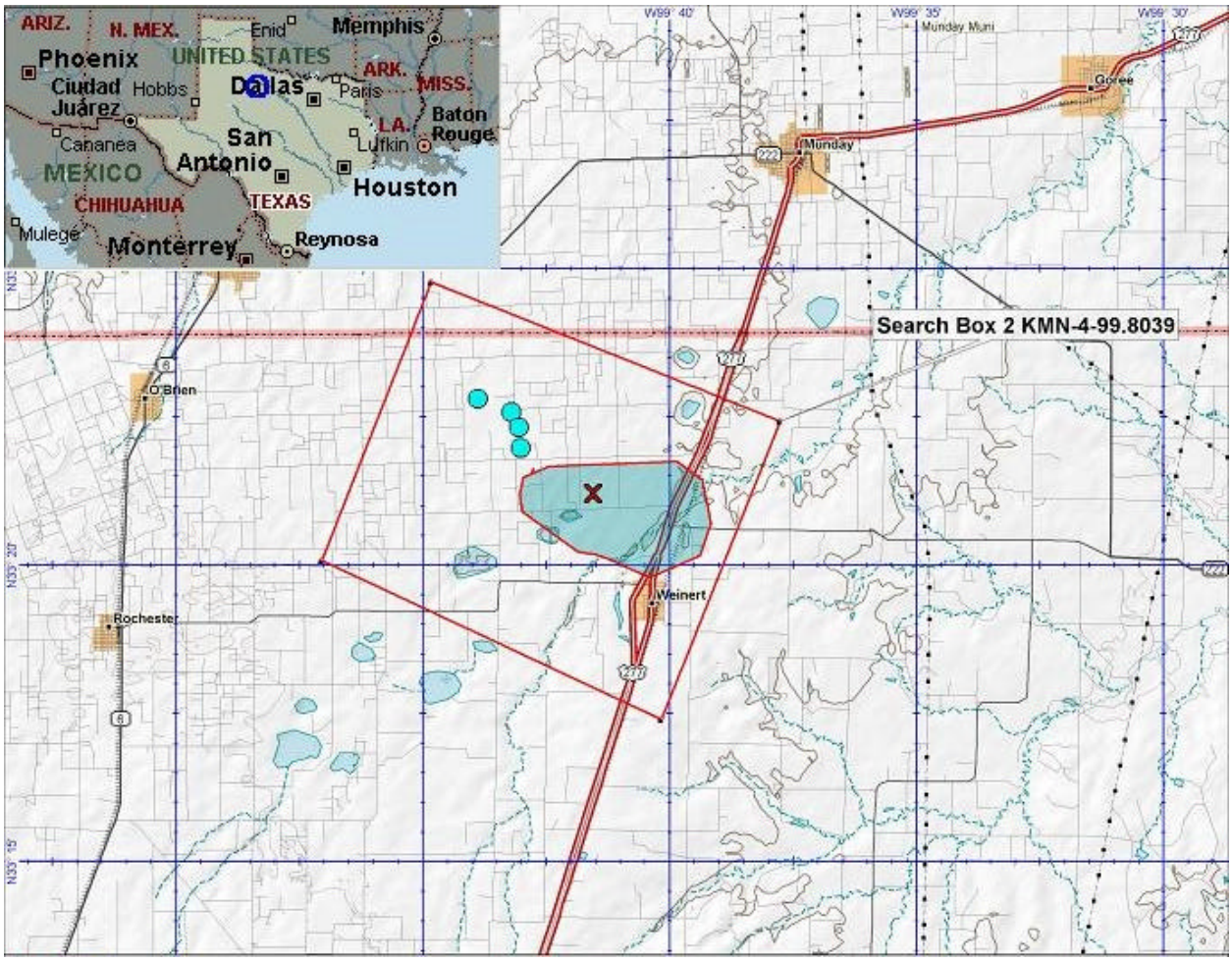

Figure 5-17: Search Box 2 Near Weinert, TX

Search Box 3 Near Floydada, TX

Number of sensors tracking: 2, 1 of these is a high rate (4.5 second sweeps) sensor
Number of tracks: 2
Total number of returns: 28
Time span: 8 minutes, 37 seconds (LBB-ASR-18-101.31) and 6 minutes, 4 seconds (QXS-10-101.433)
Ballistic footprints in proximity: Lifting 16, Non-lifting Flare 1 and Flare 2

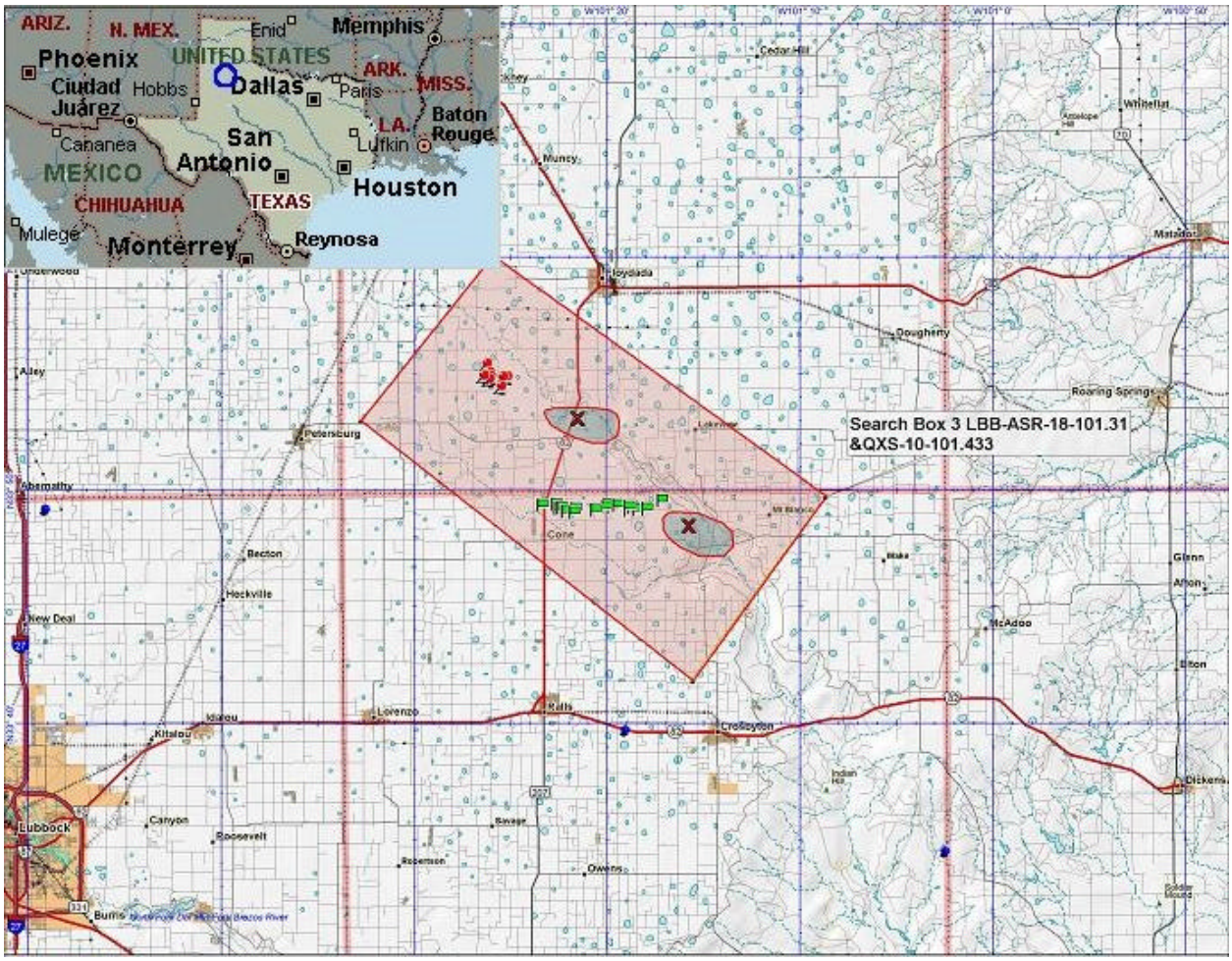

Figure 5-18: Search Box 3 Near Floydada, TX

Search Box 4 Near Brad, TX and Possum Kingdom Lake

Number of sensors tracking: 2, 1 of these is a high rate (4.5 second sweeps) sensor
Number of tracks: 2
Total number of returns: 16
Time span: 3 minutes, 53 seconds (FTW-7-098.595) and 7 minutes, 25 seconds (FTW-9-098.4887)
Ballistic footprints in proximity: Lifting - Flare 2

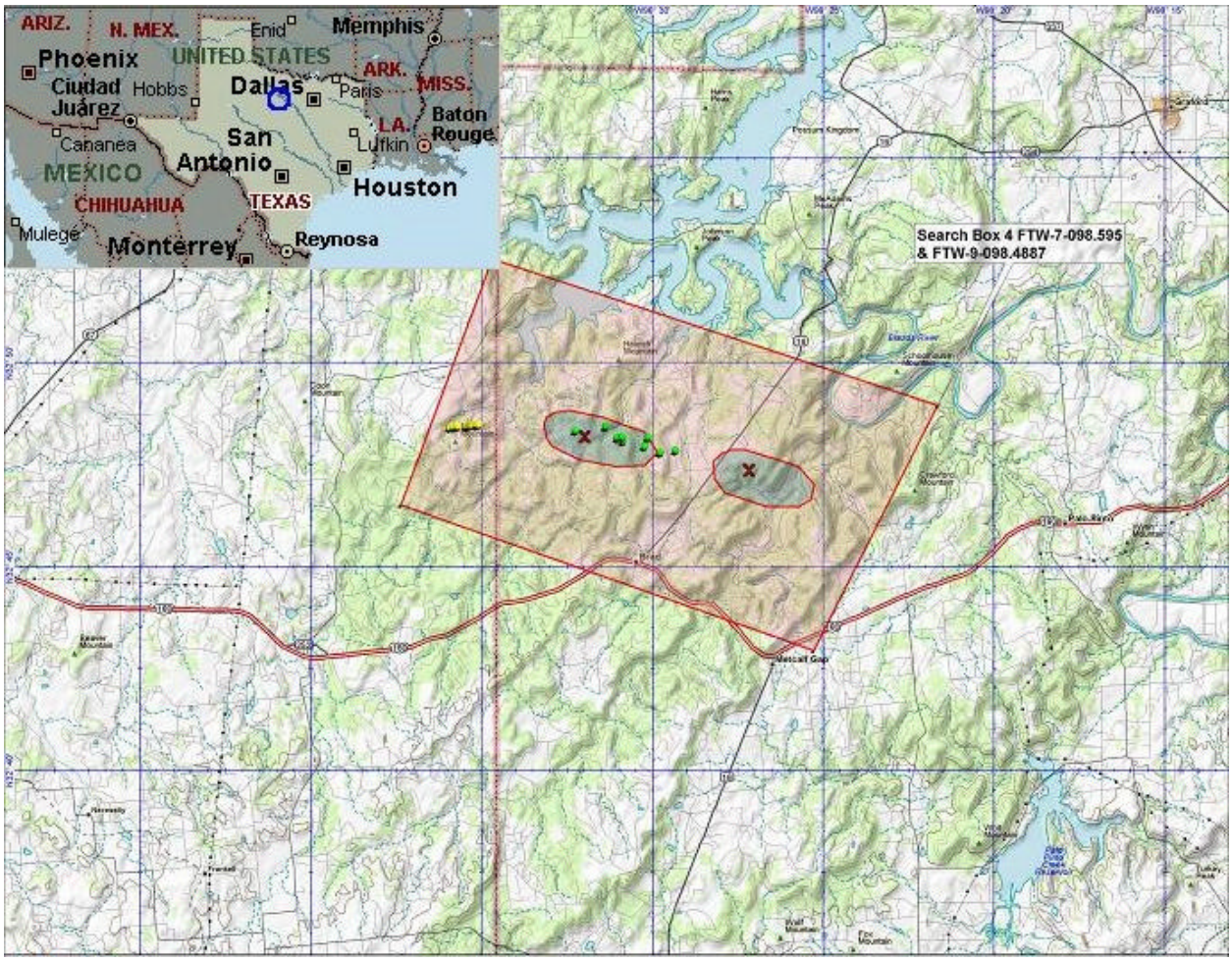

Figure 5-19: Search Box 4 Near Brad, TX and Possum Kingdom Lake

Search Box 1 Near Granbury, TX

Number of sensors tracking: 2
Number of tracks: 2
Total number of returns: 34
Time span: 5 minutes, 36.5 seconds

Tile piece found ~1000 feet north of Search Box 1 on Feb 13.
Full tile found 3.5 statute miles east of Search Box 1 on Mar 12.
Full tile found inside Search Box 1 on Apr 22.

Figure 5-20: Search Box 1 Near Granbury, TX

5.5. Implication of Radar Tests for Radar Based Search Boxes

The Air Force Research Laboratory (AFRL) at Wright-Patterson AFB, OH tested various Orbiter external materials for L-band and S-band radar cross sections. These were used to calculate maximum detection ranges for each material and all air traffic control radars near the STS-107 ground track and generic debris swath. AFRL radar testing in support of the ESAT is described in detail in Section 6.4.

While all of these materials are detectable in the air traffic control radars, the various tile, FRSI and AFRSI materials show very low detection ranges, 23 - 35 nm [15], compared to the leading edge components, 105 - 195 nm [16]. The next series of figures shows the detection ranges for all long range radars which could have tracked Columbia, plotted over the groundtrack and the generic debris swath which was described in Section 4.3.3. From these figures, it can be determined which radars have a high probability of tracking the various Orbiter materials.

Figures 5-21 through 5-23 show the detection ranges for all long range radars. Although many of the long range radars could have tracked leading edge components with a high probability of detection, only three have a high probability of detecting the various tile, FRSI and AFRSI.

Similarly, Figures 5-24 and 5-25 show the detection ranges for all short range radars. Again, although many could have tracked leading edge components with a high probability of detection, only four have a high probability of detecting the various tile, FRSI and AFRSI.

Although the larger leading edge components have much higher radar detection ranges as described in Section 4, ballistic analysis and telemetry analysis suggest the long stream of debris observed in video is comprised of smaller objects, not a series of large, near intact, leading edge components. Thus, confidence was reduced that the radar threads used as the basis for search boxes are Columbia debris.

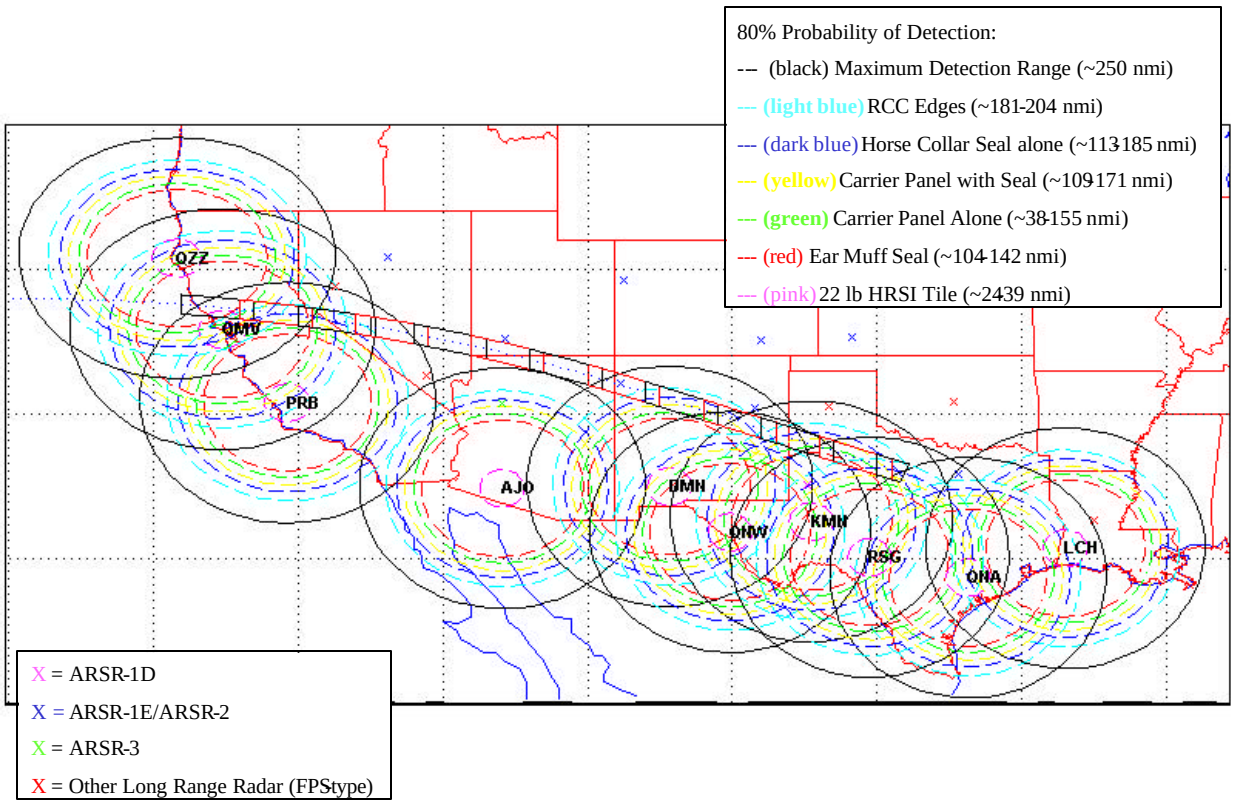

Figure 5-21: Long Range Radar (ARSR-4) Detection Ranges for Orbiter External Materials

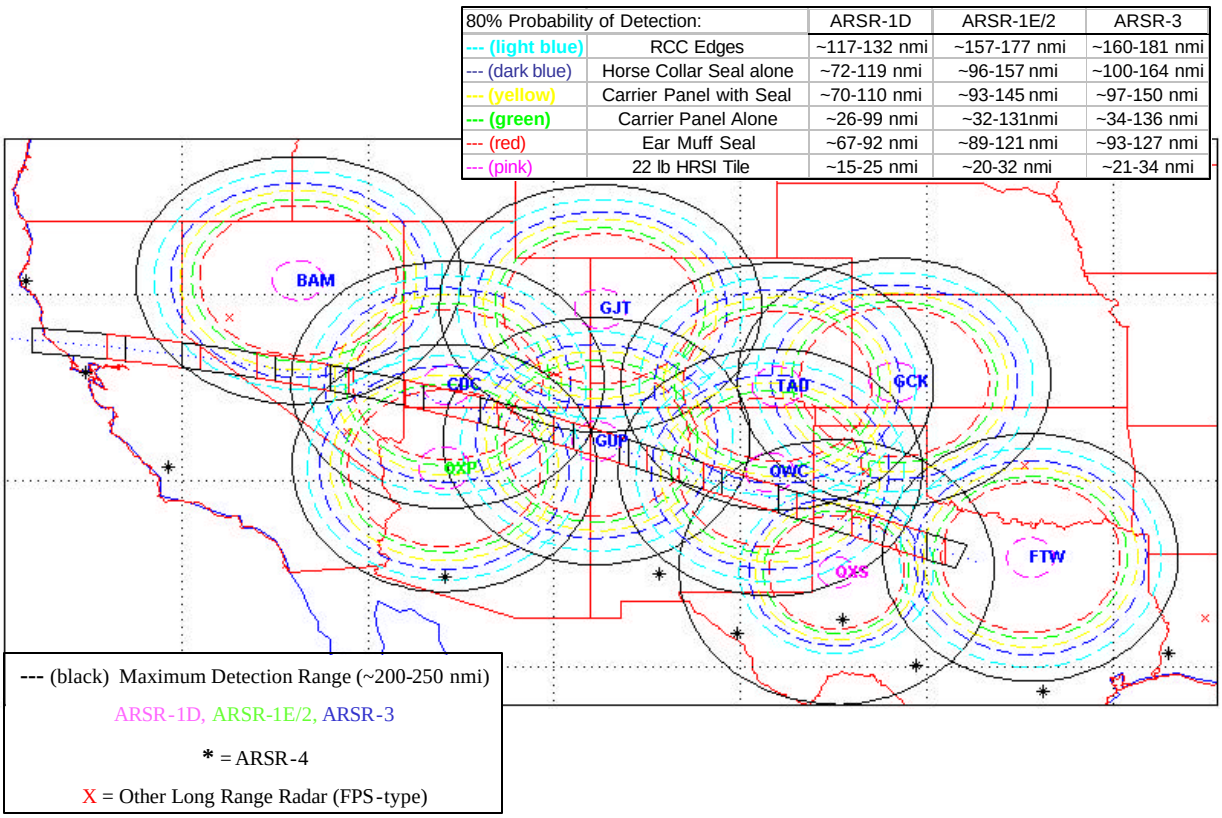

80% Probability of Detection:		ARSR-1D	ARSR-1E/2	ARSR-3
--- (light blue)	RCC Edges	~117-132 nmi	~157-177 nmi	~160-181 nmi
--- (dark blue)	Horse Collar Seal alone	~72-119 nmi	~96-157 nmi	~100-164 nmi
--- (yellow)	Carrier Panel with Seal	~70-110 nmi	~93-145 nmi	~97-150 nmi
--- (green)	Carrier Panel Alone	~26-99 nmi	~32-131nmi	~34-136 nmi
--- (red)	Ear Muff Seal	~67-92 nmi	~89-121 nmi	~93-127 nmi
--- (pink)	22 lb HRSI Tile	~15-25 nmi	~20-32 nmi	~21-34 nmi

Figure 5-22: Long Range Radar (ARSR-1D, 1E, 2 & 3) Detection Ranges for Orbiter External Materials

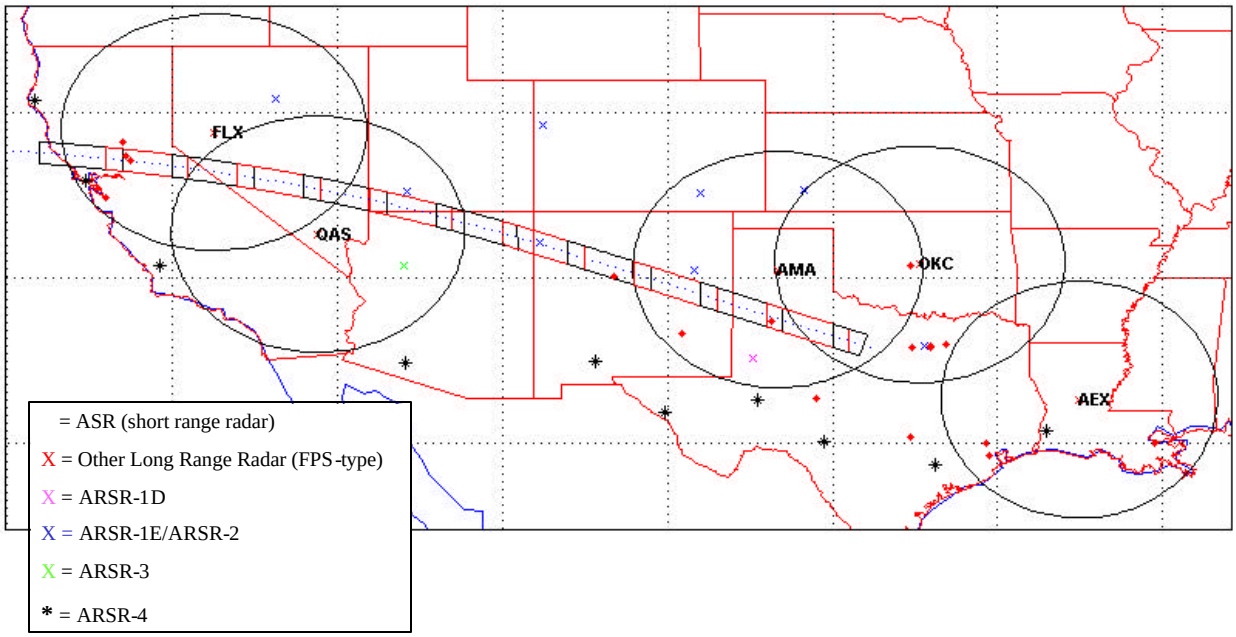

Figure 5-23: Long Range Radar (FPS, similar to the ARSR-1D, 1E, 2 & 3) Detection Ranges for Orbiter External Materials

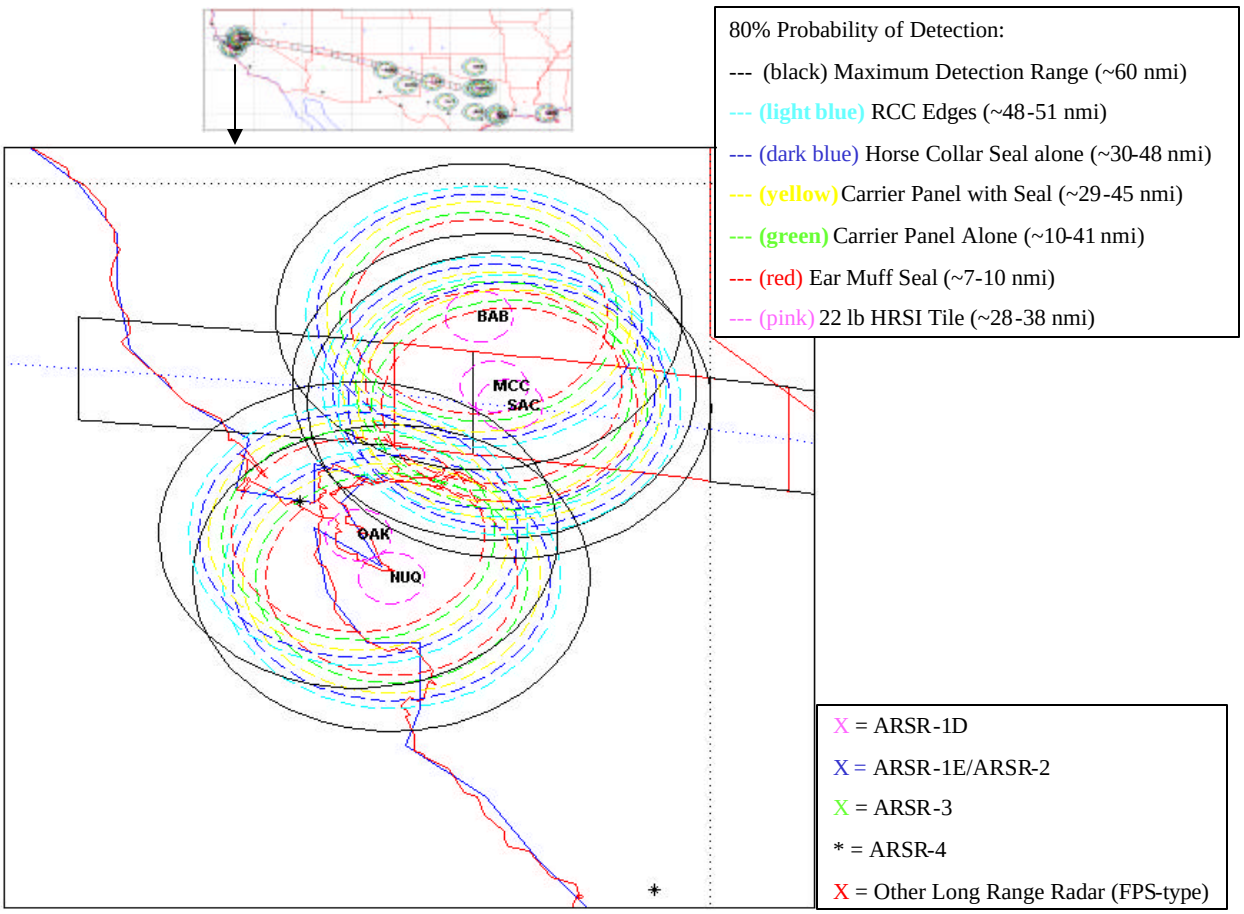

Figure 5-24: West Coast Short Range Radar (ASR-9)
Detection Ranges for Orbiter External Materials

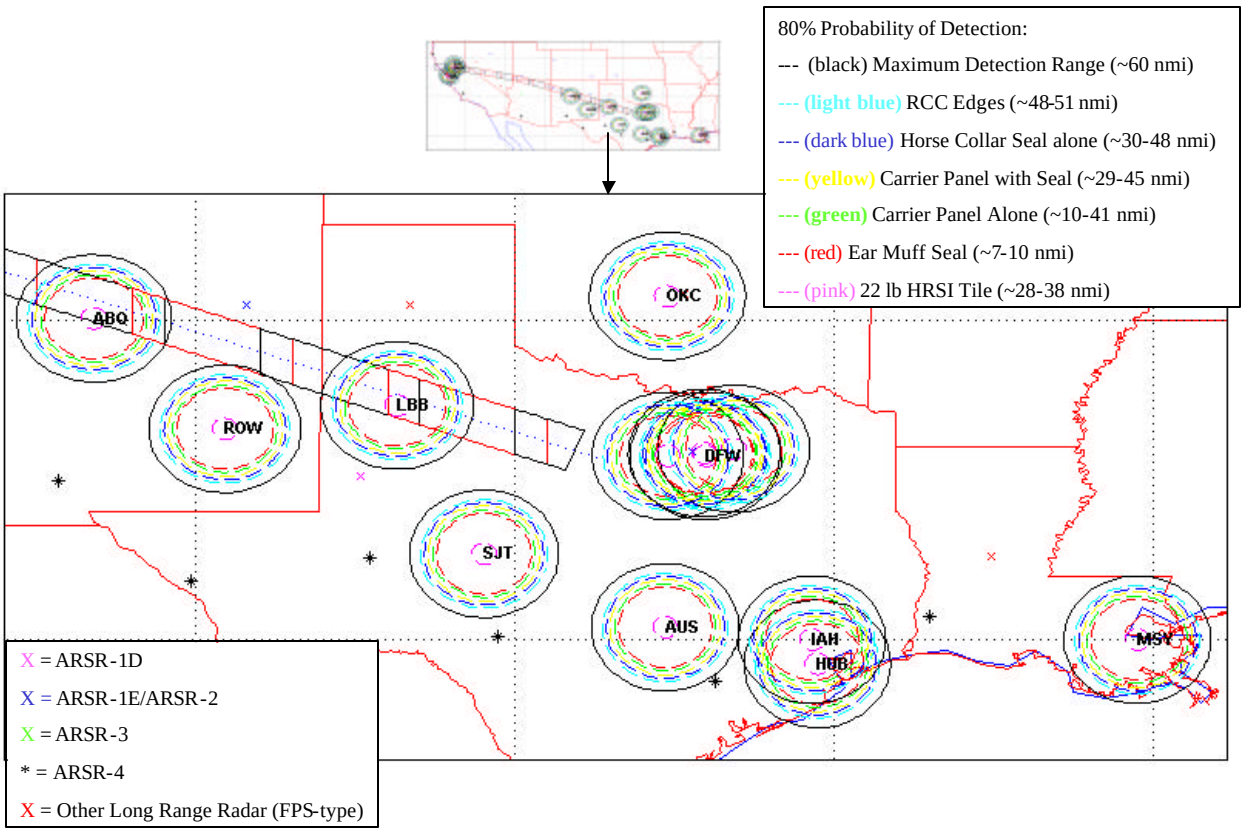

Figure 5-25: New Mexico and Texas Short Range Radar (ASR-9) Detection Ranges for Orbiter External Materials

This leaves the much larger trajectory based footprints as the most reliable predictions for pre-breakup debris ground impact, although they are too large to effectively search for debris. Radar tracks could not be ruled out altogether as returns from Columbia debris, but the associated search areas were prioritized based on their proximity to the non-lifting and lifting footprints for each debris shedding event.

Figure 5-26 shows the combined footprints for all debris shedding captured in public video. The upper plot shows the footprints, and the lower plot highlights the areas where the non-lifting footprints overlap. Of the ballistic footprints, these overlap areas are considered the highest probability areas in which to find pre-breakup Columbia debris.

Figures 5-27 through 5-29 show several of the radar based search boxes mapped with the higher probability overlap areas. Each of the radar search boxes was further prioritized based on the proximity to these overlap areas. As already described, this was then combined with witness reports and probability of detecting Orbiter materials on the given radar, resulting in the prioritized lists in Tables 5-1 and 5-2.

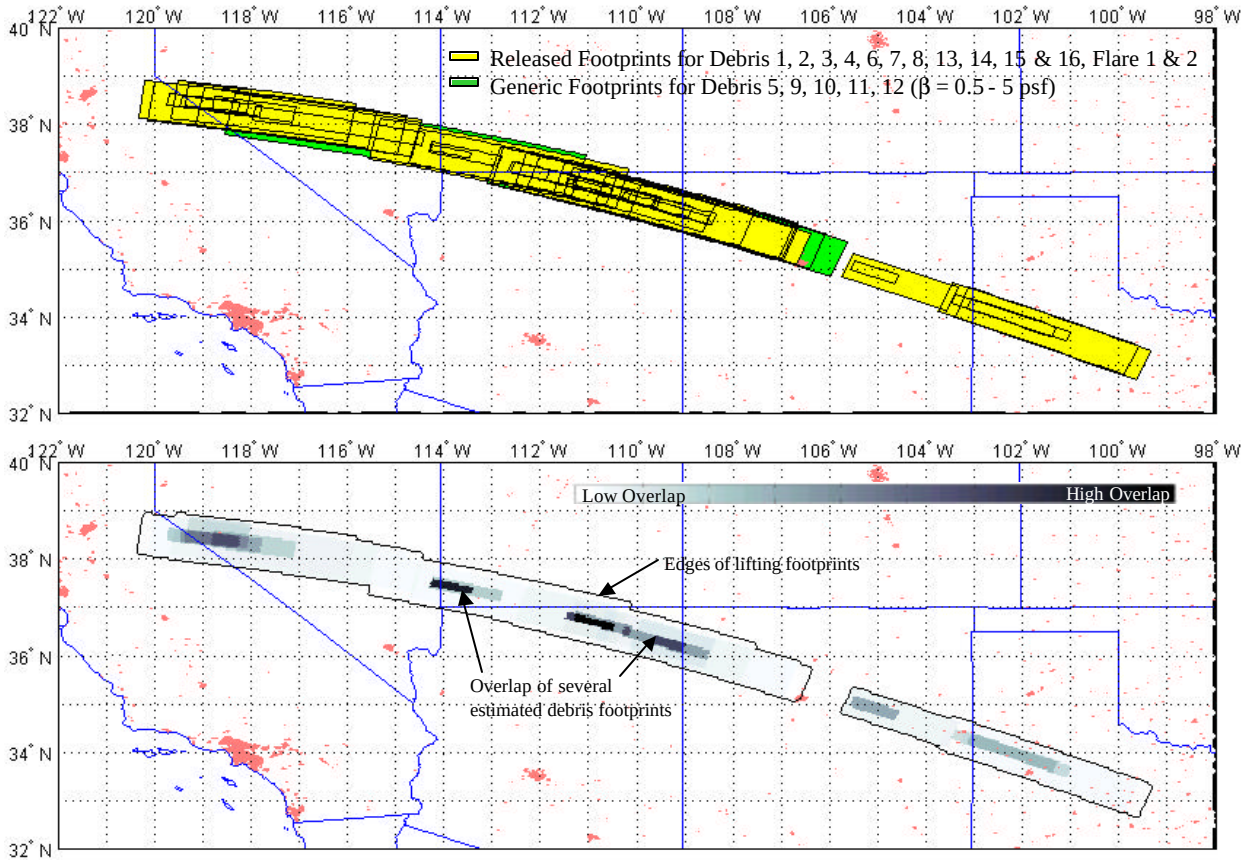

Figure 5-26: Combined Overlapping Ground Impact Footprints of Observed Debris 1 through 16

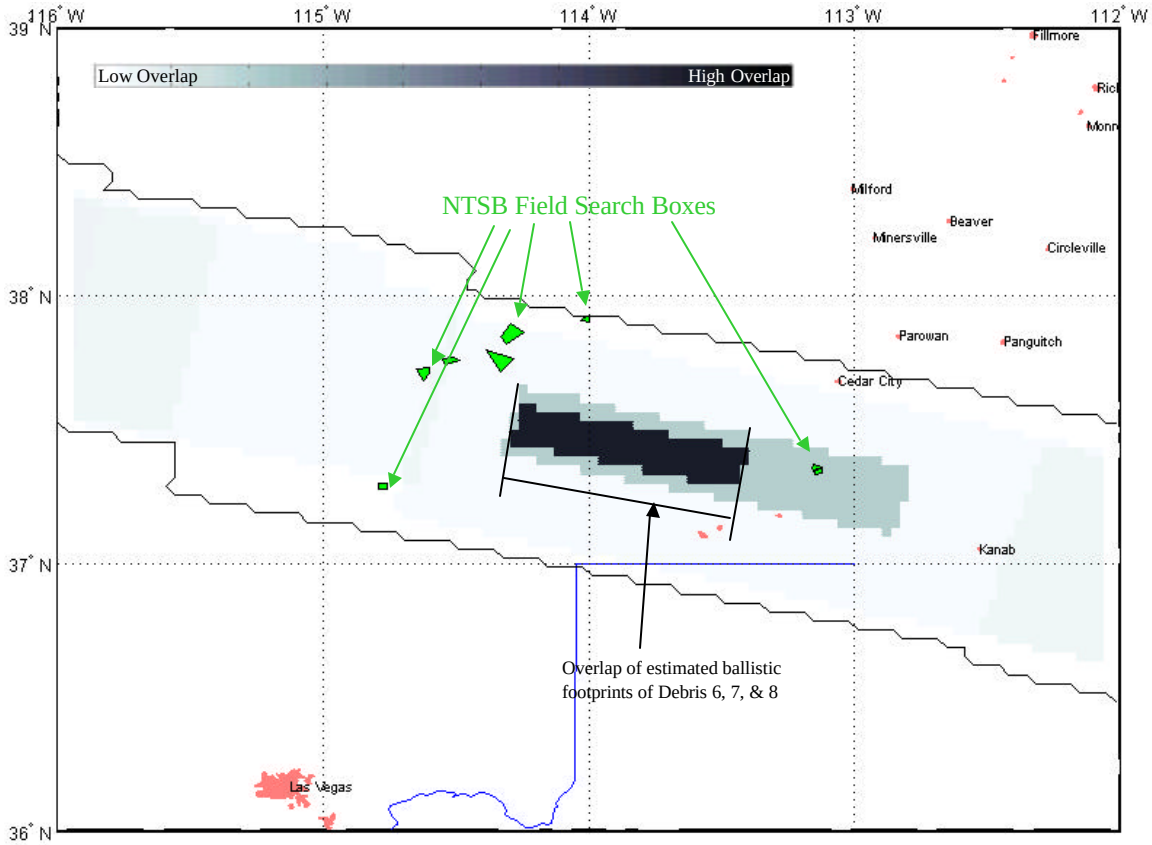

Figure 5-27: Overlap of estimated ballistic footprints of Debris 6, 7, and 8

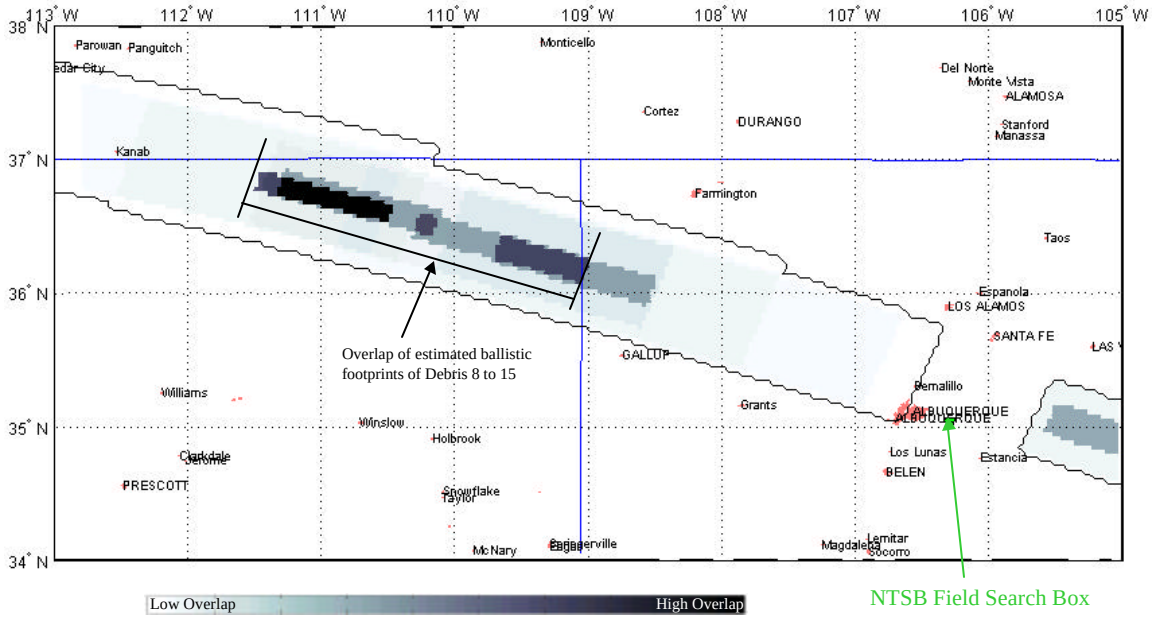

Figure 5-28: Overlap of estimated ballistic footprints of Debris 8 through 15

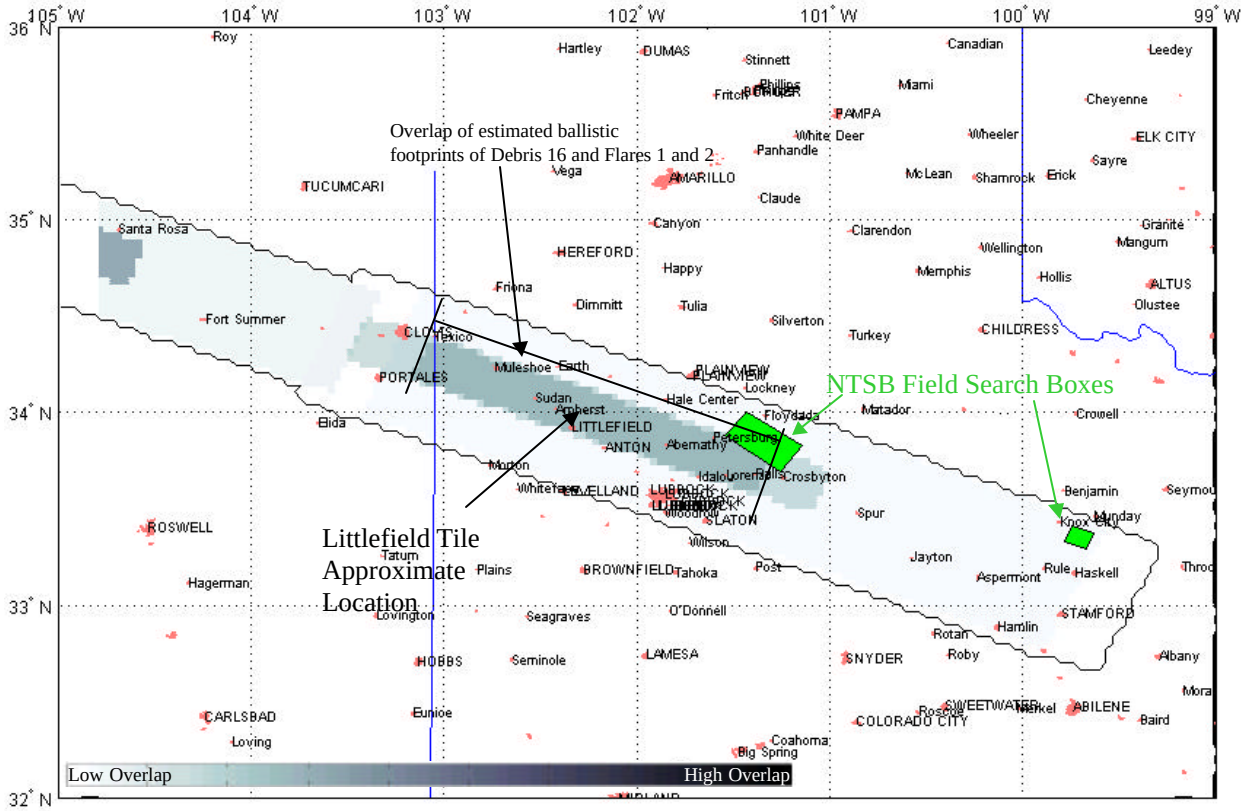

Figure 5-29: Overlap of estimated ballistic footprints of Debris 16, Flares 1 and 2

The ESAT and MIT discussed dropping candidate external Orbiter materials from balloons or aircraft in order to measure radar cross section (RCS) in actual air traffic control radar. Several options were pursued at the conceptual level through AFRL, but ultimately the results still would not have been directly comparable to debris behavior during entry. Initial velocities could not have duplicated the velocities at the altitude of debris that was shed at greater than 12,000 mph, still traveling over 200 mph at 80,000 feet. Ultimately, it was concluded that the AFRL radar test results sufficed.

As described in Section 6.4, AFRL also tested external Orbiter materials for the C-band radars which track during ascent. The C-band radar tests were added to investigate the ability to track debris during ascent, with a primary goal of quantifying the likelihood of discriminating Shuttle debris in the ascent plume and the ability to track the most likely Shuttle debris with the C-bands in general. These tests resulted in detection ranges similar to those shown above for the air traffic control radars.

The C-band data is separated into time slices that correspond with operator initiated changes to the radar characteristics. During launch, the C-band radars are manually adjusted (power/sensitivity/etc.) to optimize tracking performance. These different radar configurations

result in changes to the detection threshold. An example for each C-band radar is shown below, but the full data set is not shown in this report since they are not used for early debris sightings.

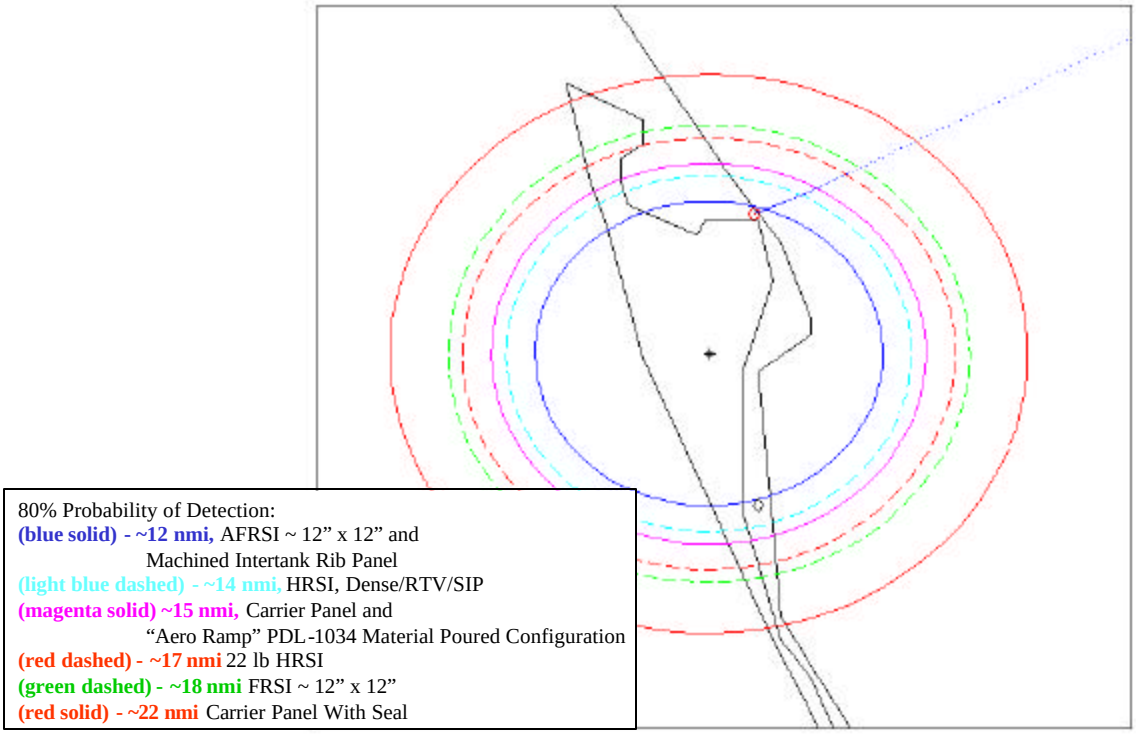

Figure 5-30: Patrick C-Band Radar 19.14, T +20 – 85 sec

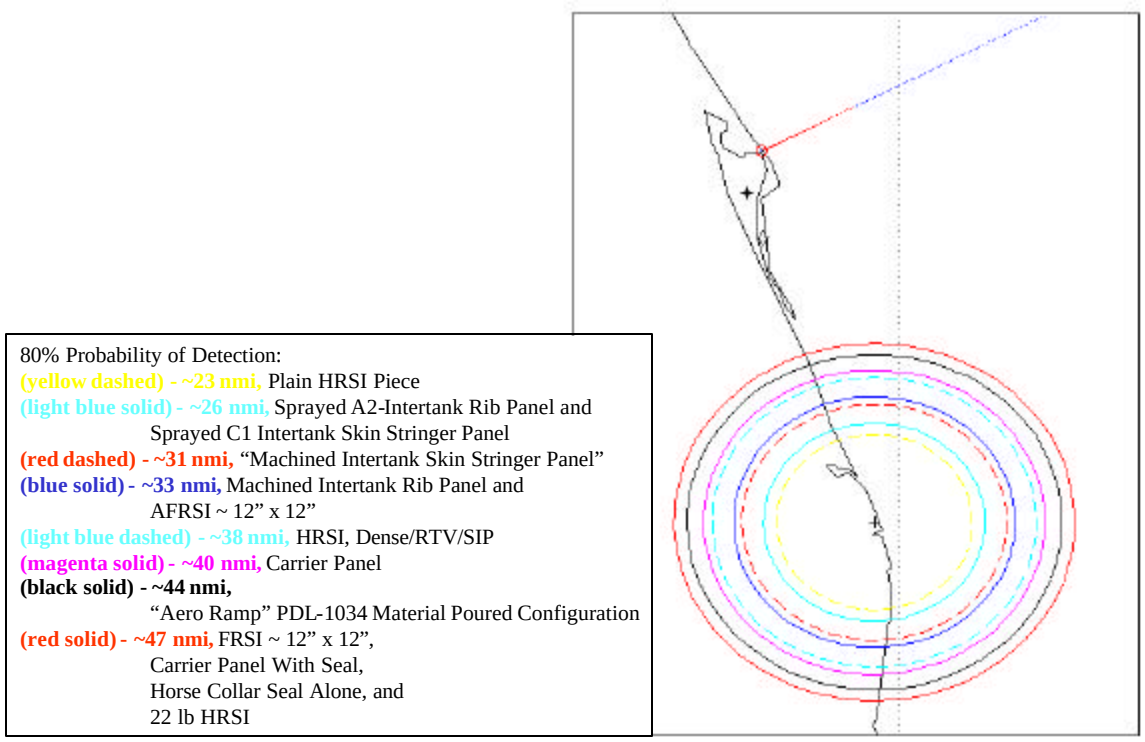

Figure 5-31: Patrick C-Band Radar 0.14, T +31– 120 sec

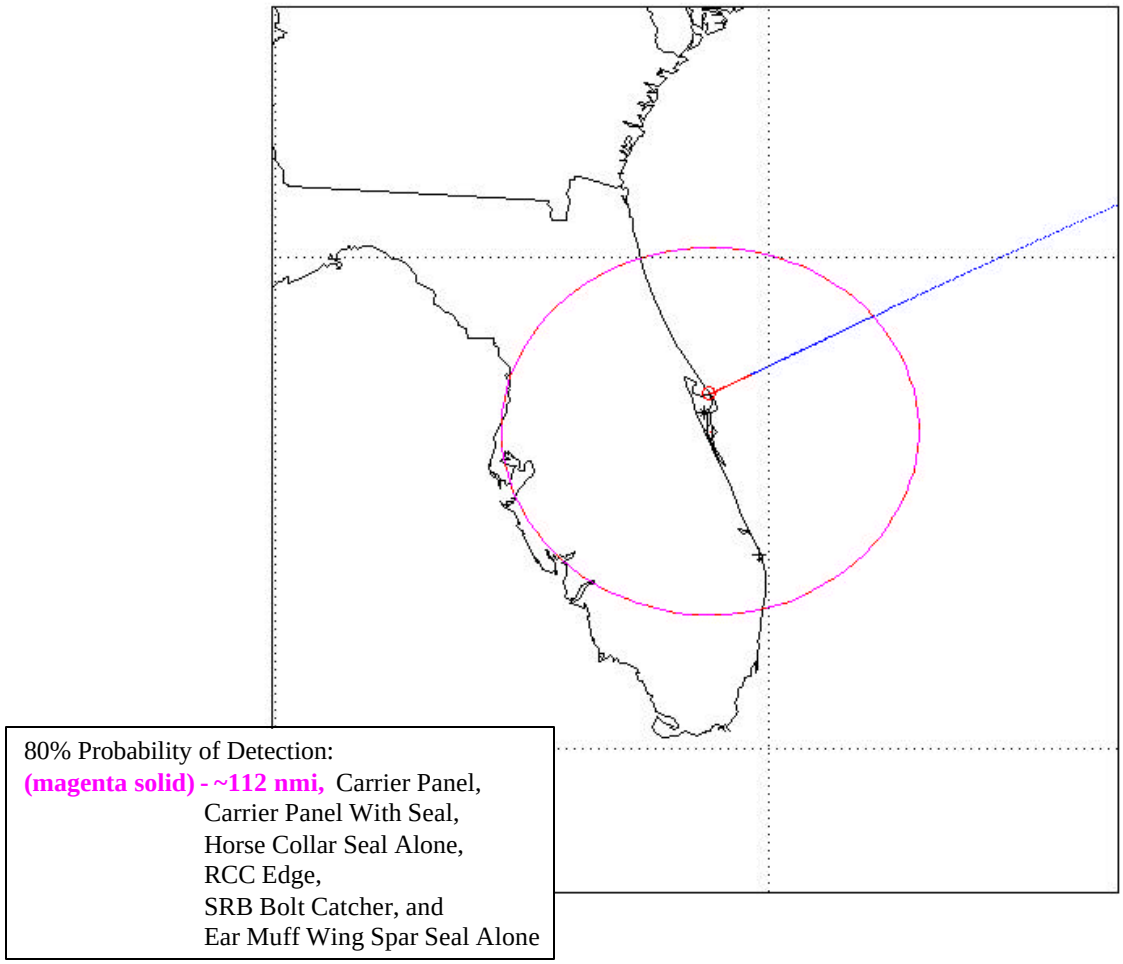

Figure 5-32: Patrick C-Band Radar 28.14, T +0 – 121 sec

5.6. Radar Search Areas Lessons Learned

1) Focus energy looking for localized “blob” tracks vice linear radar tracks.

2) Focus the search for tracks closer to the groundtrack within the non-lifting footprint.

3) Integrate eye-witness reports into radar search as early as possible.

4) Station NASA Radar Assessment Team representative at the field operations center for debris searches to help coordinate search box data and act as primary liaison between the RAT and MIT/Search Coordinators.

5) Conduct daily telecons with NTSB/FAA/RADES to discuss radar tracks, search boxes, etc.

6. Witness Reports

Unless otherwise footnoted, Section 6 is referenced to [53] Schafer, Craig P.; SAIC; Results of Search for Observed Debris Landing Events, and EOC Hotline and Database Lessons Learned for STS-107 Accident Investigation; May 16, 2003. This is included in its entirety in Appendix 10.8.

6.1. Witness Report Summary

Eyewitness reports received by the various investigation teams were routed to the ESAT for assessment and prioritization for follow up. Almost 2,000 eyewitness reports were searched for cases where objects were seen falling to earth. This collection of eyewitness reports was searched for citations of observations of objects landing within the generic debris swath that was generated by ballistics analysis.

A hand search was conducted on the ESAT's paper collection of eyewitness reports, and a keyword search of the JSC EOC and Shuttle Interagency Debris Database (SIDD) electronic databases was performed. These searches focused on eyewitness reports of debris falling to the ground in California, Nevada, Utah, Arizona, New Mexico, and Texas (west of Dallas). Because the SIDD had over 61,000 entries, an exhaustive search was not possible. However, keywords like "falling," "saw," "ground," and "earth" were used to attempt to identify pertinent reports. The resulting sightings were evaluated and put into three major confidence categories with the following criteria:

- HIGH: Eyewitness saw object(s) fall to earth. Event time and place were reasonable relative to Columbia overpass.
- MED: Eyewitness saw object(s) fall to earth. The time of the observation was fairly long after Columbia overpass, but not unreasonably so (on the order of an hour).
- LOW: Eyewitness observed debris falling in the sky but did not see any landings. Length of time (over an hour) after Columbia overpass or distance from groundtrack was considerable, but the event is not completely ruled out.
- NONE: The report was not relevant to this search (ex. sound reports), or the sighting was extremely unlikely to be related to the accident (ex. observing something the day before or after in the sky).

The search yielded two reports of enough confidence to search for radar contact correlations and, in one case, warrant a ground search. The Delamar Lake, NV and Glencoe, CA reports were rated the highest degrees of confidence. These two sightings were coordinated with the Radar Analysis Team to compare with radar contacts. In the Delamar Lake, NV case, the correlation with radar data was strong enough to warrant the dispatch of search teams.

6.2. Credible Sightings

High Confidence Sightings

2-1-1297 (Delamar Lake, NV)

The witness was camping by Delamar Lake, Nevada (about 70 miles north of Las Vegas) on the morning of the accident when he witnessed Columbia pass overhead. At some point during the overpass, he saw a bright flash from the contrail. He heard a boom about two minutes after the overpass. Between two and 10 minutes later, he observed two “twinkles” descend ("drifting down") into a mountain range between two peaks, and then wink out below the skyline. He thought the objects fell about 10 miles away east or slightly north of east of his campsite, but he did not have a compass or GPS receiver at the time to verify those directions. The sun was still below the horizon at the time of the sighting.

The witness spent two days searching the area he believed the objects fell, but did not find anything. He was confident he could show a NASA search team the exact area he saw the objects fall into. He looked up his campsite location on a map on 2/24/03 and gave the following coordinates: (N 37 deg 19 min 30 sec, W 114 deg 58 min).

His sighting was well within the preliminary lifting footprints of both Debris 1 and Debris 6 as shown in Figures 6-1 and 6-2.

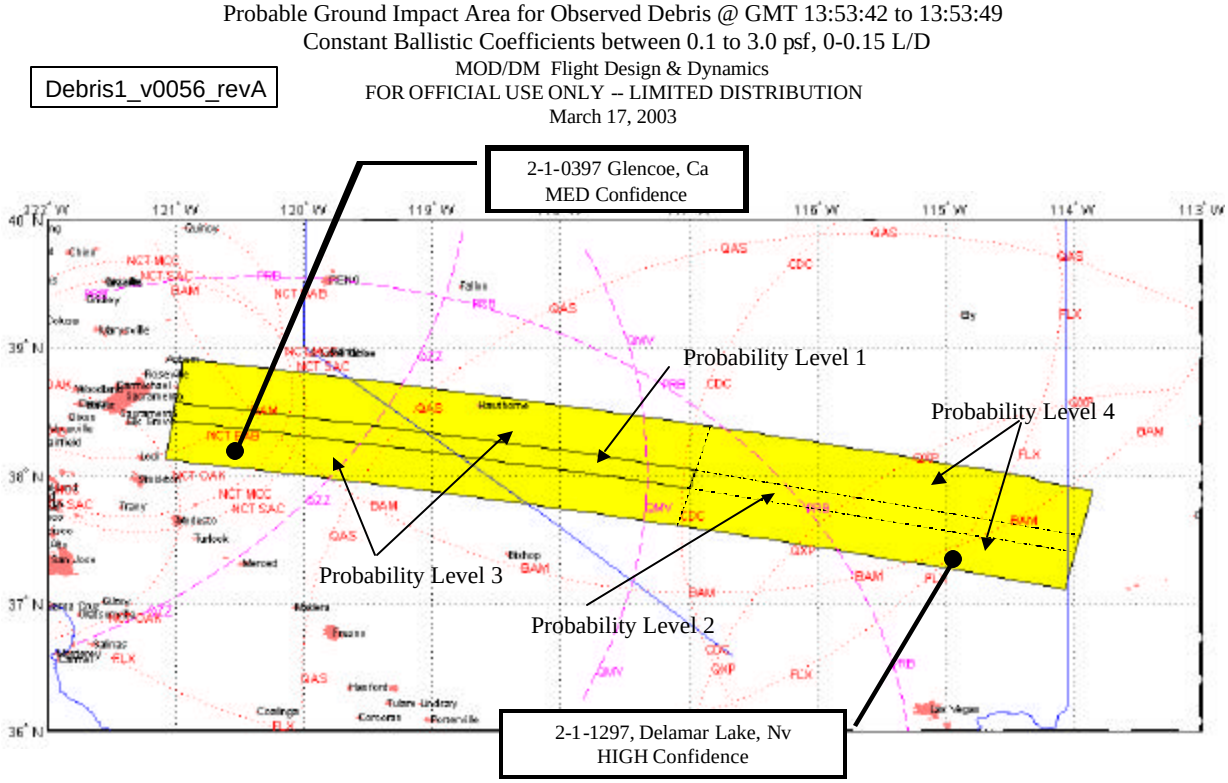

Figure 6-1: Eyewitness Correlations with a Preliminary Debris 1 Footprint

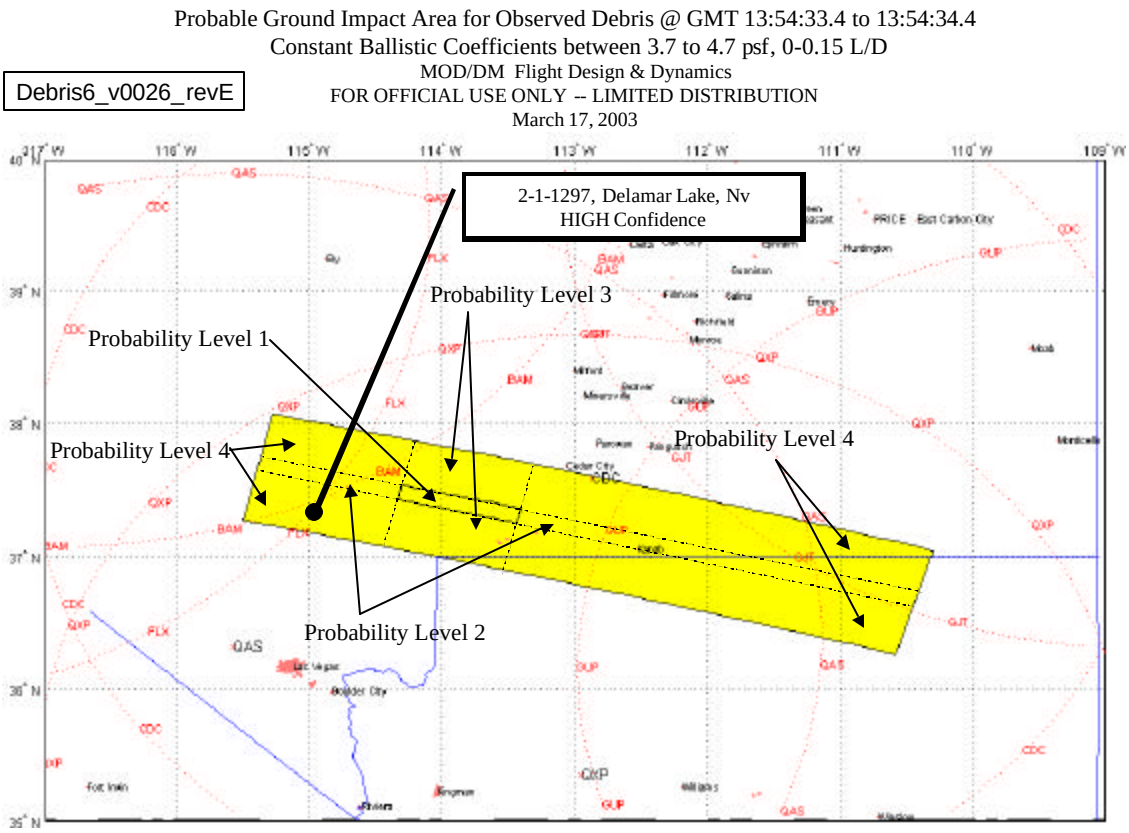

Figure 6-2: Eyewitness Correlations with a Preliminary Debris 6 Footprint

The Delamar Lake sighting is close to the dense overlap area of the ballistic footprints of Debris 6, 7, and 8. This is explained in more detail in Section 5.5, and is shown below in Figure 6-3.

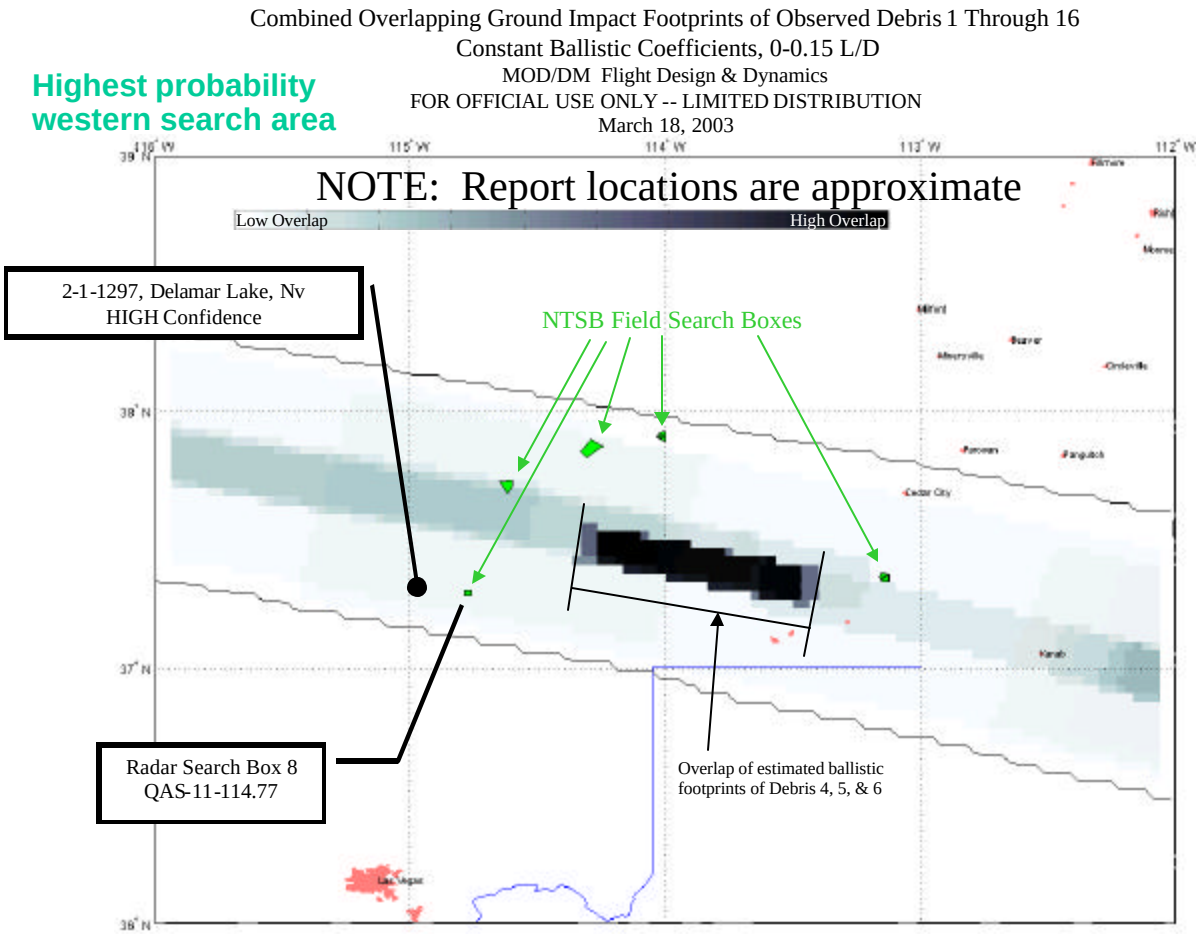

Figure 6-3: Locations of Delamar Lake, NV Campsite, Radar Based Search Box 8 and an Early Version of the Overlap of Estimated Ballistic Footprints of Debris 6, 7, and 8

This sighting is also close to the radar contacts in radar search box 8 as shown in Figure 6-4. Search box 8's location was about 10 miles E-SE of the witness' campsite and within a mile south of where he thought the objects landed.

The Figure 6-4 inset shows a comparison of the area the witness thought the objects fell into (Primary area: blue border, no shading, Secondary area: red border, no shading), and Search Box 8 (red border, yellow shading). Note the black-bordered area is an additional area of interest added by the Debris Recovery Team.

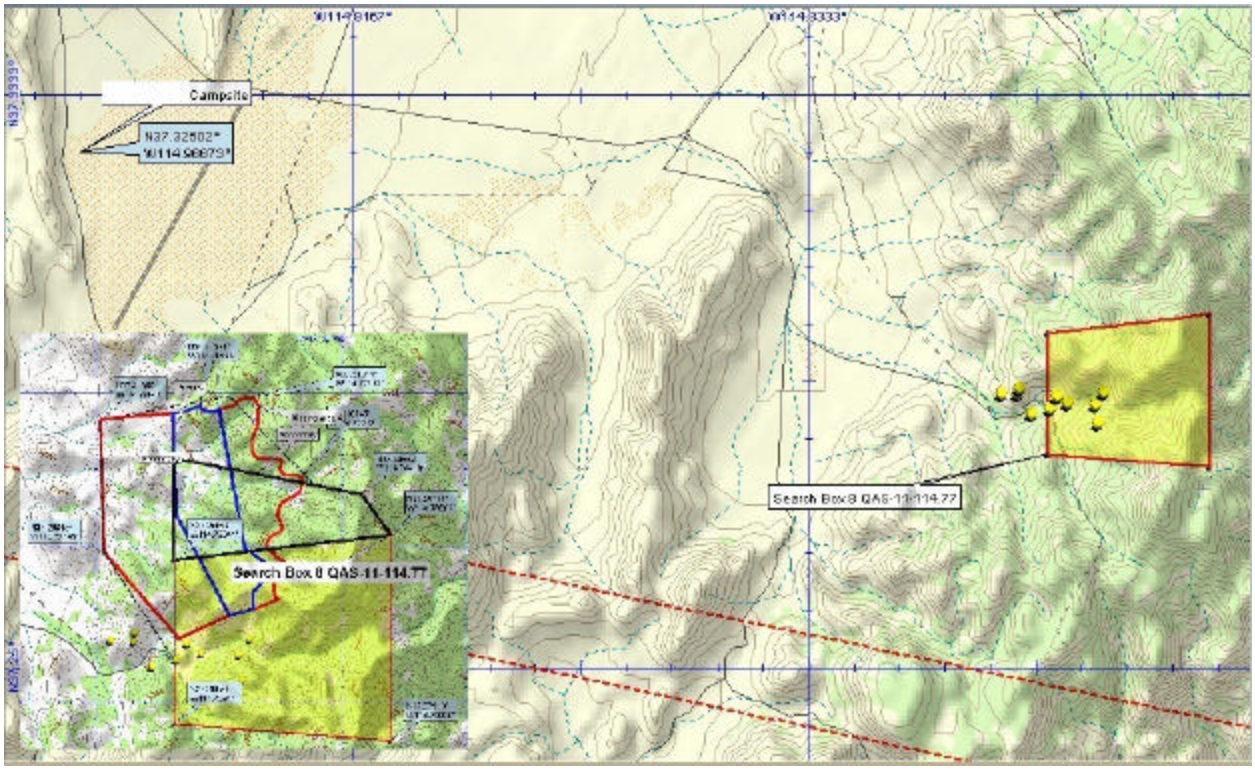

Figure 6-4: Locations of Delamar Lake, NV Campsite and Radar Based Search Box 8
Inset: Comparison of NTSB Search Box 8 and Search Area Outlined by Eyewitness

The times of the radar contacts in Search Box 8 were found to be at about the same time as the Delamar Lake sighting. It was therefore concluded that there was a strong spatial and temporal correlation between the radar contacts in Search Box 8 and the witness' sighting. A summary report was written on the case and passed on to the California/Nevada/Utah Debris Recovery Team, which made arrangements to search the area.

<u>MED Confidence Sightings</u>

2-1-0397 (Glencoe, CA)

The witness reported seeing a glowing object falling very quickly down into the Calaveras River canyon area, south of his home on the morning of Columbia's entry. Upon describing the plasma trail, he said that was not what he saw, but rather the object looked like a "shooting star" descending quickly into the canyon area. The map he drew showed the object falling about two miles south from his home, which was still well within the southern lifting footprint of Debris 1. Figure 6-1 plots the witness' approximate location relative to the preliminary Debris 1 footprint.

There were two groups of radar contacts near the area. One single contact was within a mile of where the witness may have seen an object fall, and a cluster farther to the south.

Significant doubt is cast on this report being related to Columbia because the witness' observation was about an hour after Columbia's overpass, and there are about 36 minutes between the approximate time of his observation and the time of the radar contact. The Radar

Analysis Team is continuing to investigate the disagreement between the observation and the radar contact and search though radar data, so this incident remains categorized as MED confidence.

LOW Confidence Reports

There were numerous reports between California and Western Texas from people seeing debris shedding from the main plasma trail and falling away, or seeing objects falling in the sky. Reports that indicated seeing objects falling but not landing were considered LOW Confidence. Some telephone interviews were conducted to collect additional information on these sightings. In the end, these reports did not add any new information other than confirming debris shedding from Columbia. There is a single report that should be noted because it was particularly unusual. Its details are below.

2-1-2414 (Roswell, NM)

The witness became aware of Columbia's fate about two hours after main breakup. He went outside to see if he could see anything. Looking east, he observed an object slowly 'tumbling' down at an unknown but far distance away. The object would flash then grow dark, which gave him the idea it was tumbling much the way, as he put it, a metal sheet would tumble from high in the sky. He thought it must have been something sizeable to be able to see the tumbling effect. He went inside to get his binoculars to get a closer look. By the time he was outside again, the object had fallen into the sun disc, making observation with the binoculars impossible. He thought the object traveled eastward and downward during his observation. No correlating radar contacts have been found.

This report was interesting because the object was described as a large sheet tumbling out of the sky, which is an unusual occurrence at any time. However, the time between this sighting and Columbia's overpass is quite long, and the object could have been 30 miles or more south of the generic, lifting footprint. Thus, confidence is low that the object is related to Columbia.

NONE Reports (No Confidence)

There were also a large number of reports of hearing one or more 'booms' and seeing the plasma trail. These reports were of some use in the early days of the investigation to determine Columbia was seen and heard as far back as northern California, but no more technical information was gained from them. Once it was clear that public imagery was available with near continuous coverage, these reports were of anecdotal use only.
People also reported seeing fast moving and/or falling objects days before and after the accident, which could not be reasonably attributed to Columbia's reentry.

6.3. Witness Reports Lessons Learned

NASA should consider developing a method of educating the public on how best to record future reentries so that, if such a mishap ever occurs again, the video would more easily facilitate post-flight analysis. This would include all important imagery characteristics and supporting data which are key to the analysis.

7. DOD Data

The DOD Columbia Investigation Support Team (DCIST) was formed to provide a single point of contact to NASA for all DOD sensor support. Through the DCIST, the DOD collected and analyzed all remote sensor data related to STS-107 which included deep space tracking radar, early warning radar, air traffic control radar, telescopes and infrasound. The DCIST impounded all sensor site data immediately to preserve the ability to reprocess and analyze all data.

NASA requested DOD data per the following priorities, in order from highest to lowest [7]:

1) Process all data from 1340Z -1400Z for high-energy events (include any luminosity and spectral analysis which may indicate size, mass and constituents). Key events to focus on:
   - Discrete debris shedding times.
   - Times associated with off-nominal telemetry signatures.
   - Times indicated as off nominal in infrasonic data (infrasonic data collection in work separately).
   - Bolide detonation reported from Oceanside, CA 1300-1410Z.
2) Process all data from Beale Pave Paws.
3) Confirm any and all imagery from 1 Feb 1340-1400Z has been identified, processed and received.
4) All data from de-orbit burn through break-up.
5) Process the object that has been correlated back to Columbia approx 24 hrs after launch (Flight Day 2 Object).
6) Provide trajectory data to all other national agency/organizations so they can check for related data.
7) Confirm any and all imagery from Ascent-2 Feb, 1340Z has been identified, processed and received.
8) Any "unexpected events" DoD might identify throughout duration of mission via own analysis.

7.1. Remote Sensors During Entry

In the first two weeks of the investigation, there were preliminary indications in various unclassified and classified sensors of some anomalous events during entry. In all cases, the data required considerable post-processing for analysis, and in many cases required detailed comparison to previous flight data to confirm the specific phenomena was anomalous and had not been observed during other flights. The early reports are summarized by a generic statement authorized for release by Air Force Space Command on February 24 for all such data:

> Department of Defense systems received indications of unusual Columbia mission activity at [DTG]. These indicators imply possible [debris shedding/structural flaw/object impact/increased heating/anomalous flight condition] at that time. [8]

By April 8, all preliminary indications by remote sensors during entry were either attributable to some known and nominal Orbiter entry related event or were considered indistinguishable from the background indications for the given sensor. [10] The following table lists the significant remote sensor events which were considered for the STS-107 Entry Timeline.

Date/Time	Historical or Unique?	Cause Known / Unknown?	Comments
16 Jan 15:56:22-16:01:10	Historical	Unknown	
1 Feb 13:52:19-14:10:08	Historical	Unknown	Location: 13:51:20 Initially labeled as remote sensor event 1
1 Feb 13:52:30	Historical	Known	
1 Feb 13:56:32-14:05:34	Historical	Unknown	Location: 13:55:30 Initially labeled as remote sensor event 2
1 Feb 13:56:28	Historical	Known	
1 Feb 13:56:53	Historical	Known	

Table 7-1: DOD Remote Sensor Indications during STS-107 Entry [9]

In fact, several interim versions of the timeline included “remote sensor events 1 and 2” at 13:52:30 and 13:55:30Z respectively based on initially high confidence by the sensor experts. However, as explained above, these too were better understood after more lengthy analysis and later determined to be explainable or inconclusive. In the final assessment, there are no reliable indications of debris shedding or other anomalous pre-break up phenomena in any DOD remote sensor data. [10]

7.2. Imagery: AMOS, Kirtland AFB

Columbia was imaged during 3 days of STS-107 orbit operations by the Air Force Maui Optical & Supercomputing (AMOS) Site. Columbia was also imaged during entry by employees of the Starfire Optical Range at Kirtland AFB, NM, although these images were not through the DOD optics.

These AMOS and Kirtland images are the only DOD images taken of Columbia during STS-107 from any source, unclassified or classified.

AMOS captured visible images on January 17, 22, and 28, and infrared images on January 28. These are predominantly of the upper surfaces with payload bay doors open, obscuring a significant portion of the wings. A few of the visible and infrared frames are from the front of the vehicle, but the quality or lighting is insufficient to show detail. Examples of the visible image and infrared images are shown below in Figures 6-1 and 6-2. [3][4]

Figure 7-1: Example AMOS Visible Images of Columbia during STS-107 [4]

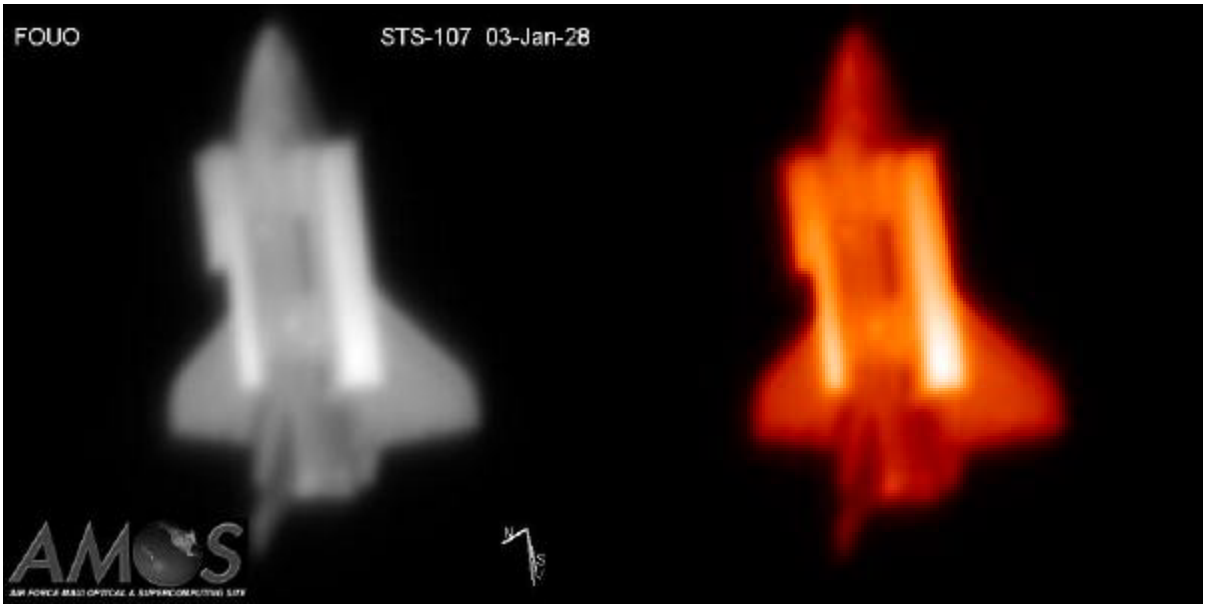

Figure 7-2: Example AMOS IR Images of Columbia during STS-107 [3]

While these images taken from the ground of a manned spacecraft in orbit are fascinating, particularly when individual frames are strung together as a video, they show no discernible damage. The post-processed infrared images and the corresponding thermal mapping shown in Figure 7-3 below suggest that this capability may be valuable on future flights for detecting significant external damage, and this is under study by NASA JSC. To facilitate use of this capability for damage detection on future flights, the Air Force Research Lab (AFRL) has requested detailed material maps of the Orbiters.

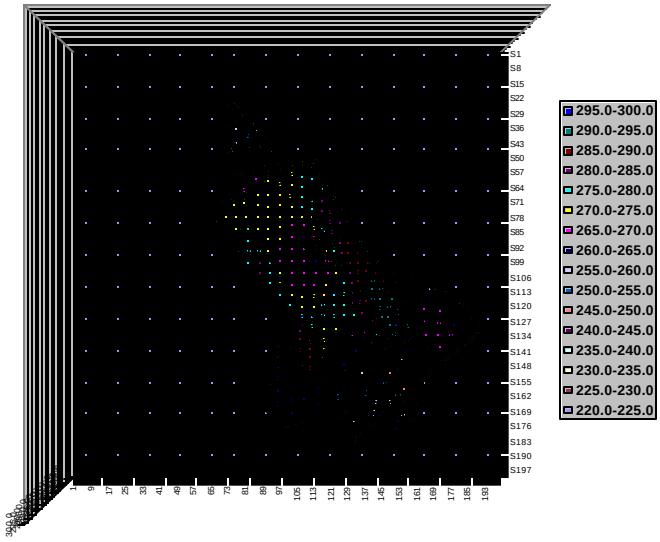

Figure 7-3: Example Thermal Mapping of Columbia
Based on AMOS IR Image during STS-107 [3]

A separate NASA tiger team was established under the Orbiter Vehicle Engineering (OVE) Working Group to study the Kirtland images for any data useful to the investigation. All

detailed descriptions and conclusions are therefore deferred to that team. This report includes only representative images and ESAT support to this study.

The images below in Figures 7-4 and 7-5 are representative of three stills and four videos taken by employees of the Starfire Optical Range at Kirtland AFB, New Mexico during STS-107 entry. They are not official DOD images and were taken through personal equipment, not the Starfire optics. Figure 7-4 is the image released to the press that sparked considerable early speculation regarding left wing leading edge damage and asymmetric wake.

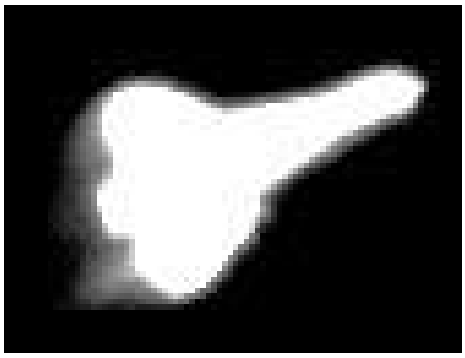

Figure 7-4: Example Raw Still Taken by Starfire Optical Range Employees during STS-107 Entry [5]

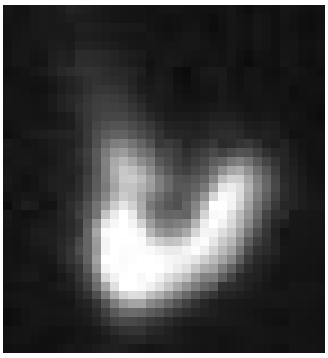

Figure 7-5: Example Frame from Raw Video Taken by Starfire Optical Range Employees during STS-107 Entry [5]

In support of this team's analysis, the ESAT provided Orbiter state vectors, a series of wire frame images of the Orbiter as viewed from Kirtland AFB throughout the pass and coordinated a series of solid model images. These Orbiter images were superimposed over the Kirtland images to help evaluate them for anomalies. Examples are shown in Figure 7-6.

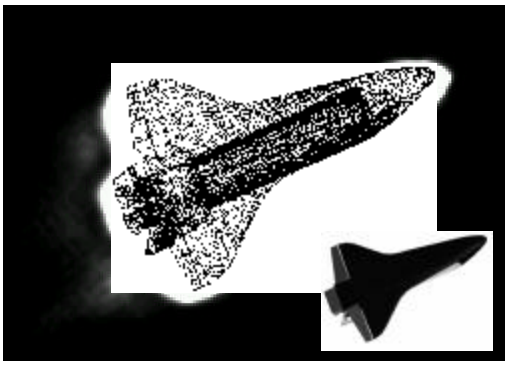

Figure 7-6: Example Orbiter Wire Frame Superimposed over Raw Still Image Taken by Starfire Optical Range Employees during STS-107 Entry and the Associated Solid Model [5]

7.3. FD2 Radar Data

A separate NASA tiger team was established under the OVE Working Group to study the Flight Day 2 object for any data useful to the investigation. All detailed descriptions and conclusions are therefore deferred to that team. This report includes only a summary of the radar data and ESAT support to this study.

During a post-flight search, Air Force Space Command discovered anomalies associated with STS-107. Uncorrelated observations from radar data were found in the same orbit as Columbia. Additional observation data was then obtained from four sensors from January 17, 18 and 19. The additional data allowed trajectory reconstruction that indicates an object separated from the Orbiter on January 17, between 1500-1615Z, Flight Day 2 of the STS-107 mission. Preliminary analysis was provided to NASA on February 9. [1]

The DCIST confirmed no other objects were tracked within 5 km of Columbia throughout STS-107.

Several passes of radar cross section versus time data were obtained by a combination of the Cape Cod and Beale UHF phased array radars and the Kwajalein VHF/UHF radar. Data from the Cape Cod passes is shown in Figures 7-7, 8 and 9. Early interpretation of this data suggested a small plate-like, spinning or tumbling object. Orbital behavior indicated a relatively lightweight object which decayed after approximately 60 hours in orbit. [2] It was also pointed out that, "had the SSN been tasked, it could have supplied additional data." [1] This will be included in a follow on activity to generically review DOD tracking capability for possible changes to routine and contingency tasking on all future Shuttle flights.

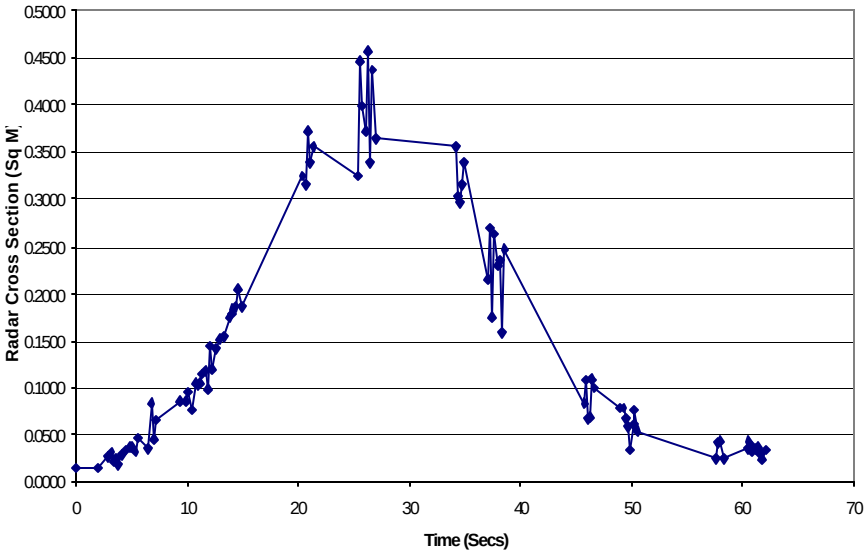

Figure 7-7: Cape Cod Track on January 17, 1857Z [2]

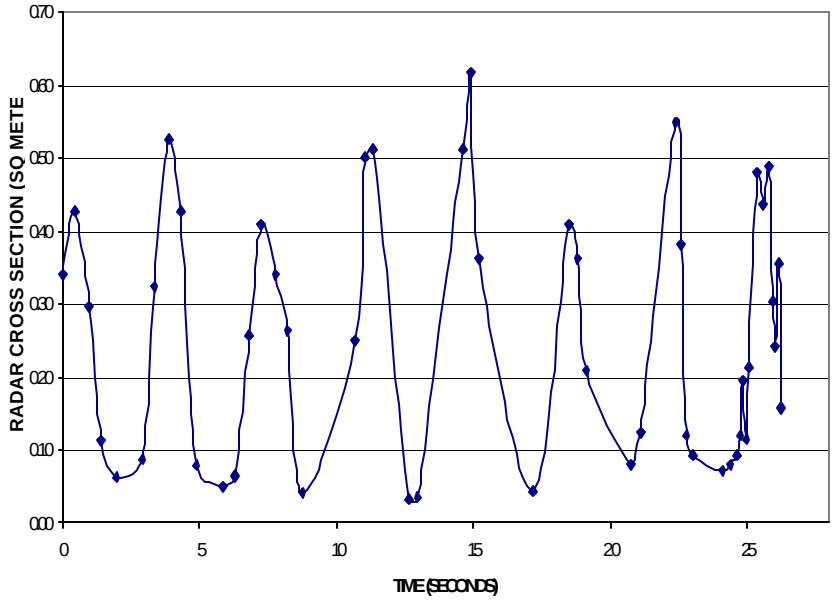

Figure 7-8: Cape Cod Track on January 18, 2029Z [2]

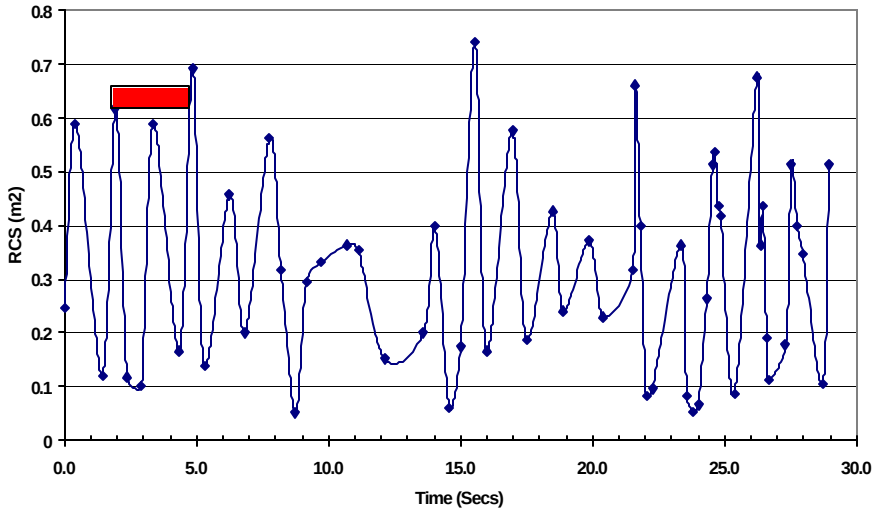

Figure 7-9: Cape Cod Track on January 19, 1539Z [2]

The radar cross section of the object in orbit varied from approximately 0.1 - 0.7 m^2. The ballistic coefficient of the object in orbit was estimated to be 0.102 m^2/kg by Air Force Space Command [2] with good agreement by JSC Engineering at 0.09 - 0.11 m^2/kg. [23]

JSC assembled a list of materials and components from the inside the payload bay and on the exterior of the Orbiter. By February 14, JSC Engineering had sent properties of these materials for correlation to the radar data. The ESAT and DCIST initiated planning for radar tests of these materials by the Air Force Research Lab at Wright-Patterson AFB, OH. This material list included all candidates for an object originating from Columbia during STS-107. (Refer to Section 7.4 Radar Tests for a complete description.)

The goal was to measure radar cross section for each of these materials in various orientations and compare the test data to the radar observation data recorded by Air Force Space Command during the mission. After radar cross sections were compared, Air Force Space Command and JSC compared ballistic coefficients for the test objects and the observed object. The overall goal was to isolate the most likely candidates for this object based on both radar cross section and ballistics.

7.4. Radar Tests

C, L, and S-band data annexes were reported to the CAIB and NASA by Air Force Research Laboratory Sensors Directorate on April 24, 2003.

Uncertainty in evaluating the deep space tracking radar data from the Flight Day 2 object led to a series of radar tests at Wright-Patterson AFB, OH for materials and components inside the payload bay and on the exterior of the Orbiter. These tests were tuned to the specific radars that recorded observations of this object with a goal to compare the test data to the radar observation data recorded by Air Force Space Command during the mission.

On March 7, these tests were expanded for the external materials and components to include the C-band radars which track during ascent and the air traffic control radars which are flown over during entry. The C-band radar tests were added to investigate the ability to track debris during ascent, with a primary goal of quantifying the likelihood of discriminating Shuttle debris in the ascent plume and the ability to track the most likely Shuttle debris with the C-bands in general. L-band and S-band air traffic control radars were added to quantify the ability to for these radars to have detected the most likely Orbiter debris during entry over the CONUS.

The goal was to measure radar cross section (RCS) for each of these materials and components in various orientations and compare the test data to the radar observation data during the mission. Ideally, this would reduce the candidate list for the Flight Day 2 object and provide a reasonableness check for the entry debris radar searches described in Section 5.

Items from the exterior of the Orbiter included: thermal blankets (FRSI, AFRSI) and heat tiles (HRSI). Items from the Orbiter wing leading edge included: Reinforced Carbon-Carbon (RCC) panel, ear muff, carrier panel with horse collar seal and an RCC T-seal. Items from inside the payload bay included: thermal blankets (beta cloth), thermal blankets (aluminized), and beta cloth logo panels. These are shown in Figures 7-10, 11, 12 and 13. [11]

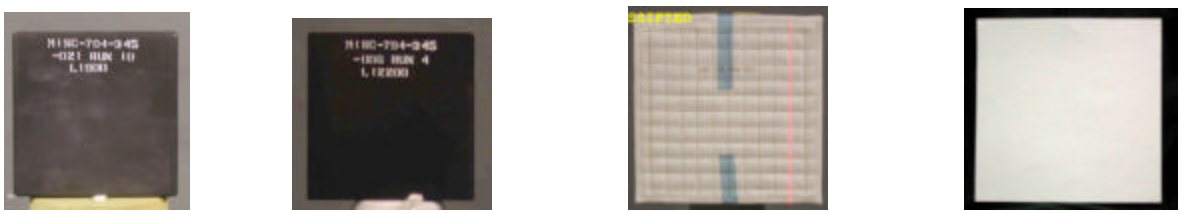

LI 900 Tile | LI 2200 Tile | AFRSI | FRSI

Figure 7-10: External Thermal Protection System Constituent Materials [11]

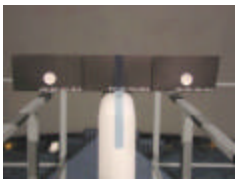

Carrier Panel Segment

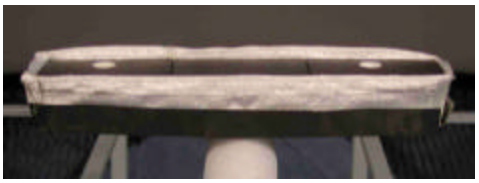

Carrier Panel Segment with Horse Collar

Horse Collar

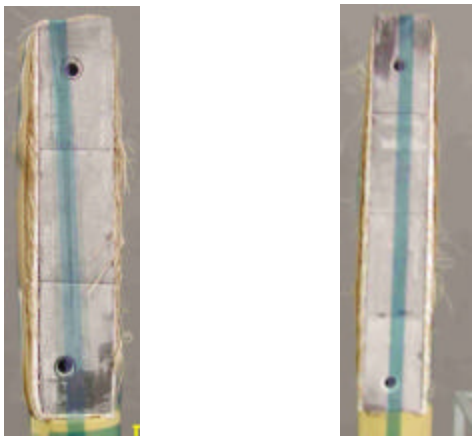

3 and 4 Tile Carrier Panels with Horse Collar

Figure 7-11: Carrier Panel Combinations [11]

RCC Leading Edge Panel

RCC T-Seal

Incoflex “Ear Muff”

Figure 7-12: Wing Leading Edge Components [11]

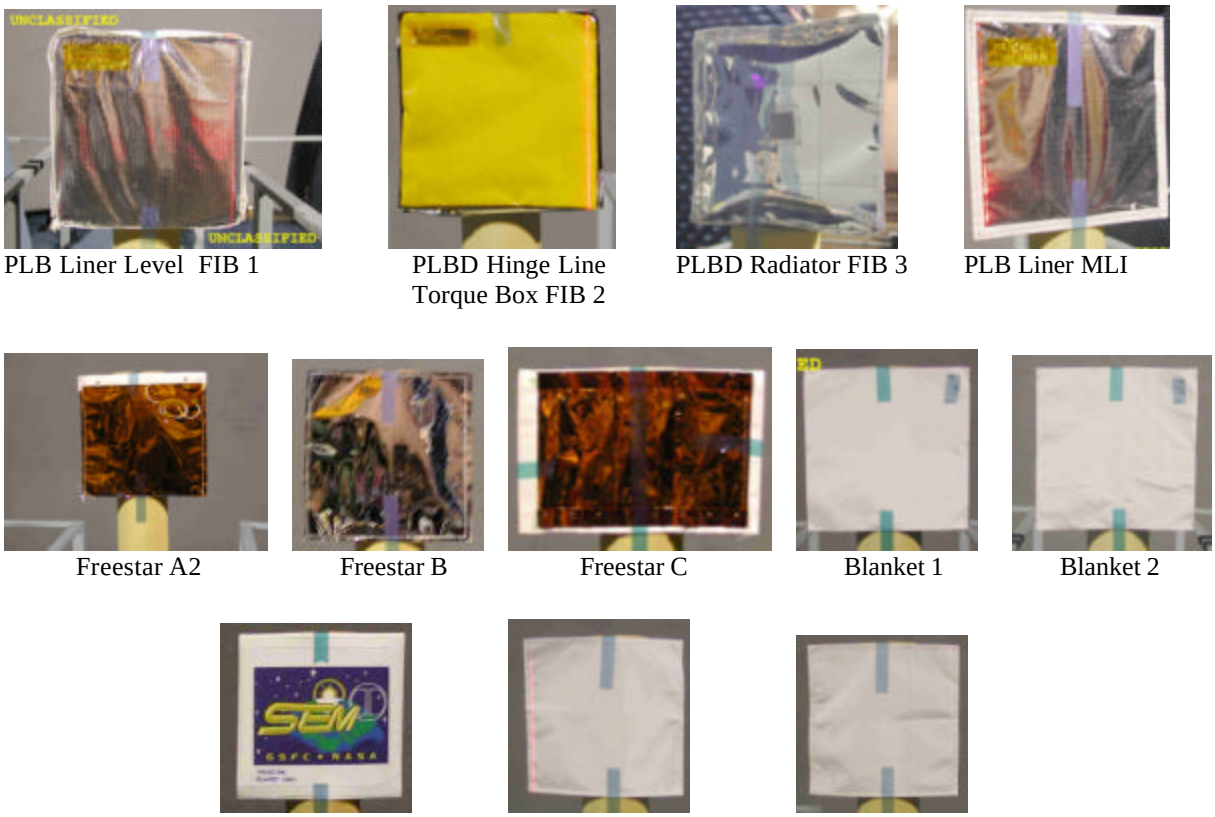

PLB Liner Level FIB 1 | PLBD Hinge Line Torque Box FIB 2 | PLBD Radiator FIB 3 | PLB Liner MLI

Freestar A2 | Freestar B | Freestar C | Blanket 1 | Blanket 2

Freestar Logo | Beta Cloth | Beta Cloth w/ Metal Quilting

Figure 7-13: Payload Bay and Payload Insulation Materials [11]

Similar items were identified informally as generic ascent debris candidates from the Shuttle External Tank (ET) and Solid Rocket Boosters (SRB). These components were also tested by AFRL for C-band radar frequencies. For the ET, these include: Aero Ramp PDL-1034; Intertank Skin Stringer Panel; Intertank Rib Panel; Intertank/LH2 Flange Divot simulator; A2-Intertank Rib Panel; C1 Intertank Skin Stringer Panel. For the SRB, these include: Solid Rocket Motor Booster Bolt Catcher; and Solid Rocket Motor Booster Bolt Catcher insulation.

Ultimately, AFRL tested thirty-eight different materials and combinations of wing leading edge components. [12] Table 7-2 summarizes the materials, combinations of leading edge components and the radar frequencies tested.

AFRL Part #	NASA Part Description	RCS Test Data Acquired						RCS Test Data Reported					
		VV On-Orbit	HH On-Orbit	Descent	Descent	Ascent		VV On-Orbit	HH On-Orbit	Descent	Descent	Ascent	
		UHF 433 MHz	UHF 433 MHz	L 1.2-1.4 GHz	S 2.7-2.9 GHz	C 5.68-5.7 GHz	Wideband 1-6 GHz	UHF 433 MHz	UHF 433 MHz	L 1.2-1.4 GHz	S 2.7-2.9 GHz	C 5.68-5.7 GHz	Wideband 1-6 GHz
1	AFRSI(Fibrous) 12" x 12	Y	Y	Y	Y	Y	Y	Y	Y	Y	Y	Y	Y
2	FRSI 12" x 12"	Y	Y	Y	Y	Y	Y	Y	Y	Y	Y	Y	Y
3	HRSI (No Backing)	Y	Y	Y	Y	Y	Y	Y	Y	Y	Y	Y	Y
4	HRSI (Dense/RTV/SIP)	Y	Y	Y	Y	Y	Y	Y	Y	Y	Y	Y	Y
5	"Fibrous 001"	Y	Y	N/A	N/A	N/A	N/A	Y	Y	N/A	N/A	N/A	N/A
6	"Fibrous 002"	Y	Y	N/A	N/A	N/A	N/A	Y	Y	N/A	N/A	N/A	N/A
7	"Fibrous 003"	Y	Y	N/A	N/A	N/A	N/A	Y	Y	N/A	N/A	N/A	N/A
8	Beta Cloth (No Conductive Quilt Thread	Y	Y	N/A	N/A	N/A	N/A	Y	Y	N/A	N/A	N/A	N/A
9	Beta Cloth (Conductive Quilt Thread)	Y	Y	N/A	N/A	N/A	N/A	Y	Y	N/A	N/A	N/A	N/A
10	MLI 004 13" x 13" Piece	Y	Y	N/A	N/A	N/A	N/A	Y	Y	N/A	N/A	N/A	N/A
11	"Freestar panel a2"	Y	Y	N/A	N/A	N/A	N/A	Y	Y	N/A	N/A	N/A	N/A
12	"Freestar panel b"	Y	Y	N/A	N/A	N/A	N/A	Y	Y	N/A	N/A	N/A	N/A
13	"Freestar panel c"	Y	Y	N/A	N/A	N/A	N/A	Y	Y	N/A	N/A	N/A	N/A
14	"Freestar panel logo piece"	Y	Y	N/A	N/A	N/A	N/A	Y	Y	N/A	N/A	N/A	N/A
15	"Insulation Blanket Sample 1"	Y	Y	N/A	N/A	N/A	N/A	Y	Y	N/A	N/A	N/A	N/A
16	"Insulation Blanket Sample 2"	Y	Y	N/A	N/A	N/A	N/A	Y	Y	N/A	N/A	N/A	N/A
17	Aero Ramp" PDL-1034	N/A	N/A	N/A	N/A	Y	N/A	N/A	N/A	N/A	N/A	Y	N/A
18	Intertank Skin Stringer Panel"	N/A	N/A	N/A	N/A	Y	N/A	N/A	N/A	N/A	N/A	Y	N/A
19	"Intertank Rib Panel"	N/A	N/A	N/A	N/A	Y	N/A	N/A	N/A	N/A	N/A	Y	N/A
20	"Intertank/LH2 Flange Divot Simulation"	N/A	N/A	N/A	N/A	Y	N/A	N/A	N/A	N/A	N/A	Y	N/A
21	"A2-Intertank Rib Panel"	N/A	N/A	N/A	N/A	Y	N/A	N/A	N/A	N/A	N/A	Y	N/A
22	"C1 Intertank Skin Stringer Panel",	N/A	N/A	N/A	N/A	Y	N/A	N/A	N/A	N/A	N/A	Y	N/A
23	"Carrier Panel" section by itself - **Rcvd 3/17/03**	Y	Y	Y	Y	Y	Y	Y	Y	Y	Y	Y	Y
24	"Carrier Panel" with "Horse-shoe" seal installed	Y	Y	Y	Y	Y	Y	Y	Y	Y	Y	Y	AT
25	"Horse Shoe Seal"	Y	Y	Y	Y	Y	Y	Y	Y	Y	Y	Y	AT
26	RCC Edge Flight Spare from Columbia	Y	Y	Y	Y	Y	Y	Y	Y	Y	Y	Y	Y
27	Recovered STS-107 RCC Component	N/A	N/A	N/A	N/A	N/A	N/A	N/A	N/A	N/A	N/A	N/A	N/A
28	Highly Densified Shuttle tile 6"x6"x1.5"	Y	Y	Y	Y	Y	Y	Y	Y	AT	AT	AT	AT
29	Solid Rocket Motor Booster Bolt Catcher	N/A	N/A	N/A	N/A	Y	N/A	N/A	N/A	N/A	N/A	AT	N/A
30	"Ear Muff" Wing Spar Insulation	Y	Y	Y	Y	Y	Y	Y	Y	Y	Y	Y	AT
31	Highly Densified Shuttle tile 6"x6"x2"	Y	Y	Y	Y	Y	Y	Y	Y	Y	Y	Y	AT
32	Solid Rocket Motor Booster Bolt Catcher insulation	N/A	N/A	N/A	N/A	TBD	N/A	N/A	N/A	N/A	N/A	TBD	N/A
33	Carrier Panel w/yoke LH 14, SN AF7843	Y	Y	N/A	N/A	N/A	N/A	Y	Y	N/A	N/A	N/A	N/A
34	Carrier Panel w/yoke LH 4, SN ANG391	Y	Y	N/A	N/A	N/A	N/A	Y	Y	N/A	N/A	N/A	N/A
35	Tee Seal (3 orientations) - From panel 21	Y	Y	N/A	N/A	N/A	N/A	Y	Y	N/A	N/A	N/A	N/A
36	51311 (8" x 13" RCC Fragment with lip)	Y	Y	N/A	N/A	N/A	N/A	N	N	N/A	N/A	N/A	N/A
37	37736 (Compund Curve RCC Fragment)	Y	Y	N/A	N/A	N/A	N/A	N	N	N/A	N/A	N/A	N/A
38	2018 (RCC Flat acrage ~8" x 11")	Y	Y	N/A	N/A	N/A	N/A	N	N	N/A	N/A	N/A	N/A
39	51313 (Upper half RS RCC Tee Seal 9/10)	Y	Y	N/A	N/A	N/A	N/A	N	N	N/A	N/A	N/A	N/A
40	Upper Carrier Panel 9/10	N	N	N/A	N/A	N/A	N/A	N	N	N/A	N/A	N/A	N/A

Notes

AT = Awaiting RCS Testing or Test Resullts
In Process = RCS Test Done, data being reduced
N = no or not completed
N/A = Not Applicable or data not required
TBD - To be determined by NASA and CAIB
BAS = Boxed and Awaiting Shipment Paperwork

Table 7-2: AFRL Advanced Compact Range Shuttle Parts Test Status as of April 25, 2003 [12]

The final evaluation of the test data versus the radar observations from the Flight Day 2 object are shown in Table 7-3. Detailed test results are included on the ESAT data CD. As mentioned above, detailed discussion of the RCS and ballistic comparisons to the Flight Day 2 object are deferred to the tiger team formed under the OVE WG.

Test Article	RCS Result	Other Considerations	Comments
AFRSI 12" x 12"	Excluded		RCS was orders of magnitude too low
FRSI 12" x 12"	Excluded		RCS was orders of magnitude too low
HRSI LI 900	Excluded		RCS was orders of magnitude too low
HRSI LI 900 (Densified Layer/RTV/SIP)	Excluded		RCS was orders of magnitude too low
"Fibrous 001" - Bulk Insulation Blanket, Cargo Bay Liner Level	NOT Excluded		Cd*A/M was off by >factor of 7
"Fibrous 002" - PLBD Hinge Line Torque Box	NOT Excluded		Cd*A/M was off by >factor of 7
"Fibrous 003" - Beneath Radiator	NOT Excluded		Cd*A/M was off by >factor of 7
Beta Cloth (without Conductive Quilt Thread)	Excluded		Cd*A/M was off by >factor of 7
Beta Cloth (with Conductive Quilt Thread)	Unlikely		Cd*A/M was off by >factor of 7
Cargo Bay Liner MLI 004 13" x 13" Piece	NOT Excluded		Cd*A/M was off by >factor of 7
Freestar Panel A2	NOT Excluded		
Freestar Panel B	NOT Excluded		
Freestar Panel C	NOT Excluded		
Freestar Logo	Excluded		
Insulation Blanket Sample 1	NOT Excluded		
Insulation Blanket Sample 2	NOT Excluded		
Carrier Panel SEGMENT	Excluded	Excluded if debris is positively identified AND is in region of interest	Object is unlikely from an RCS perspective unless Cape Cod radar was off by ~5 dB
Carrier Panel SEGMENT with "Horse-Collar"	Excluded	Excluded if debris is positively identified AND is in region of interest	Object is unlikely from an RCS perspective unless Cape Cod radar was off by ~5 dB
"Horse Collar" Seal	Excluded	Excluded if debris is positively identified AND is in region of interest	Object is unlikely from an RCS perspective unless Cape Cod radar was off by ~5 dB
RCC Leading Edge Panel with Attachment Hardware (Flight Hardware Spare)	Excluded		Object was too large in each characteristic dimension.
HRSI LI 2200 Tile	Excluded		
"Ear Muff" Wing Spar Insulation	NOT Excluded	Excluded because Incoflex has no path to depart Shuttle UNLESS RCC panel assumed missing while on orbit	
4 Tile Carrier Panel with Horse Collar (Flight Hardware)	Excluded	Excluded because Incoflex has no path to depart Shuttle UNLESS RCC panel assumed missing while on orbit	
3 Tile Carrier Panel with Horse Collar (Flight Hardware)	Excluded	Excluded because Incoflex has no path to depart Shuttle UNLESS RCC panel assumed missing while on orbit	
Reinforced Carbon-Carbon T-Seal	NOT Excluded		
RCC Panel "Acreage"	In Work		

Table 7-3: Summary of UHF RCS Test Results [14]

L-band and S-band radar testing provided maximum detection ranges with an 80 percent probability of detection. While all of these materials are detectable in the air traffic control radars, the various tile, FRSI and AFRSI materials show very low detection ranges, 23 - 35 nm [15], compared to the leading edge components, 105 - 195 nm [16]. This is shown in Figure 7-14 for the standard ARSR-4 L-band radar. Figure 7-15 shows the ROC curves for all ARSR-4 variants, all of which have similar detection ranges. The ARSR-9 S-band radar detection ranges are lower than the L-band radars as shown in Figure 7-16. The implications of these relatively low detection ranges are discussed in Section 5.

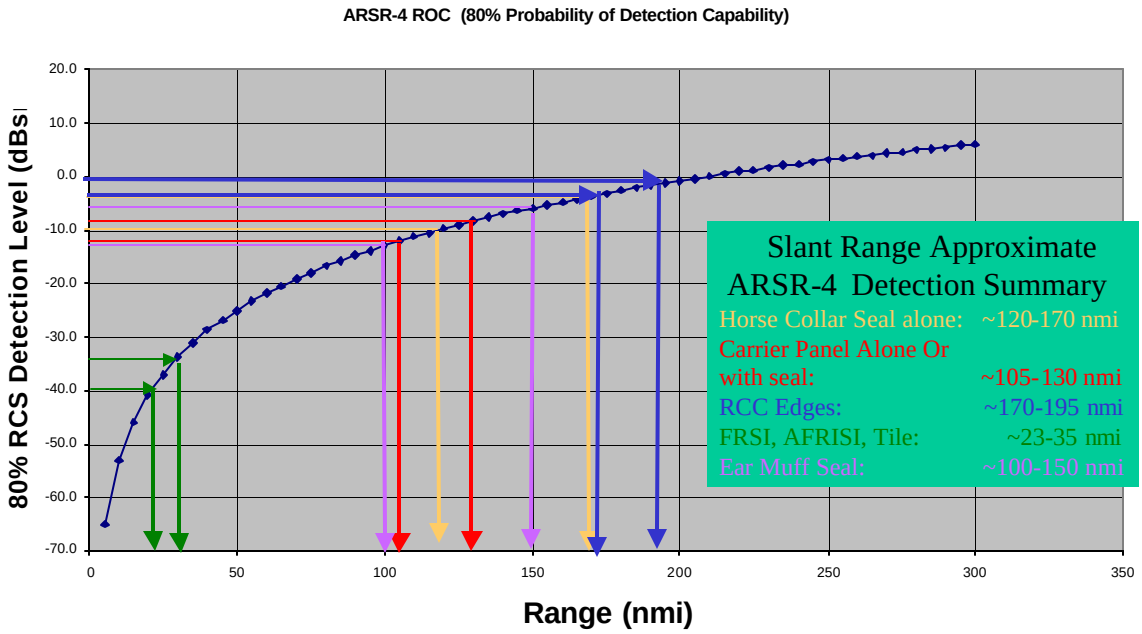

Figure 7-14: ARSR-4 L-Band ROC Curve (slant range, line of sight, perfect weather) [15][16]

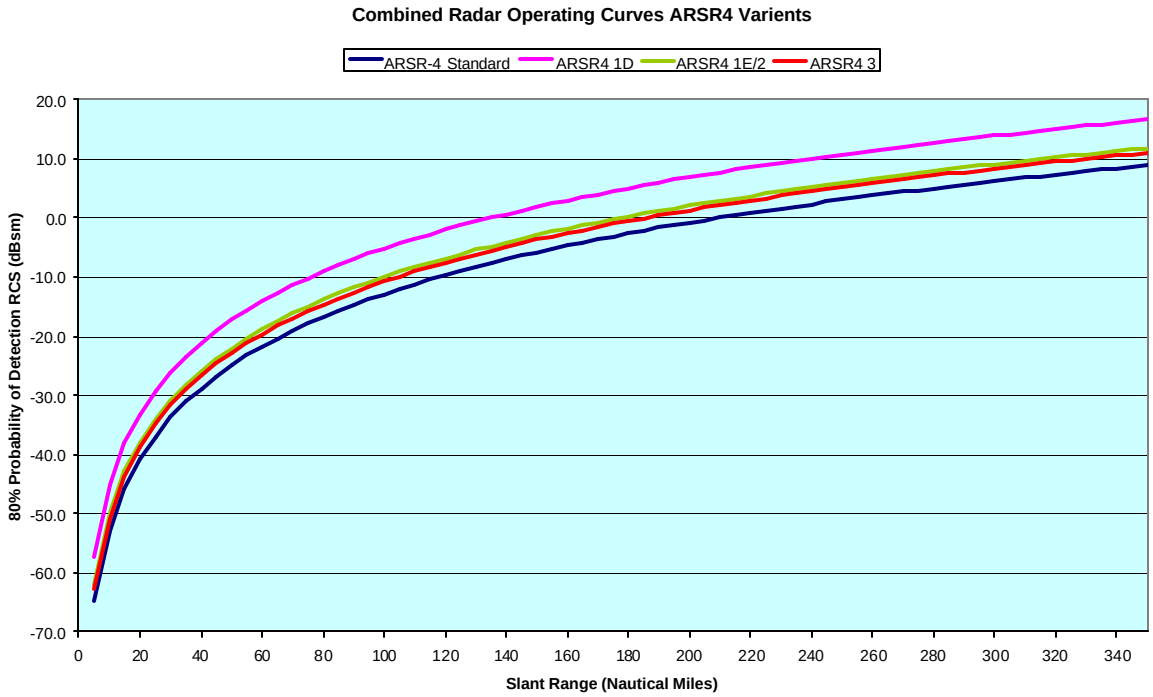

Figure 7-15: All ARSR-4 Variant L-Band ROC Curves
(slant range, line of sight, perfect weather) [59]

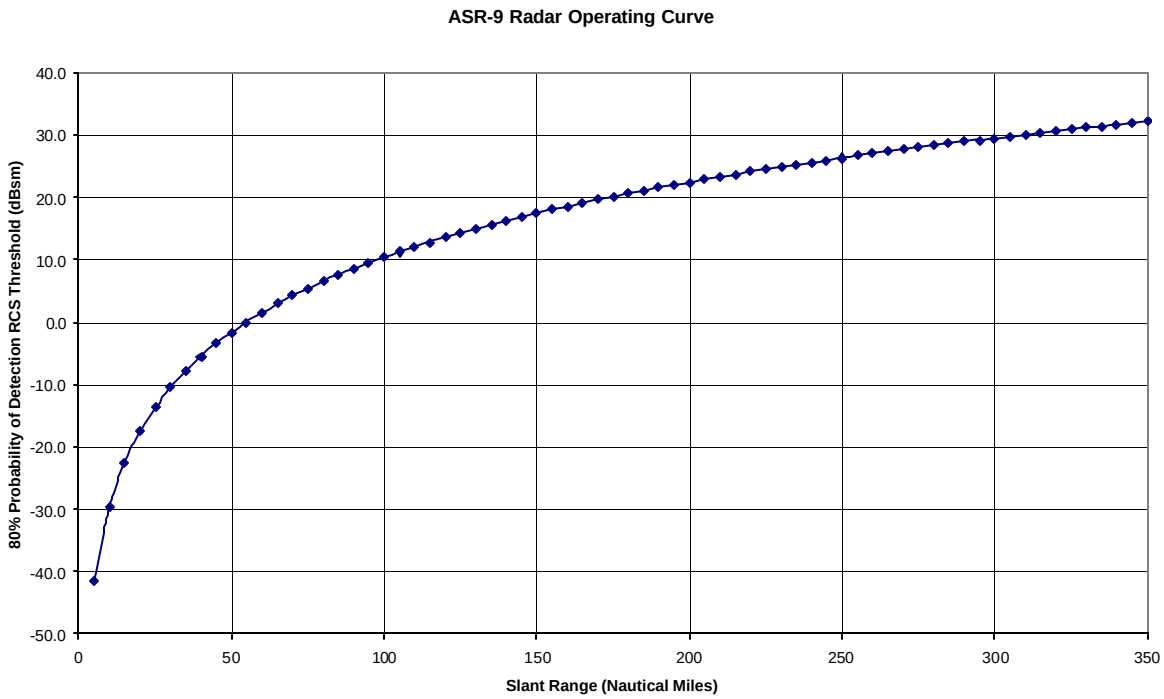

Figure 7-16: ARSR-9 S-Band ROC Curve (slant range, line of sight, perfect weather) [59]

Similar data were produced for the C-band radar and are plotted in Figures 7-17 through 7-19. A series of ROC curves is shown for each C-band radar since these radars' parameters are changed during ascent to optimize tracking as the Orbiter travels down range. Examples of the corresponding coverage for one set of data from each radar is shown in Section 6. Detailed analyses of this data and any implications for detecting debris during ascent are not included in this report.

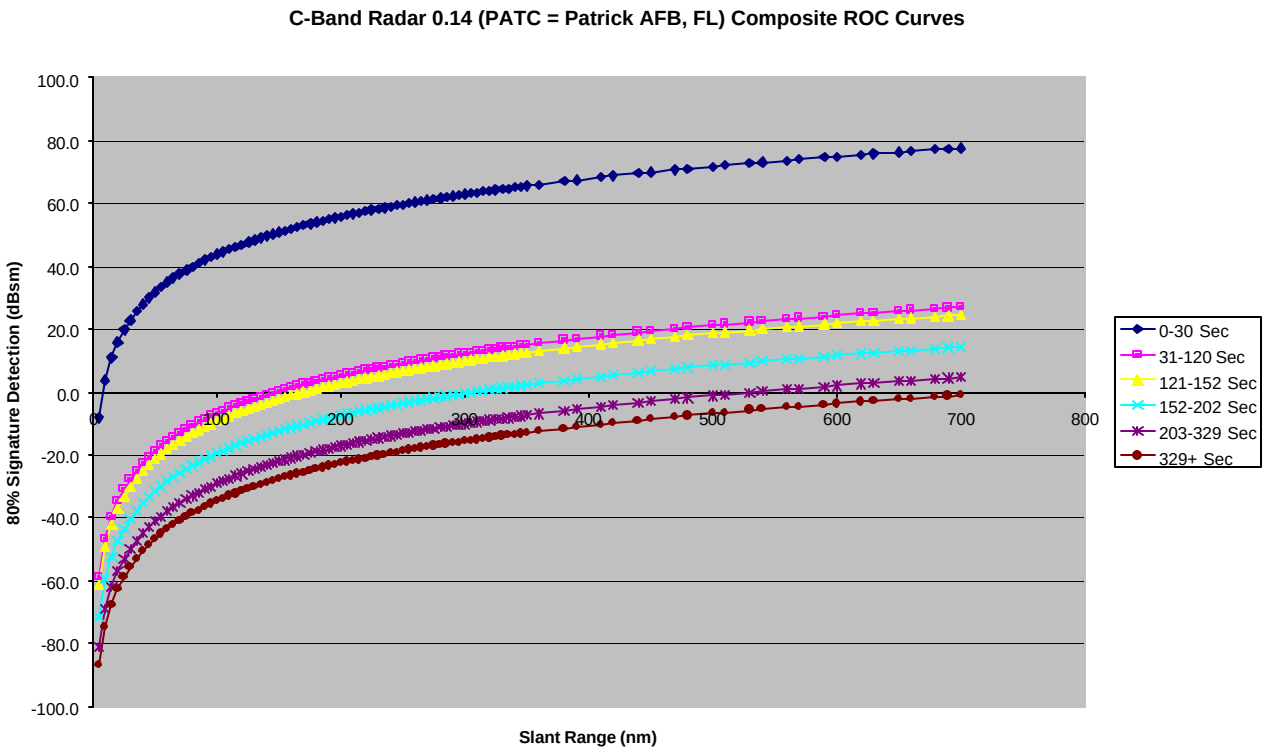

Figure 7-17: C-Band 0.14 Radar ROC Curves
(slant range, line of sight, perfect weather) [58]

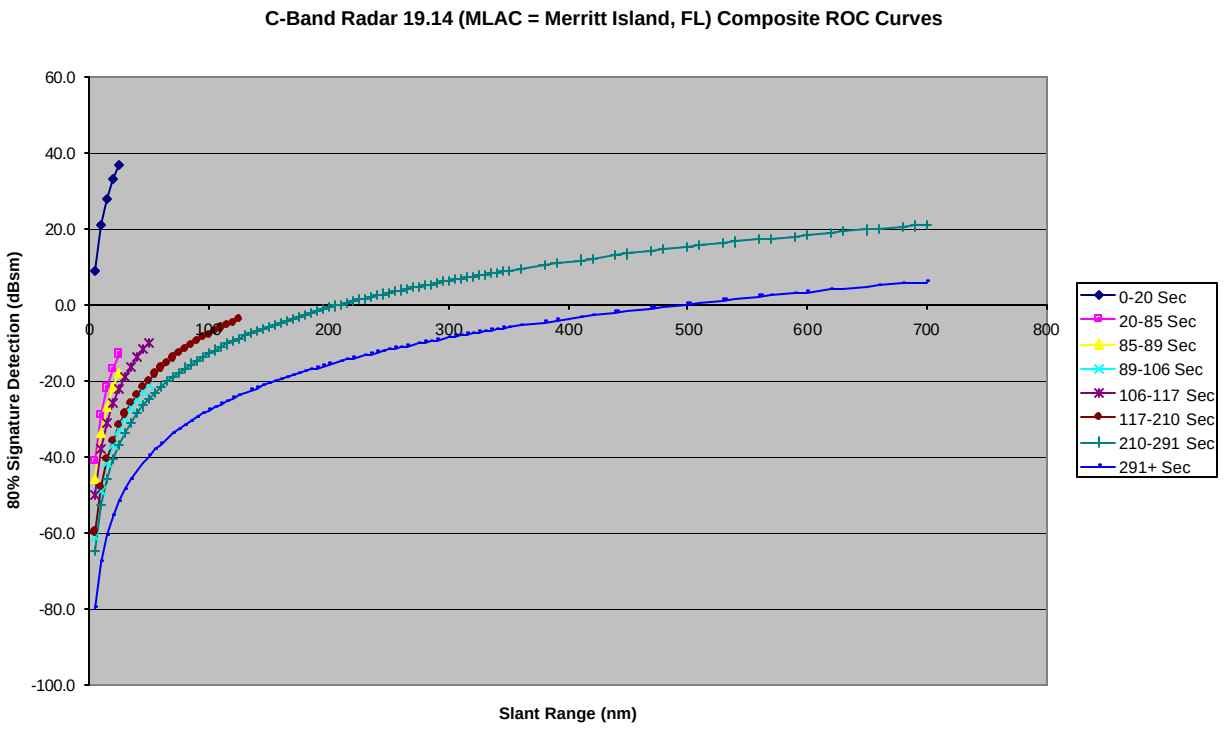

Figure 7-18: C-Band 19.14 Radar ROC Curve
(slant range, line of sight, perfect weather) [58]

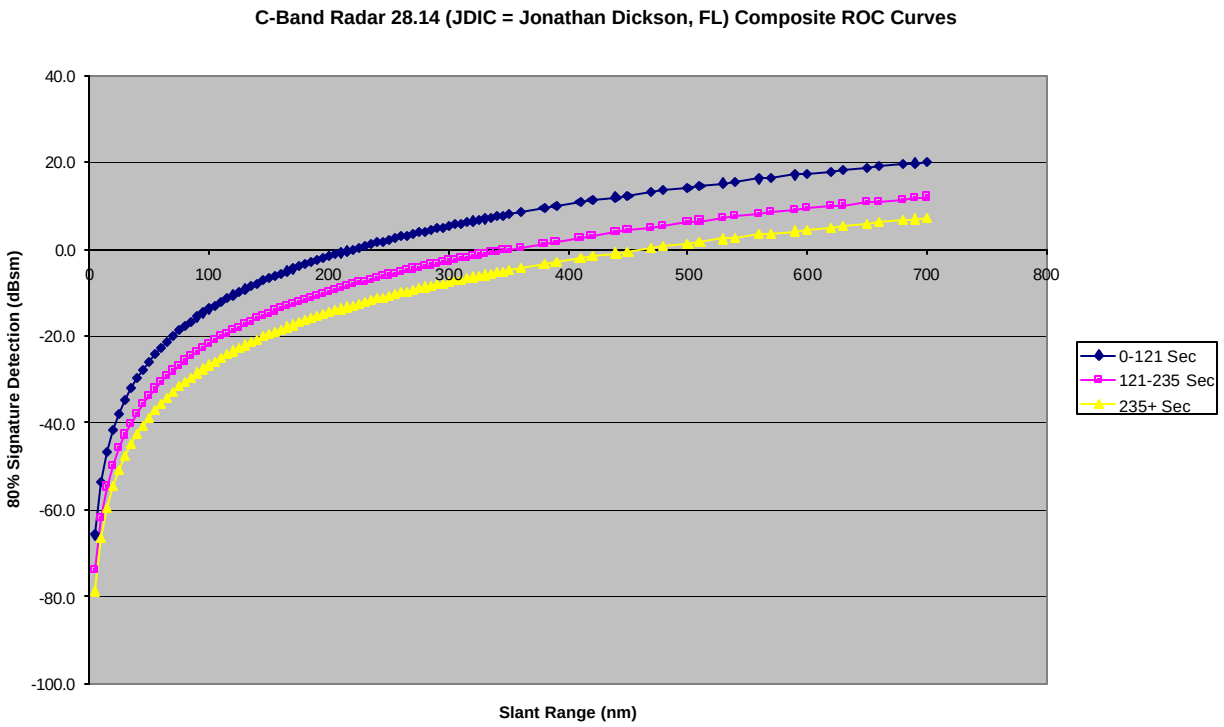

Figure 7-19: C-Band 28.14 Radar ROC Curve
(slant range, line of sight, perfect weather) [58]

7.5. Miscellaneous Other DOD Data

7.5.1. 16 Jan, 15:56:22-16:01:10

Post-flight analysis of remote sensor data suggested anomalous signatures after ascent. Similar to the remote sensor data during entry, this required considerable post-processing and detailed comparison to previous flight data. In the final assessment, this signature also was concluded to have been seen on multiple previous missions and was not studied further.

7.5.2. Ascent Radar

STS-107 was tracked during ascent by Eastern Test Range C-band radar. This data was analyzed and reported by the 45th Space Wing, Patrick AFB, Florida. None of the radars detected debris prior to SRB separation. From T+150 to T+230 seconds, radar 0.14 detected 21 objects and radar 28.14 detected 6 objects. The radar return signal strengths were not adequate to determine debris properties, but the data were considered to be consistent with observations from previous Shuttle missions. [54]

7.5.3. Other Entry Radar

No ship based or AWAC's radar tracked Columbia during entry. [55]

The UHF radar at Beale AFS, CA recorded two observations of Columbia during entry. No debris was detected. [56]

The Naval Space Surveillance System recorded 5 distinct radar detections during Columbia's entry over the CONUS. Although several of the cases showed anomalous characteristics, there is no conclusive evidence of pre-break up debris detected in any of this data. [57]

All DOD air traffic control radar during STS-107 entry was recorded by the 84th RADES. This data was included in the radar searches as described in detail in Section 5.

7.5.4. Infrasound

Infrasound signals were recorded by DOD stations during STS–107 entry. Analysis to date provides no data that can be positively identified as off-nominal. This analysis is summarized in Section 8.1, and a complete discussion can be found in Appendix 10.9 of this report.

7.6. DOD Data Lessons Learned

1) A single DOD POC, located at the NASA center conducting the investigation is essential to effectively exchanging data and requesting additional support.

2) Generic DOD tracking capability and the resulting routine taskings on Shuttle flights should be reviewed and updated as required for all phases of flight.

3) Generic DOD imaging/sensor capability and the resulting routine and contingency taskings on Shuttle flights should be reviewed and updated as required for all phases of flight.

4) NASA and the USAF should study the use of Orbiter-specific material maps to facilitate AMOS' thermal mapping of all Orbiters during Orbit operations.

8. Other Sensor Data

8.1. Infrasonic

Dr Henry Bass, Director of the National Center for Physical Acoustics, University of Mississippi, led a collection of DOD and other infrasound researchers from several institutions in the United States. This team analyzed data recorded on infrasound monitoring stations across the United States to assist the Columbia accident investigation. This was a collaborative effort with support from DOD, DOE and NOAA.

Infrasound signals were recorded by ten stations during STS–107 entry. These stations recorded clear signals from several previous missions as well. These infrasound arrays can determine the direction of the signal, and it was hypothesized that analyzing the signals would yield data on Columbia debris shedding or some other high energy events during entry over the CONUS. Analysis to date, however, does not provide any data that can be positively identified as off-nominal. A complete discussion can be found in Appendix 10.9 of this report.

The Orbiter was first detected as it crossed the California coast and was observed all the way to break-up over Texas. All stations observed multiple signals associated with sound generated during the entry. These signals may be explained by various atmospheric multi-pathing phenomena, but it is possible that some come from debris. When combining the data with the entry trajectory, it was concluded that there do not appear to be other sources of infrasound in the vicinity of the Orbiter. [18]

Figure 8-1: Projected track, altitude, time GMT, and infrasonic detections for the Columbia reentry based on using PMCC with time windows greater than 30 s.
(The red lines indicate the observed azimuth of the first arrival, and the blue lines the azimuth of any secondary arrivals.) [18]

Dr. Al Bedard at the NOAA Environmental Technology Laboratory in Boulder, Colorado has routinely detected both Orbiter entries and naturally occurring bolides and meteorites. The infrasonic data from past entries show very consistent and identifiable patterns. His observations

have shown that specific Orbiters can be discerned from infrasonics. [20] Dr. Bass' team compared signals from STS-107 to STS-77, STS-78, and STS-90 which had similar entry trajectories but fewer infrasound stations on line.

The state of knowledge of infrasonics makes interpreting signal differences problematic. Both Dr. Bass and Dr. Bedard note the sonic boom waveforms from each mission were different in detail. Dr. Bass concludes these were essentia lly the same in major features, with noticeable differences in the STS-107 signals, especially a long acoustic signal following the sonic boom coming from the West. [18] Dr. Bedard concludes there are distinct energy bursts which can be traced to specific points in the trajectory. He also notes overall frequency shift of the signal is inconsistent with past data. The frequency shift was consistent with the data observed for meteorites. [20]

As described above, there is insufficient data from previous missions to determine such waveform changes are expected. [18] Analysis to date has not correlated any infrasonic data to debris shedding events.

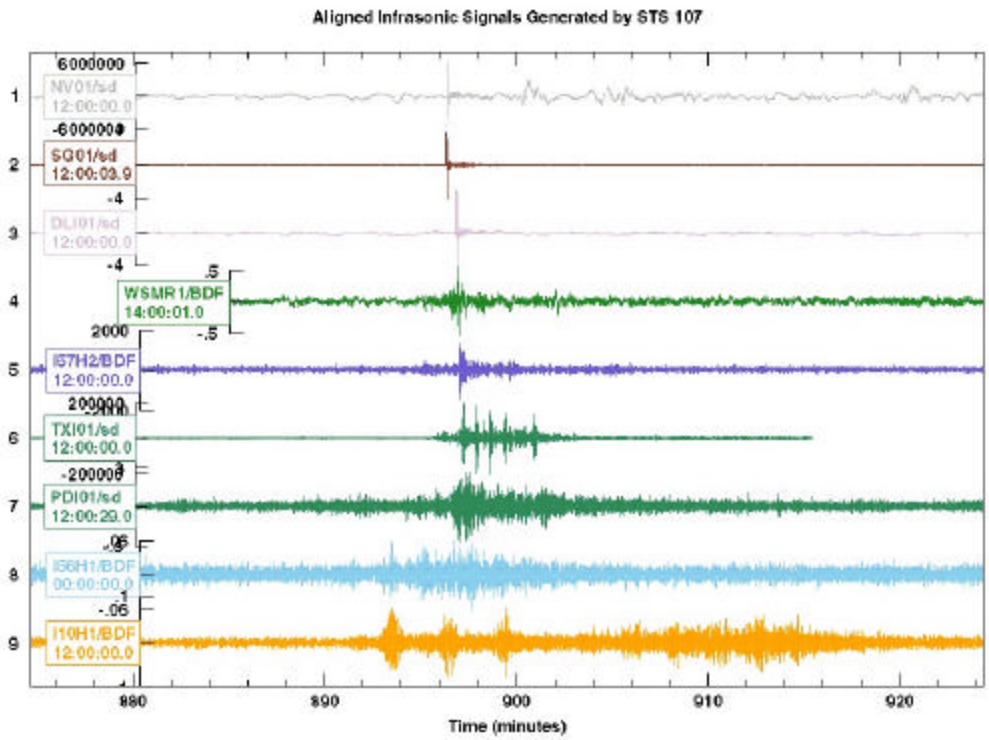

Figure 8-2: Single-channel traces from each of the infrasound arrays whose data were analyzed. [18]

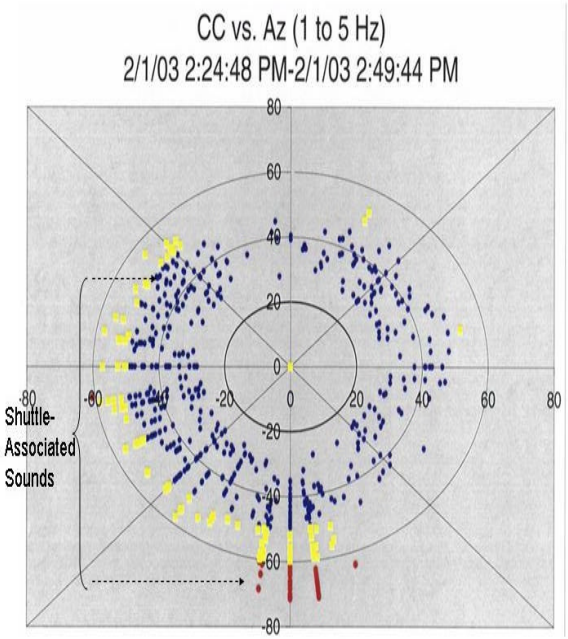

Figure 8-3. Polar plot direction of arrival plot covering the interval 1412 to 1452 UTC on 1 February 2003. The angle indicates the direction from which the acoustic signal is arriving. The radial distance from the origin is a measure of signal quality. The red data points indicate excellent signals, the yellow good signals and the blue data points weak signals or noise. [20]

8.2. Seismic

The STS-107 entry was observed by a number of seismograph stations distributed throughout the southwest CONUS with a significant concentration in southern California. The majority of the stations are members of the Princeton Earth Physics Program or the Public Seismic Network. Dr. David Oppenheimer of the United States Geological Survey, Northern California Seismic Network Office compiled the data. Like the infrasonic data analysis, it was hypothesized that analyzing the seismic recordings would yield data on Columbia debris shedding or some other high energy events during entry over the CONUS. Again, however, analysis to date, does not provide any data that can be positively identified as off-nominal. A complete discussion can be found in Appendix 10.10 of this report.

Several stations recorded the bow shock wave as well as some secondary signals associated with the Orbiter flyby. In order to assess unique features of this entry, NASA provided the STS 107 trajectory and four past missions that over flew the southwestern United States. Unfortunately the seismic stations do not routinely record non-earthquake data. Thus, very limited comparisons could be made to previous entries. However, this entry appeared consistent with others that have been observed in the past, and no distinctive features were seen in the STS-107 data. No specific conclusions could be made with regard to the secondary signals, and no obvious signals were present that indicated any debris impacts along the flight path. [19]

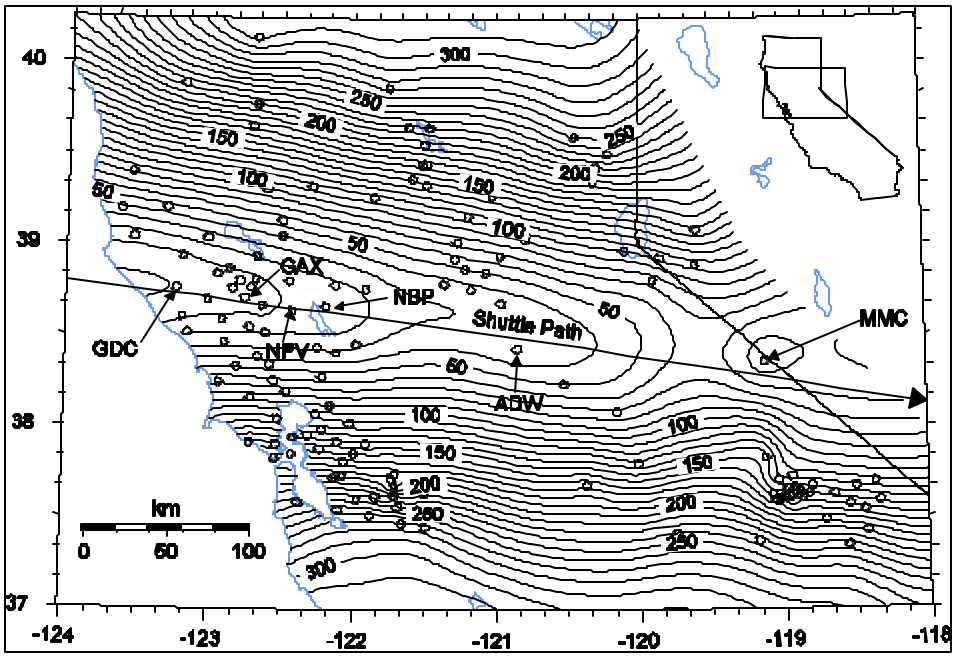

Figure 8-4. Contour map of observed arrival times of sonic boom from Space Shuttle Columbia. Contour interval is 10 s. Open circles depict locations of seismic stations recording the sonic boom. Shuttle path is shown as a straight arrow. [19]

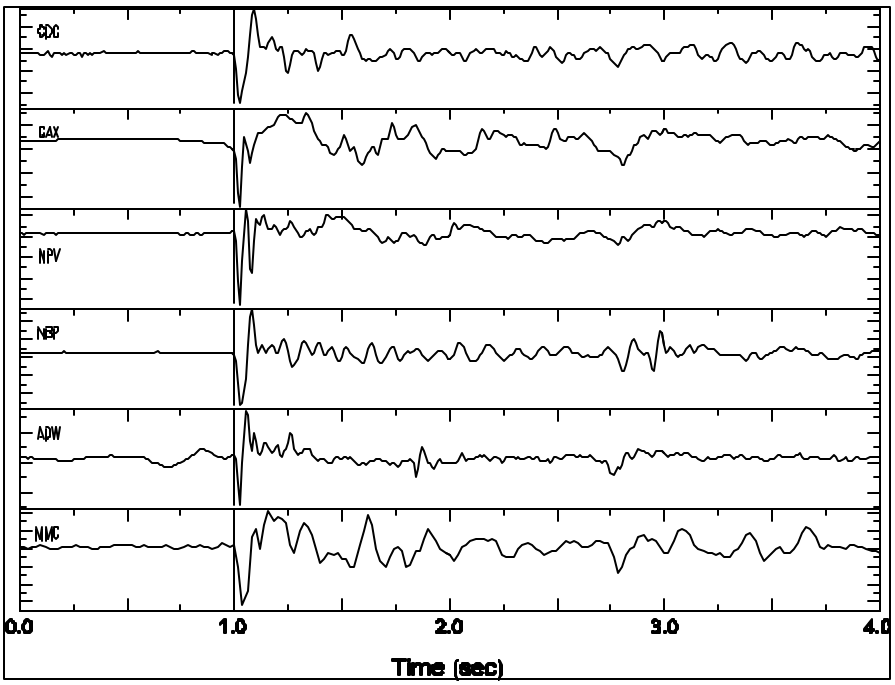

Figure 8-5. Examples of sonic boom N-waves from 6 stations along the shuttle path (see Figure 8-4 for station locations). All seismograms were recorded on a vertical 1-Hz geophone using analog telemetry and sampled at 100sps. Seismograms are shifted in time to align on arrival time. Amplitudes are normalized. [19]

8.3. Other Sensor Data Lessons Learned

1) The state of the art for infrasonic and seismic data does not support their use for monitoring Orbiter entry.

2) The state of the art for infrasonic and seismic data does not provide significant engineering value for Columbia's post-incident investigation.

9. References

[1] Visel, Lt Col Cyndie; Information Paper on Object Associated with STS-107; March 13, 2003.

[2] HQ AFSPC/XPY; FD2 Piece Characterization (RCS and Area/Mass Ratio) Preliminary Results; April 18, 2003.

[3] Witte, Dave and Lt Col Jeff McCann; AMOS, AFRL/DE; Quick-look Surface Temperature Mapping of STS-107 Using Long-Wave Infrared Imagery Collected on 28 Jan 03 from the Air Force Maui Optical & Supercomputing (AMOS) Site; March 4, 2003.

[4] Air Force Maui Optical & Supercomputing (AMOS) Detachment; Data CD: AMOS STS1-107; EOC #2-4-0124; February 2003.

[5] Jarvis, Kandy; JSC/SX; STS-107 Investigation Kirtland Photo Tiger Team; April 21, 2003.

[6] Roeh, William; JSC/JA171; Report Tallies e-mail; April 30, 2003.

[7] Hill, Paul S.; JSC/DA8; NASA-DOD Data Exchange; February 28, 2003.

[8] Shelton, William L., BGen; HQ AFSPC/XO, Peterson AFB, CO; AFSPC Data Classification Guidance; February 24, 2003.

[9] Anthony, Jack, Col; AFSPC/DP, Peterson AFB, CO; Remote Sensor Summary; April 17, 2003.

[10] Summary of classified and unclassified phone conversations and meetings at JSC in March and April 2003.

[11] Rickman, Steven L.; JSC/ES3; Summary of Radar Cross Section (RCS)Testing and Ballistic Analysis of the STS 107 Flight Day 2 Object; 22 April 2003.

[12] Kent, Brian, Dr.; AFRL, Wright-Patterson AFB, OH; AFRL Advanced Compact Range Shuttle Parts Testing/Reporting Status; April 25, 2003.

[23] Broome, Joey and Carlos H. Westhelle; JSC/EG; STS-107 Flight Day 2 Debris Trajectory Analysis Ballistic Number Range Definition; April 24, 2003

[14] Rickman, Steve; JSC/ES3; Summary of UHF RCS and Ballistic Results REV A; April 17, 2003.

[15] Kent, Brian, Dr.; AFRL, Wright-Patterson AFB, OH; RCS Assessment of STS-107 Debris Candidates; March 14, 2003

[16] Kent, Brian, Dr.; AFRL, Wright-Patterson AFB, OH; RCS Assessment of STS-107 Debris Candidates, L-Band Measurements of Carrier Panel, RCC Edge, High Density Tile; March 28, 2003.

[17] Spencer, James. R.; JSC/DM; Debris Hot list; May 13, 2003.

[18] Bass, H., Editor, National Center of Physical Acoustics, University of Mississippi; Interim Report to the Department of Defense on Infrasonic Re-Entry Signals from the Space Shuttle Columbia (STS-107) (Revision 3.0); March 31, 2003.

[19] Oppenheimer, David; U.S. Geological Survey; Analysis of Sonic Booms from the Reentry of the Space Shuttle Columbia over California and Nevada; May 8, 2003.

[20] Bedard, A.J; Infrasonics Group Leader, NOAA Environmental Technology Laboratory Microwave Systems Development Division; Boulder, Colorado; Infrasound Originating from the 1 February 2003 Reentry of the Space Shuttle Columbia (STS-107), A Summary of Sub-Audible Sound Bursts Detected Near Boulder, Colorado for use by NASA and Others Studying this Accident, Draft V1.2; May 7, 2003.

[21] Byrne, Greg; JSC-SX; Image Analysis Team - Rev 5 Entry Debris Timeline; April 12, 2003.

[22] Spencer, J.R.; JSC-DM; STS-107 Early Entry Debris Sighting Timeline; May 2003.

[23] Abadie, M.; JSC-DM; STS-107 ESAT Final Report Relative Motion and Ballistics Analysis; May 20, 2003.

[24] Mrozinksi, R.B; JSC-DM; STS-107 Columbia Accident Debris Footprint Boundary Estimates; June 3, 2003.

[25] Hartman, S.; JSC-DM; JSC Radar Assessment Team Final Report; May 23, 2003.

[26] Mrozinski, R. B., "CRV Deorbit Opportunities, v1.0h," internal memorandum, NASA Johnson Space Center, Houston, Texas, January 24, 2000.

[27] Mrozinski, R. B., “NASA Pre-Event Debris Footprint Estimates for the Deorbit of Space Station Mir," Proceedings of the International Workshop Mir Deorbit, European Space Operations Center, Darmstadt, Germany, May 14, 2001, pgs. 45 - 55.

[28] Mrozinski, R. B., “Entry Debris Field Estimation Methods and Application to Compton Gamma Ray Observatory Disposal,” proceedings 2001 Flight Mechanics Symposium, NASA Goddard Space Flight Center, Greenbelt, Maryland, June, 2001, pp. 455 - 469.

[29] Berning, M. J., Sagis, K. D., “User’s Guide for the Simulation and Optimization of Rocket Trajectories (SORT) Program, Version 7,” NAS9-17900, Lockheed Engineering & Sciences Company, Houston, Texas, October, 1992.

[30] Hallman, W. P., Moody, D. M., Patera, R. P., Stern, R., “Analyses of Videos of the STS-107 Reentry,” Aerospace ATR, The Aerospace Corporation, Los Angeles, California, May 27, 2003.

[31] Scheffe, H., Tukey, J. W., “A Formula for Sample Sizes for Population Tolerance Limits,” Annals of Mathematical Statistics, Vol. 15, p. 217, 1944.

[32] Oram, T. D., “Final Atmosphere Update,” e-mail communication, NASA Johnson Space Center, Houston, Texas, April 11, 2003.

[33] Jones, R. S., conversation, NASA Johnson Space Center, Houston, Texas, February 03, 2003.

[34] Oram, T. D. “RE: Weather Uncertainties,” e-mail communication, NASA Johnson Space Center, Houston, Texas, April 25, 2003.

[35] Rao, P. P., Woeste, M. A., "Monte Carlo Analysis of Satellite Debris Footprint Dispersion," AIAA 79-1628, 1979.

[36] Herdrich, R. J., Nguyen, P. D., “Super Lightweight Tank (SLWT) Footprint Analysis: Technical Report,” JSC-27712, NASA Johnson Space Center, Houston, Texas, March 01, 1997.

[37] Cerimele, C. J., conversation, NASA Johnson Space Center, Houston, Texas, May 03, 2000.

[38] Jones, R. S., “Checkout Monitor 1,” screen printout, NASA Johnson Space Center, Houston, Texas, February 01, 2003.

[39] Nagle, S. M., telephone conversation, United Space Alliance, NASA Johnson Space Center, Houston, Texas, February 01, 2003.

[40] Carman, G. L., “FW: TRAJ_GPS.txt,” e-mail communication, NASA Johnson Space Center, Houston, Texas, February 05, 2003.

[41] Silvestri, R. T., “FW: Inertial V, gamma, azimuth,” e-mail communication, NASA Johnson Space Center, Houston, Texas, February 10, 2003.

[42] Oram, T. D., “RE: Weather Uncertainties,” e-mail communication, NASA Johnson Space Center, Houston, Texas, March 26, 2003.

[43] Carman, G. L., “FW: 10HZ_BET.txt,” e-mail communication, NASA Johnson Space Center, Houston, Texas, March 20, 2003.

[44] Nuss, R. W., “STS107 GPS post-LOS data,” e-mail communication, NASA Johnson Space Center, Houston, Texas, March 19, 2003.

[45] Feustel, A. J., "FW: Ballistic 100," e-mail communication, NASA Johnson Space Center, Houston, Texas, March 14, 2003.

[46] Mendoza, A. C., "Updated SRIL," e-mail communication, NASA Kennedy Space Center, Kennedy Space Center, Florida, May 29, 2003.

[47] http://usaflwas1.ksc.nasa.gov/fl/debris/index.cfm?fuseaction=reports.roReport&CFID=36890&CFTOKEN=19948634&fakey=64394, NASA Kennedy Space Center, Kennedy Space Center, Florida.

[48] http://usaflwas1.ksc.nasa.gov/fl/debris/index.cfm?fuseaction=reports.roReport&CFID=36890&CFTOKEN=19948634&fakey=66424, NASA Kennedy Space Center, Kennedy Space Center, Florida.

[49] http://usaflwas1.ksc.nasa.gov/fl/debris/index.cfm?fuseaction=reports.roReport&CFID=36890&CFTOKEN=19948634&fakey=38885, NASA Kennedy Space Center, Kennedy Space Center, Florida.

[50] "STS-107 Radar Database, Long Range Radar Returns (2/1/03, 13:30Z to 15:00Z)," National Transportation Safety Board and Federal Aviation Administration, Washington, D. C., February 10, 2003.

[51] Rochelle, W. C., Smith, R. N., Dobarco-Otero, J., "ORSAT Results of STS-107 (Columbia) Early and Late Break-Up Debris Analysis," presentation, NASA Johnson Space Center, Houston, Texas, March 07, 2003.

[52] http://usaflwas1.ksc.nasa.gov/fl/debris/index.cfm?fuseaction=reports.roReport&fakey=14768&goback=2&CFID=36890&CFTOKEN=19948634, NASA Kennedy Space Center, Kennedy Space Center, Florida.

[53] Schafer, Craig P.; SAIC; Results of Search for Observed Debris Landing Events, and EOC Hotline and Database Lessons Learned for STS-107 Accident Investigation; May 16, 2003.

[54] 45 RMS/RMSS; PAFB, FL; Shuttle STS-107 Debris Analysis - Instrumentation Systems Analysis Special Report, CDR A205; February 14, 2003.

[55] Roberts, Katherine E., Col;USSTRATWEST/J3V; e-mail communication; February 21, 2003.

[56] Roberts, Katherine E., Col;USSTRATWEST/J3V; e-mail communication; March 26, 2003.

[57] Brad, J., Lydick, E.D., Schumacher Jr., P.W.; Naval Network and Space Operations Command; Dahlgren VA; Analysis of Fence Observations of STS-107 Reentry - NNSOC Technical Report 03-001; February 28, 2003.

[58] Kent, Brian, Dr.; AFRL, Wright-Patterson AFB, OH; e-mail communication; May 21, 2003.

[59] Kent, Brian, Dr.; AFRL, Wright-Patterson AFB, OH; e-mail communication; May 14, 2003.

10. Appendices

10.1. Team Members and Contributors

Early Sighting Assessment Team Members	
Hill, Paul - Flight Director	ESAT Lead - DA8
Koerner, Cathy - Flight Director	Co-Lead - DA8
Oliver, Greg	Management Coordination (DM4)
Anthony, Col Jack	DCIST POC to NASA
Bryant, Jeralynn	Admin support-DA8
Shaw, Jackie	Admin support-DA8
Moore, Patti	DB Tracking-DA8
Spohr, Rob	DB Tracking-DA8
Conover, Sharon	Sighting Reports - OA/MA
Craig Schafer	Sighting Reports, DB Tracking - OZ4/SAIC
Beck, Kelly - Flight Director	Sighting Reports-DA8
Ceccacci, Tony Flight Director	Sighting Reports-DA8
Curry, John - Flight Director	Sighting Reports-DA8
Knight, Norm - Flight Director	Sighting Reports-DA8
Lunney, Bryan - Flight Director	Sighting Reports-DA8
Abadie, Marc J.	Ballistics (Co-lead) (DM4)
Gowan, John W.	Ballistics (Co-lead) (DM4)
Conte, Barbara A. (DM44 Lead)	Ballistics, Group Lead (DM4)
Mrozinski, Richard (Rich) B.	Footprints (Lead) (DM4)
Graybeal, Sarah R.	Footprints (DM4)
Kadwa, Binaifer (Bini) K. (Co-Op)	Footprints (DM4)
Mendeck, Gavin F.	Footprints (DM4)
Chi, George	Footprints/Groundtrack QA (DM4)
Rask, John (Doug) D.	Ground tracks/Timelines (DM4)
Hartman, Scott A.	RAT (Radar Analysis Team) (lead) (DM4)
Herron, Marissa S.	RAT (b/u lead) (DM4)
Evans, Michael	RAT (DM2)
Brogan, Jonathan	RAT (DM3)
Zaczek, Mario	RAT (DM3)
Braun, Angela N.	RAT (DM4)
Cutri-Kohart, Rebecca M.	RAT (DM4)
Shaver, Matthew (Matt) D.	RAT (USA Navigation)

Early Sighting Assessment Team Members	
Spencer, James R. (Ron)	Sighting - Video Screening (Lead) (DM4)
Edelen, James C. (Chris)	Sighting - Video Screening (DM4)
Proud, Ryan W.	Sighting - Video Screening (DM4)
Bentley, Dennis L.	Sighting Team Support (DM4)
Branham, Doug	Sighting Team Support - DF
Campa, Todd	Sighting Team Support - DF
Hendrickson, Larry A.	Sighting Team Support (DM4)
Horlacher, Gary	Sighting Team Support - DF
Jarvis, Bobby	Sighting Team Support - DF
Schmidt, Tom	Sighting Team Support (DM4)
Schottel, Matthew L. (Matt)	Sighting Team Support (DM4)
Lawson, Keith	Infrasonics, Seismic, Pointing-DO
Dworak, Natalie	Infrasonics, Pointing-DO
Watts, Karen	Pointing-DO
Johnson, Nick	Orbital Debris-SX
Stansbery, Eugene	Orbital Debris-SX

Individuals in bold invested considerable time to support ESAT

Early Sighting Assessment Team Contributors	
Silvestri, Ray (DM42 Lead)	Footprints Group Lead - (DM4)
Carman, Gilbert	BET vector Transformations (DM4)
Pogue, Glenn	BET/GPS Vector Transformations (DM4)
Blanton, Mark	Pointing-DO
Hemingson, Greg "Ernie"	Pointing-DO
McKinley, David	Pointing-DO
Stocco, Marcos	Pointing-DO
Kling, Jeff	Shuttle Systems, MMACS-DF
Lenort, Dean	Shuttle Systems, PROP - DF
Marasia, Amy	Shuttle Systems, PROP - DF
McCluney, Kevin	Shuttle Systems, MMACS-DF
Cerimele, Chris	Management (EG)
Stuart, Phil	Aero Ballistics (EG3)
Rochelle, Bill	Aero Heating Analysis (EA/LMCO)
Smith, Reis	Aero Heating Analysis (EA)
Dobarco-Otero, Jose	Aero Heating Analysis (EA/LMCO)
Bryant, Lee	Backward Propagation (EG5)
Sostaric, Ron	Ballistics (EG)
Tigges, Mike	Footprints (EG)
Broome, Joey	Mapping (EG5)
Gaffney, Bob	EOC - JA
Perrin, Dennis	EOC - JA
Roeh, Bill	EOC - JA
Curry, Don	Radar Test Support - JSC-ES
Rickman, Steve	Radar Test Support - ES
Schomburg, Calvin	Radar Test Support - JSC-EA
Austin, Larry	Radar Test Support - KSC
Banks, Marvin E.	Radar Test Support - KSC
Chambers, Tony	Radar Test Support - KSC
Henn, Becky	Radar Test Support - KSC
Stoner, Mike	Radar Test Support - KSC
Bower, Dan	Radar Assessment Team - NTSB
Brazy, Doug	Radar Assessment Team - NTSB
Crider, Dennis	Radar Assessment Team - NTSB

Early Sighting Assessment Team Contributors	
Duhham, Scott	Radar Assessment Team - NTSB
Fox, Todd	Radar Assessment Team - NTSB
Gregor, Joe	Radar Assessment Team - NTSB
Grossi, Dennis	Radar Assessment Team - NTSB
Kakar, Abdullah	Radar Assessment Team - NTSB
Kolly, Joe	Radar Assessment Team - NTSB
O'Callaghan, John	Radar Assessment Team - NTSB
Park, Alice	Radar Assessment Team - NTSB
Pereira, Charley	Radar Assessment Team - NTSB
Beaulieu, Steve	Radar Assessment Team - FAA
Olsen, Mark	Radar Assessment Team - FAA
Clark, Chris	Radar Tests - AFRL, WPAFB, OH
Fails, Frank	Radar Tests - AFRL, WPAFB, OH
Forster, William	Radar Tests - AFRL, WPAFB, OH
Kent, Brian	Radar Tests - AFRL, WPAFB, OH
Turner, Dan	Radar Tests - AFRL, WPAFB, OH
Ailor, William	Aerospace Ballistics Management
Hallman, Wayne	Aerospace Corp. Ballistics Lead
Moody, Douglas	Aerospace Corp. Ballistics
Patera, Russell	Aerospace Corp. Ballistics
Rudy, Donald	Aerospace Corp. Video Analysis
Stern, Richard	Aerospace Corp. Ballistics
Bellue, Dan	SMG - Atmospheres (ZS8)
Garner, Tim	SMG - Atmospheres (ZS8)
Lafosse, Richard	SMG - Atmospheres (ZS8)
Oram, Tim	SMG - Atmospheres (ZS8)
Rotzoll, Doris	SMG - Atmospheres (ZS8)
Chimes, Patrick	Image process - GP
Fennelly, Jason	Video processing - GA
Gross, Debbie	Image process - GP
White, Maura	Still image processing - GA
Zarella, Susan	Video processing - GA

DCIST Support	
Maj Gen Hamel	DCIST CHIEF
Col Roberts	DCIST DEPUTY
Lt Col John Amrine	14AF Spt
Maj Brian Renga	14AF Spt
Capt Kevin D. Brooks	14AF Spt
SSgt Tom Dickerson	14AF Spt
Mr Jim Gin	14AF Spt
Lt Col Cyndie Visel	STRATWEST/J33
Maj Paul Pease	STRATWEST/J33
Roger Simpson	NASA LNO to USSTRAT
Stan Newberry	NASA LNO to AFSPC
Lt Col John Kress	AFSPC/XOCS
Maj Eric Olson	AFSPC/XOCS
Gary W. Dahlen	AEROSPACE
Marc Dinnerstein	AEROSPACE
Ruth Matias	AEROSPACE
Eric Urig	AEROSPACE
Doug Vier	AEROSPACE
Col Kenneth Schroer	AFSPC/JA
Maj Robert Ramey	AFSPC/JA
Lt Col Mary Ensminger	AFSPC/FM
Lt Col Andy Roake	AFSPC/PA
DR Finkleman	NORTHCOM/AN
Col Linda Marchione	STRATCOM/J33
Lt Col Rod Burnett	STRATCOM/J33
Maj Jeff Lamb	STRATCOM/J33
Capt Aaron Spaans	STRATCOM/J33
Capt James Taylor	STRATCOM/PA
Julie Holland	STRATCOM/PA

DCIST Support	
Maj John Paradis	STRATCOM/PA
Capt Brett Ashworth	STRATCOM/PA
MSgt Planki	STRATCOM/FM
Capt Mary McLendon	NNSOC
Dr Paul Schumacher	NNSOC
Jon Boers	NNSOC
Larry Gallop	NNSOC
CDR Mark Sanford	NNSOC
Col Pierson	ARSPACE
Matt Scott	ARSPACE
Jay Donnelly	ARSPACE
Dave Svetz	NRO
Lt Col Gene Brown	NRO
Frank Giegerich	NRO
Eleanor Padgett	NSA/DEFSMAC
Jack Bobela	NSA/DEFSMAC
Mr Christian Chatfield	DCI Rep
Mr Joseph Convery	DIA Rep
Maj Jeff Wohlford	CMOC/J3S
MSgt Tom Dickerson	SPACEAF
Maj Bob Rochester	1 SPCS
Robin Thurston	1 SPCS
Chris Irrgang	1 SPCS
Bill Barker	1 SPCS
Steve Casali	1 SPCS
Todd Bunker	1 SPCS
Bill Schick	1 SPCS
Lt Col Bob Gibson	2SWS
6SWS: Bernadette VanBurskirk	21 SW
Norm Davis	21 SW

DCIST Support	
Mike Ayres	21 SW
7SWS: Chet Burress	21 SW
Lt Col Cynthia Grey	45 SW
Maj John Talarico	50 SW
Capt Chris Collins	50 SW
MGen Paul D. Nielsen	AIR FORCE RESEARCH LAB (AFRL)
Col Mark D. Stephen	AIR FORCE RESEARCH LAB (AFRL)
Lt Col Mike Caylor	AIR FORCE RESEARCH LAB (AFRL)
Lt Col Jeff McCann	AFRL/AMOS
Tom Glesny/Dan Diehl	AFRL/AMOS
LtCol Joseph Pugliese	AFRL/STARFIRE
Mr Patrick Serna	AFRL/ RF TW/AR
Herbert (John) Mucks	AFRL/IFEA
Jay Jesse	AFRL/IFEA
Robert Morris	AFRL/VSV
Col Neil R. Wyse	45TH WEATHER SQUADRON
Lt Col Harms	45TH WEATHER SQUADRON
Mr. Bill Roeder	45TH WEATHER SQUADRON
Maj Robert Hauser	AFWA
Capt Herb Keyser	AFWA
Lt Col Rick Rehs	84th RADES
Lanny Clelland	84th RADES
Lt Steve Cruz	84th RADES
TSgt Kevin Powell	84th RADES
Kirk Sharp (NASA POC to 84 RADES)	84th RADES
MSgt John Muir	AFTAC
Alt: Paula Patterson	AFTAC
TSgt Kenneth B. Edgcombe	AFTAC

DCIST Support	
INFRASONIC POCS AND DATA	
Stephen Tenney	Army Research Lab (ARL)
Pam Clark	Army Research Lab (ARL)
Dr Doug Drob	Navy Research Lab (NRL)
Mr. Patrick Wakefield	OUSD (AT&L)/NCB
Dr. Stephen Mangino	OUSD (AT&L)/NCB
Bob North	CMR
Dr Xiaoping Yang	CMR
Dr Joydeep Bhattacharyya	CMR
Dr Hans Israelsson	CMR
Mr. Michael Skov	CMR
Dr Bob Woodward	CMR
Dr Rob Gibson	BBN Inc
Dr David Norris	BBN Inc
Dr Gene Herrin	SMU
Chris Hayward	SMU
Alfred J. Bedard, Jr	NOAA/ETO
Dr. Rod Whitaker	LANL
Dr Doug Revelle	LANL
Dr Milton Garces	University of Hawaii
Dr Hank Bass	University of Mississippi
Dr Michael Hedlin	UC at San Diego
Dr Gerald D'Spain	UC at San Diego
Dave Derosher	AEROSPACE
Larry L. Benson	National Air Intelligence Center (NAIC)
Korin Elder	National Air Intelligence Center (NAIC)
TSGT Par Soulati	National Air Intelligence Center (NAIC)
Mr. Randall Bostick (Infrasonic POC)	National Air Intelligence Center (NAIC)

DCIST Support	
Lt Col Dale Smith	Aerospace Fusion Center (AFC)
Peter Soller	Aerospace Fusion Center (AFC)
Todd Beltracci	Aerospace Fusion Center (AFC)
Steve Hammes	Aerospace Fusion Center (AFC)
Maj Anthony Cruciani	Aerospace Research Center (ARC)(Los Angeles)
Col TS Kelso, PhD	Air Force Space Analysis Center (ASAC)
Bob Morris	Air Force Space Analysis Center (ASAC)
Taft Devere	Air Force Space Analysis Center (ASAC)
Nancy Ericson	Air Force Space Analysis Center (ASAC)
Bruce Bowman	Air Force Space Analysis Center (ASAC)

10.2. Entry Debris Events Timeline, Version 6 - 05/27/03

Photo/TV Analysis Team

STS-107 Investigation

Entry Debris Events Timeline

Photo/TV Analysis Team
Version 6 - 05/27/03

This revision slightly modifies the times of debris events 7, 8, and 15 based on a resynchronization of four videos based on ballistic calculations.

Data Summary

The Photo Analysis Team has screened over 140 videos received from the public. Approximately 25 contain good records of debris emanating from the Orbiter plasma envelope. Our emphasis has been on obtaining the most accurate GMT's possible for the debris observations. This report documents the 28 Western-most events identified to date. In addition, the four Eastern-most events for which GMT's have been determined are also listed. The Photo/TV Analysis Team currently does not have any good quality video that covers Eastern Arizona to Central Texas and no video at all that covers Eastern New Mexico to Central Texas. This makes it impossible to link the Western and Eastern segments into a single unified timeline. Finally, all of the videos contain short periods when the Orbiter is out of the camera's field of view, obscured by clouds, or is out of focus. As a result, it is possible that additional events may have occurred which to date have not been seen on available videos.

Event Timing

The GMT's for the Western-most seven events (Debris 1-6 and Flash 1) were based upon passage of the Orbiter envelope near celestial objects recorded in three separate videos (EOC2-4-0055, 0034, 0064). The times for Debris 7A and 9 - 14 were based upon passage of the Orbiter envelope near celestial objects recorded in two separate videos (EOC2-4-0098, 0161). Video EOC2-4-0030 overlaps the time period from Debris 6 through Debris 14, providing a unified time check between the former celestial time-referenced events (Debris 1-6 and Flash 1) and latter celestial time-referenced events (Debris 7A, 9 –15). Key overlapping events were then cross-referenced with other videos that did not have a time reference, in order to compute GMT's for Debris 16.

The time for Debris 7, 8 and 15 were computed by synchronizing the videos in which they were seen to other synchronized videos based on the time of separation of the debris from the vehicle based on ballistic calculations made from these videos.

The GMT's for Flares 1 and 2, which occurred over Eastern Arizona and New Mexico, were based on a verified GMT embedded in the telescope video in which they are seen (EOC2-4-0148-4).

GMT's for the Eastern-most 4 events are based on a GPS time synchronization contained in a video provided by a military source. We then cross-referenced events seen in the military imagery with videos that did not have a time reference. The accuracy of the GPS reference has been verified to be correct.

Notes

Each event time, reported below, represents the earliest moment in time when we can distinguish an event outside the Orbiter plasma envelope. Debris times do not represent the point in time when debris physically separated from Columbia, because the Orbiter is not visible within the plasma envelope. A report entitled "STS-107 Early Debris Ballistics Results;" produced by the Early Sighting Assessment Team (EAST) lists the computed separation time from the vehicle of some of the debris events based on ballistic calculations from these entry videos (contact Marc Abadie @ 281-244-5434 or John Gowan @ 281-483-1923 for more information).

Plasma anomalies (sudden widening and/or brightening in the plasma trail) have been added to the description because after screening a number of videos there is strong evidence to show that when a plasma anomaly is seen, a debris event has almost always occurred.

Western Debris Events			
Event	**GMT**	**EOC Video Number**	**Description**
Debris 1	13:53:46 (+/- 1 sec)	EOC2-4-0056 EOC2-4-0064 EOC2-4-0201 Plasma Anomaly seen in EOC2-4-0136	Seen just aft of Orbiter envelope, one second after a plasma anomaly which consisted of a noticeably luminescent section of the plasma trail.
Debris 2	13:53:48 (+/- 2 sec)	EOC2-4-0056 EOC2-4-0064 EOC2-4-0201	Seen just aft of Orbiter envelope.
Debris 3	13:53:56 (+/- 2 sec)	EOC2-4-0055 Δ EOC2-4-0056 Plasma Anomaly seen in EOC2-4-0064 EOC2-4-0136	Seen just aft of Orbiter envelope followed one second later by a plasma anomaly which consisted of a noticeably luminescent section of the plasma trail.
Debris 4	13:54:02 (+/- 2 sec)	EOC2-4-0055 Δ EOC2-4-0056	Seen just aft of Orbiter envelope.
Debris 5	13:54:09 (+/- 2 sec)	EOC2-4-0055 EOC2-4-0056	Seen just aft of Orbiter envelope at the head of a plasma anomaly.
Flash 1	13:54:33.6 (+/- 0.3 sec)	EOC2-4-0009-B EOC2-4-0055 Δ EOC2-4-0034 EOC2-4-0066 EOC2-4-0070	Orbiter envelope suddenly brightened (duration 0.3 sec), leaving noticeably luminescent signature in plasma trail.
Debris 6	13:54:36 (+/- 1 sec)	EOC2-4-0009-B EOC2-4-0055 Δ EOC2-4-0030 EOC2-4-0066 EOC2-4-0070	Very bright debris seen just aft of Orbiter envelope.
Debris 7	**13:55:05 (+/- 1 sec)**	EOC2-4-0030	Seen just aft of Orbiter envelope.
Debris 7A	13:55:18 (+/- 1 sec)	EOC2-4-0161	Seen just aft of Orbiter envelope.
Debris Shower A	13:55:23 to 13:55:27 (+/- 1 sec)	Saw Debris EOC2-4-0098 EOC2-4-0161 EOC2-4-0005 EOC2-4-0030 Saw Shower EOC2-4-0017 EOC2-4-0021 EOC2-4-0028	Seen just aft of Orbiter envelope. Over the course of these four seconds a luminescent section of plasma trail is observed which appears to contain a shower of indefinite particles and multiple, larger discrete debris that includes Debris 8, 9 and 10.

D EOC2-4-0055 Replaces a lower quality VHS copy EOC2-4-0026.

Western Debris Events (continued)			
Event	**GMT**	**EOC Video Number**	**Description**
Debris 8	**13:55:23 (+/- 2 sec)**	EOC2-4-0030 EOC2-4-0098 EOC2-4-0161	Seen aft of Orbiter envelope inside the aforementioned Debris Shower A.
Debris 9	13:55:26 (+/- 2 sec)	EOC2-4-0005 EOC2-4-0098	Seen aft of Orbiter envelope inside the aforementioned Debris Shower A.
Debris 10	13:55:27 (+/- 2 sec)	EOC2-4-0005	Seen aft of Orbiter envelope inside the aforementioned Debris Shower A.
Debris 11	13:55:37 (+/- 2 sec)	EOC2-4-0050 EOC2-4-0098	Appears at the head of a secondary parallel plasma trail well aft of Orbiter envelope. A second piece of debris is also seen in the secondary plasma trail.
Debris 11A	13:55:39 (+/- 1 sec)	EOC2-4-0098	Seen just aft of Orbiter envelope.
Debris 11B	13:55:40 (+/- 2 sec)	EOC2-4-0098	Seen at head of a parallel plasma trail aft of the Orbiter envelope.
Debris 11C	13:55:44 (+/- 2 sec)	Sees debris and parallel trail: EOC2-4-0098 Sees parallel plasma trail only: EOC2-4-0028, EOC2-4-0050	Seen at head of a parallel plasma trail well aft of the Orbiter envelope.
Debris 12	13:55:45 (+/- 1 sec)	EOC2-4-0028 EOC2-4-0050 EOC2-4-0098	Seen aft of Orbiter envelope followed by secondary plasma trails.
Debris 13	13:55:56 (+/- 2 sec)	EOC2-4-0005 EOC2-4-0017 EOC2-4-0021 EOC2-4-0161	Seen well aft of Orbiter envelope with momentary brightening of plasma trail adjacent to debris.
Debris 14	13:55:58 (+/- 1 sec)	EOC2-4-0005 EOC2-4-0017 EOC2-4-0021 EOC2-4-0028 EOC2-4-0030	Very bright debris just aft of Orbiter envelope.
Debris 15	**13:56:10 (+/- 2 sec)**	EOC2-4-0017	Seen just aft of Orbiter envelope.
Debris 16	13:57:24 (+/- 5 sec)	EOC2-4-0148-2	Very faint debris just aft of Orbiter.
Flare 1	13:57:54.5 (+/- 1 sec)	EOC2-4-0148-4	Asymmetrical brightening of Orbiter shape.
Flare 2	13:58:00.5 (+/- 1 sec)	EOC2-4-0148-4	Asymmetrical brightening of Orbiter shape.

The Photo/TV Analysis Team currently does not have any good quality video that covers Eastern Arizona to Central Texas (no video is available that covers Eastern New Mexico to Central Texas), making it impossible to link the Western and Eastern segments into a single unified timeline.

Eastern Debris Events			
Event	**GMT**	**EOC Video Number**	**Description**
Debris "A"	14:00:04 (+/-2 sec)	EOC2-4-0024 EOC2-4-0018 EOC2-4-0118	Large debris seen falling rapidly away from the Orbiter envelope.
Debris "B"	14:00:19 (+/-2 sec)	EOC2-4-0024 EOC2-4-0118	Time is for debris first seen well aft of Orbiter envelope.
Debris "C"	14:00:20 (+/-2 sec)	EOC2-4-0024 EOC2-4-0118	Time is for debris first seen aft of Orbiter envelope.
Main Body Breakup	14:00:23 (+/-2 sec)	EOC2-4-0024 EOC2-4-0018	Onset of the main body breakup.

These times represent a consensus among photo team members from SX, DM, DF and Boeing.

The following list of viewer's locations is provided to correct inaccurate information displayed on some publicly released maps.

*Viewer locations are rounded and only displayed to two decimal places to protect the individual privacy of the viewer.

STS-107 View Location Data					
EOC	**Location**	**North Latitude* (degrees)**	**West Longitude* (degrees)**	**First View of Vehicle (GMT)**	**Last view of vehicle (GMT)**
EOC2-4-0064	**Fairfield, CA**	**38.28**	**122.01**	**13:53:15**	**13:54:17**
EOC2-4-0056	**Mt. Hamilton, CA**	**37.34**	**121.64**	**13:53:28**	**13:54:29**
EOC2-4-0034	**Reno, NV**	**39.47**	**119.79**	**13:54:04**	**13:54:45**
EOC2-4-0055 (Replaces a lower quality VHS copy EOC2-4-0026)	**Sparks, NV**	**39.54**	**119.76**	**13:53:38**	**13:54:51**
EOC2-4-0009-B	**Springville, CA**	**36.22**	**118.81**	**13:54:17**	**13:55:13**
EOC2-4-0030	**Las Vegas, NV**	**36.31**	**115.27**	**13:54:37**	**13:56:06**
EOC2-4-0017	**North of Flagstaff, AZ**	**35.57**	**111.53**	**13:54:45**	**13:57:30**
EOC2-4-0005	**Ivins, UT**	**37.17**	**113.66**	**13:55:18**	**13:56:10**
EOC2-4-0028	**St. George, UT**	**37.10**	**113.57**	**13:55:05**	**13:56:02**
EOC2-4-0021	**St. George, UT**	**37.10**	**113.56**	**13:55:13**	**13:56:16**
EOC2-4-0050	**St. George, UT**	**37.22**	**113.62**	**13:55:31**	**13:55:55**
EOC2-4-0098	**Santa Clara, UT**	**37.13**	**113.65**	**13:55:10**	**13:56:10**
EOC2-4-0161	**Kolob Arch, UT**	**37.49**	**113.23**	**13:55:14**	**13:56:11**
EOC2-4-0136	**Mill Valley, CA**	**37.90**	**122.51**	**13:55:33**	**13:54:19**

STS-107 View Location Data (continued)					
EOC	**Location**	**North Latitude* (degrees)**	**West Longitude* (degrees)**	**First View of Vehicle (GMT)**	**Last view of vehicle (GMT)**
EOC2-4-0070	**Bishop, CA**	**37.28**	**118.39**	**13:54:12**	**13:55:03**
EOC2-4-0066	**Ramona, CA**	**33.03**	**116.93**	**13:54:29**	**13:54:56**
EOC2-4-0201	**St. Helena, CA**	**38.51**	**122.47**	**13:53:25**	**13:54:01**
EOC2-4-0148-2	**Kirtland AFB, NM**	**34.97**	**106.46**	**13:56:48**	**13:58:12**
EOC2-4-0148-4	**Kirtland AFB, NM**	**34.97**	**106.46**	**13:56:49**	**13:58:01**
EOC2-4-0024	**Arlington, TX**	**32.74**	**97.11**	**14:00:00**	**14:00:35**
EOC2-4-0118	**Arlington, TX**	**32.63**	**97.11**	**14:00:04**	**14:00:21**
EOC2-4-0018	**Duncanville, TX**	**32.67**	**96.90**	**13:59:59**	**14:00:53**
EOC2-4-0025	**Camp Swift, TX**	**30.26**	**97.30**	**14:00:21**	**14:01:01**
MIT DVCAM 0001	**Fort Hood, TX**	**31.18**	**97.58**	**14:00:26**	**14:01:19**

Note: This list does not include all 140+ videos that have been submitted to date by the public. Although all videos received to date have been screened by the NASA Entry Screening Team; this list shows the most useful of the videos that have been assembled to document STS-107 entry debris events as fully as possible.

10.3. DOD - JSC Actions

DOD Data Priorities

1) Process all data from 1340Z -1400Z for high-energy events (include any luminosity and spectral analysis which may indicate size, mass and constituents). Key events to focus on:
   - Discrete debris shedding times.
   - Times associated with off-nominal tlm signatures.
   - Times indicated as off-nominal in infrasonic data (infrasonic data collection in work separately)
   - Bolide detonation reported from Oceanside, CA 1300-1410Z
2) Process all data from Beale Pave Paws
3) Confirm any and all imagery from 1 Feb 1340-1400Z has been identified, processed and received
4) All data from de-orbit burn through break-up
5) Process the object that has been correlated back to Columbia approx 24 hrs after launch
6) Provide trajectory data to all other national agency/organizations so they can check for data
7) Confirm any and all imagery from Ascent-2 Feb, 1340Z has been identified, processed and received
8) Any "unexpected events" DOD might identify throughout duration of mission via own analysis

Closed	Priority	Actionee	Request
	1	DOD	Detailed data from NAVSPASUR re AZ, NM fence detects. In work. Expected 2/28.
	1	DOD	Pam Clark, Army Research Lab pclark@arl.army.mil 410-203-2133, 301-394-3447 Apparently passed on classified information to Dave Hess regarding infrasonic data recorded by a military sensor which shows an event over Arizona. It mentions that this was recorded by White Sands. Suggests they have time, range, altitude. Please follow up May be rolled into the action below.
	1	DOD	Coordinate with Fusion Analysis Cell on infrasonic data and other sensor data for: entry day bolide reports, other infrasonic event correlation to Shuttle timeline and ground track.
	6	JSC	In a separate run of the ephemerides, add the following locations: Alice Springs, 23.5 deg S X 134 deg E; Longreach, 22 deg S X 144 deg E; and Laverton, 28.66 deg S X 122.5 deg E. If they show possible acquisitions, especially for the entry ephemeris, then NASA should pursue getting the data from Australia. DM has it and will add it to the hopper.
	6	DOD	Can you reach into civilian intelligence databases for assets which may have been tasked to regions Columbia overflew in the event they captured images? Optical assets over the Middle East come to mind if there are any, since we flew over and I'd expect it to be a hot intel area now. In work.
2/7/2003	9	DOD	DOD approved Kirtland photo for released. NASA released it.
2/8/2003	1	JSC	DM/Greg Oliver sent Columbia GPS data to Simpson.
2/8/2003	1	DOD	DOD confirmed no other fences similar to NAVSPASUR.
2/8/2003	9	DOD, JSC	Confirmed JSC Orbital Debris Program will request data through the NASA and DOD POCs. Normal working relationships permitted to continue with POCs in the loop.

Closed	Priority	Actionee	Request
2/9/2003	1	DOD	Ames is offering help with photo/video analysis. They suggested that DOD may have spectral data from entry that would help them estimate size, material and mass of the debris. Ring a bell, and if so, are you expecting data back? I'll forward Ames contact info to you for security clearance verification on any classified (including the data you brought last week).
2/9/2003	9	JSC	Updated NASA data request priorities.
2/10/2003	1	DOD	DM/Greg Oliver is interested in getting help from Dick Stearns. Mr. Stearns has been notified.
2/12/2003	5	JSC	Provide DOD with the following for FD2 radar analysis: - Precision ephemeris on the Shuttle for day 17 - The density (gm/cm**3) of heat tiles, carbon-carbon leading edge, spacecraft aluminum, and tool steel - A summary chart of the accelerometer events for all of day 17 Density data e-mailed 2/12/03. Full flight ephemeris e-mailed 2/12/2003. DF6/Sarafin and Allega working accel tlm.
2/12/2003	5	JSC	ES3/Steve Rickman sent material descriptions and densities for external components, specifically various TPS materials.
2/12/2003	6	JSC	Entire ephemeris (on orbit and entry) for STS-107 through the SAT ACQ program using every sensor that they have in their database with an elevation angle of -5 degrees E-mailed 2/12/2003 by DM/Leleux.
2/12/2003	6	JSC	Ephemeris for the entire flight. At this time vectors every 6 hours in the ECI format would suffice. In work. E-mailed M50 2/12/2003 by DM/Leleux
2/14/2003	1	DOD	E-mailed unclass DOD data estimating possible Orbiter debris shedding events and impact locations.
2/14/2003	3	DOD	Confirm Maui and Kirtland do not have any other images, classified or unclass, which would help evaluate both leading edges and the bottom surface of the orbiter, whether in orbit ops or during entry. Confirmed no other entry images 2/11/2003. Confirmed no other orbit ops images exist 2/14/2003 via JSC call to Maui.
2/14/2003	5	JSC/DOD	Telecon with Bob Morris re other thermal insulation on the exterior and PLB.
2/17/2003	8	DOD	Approve normal working interface between individual below and JSC Engineering to discuss and obtain any available information concerning the properties of Kapton (polyimide) insulated wire in high/extreme heat conditions. This may help in precluding duplicate testing already performed by the DoD or guide us better in developing our own test to characterize the data seen on STS-107. George A. Slenski AFRL/MLSA 2179 12th Street, B652 Rm 25 WPAFB, OH 45433-7718 Phone: 937-656-9147 e-mail: george.slenski@wpafb.af.mil
2/18/2003	1	DOD	Provide any DOD ascent video for NASA review and analysis. DCIST approved Patrick AFB provide their asc video to NASA.
2/18/2003	3	DOD	Provide Kirtland camera location and pointing information in support of entry photo. Also provide Kirtland POC to discuss engineering analysis.

Closed	Priority	Actionee	Request
2/19/2003	3	DOD	Post-process AMOS imagery for: indications of upper surface leading edge damage; missing thermal insulation in the payload bay, including but not limited to the SpaceHab trunnions.
2/19/2003	8	DOD	Provide OAFS/VTS data per GSFC- Ted Sobchak/ND, (301) 286-7813 Approved 2/13/03. In work.
2/21/2003	4	DOD	Confirmed no ship based or AWACS radar data taken during entry.
2/21/2003	5	DOD, JSC	It was reported to JSC-SX/Nick Johnson from DOD that an object was tracked separating from the orbiter at 5 m/s, 17 Jan, 1600Z (STS-107 flight day 2). JSC is pulling timeline data for water dumps, which may account for this. We will also evaluate accelerometer data much more closely on this day. We had already decided to screen all accelerometer data for the full mission. No water dumps. Manual fuel cell purge initiated 1625Z. Accelerometer data tracked in another action.
2/21/2003	8	DOD	Confirmed no tracks objects approached within 5 km of Columbia throughout orbit ops.
2/24/2003	1	JSC	Debris sighting data on timeline. In work. Sent ground track with rev 12.1 but no sightings on 2/12/2003. 1st 6 discrete shedding times to ship 2/13. Remainder expected 2/20.
2/27/2003	1	DOD	On a similar note, we're hearing from NOAA that there is some DOD site on the west coast with infrasonic capability similar to what NOAA is sending us from Boulder, CO. He suggests that the west coast data could show us good data over the Pacific. DOD request went to AFTAC for this data. JSC requested direct support to NOAA-LANL review in Colorado. Message 2/18/2003: The “Center for Monitoring Research at the Defense Threat Reduction Agency in Arlington, VA” has apparently “forbidden” DOE to get involved in the investigation. Various data is being withheld from LANL, including Air Force Technical Applications Center data. DOD data analysis in work.
2/27/2003	2	DOD	Confirm Vandenburg and/or any other DOD tracking did not track Columbia. Provide raw tracking radar data for debris searches. 84th RADES has all DOD ATC radar.
2/27/2003	5	DOD	Based on the possible FD2 debris strike, focus radar searches to obtain skin paints before 17 Jan 1600Z, any time after, and as late as possible before deorbit. No data.